



Modern radical chemistry

Edited by Huan-Ming Huang

Imprint

Beilstein Journal of Organic Chemistry
www.bjoc.org
ISSN 1860-5397
Email: journals-support@beilstein-institut.de

The *Beilstein Journal of Organic Chemistry* is published by the Beilstein-Institut zur Förderung der Chemischen Wissenschaften.

Beilstein-Institut zur Förderung der
Chemischen Wissenschaften
Trakehner Straße 7–9
60487 Frankfurt am Main
Germany
www.beilstein-institut.de

The copyright to this document as a whole, which is published in the *Beilstein Journal of Organic Chemistry*, is held by the Beilstein-Institut zur Förderung der Chemischen Wissenschaften. The copyright to the individual articles in this document is held by the respective authors, subject to a Creative Commons Attribution license.



Photoredox catalysis enabling decarboxylative radical cyclization of γ,γ -dimethylallyltryptophan (DMAT) derivatives: formal synthesis of 6,7-secoagroclavine

Alessio Regni, Francesca Bartoccini and Giovanni Piersanti*

Full Research Paper

Open Access

Address:

Department of Biomolecular Sciences, University of Urbino, Carlo Bo
Piazza Rinascimento 6, 61029 Urbino, PU, Italy

Email:

Giovanni Piersanti* - giovanni.piersanti@uniurb.it

* Corresponding author

Keywords:

decarboxylative cyclization; DMAT; ergot alkaloids; photoredox
catalysis; radicals

Beilstein J. Org. Chem. **2023**, *19*, 918–927.

<https://doi.org/10.3762/bjoc.19.70>

Received: 15 February 2023

Accepted: 15 June 2023

Published: 26 June 2023

This article is part of the thematic issue "Modern radical chemistry".

Guest Editor: H.-M. Huang



© 2023 Regni et al.; licensee Beilstein-Institut.
License and terms: see end of document.

Abstract

An unusual photoredox-catalyzed radical decarboxylative cyclization cascade reaction of γ,γ -dimethylallyltryptophan (DMAT) derivatives containing unactivated alkene moieties has been developed, providing green and efficient access to various six-, seven-, and eight-membered ring 3,4-fused tricyclic indoles. This type of cyclization, which was hitherto very difficult to comprehend in ergot biosynthesis and to accomplish by more conventional procedures, enables the synthesis of ergot alkaloid precursors. In addition, this work describes a mild, environmentally friendly method to activate, reductively and oxidatively, natural carboxylic acids for decarboxylative C–C bond formation by exploiting the same photocatalyst.

Introduction

Visible-light photoredox catalysis is rapidly changing the way organic chemists approach the design and synthesis of molecules by offering new synthetic disconnection opportunities that are usually more convergent, enabling a more diverse chemical space in a rapid fashion [1–15]. Currently, increasing numbers of synthetic chemists are developing photocatalytic processes to make molecules efficiently and in an environmentally friendly manner due to their intrinsic mildness and broad substrate compatibility [16–20]. This transformative synthetic tool often utilizes direct single-electron transfer (SET) between an elec-

tronically excited photoredox catalyst and an organic substrate, resulting in oxidation or reduction, to easily generate reactive open-shell radical species and/or intermediates. The substrate is consequently activated for bond cleavage, atom abstraction, or nucleophilic or electrophilic attack. After quenching, the oxidized or reduced photocatalyst regains or loses an electron to return to the starting ground state catalyst [21–26].

While early research has focused on methods for the functionalization of relatively simple hydrocarbons [27–30], develop-

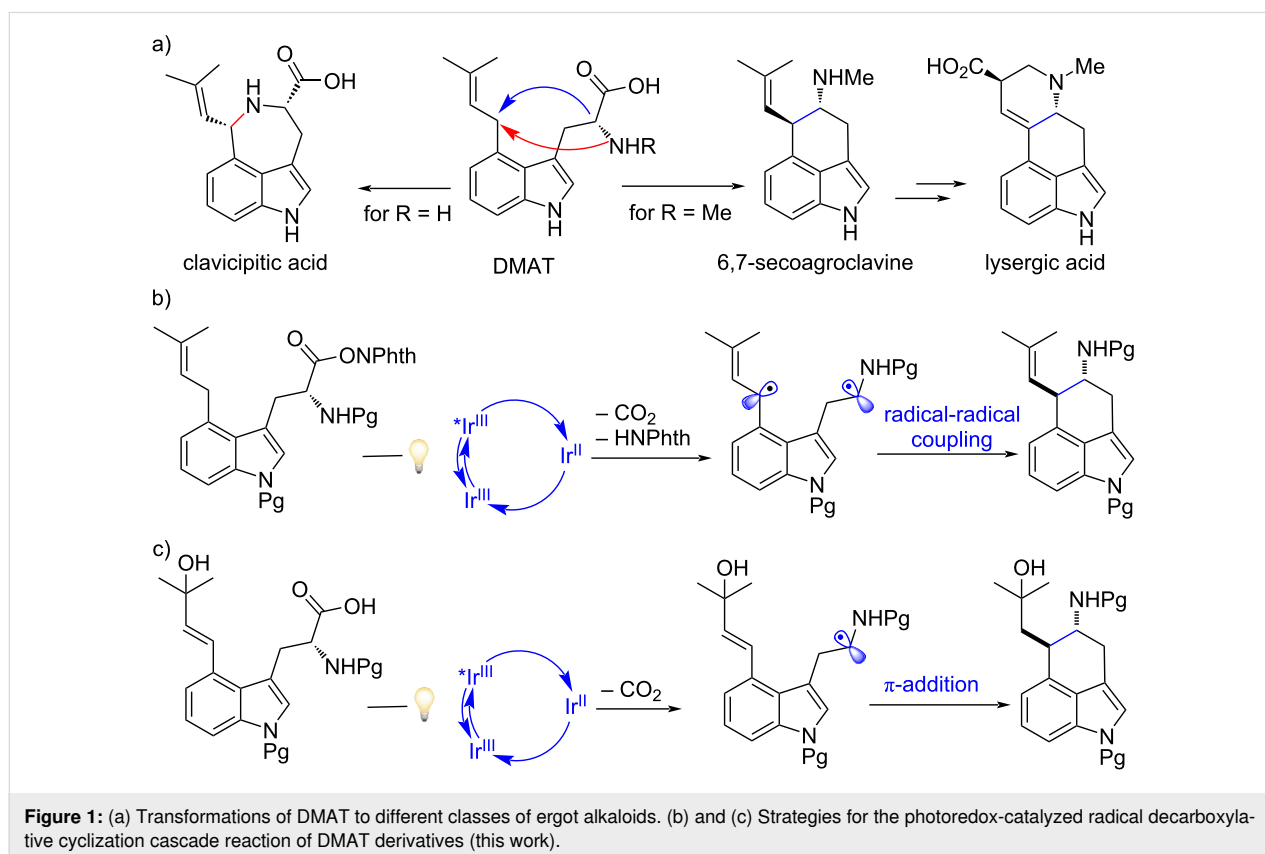
ments in photoredox catalysis have gained traction recently as a viable strategy for the total synthesis of natural products [31–33], modification of biomacromolecules [34], and relatively complex pharmaceutical agents [35–38]. Photocatalysis tremendously enriches the synthetic compound library, providing a precious alternative to directly modify abundant natural substrates, including biomass, which usually requires a multistep process in conventional chemical synthesis [39–41]. Among the various widely available and abundant substrates for photocatalyzed reactions, natural and unnatural α -amino acids play a very important role, given their paramount importance across several chemistry fields as well as their ability to participate in either redox step of the catalytic cycle [42–45]. For example, the main use of α -amino acids in syntheses via photoredox catalysis is as readily available precursors of regioselective α -amino radicals by decarboxylative transformations, by oxidation of the carboxylate anion and/or reduction of the corresponding *N*-hydroxyphthalimide- (NHPI)-derived redox-active ester, although it destroys their stereochemical information [46–51]. In addition, the side-chains of aromatic amino acids (mainly electron-rich tryptophan and tyrosine) can be selectively targeted by photoredox catalysis to enable unprecedented modification of the amino acid. In this context, it is worth mentioning that the single-electron oxidation of the indole moiety in tryptophan provides the radical cation, which enables selective C-radical

generation at the weaker benzylic position via a sequential electron transfer–proton transfer (ET/PT) [52–59].

With our ongoing interest of establishing new methods for the asymmetric synthesis of nonproteinogenic tryptophan derivatives as well as their associated indole alkaloid natural products [60–67], we became fascinated in exploring whether photoredox catalysis could be applied for the activation of such unnatural amino acids to expedite the development of completely new synthetic pathways. In particular, 4-dimethylallyltryptophan (DMAT) is of interest for the following reasons: 1) it functions as the central intermediate in the biosynthetic pathways leading to numerous prenylated indole alkaloids, such as ergot alkaloids in normal biosynthesis and clavicipitic acid in derailment biosynthesis [68–71]; and 2) the mechanism of the fundamental central C-ring formation of all ergot alkaloids, specifically the decarboxylative cyclization of DMAT, is still a puzzle even though a radical mechanism has been proposed (Figure 1a) [72,73].

Results and Discussion

Herein, we propose that visible light irradiation of the cationic iridium photocatalyst $\text{Ir}[\text{dF}(\text{CF}_3)\text{ppy}]_2(\text{dtbbpy})\text{PF}_6$ ($E_{1/2}^{*\text{III}/\text{II}} = +1.21 \text{ V}$, $E_{1/2}^{\text{III}/\text{II}} = -1.37$; $E_{1/2}^{\text{IV}/*\text{III}} = -0.89$, $E_{1/2}^{\text{IV}/\text{III}} = +1.69 \text{ V}$) [74] would permit efficient radical generation and



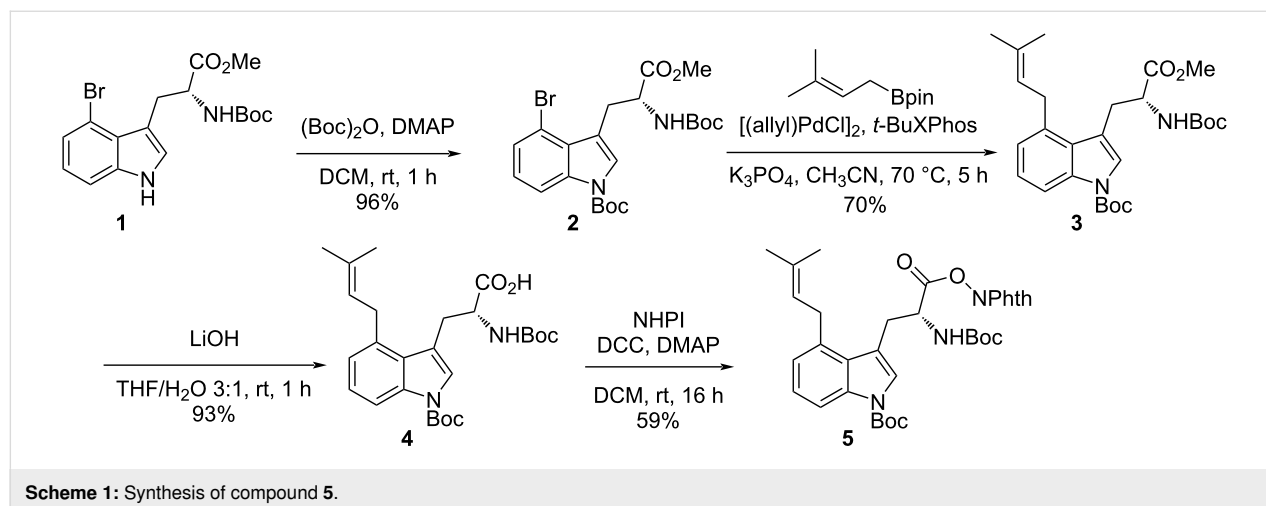
C(sp³)–C(sp³) bond formation either by challenging selective radical–radical cross-coupling or by radical addition to a π -bond, enabling a rare example of intramolecular decarboxylative cyclization with the formation of the 3,4-fused indole carbocycle rings (Figure 1b,c). In detail, the photocatalytic strategy for accessing the two C(sp³) radicals of DMAT derivatives envision the formation of a relatively stabilized allylic-benzylic carbon-centered radical by proton transfer from the oxidized indole radical cation [75], generated by SET from the activated photocatalyst. The α -amino radical generated by reductive decarboxylation of a DMAT derivative with a redox-active ester (–1.26 V to –1.37 V vs a saturated calomel electrode) would enable turnover of the photoredox cycle (Figure 1b). Alternatively, we envisioned a more established approach expecting the direct oxidative photoredox decarboxylation of the carboxylic acid/carboxylate (by SET from the activated photocatalyst) of DMAT to generate the α -aminoalkyl radical that might readily be captured/trapped intramolecularly with the C4-pendant prenyl side-chain previously oxidized [76]. Closure of the photoredox catalytic cycle would then involve SET reduction, and protonation would deliver the desired carbocyclic ring (Figure 1c). If this cyclization reaction could be realized in either way, it would shorten the synthetic route of ergot alkaloids and may offer new opportunities for drug discovery and biochemistry applications.

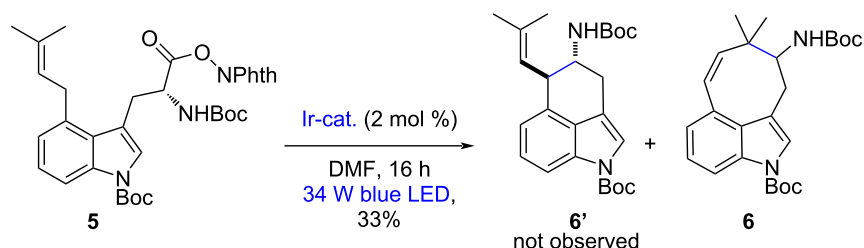
As natural and unnatural tryptophan-derived redox-active *N*-hydroxyphthalimide esters have already been used in photoredox catalysis, we decided to use them as the initial substrates [77–85]. To test this concept, we turned our attention to the synthesis of key intermediate **5** (Scheme 1). The synthesis began with protection of the indole nitrogen of the known compound **1**, which is readily available from commercially available 4-bromoindole in one step [62]. Regioselective palladium-catalyzed prenylation of **2** with prenylboronic acid pinacol ester

and subsequent hydrolysis with LiOH provided the linear prenylated acid **4** in good yield. Coupling acid **4** with *N*-hydroxyphthalimide using DCC and a catalytic amount of DMAP afforded the key intermediate **5** in 59% yield.

With compound **5** in hand, the required radical–radical coupling was investigated next, and some of the representative results are shown in Table S1 (see Supporting Information File 1). Irradiation from blue light-emitting diodes (LEDs) in the presence of 2 mol % of the photocatalyst [Ir(dF(CF₃)ppy)₂(dtbpy)]PF₆ in CH₂Cl₂ at room temperature using our integrated photoreactor enabled efficient cyclization to give a decarboxylated compound with the correct mass (*m/z* 426.2) after 16 h. While we were delighted to find that the proposed radical–radical coupling in the synthesis of extracyclic fused indoles was feasible under these conditions, the observed reaction efficiency was poor (14–33% yield). However, on the ¹H NMR spectrum, some unexpected signals were observed. The appearance of equilibrating species such as rotamers in the ¹H NMR spectrum (see the variable-temperature NMR experiments in Supporting Information File 1, Figure S1) due to the protecting groups complicates the analysis of the reaction products. However, the olefinic signals were a pair of two doublets representing two vicinal vinylic protons [6.48 (d, *J* = 8.0 Hz, 1H), 6.29 (d, *J* = 8.0 Hz, 1H), 5.31 (d, *J* = 8.0 Hz, 1H), and 5.28 (d, *J* = 8.0 Hz, 1H)], strongly indicating that this product is not the desired structure **6'** but the eight-membered cycloalkene structure **6**, shown in Scheme 2. Based on these results and previous reports on the benzylic and allylic C–H bond functionalization enabled by metallaphotoredox catalysis [86], we propose a tentative mechanism (Figure 2).

First, the radical cation **I** was generated via the oxidation of indole **5** by the excited Ir-based photocatalyst, followed by sequential regioselective proton transfer on the benzylic





Scheme 2: Photoredox-catalyzed radical decarboxylative cyclization of **5**.

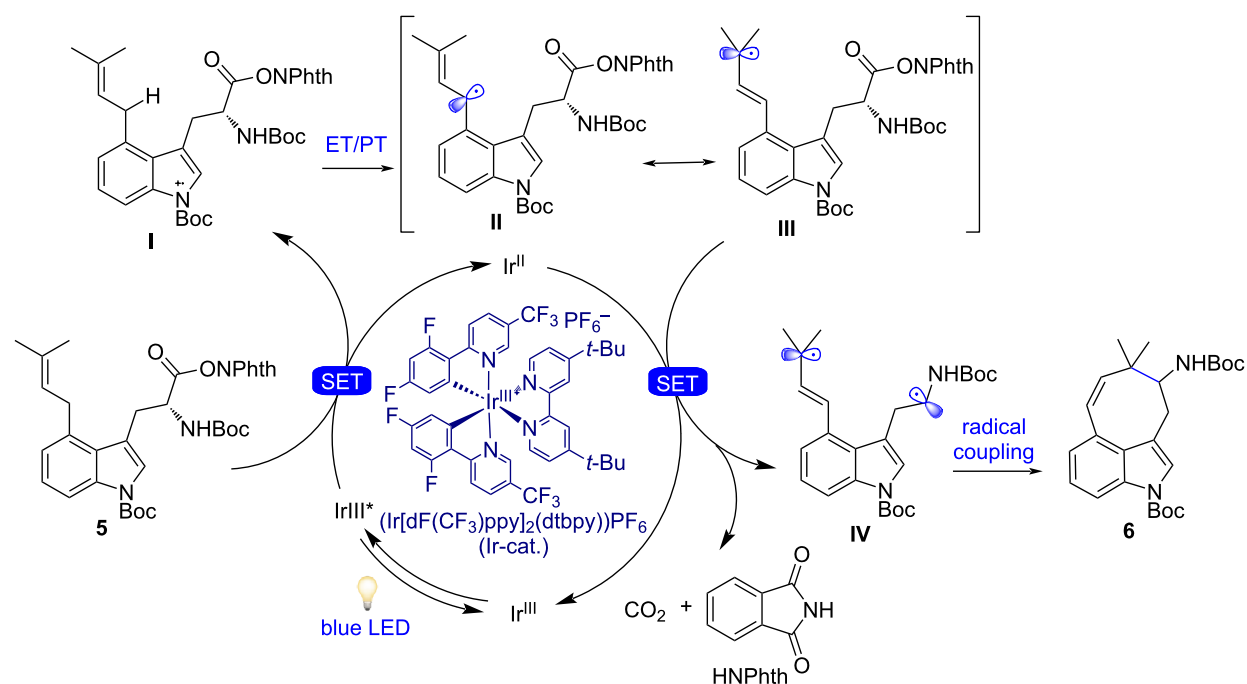


Figure 2: Proposed reaction mechanism for photoredox-catalyzed radical decarboxylative cyclization.

dimethylallyl unit C–H bond of the C4 side-chain, thereby generating **II**. Here, the radical is stabilized by both the indole ring and the Δ^2 -olefin. Next, the resonance-stabilized radical intermediate **III** was trapped by the active α -aminoalkyl radical, generated by reductive decarboxylation by Ir(II) produced in the photocatalytic cycle (which undergoes oxidation to afford the Ir(III) complex and to close the cycle), thus furnishing compound **6** comprised of an eight-membered ring. The related stabilization effect of the conjugated product **6** might be the thermodynamic driving force for this radical coupling. An alternative route (not shown) would be that, the α -amidoalkyl radical generated by reductive decarboxylation, could add in an 8-*endo*-trig manner (common in radical chemistry) to the alkene and the resulting radical could be oxidized to the cation by the oxidized form of the photocatalyst to close the photocatalytic cycle, followed by formation of the double bond. Even though

no desired cyclized product was observed, an interesting aspect of this reaction was the access of an attractive, unusual, and highly functionalized 3,4-fused eight-membered tricyclic indole, whose ring closure would not have been possible or at least very difficult in the ground state [87–89].

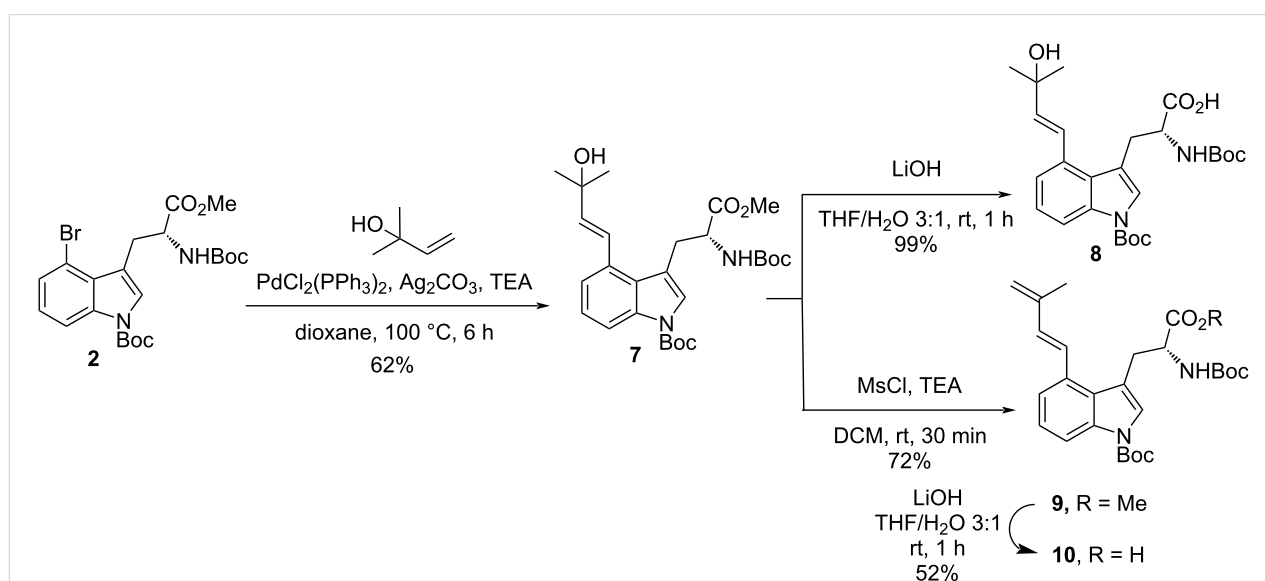
Although not yet completely clarified, some previous studies on the detailed mode of closure of the C ring in ergot alkaloids from DMAT have been shown to involve, before decarboxylative cyclization, oxidation on the C4-prenyl chain to give the stable rearranged allyl alcohol and/or the relatively unstable diene [90,91]. In addition, these results support the hypothesis that the decarboxylative cyclization can occur through subsequent selective 6-*exo*-trig radical addition. It also has been reported that it is difficult to detect which intermediate is really involved, since they are easily interconvertible to each other by

hydration or dehydration, i.e., a plausible precursor of the allylic alcohol would be the diene, and vice versa [90]. Since both **8** and **10** are easily obtainable from **2** by Mozoroki–Heck coupling with commercially available 2-methyl-3-buten-2-ol, ester hydrolysis (LiOH in THF/H₂O), and, finally for **10**, dehydration of the tertiary alcohol (mesylation and elimination) (Scheme 3), we decided to test their roles in the photoredox-catalyzed decarboxylative cyclization. With **8** and **10** in hand with the C4-prenyl side-chain already oxidized/functionalized, we recognized that this cyclization event would be triggered using their innate functionality, namely the α -amino carboxylate, through photoredox-mediated oxidative activation and CO₂ extrusion, without the need for acid prefunctionalization to the redox-activated ester. Consequently, a technique involving direct generation of α -aminoalkyl radicals from free carboxylic acids of **8** and **10** under mild conditions would make the approach even more efficient and more biosimilar; nevertheless, issues regarding the regioselectivity of the ring formation could be raised, since both the 6-*exo*-trig and 7-*endo*-trig cyclization are both favorable, according to the Baldwin rules [92].

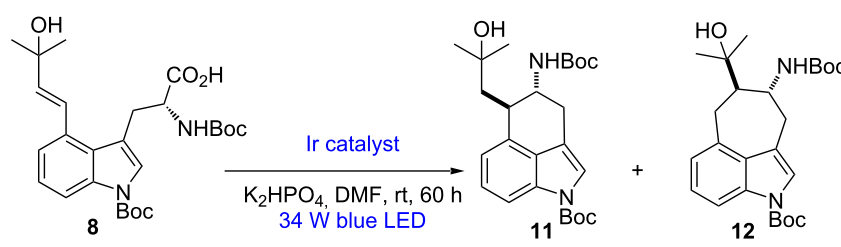
We began our investigation of the proposed decarboxylative cyclization by exposing the *N*-Boc derivative **8**, Ir catalyst, and K₂HPO₄ in DMF to a 34 W blue LED lamp at room temperature (Table 1) [93–97]. To our delight, cyclization was observed under these preliminary conditions, albeit in low yield (35% yield) and low regioselectivity (1:1) (Table 1, entry 1). No regiocontrol was observed; but remarkably, the regioisomers exhibited distinct retention factors on silica gel, allowing **11** and **12** to be isolated separately in good yield as single *trans* diastereomers [98]. Reducing the substrate concentration in-

creased efficiency while assisting in avoiding the oligomerization pathways (Table 1, entries 2 and 3). Higher photocatalyst loadings resulted in an increased yield (Table 1, entry 4). Control experiments showed that both the photocatalyst and light were essential for product production (Table 1, entries 6 and 7), despite the fact that the removal of base did not result in a significantly reduced efficiency (Table 1, entry 5). The regioselectivity outcome was explained by the relative stability of the intermediate radicals involved, with strong evidence of the importance of steric effects [99]. Indeed, while the addition of the nucleophilic α -amino radical to the α -styrenyl position affords the 6-membered ring (kinetic product via intramolecular 6-*exo*-trig ring closure) [100] the resulting radical is unstabilized, the 7-membered ring (obtained via intramolecular 7-*endo*-trig ring closure) may well be the thermodynamic product based on the more stabilized benzylic radical that is produced [101].

As largely reported in the literature [102,103], radicals generated next to alcohols do not normally undergo β -elimination to give alkene/carbon–carbon double-bond formation and a hydroxyl radical (\cdot OH). However, it is possible to transform an alcohol into a leaving group, in the radical sense, by converting it into a halide or pseudohalide derivative [104,105]. For alcohol **8**, all attempts to make a better leaving group, including phenyl sulfone derivative, to have radical addition–fragmentation on the latter and most likely to shift the regioselectivity towards 6-*exo*-trig by a favorable interplay of polar effects [99] failed and furnished only the 1,3-diene **10**. Unfortunately, when substrate **10** was subjected to the reaction conditions shown above, only tarry compounds were obtained; this result was probably due to the competitive cycloaddition and polymeriza-



Scheme 3: Synthesis of tryptophan derivatives **8** and **10**.

Table 1: Photoredox-catalyzed radical decarboxylative cyclization of **8**.^a


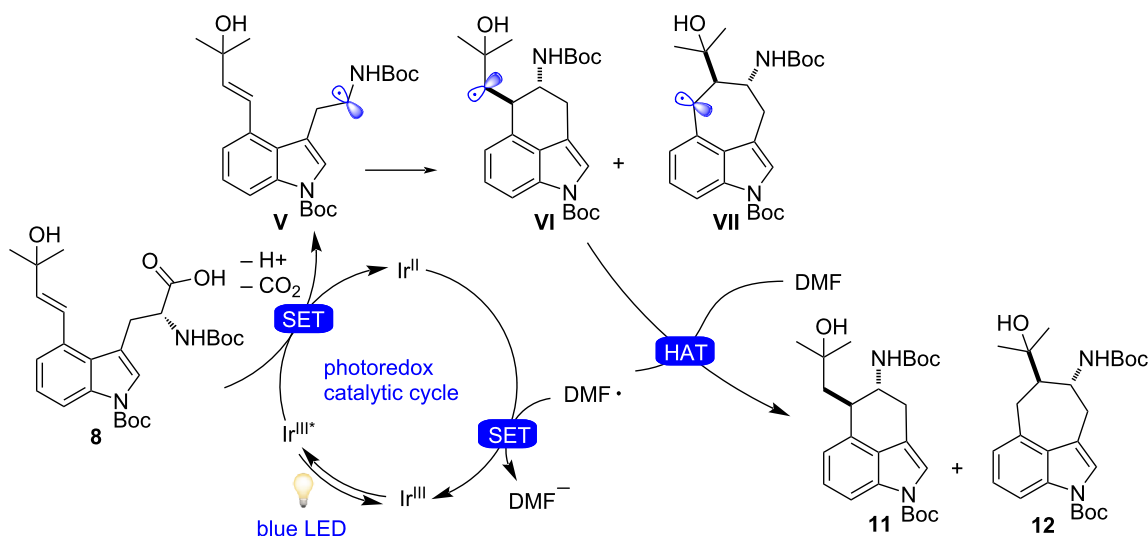
Entry	Conditions	Concentration of 8	Ir catalyst (mol %)	Ratio of 11/12 ^b	Yield of 11 and 12 ^c
1	as shown	10 mM	2	1:1	35%
2	as shown	5 mM	2	1:0.7	39%
3	as shown	2.5 mM	2	1:0.6	42%
4	as shown	2.5 mM	4	1:0.7	59%
5	no base	2.5 mM	4	1:0.7	53%
6	no photocatalyst	2.5 mM	—	—	N.D. ^d
7	no light	2.5 mM	4	—	N.D. ^d
8	DMSO instead of DMF	2.5 mM	4	0.7:1	33%
9	DCE instead of DMF	2.5 mM	4	1:0.7	40%

^aReaction conditions: **8** (0.1 mmol), K₂HPO₄ (0.12 mmol), catalyst (x mol %), solvent (4 mL), irradiation with 34 W blue LEDs for 60 h. ^bRatio of **11/12** was determined by ¹H NMR analysis. ^cIsolated yields. ^dN.D., not detected.

tion reactions and decomposition of the diene moiety, which is unstable and very sensitive to acidic and basic conditions [106].

As shown in Figure 3 and anticipated above, our proposed mechanism begins with visible-light irradiation of the photoredox catalyst [Ir(dF(CF₃)ppy)₂(dtbpy)]PF₆ to access the excited state *[Ir(dF(CF₃)ppy)₂(dtbpy)]PF₆, which can trigger SET oxidation of **8**. Rapid decarboxylation leads to α-amino

radical **V** (and the reduced photocatalyst), which is intercepted by the pendant double bond to forge the desired six-membered ring through a key C–C bond formation while furnishing secondary radical **VI** and the undesired seven-membered-ring compound **VII**. Closure of the photoredox catalytic cycle would then involve either SET reduction of the radical **VI** and **VII** (which upon protonation would deliver the desired product **11** and the undesired product **12**), or an hydrogen-atom-transfer

**Figure 3:** Proposed reaction mechanism for photoredox-catalyzed radical decarboxylative cyclization.

(HAT) process (which would not place a formal negative charge onto the molecule), where the hydrogen atom required for this possible final HAT step originates from the solvent (DMF) itself [107]. Therefore, we tested the reaction in *N,N*-dimethylformamide-*d*₇ (DMF-*d*₇), which showed almost quantitative deuterium incorporation. While this result was surprising, further studies into this complex mechanism are ongoing and will be reported in due course.

The synthetic potential and utility of this method was further demonstrated by the formal total synthesis of (±)-6,7-secoagroclavine (Scheme 4) [108–114]. Towards this end, compound **11** was methylated efficiently and selectively at the secondary amide by treatment with methyl iodide in DMF to afford compound **13**. In additional two steps, intermediate **13** was transformed to (±)-6,7-secoagroclavine in enantiopure form, as reported previously by the Bisai group in 2018 [115]. All the spectroscopic data of **13** were in agreement with those reported in the literature, confirming that the radical addition reaction provided the *trans* amino group due to steric hindrance.

Conclusion

In summary, this work illustrates, once more, the synthetic potential of an Ir-polypyridyl complex as a photoredox catalyst that can efficiently convert visible light into chemical energy. In addition, this catalyst was applied to demonstrate the proposed radical mechanism involved in the biosynthetic formation of the central C ring of several DMAT derivatives. The results presented here lend strong credence to decarboxylation and cyclization to form the six-membered ring as well as the nature of the stable oxidized intermediates concerned. Moreover, unprecedented and functionalized 3,4-fused tricyclic indoles with medium-sized rings (seven and eight), which have been largely neglected in previous studies, can be synthesized by this new protocol. Notably, the reaction has been successfully applied in the formal synthesis of (±)-6,7-secoagroclavine, a key intermediate for a common synthetic route to ergot alkaloids, providing an advantageous synthetic method for this class of natural products. Further studies on the utility of the

decarboxylative radical cyclization and their applications are currently being investigated in our laboratory.

Supporting Information

Supporting Information File 1

Experimental and copies of spectra.

[<https://www.beilstein-journals.org/bjoc/content/supplementary/1860-5397-19-70-S1.pdf>]

Acknowledgements

The authors thank Dott. Michele Retini for helpful discussion. We also thank Dott. Vittorio Ciccone, an undergraduate student in the Piersanti group, for preliminary exploratory studies. Prof. Michele Menotta and Federica Biancucci for assistance with HRMS analysis.

Funding

This work was supported by the Italian Ministry for University and Research (MUR, PRIN 2020, 2020AEX4TA project) and University of Urbino grants (DISB_PERSANTI_PROG_SIC_ALIMENTARE).

ORCID® iDs

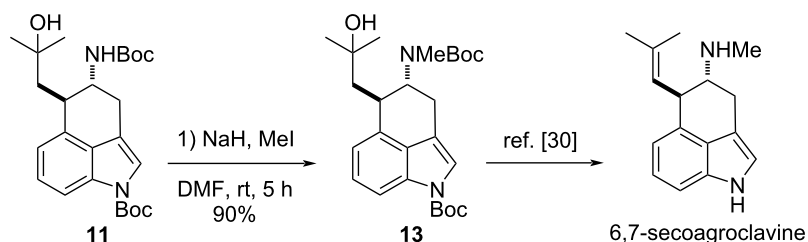
Alessio Regni - <https://orcid.org/0000-0002-2188-1789>

Francesca Bartocchini - <https://orcid.org/0000-0003-0400-7771>

Giovanni Piersanti - <https://orcid.org/0000-0003-0418-7143>

References

- Nicewicz, D. A.; MacMillan, D. W. C. *Science* **2008**, *322*, 77–80. doi:10.1126/science.1161976
- Ischay, M. A.; Anzovino, M. E.; Du, J.; Yoon, T. P. *J. Am. Chem. Soc.* **2008**, *130*, 12886–12887. doi:10.1021/ja805387f
- Narayanam, J. M. R.; Tucker, J. W.; Stephenson, C. R. J. *J. Am. Chem. Soc.* **2009**, *131*, 8756–8757. doi:10.1021/ja9033582
- Narayanam, J. M. R.; Stephenson, C. R. J. *Chem. Soc. Rev.* **2011**, *40*, 102–113. doi:10.1039/b913880n
- Xuan, J.; Xiao, W.-J. *Angew. Chem., Int. Ed.* **2012**, *51*, 6828–6838. doi:10.1002/anie.201200223



Scheme 4: Methylation of **11** and the formal total synthesis of (±)-6,7-secoagroclavine.

6. Prier, C. K.; Rankic, D. A.; MacMillan, D. W. C. *Chem. Rev.* **2013**, *113*, 5322–5363. doi:10.1021/cr300503r
7. Schultz, D. M.; Yoon, T. P. *Science* **2014**, *343*, 1239176. doi:10.1126/science.1239176
8. Ravelli, D.; Protti, S.; Fagnoni, M. *Chem. Rev.* **2016**, *116*, 9850–9913. doi:10.1021/acs.chemrev.5b00662
9. Shaw, M. H.; Twilton, J.; MacMillan, D. W. C. *J. Org. Chem.* **2016**, *81*, 6898–6926. doi:10.1021/acs.joc.6b01449
10. Tellis, J. C.; Kelly, C. B.; Primer, D. N.; Jouffroy, M.; Patel, N. R.; Molander, G. A. *Acc. Chem. Res.* **2016**, *49*, 1429–1439. doi:10.1021/acs.accounts.6b00214
11. Marzo, L.; Pagire, S. K.; Reiser, O.; König, B. *Angew. Chem., Int. Ed.* **2018**, *57*, 10034–10072. doi:10.1002/anie.201709766
12. McAtee, R. C.; McClain, E. J.; Stephenson, C. R. J. *Trends Chem.* **2019**, *1*, 111–125. doi:10.1016/j.trechm.2019.01.008
13. Zhu, C.; Yue, H.; Chu, L.; Rueping, M. *Chem. Sci.* **2020**, *11*, 4051–4064. doi:10.1039/d0sc00712a
14. Stephenson, C.; Yoon, T.; MacMillan, D. W. C. *Visible Light Photocatalysis in Organic Chemistry*; Wiley-VCH: Weinheim, Germany, 2018. doi:10.1002/9783527674145
15. König, B., Ed. *Chemical Photocatalysis*, 2nd ed.; De Gruyter: Berlin, Germany, 2020. doi:10.1515/9783110576764
16. Yoon, T. P.; Ischay, M. A.; Du, J. *Nat. Chem.* **2010**, *2*, 527–532. doi:10.1038/nchem.687
17. Oelgemöller, M. *Chem. Rev.* **2016**, *116*, 9664–9682. doi:10.1021/acs.chemrev.5b00720
18. Cambié, D.; Bottecchia, C.; Straathof, N. J. W.; Hessel, V.; Noël, T. *Chem. Rev.* **2016**, *116*, 10276–10341. doi:10.1021/acs.chemrev.5b00707
19. Zhou, L.; Lokman Hossain, M.; Xiao, T. *Chem. Rec.* **2016**, *16*, 319–334. doi:10.1002/tcr.201500228
20. Crisenza, G. E. M.; Melchiorre, P. *Nat. Commun.* **2020**, *11*, 803. doi:10.1038/s41467-019-13887-8
21. Romero, N. A.; Nicewicz, D. A. *Chem. Rev.* **2016**, *116*, 10075–10166. doi:10.1021/acs.chemrev.6b00057
22. Capaldo, L.; Ravelli, D.; Fagnoni, M. *Chem. Rev.* **2022**, *122*, 1875–1924. doi:10.1021/acs.chemrev.1c00263
23. Cao, H.; Tang, X.; Tang, H.; Yuan, Y.; Wu, J. *Chem Catal.* **2021**, *1*, 523–598. doi:10.1016/j.jcatal.2021.04.008
24. Bell, J. D.; Murphy, J. A. *Chem. Soc. Rev.* **2021**, *50*, 9540–9685. doi:10.1039/d1cs00311a
25. Buzzetti, L.; Crisenza, G. E. M.; Melchiorre, P. *Angew. Chem., Int. Ed.* **2019**, *58*, 3730–3747. doi:10.1002/anie.201809984
26. Arias-Rotondo, D. M.; McCusker, J. K. *Chem. Soc. Rev.* **2016**, *45*, 5803–5820. doi:10.1039/c6cs00526h
27. Ciamician, G. *Science* **1912**, *36*, 385–394. doi:10.1126/science.36.926.385
28. Klán, P.; Wirz, J. *Photochemistry of Organic Compounds: From Concepts to Practice*; John Wiley & Sons: Chichester, UK, 2009. doi:10.1002/9781444300017
29. Hu, A.; Guo, J.-J.; Pan, H.; Zuo, Z. *Science* **2018**, *361*, 668–672. doi:10.1126/science.aat9750
30. Laudadio, G.; Deng, Y.; van der Wal, K.; Ravelli, D.; Nuño, M.; Fagnoni, M.; Guthrie, D.; Sun, Y.; Noël, T. *Science* **2020**, *369*, 92–96. doi:10.1126/science.abb4688
31. Nicholls, T. P.; Leonori, D.; Bissember, A. C. *Nat. Prod. Rep.* **2016**, *33*, 1248–1254. doi:10.1039/c6np00070c
32. Liu, X.-Y.; Qin, Y. *Acc. Chem. Res.* **2019**, *52*, 1877–1891. doi:10.1021/acs.accounts.9b00246
33. Pitre, S. P.; Overman, L. E. *Chem. Rev.* **2022**, *122*, 1717–1751. doi:10.1021/acs.chemrev.1c00247
34. Lechner, V. M.; Nappi, M.; Deneny, P. J.; Folliet, S.; Chu, J. C. K.; Gaunt, M. J. *Chem. Rev.* **2022**, *122*, 1752–1829. doi:10.1021/acs.chemrev.1c00357
35. Capaldo, L.; Quadri, L. L.; Ravelli, D. *Green Chem.* **2020**, *22*, 3376–3396. doi:10.1039/d0gc01035a
36. Douglas, J. J.; Sevrin, M. J.; Stephenson, C. R. J. *Org. Process Res. Dev.* **2016**, *20*, 1134–1147. doi:10.1021/acs.oprd.6b00125
37. Li, P.; Terrett, J. A.; Zbieg, J. R. *ACS Med. Chem. Lett.* **2020**, *11*, 2120–2130. doi:10.1021/acsmmedchemlett.0c00436
38. Candish, L.; Collins, K. D.; Cook, G. C.; Douglas, J. J.; Gómez-Suárez, A.; Jolít, A.; Keess, S. *Chem. Rev.* **2022**, *122*, 2907–2980. doi:10.1021/acs.chemrev.1c00416
39. Nguyen, S. T.; Murray, P. R. D.; Knowles, R. R. *ACS Catal.* **2020**, *10*, 800–805. doi:10.1021/acscatal.9b04813
40. Zhang, J. *ChemSusChem* **2018**, *11*, 3071–3080. doi:10.1002/cssc.201801370
41. Scott, E.; Peter, F.; Sanders, J. *Appl. Microbiol. Biotechnol.* **2007**, *75*, 751–762. doi:10.1007/s00253-007-0932-x
42. Liu, J.-Q.; Shatskiy, A.; Matsuura, B. S.; Kärkäs, M. D. *Synthesis* **2019**, *51*, 2759–2791. doi:10.1055/s-0037-1611852
43. Bottecchia, C.; Noël, T. *Chem. – Eur. J.* **2019**, *25*, 26–42. doi:10.1002/chem.201803074
44. Aguilar Troyano, F. J.; Merckens, K.; Anwar, K.; Gómez-Suárez, A. *Angew. Chem., Int. Ed.* **2021**, *60*, 1098–1115. doi:10.1002/anie.202010157
45. King, T. A.; Mandrup Kandemir, J.; Walsh, S. J.; Spring, D. R. *Chem. Soc. Rev.* **2021**, *50*, 39–57. doi:10.1039/d0cs00344a
46. Zuo, Z.; MacMillan, D. W. C. *J. Am. Chem. Soc.* **2014**, *136*, 5257–5260. doi:10.1021/ja501621q
47. Schwarz, J.; König, B. *Green Chem.* **2016**, *18*, 4743–4749. doi:10.1039/c6gc01101b
48. Liao, L.-L.; Cao, G.-M.; Jiang, Y.-X.; Jin, X.-H.; Hu, X.-L.; Churma, J. J.; Sun, G.-Q.; Gui, Y.-Y.; Yu, D.-G. *J. Am. Chem. Soc.* **2021**, *143*, 2812–2821. doi:10.1021/jacs.0c11896
49. Li, Y.; Dai, C.; Xie, S.; Liu, P.; Sun, P. *Org. Lett.* **2021**, *23*, 5906–5910. doi:10.1021/acs.orglett.1c02014
50. Xuan, J.; Zhang, Z.-G.; Xiao, W.-J. *Angew. Chem., Int. Ed.* **2015**, *54*, 15632–15641. doi:10.1002/anie.201505731
51. Rahman, M.; Mukherjee, A.; Kovalev, I. S.; Kopchuk, D. S.; Zyryanov, G. V.; Tsurkan, M. V.; Majee, A.; Ranu, B. C.; Charushin, V. N.; Chupakhin, O. N.; Santra, S. *Adv. Synth. Catal.* **2019**, *361*, 2161–2214. doi:10.1002/adsc.201801331
52. Schmittel, M.; Burghart, A. *Angew. Chem., Int. Ed. Engl.* **1997**, *36*, 2550–2589. doi:10.1002/anie.199725501
53. Roth, H. G.; Romero, N. A.; Nicewicz, D. A. *Synlett* **2016**, *27*, 714–723. doi:10.1055/s-0035-1561297
54. Yu, Y.; Zhang, L.-K.; Buevich, A. V.; Li, G.; Tang, H.; Vachal, P.; Colletti, S. L.; Shi, Z.-C. *J. Am. Chem. Soc.* **2018**, *140*, 6797–6800. doi:10.1021/jacs.8b03973
55. Laroche, B.; Tang, X.; Archer, G.; Di Sanza, R.; Melchiorre, P. *Org. Lett.* **2021**, *23*, 285–289. doi:10.1021/acs.orglett.0c03735
56. Rahimidashghoul, K.; Klimánková, I.; Hubálek, M.; Matoušek, V.; Filgas, J.; Slaviček, P.; Slanina, T.; Beier, P. *ChemPhotoChem* **2021**, *5*, 43–50. doi:10.1002/cptc.202000214
57. Lima, R. N.; Delgado, J. A. C.; Bernardi, D. I.; Berlink, R. G. S.; Kaplaneris, N.; Ackermann, L.; Paixão, M. W. *Chem. Commun.* **2021**, *57*, 5758–5761. doi:10.1039/d1cc01822a

58. Weng, Y.; Ding, B.; Liu, Y.; Song, C.; Chan, L.-Y.; Chiang, C.-W. *Org. Lett.* **2021**, *23*, 2710–2714. doi:10.1021/acs.orglett.1c00609
59. Hoopes, C. R.; Garcia, F. J.; Sarkar, A. M.; Kuehl, N. J.; Barkan, D. T.; Collins, N. L.; Meister, G. E.; Bramhall, T. R.; Hsu, C.-H.; Jones, M. D.; Schirle, M.; Taylor, M. T. *J. Am. Chem. Soc.* **2022**, *144*, 6227–6236. doi:10.1021/jacs.1c10536
60. Bartoccini, F.; Regni, A.; Retini, M.; Piersanti, G. *Eur. J. Org. Chem.* **2022**, e202200315. doi:10.1002/ejoc.202200315
61. Bartoccini, F.; Regni, A.; Retini, M.; Piersanti, G. *Org. Biomol. Chem.* **2021**, *19*, 2932–2940. doi:10.1039/d1ob00353d
62. Bartoccini, F.; Fanini, F.; Retini, M.; Piersanti, G. *Tetrahedron Lett.* **2020**, *61*, 151923. doi:10.1016/j.tetlet.2020.151923
63. Bartoccini, F.; Venturi, S.; Retini, M.; Mari, M.; Piersanti, G. *J. Org. Chem.* **2019**, *84*, 8027–8034. doi:10.1021/acs.joc.9b00879
64. Bartoccini, F.; Bartolucci, S.; Mari, M.; Piersanti, G. *Org. Biomol. Chem.* **2016**, *14*, 10095–10100. doi:10.1039/c6ob01791f
65. Bartoccini, F.; Casoli, M.; Mari, M.; Piersanti, G. *J. Org. Chem.* **2014**, *79*, 3255–3259. doi:10.1021/jo500245s
66. Lucarini, S.; Bartoccini, F.; Battistoni, F.; Diamantini, G.; Piersanti, G.; Righi, M.; Spadoni, G. *Org. Lett.* **2010**, *12*, 3844–3847. doi:10.1021/ol101527j
67. Bartoccini, F.; Piersanti, G. *Synthesis* **2021**, *53*, 1396–1408. doi:10.1055/a-1340-3423
68. Tasker, N. R.; Wipf, P. Biosynthesis, Total Synthesis, and Biological Profiles of Ergot Alkaloids. *The Alkaloids: Chemistry and Biology*; Academic Press: Cambridge, MA, USA, 2021; Vol. 85, pp 1–112. doi:10.1016/bs.alkal.2020.08.001
69. Liu, H.; Jia, Y. *Nat. Prod. Rep.* **2017**, *34*, 411–432. doi:10.1039/c6np00110f
70. McCabe, S. R.; Wipf, P. *Org. Biomol. Chem.* **2016**, *14*, 5894–5913. doi:10.1039/c6ob00878j
71. Jakubczyk, D.; Cheng, J. Z.; O'Connor, S. E. *Nat. Prod. Rep.* **2014**, *31*, 1328–1338. doi:10.1039/c4np00062e
72. Yao, Y.; An, C.; Evans, D.; Liu, W.; Wang, W.; Wei, G.; Ding, N.; Houk, K. N.; Gao, S.-S. *J. Am. Chem. Soc.* **2019**, *141*, 17517–17521. doi:10.1021/jacs.9b10217
73. Ma, Y.; Yan, J.; Yang, L.; Yao, Y.; Wang, L.; Gao, S.-S.; Cui, C. *Front. Bioeng. Biotechnol.* **2022**, *10*, 1095464. doi:10.3389/fbioe.2022.1095464
And references cited therein.
74. Lowry, M. S.; Goldsmith, J. I.; Slinker, J. D.; Rohl, R.; Pascal, R. A.; Malliaras, G. G.; Bernhard, S. *Chem. Mater.* **2005**, *17*, 5712–5719. doi:10.1021/cm051312+
75. Walden, S. E.; Wheeler, R. A. *J. Phys. Chem.* **1996**, *100*, 1530–1535. doi:10.1021/jp951838p
76. Ge, Y.; Wang, H.; Wang, H.-N.; Yu, S.-S.; Yang, R.; Chen, X.; Zhao, Q.; Chen, G. *Org. Lett.* **2021**, *23*, 370–375. doi:10.1021/acs.orglett.0c03867
77. Yang, J.; Zhang, J.; Qi, L.; Hu, C.; Chen, Y. *Chem. Commun.* **2015**, *51*, 5275–5278. doi:10.1039/c4cc06344a
78. Jin, Y.; Jiang, M.; Wang, H.; Fu, H. *Sci. Rep.* **2016**, *6*, 20068. doi:10.1038/srep20068
79. Cheng, W.-M.; Shang, R.; Fu, Y. *ACS Catal.* **2017**, *7*, 907–911. doi:10.1021/acscatal.6b03215
80. Cheng, W.-M.; Shang, R.; Fu, M.-C.; Fu, Y. *Chem. – Eur. J.* **2017**, *23*, 2537–2541. doi:10.1002/chem.201605640
81. Liu, X.; Liu, Y.; Chai, G.; Qiao, B.; Zhao, X.; Jiang, Z. *Org. Lett.* **2018**, *20*, 6298–6301. doi:10.1021/acs.orglett.8b02791
82. Proctor, R. S. J.; Davis, H. J.; Phipps, R. J. *Science* **2018**, *360*, 419–422. doi:10.1126/science.aar6376
83. Xiao, Z.; Wang, L.; Wei, J.; Ran, C.; Liang, S. H.; Shang, J.; Chen, G.-Y.; Zheng, C. *Chem. Commun.* **2020**, *56*, 4164–4167. doi:10.1039/d0cc00451k
84. He, S.; Li, H.; Chen, X.; Krylov, I. B.; Terent'ev, A. O.; Qu, L.; Yu, B. *Chin. J. Org. Chem.* **2021**, *41*, 4661–4689. doi:10.6023/cjoc202105041
85. Dong, W.; Yen-Pon, E.; Li, L.; Bhattacharjee, A.; Jolit, A.; Molander, G. A. *Nat. Chem.* **2022**, *14*, 1068–1077. doi:10.1038/s41557-022-00979-0
86. Yue, H.; Zhu, C.; Huang, L.; Dewanjji, A.; Rueping, M. *Chem. Commun.* **2022**, *58*, 171–184. doi:10.1039/d1cc06285a
87. Nemoto, T.; Harada, S.; Nakajima, M. *Asian J. Org. Chem.* **2018**, *7*, 1730–1742. doi:10.1002/ajoc.201800336
88. Yuan, K.; Jia, Y. *Chin. J. Org. Chem.* **2018**, *38*, 2386–2399. doi:10.6023/cjoc201705058
89. Connon, R.; Guiry, P. J. *Tetrahedron Lett.* **2020**, *61*, 151696. doi:10.1016/j.tetlet.2020.151696
90. Kozikowski, A. P.; Chen, C.; Wu, J. P.; Shibuya, M.; Kim, C. G.; Floss, H. G. *J. Am. Chem. Soc.* **1993**, *115*, 2482–2488. doi:10.1021/ja00059a051
91. Wong, G.; Lim, L. R.; Tan, Y. Q.; Go, M. K.; Bell, D. J.; Freemont, P. S.; Yew, W. S. *Nat. Commun.* **2022**, *13*, 712. doi:10.1038/s41467-022-28386-6
92. Jasperse, C. P.; Curran, D. P.; Fevig, T. L. *Chem. Rev.* **1991**, *91*, 1237–1286. doi:10.1021/cr00006a006
93. Chu, L.; Ohta, C.; Zuo, Z.; MacMillan, D. W. C. *J. Am. Chem. Soc.* **2014**, *136*, 10886–10889. doi:10.1021/ja505964r
94. Noble, A.; McCarver, S. J.; MacMillan, D. W. C. *J. Am. Chem. Soc.* **2015**, *137*, 624–627. doi:10.1021/ja511913h
95. Xiao, T.; Li, L.; Zhou, L. *J. Org. Chem.* **2016**, *81*, 7908–7916. doi:10.1021/acs.joc.6b01620
96. Ernouf, G.; Chirkin, E.; Rhyman, L.; Ramasami, P.; Cintrat, J.-C. *Angew. Chem., Int. Ed.* **2020**, *59*, 2618–2622. doi:10.1002/anie.201908951
97. Li, J.-T.; Luo, J.-N.; Wang, J.-L.; Wang, D.-K.; Yu, Y.-Z.; Zhuo, C.-X. *Nat. Commun.* **2022**, *13*, 1778. doi:10.1038/s41467-022-29464-5
98. It should be mentioned that racemization was found in products **11** and **12** from the chiral intermediate **V**, which is common in this radical coupling reaction. See reference [76].
99. McCarver, S. J.; Qiao, J. X.; Carpenter, J.; Borzilleri, R. M.; Poss, M. A.; Eastgate, M. D.; Miller, M. M.; MacMillan, D. W. C. *Angew. Chem., Int. Ed.* **2017**, *56*, 728–732. doi:10.1002/anie.201608207
100. Blackwell, J. H.; Harris, G. R.; Smith, M. A.; Gaunt, M. J. *J. Am. Chem. Soc.* **2021**, *143*, 15946–15959. doi:10.1021/jacs.1c07402
101. Lovett, G. H.; Sparling, B. A. *Org. Lett.* **2016**, *18*, 3494–3497. doi:10.1021/acs.orglett.6b01712
102. Renaud, P.; Sibi, M. P., Eds. *Radicals in Organic Synthesis*; Wiley-VCH: Weinheim, Germany, 2001; Vol. 1 and 2. doi:10.1002/9783527618293
103. Zard, S. Z. *Radicals Reactions in Organic Synthesis*; Oxford University Press: Oxford, UK, 2003.
104. Beckwith, A. L. J.; Crich, D.; Duggan, P. J.; Yao, Q. *Chem. Rev.* **1997**, *97*, 3273–3312. doi:10.1021/cr950207o
105. Crich, D.; Brebion, F.; Suk, D.-H. *Top. Curr. Chem.* **2006**, *263*, 1–38. doi:10.1007/128_024
106. Hurlley, A. E.; Lu, Z.; Yoon, T. P. *Angew. Chem., Int. Ed.* **2014**, *53*, 8991–8994. doi:10.1002/anie.201405359

107. Capaldo, L.; Ravelli, D. *Eur. J. Org. Chem.* **2017**, 2056–2071. doi:10.1002/ejoc.201601485
108. Yamada, F.; Makita, Y.; Somei, M. *Heterocycles* **2007**, 72, 599–620. doi:10.3987/com-06-s(k)55
109. Somei, M.; Yamada, F.; Ohnishi, H.; Makita, Y.; Kuriki, M. *Heterocycles* **1987**, 26, 2823–2828. doi:10.3987/r-1987-11-2823
110. Somei, M.; Ohnishi, H.; Shoken, Y. *Chem. Pharm. Bull.* **1986**, 34, 677–681. doi:10.1248/cpb.34.677
111. Oppolzer, W.; Grayson, J. I.; Wegmann, H.; Urrea, M. *Tetrahedron* **1983**, 39, 3695–3705. doi:10.1016/s0040-4020(01)88608-7
112. Somei, M.; Tsuchiya, M. *Chem. Pharm. Bull.* **1981**, 29, 3145–3157. doi:10.1248/cpb.29.3145
113. Somei, M.; Yamada, F.; Karasawa, Y.; Kaneko, C. *Chem. Lett.* **1981**, 10, 615–618. doi:10.1246/cl.1981.615
114. Natsume, M.; Muratake, H. *Heterocycles* **1980**, 14, 1101–1105. doi:10.3987/r-1980-08-1101
115. Chaudhuri, S.; Bhunia, S.; Roy, A.; Das, M. K.; Bisai, A. *Org. Lett.* **2018**, 20, 288–291. doi:10.1021/acs.orglett.7b03683

License and Terms

This is an open access article licensed under the terms of the Beilstein-Institut Open Access License Agreement (<https://www.beilstein-journals.org/bjoc/terms>), which is identical to the Creative Commons Attribution 4.0 International License (<https://creativecommons.org/licenses/by/4.0>). The reuse of material under this license requires that the author(s), source and license are credited. Third-party material in this article could be subject to other licenses (typically indicated in the credit line), and in this case, users are required to obtain permission from the license holder to reuse the material.

The definitive version of this article is the electronic one which can be found at:
<https://doi.org/10.3762/bjoc.19.70>



Radical ligand transfer: a general strategy for radical functionalization

David T. Nemoto Jr, Kang-Jie Bian, Shih-Chieh Kao and Julian G. West*

Perspective

Open Access

Address:
Department of Chemistry, Rice University, 6100 Main St MS 602,
Houston, TX 77005, USA

Email:
Julian G. West* - jgwest@rice.edu

* Corresponding author

Keywords:
catalysis; cooperative catalysis; earth abundant elements;
photocatalysis; radicals

Beilstein J. Org. Chem. **2023**, *19*, 1225–1233.
<https://doi.org/10.3762/bjoc.19.90>

Received: 22 June 2023
Accepted: 04 August 2023
Published: 15 August 2023

This article is part of the thematic issue "Modern radical chemistry".

Guest Editor: H.-M. Huang



© 2023 Nemoto et al.; licensee Beilstein-Institut.
License and terms: see end of document.

Abstract

The place of alkyl radicals in organic chemistry has changed markedly over the last several decades, evolving from challenging-to-generate “uncontrollable” species prone to side reactions to versatile reactive intermediates enabling construction of myriad C–C and C–X bonds. This maturation of free radical chemistry has been enabled by several advances, including the proliferation of efficient radical generation methods, such as hydrogen atom transfer (HAT), alkene addition, and decarboxylation. At least as important has been innovation in radical functionalization methods, including radical–polar crossover (RPC), enabling these intermediates to be engaged in productive and efficient bond-forming steps. However, direct engagement of alkyl radicals remains challenging. Among these functionalization approaches, a bio-inspired mechanistic paradigm known as radical ligand transfer (RLT) has emerged as a particularly promising and versatile means of forming new bonds catalytically to alkyl radicals. This development has been driven by several key features of RLT catalysis, including the ability to form diverse bonds (including C–X, C–N, and C–S), the use of simple earth abundant element catalysts, and the intrinsic compatibility of this approach with varied radical generation methods, including HAT, radical addition, and decarboxylation. Here, we provide an overview of the evolution of RLT catalysis from initial studies to recent advances and provide a conceptual framework we hope will inspire and enable future work using this versatile elementary step.

Introduction

The behavior of alkyl radicals has been studied rigorously for decades, though only recently have these come to be widely viewed as selective and useful synthetic intermediates [1–4]. This sea change has been driven by innovations in both the generation and functionalization of alkyl radicals, with successful

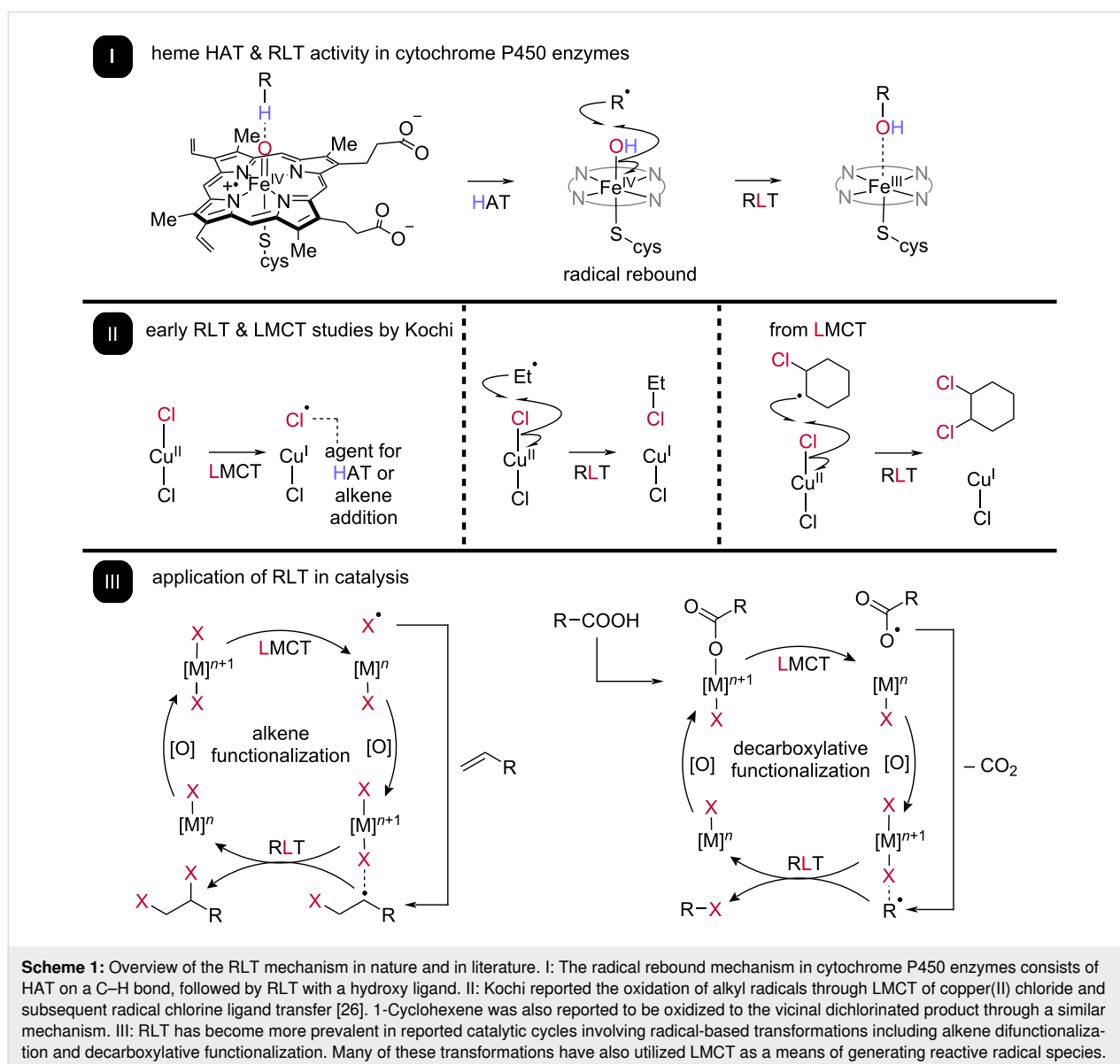
synthetic reactions requiring efficiency and selectivity in both of these processes and inherent compatibility between each. Radical generation has benefitted from many general mechanistic approaches, including hydrogen atom transfer (HAT) [5], alkene addition [6], and decarboxylation [7], enabling these

intermediates to be easily accessed from diverse starting materials. Functionalization methods have also seen significant development, with elementary steps such as radical–polar crossover (RPC) finding significant purchase [8]; however, these steps are not amenable to all radical generation approaches/substrate classes nor can they form all desired bonds from alkyl radical intermediates, limiting the toolkit of radical reactions.

Recently, radical ligand transfer (RLT) [9–11] has emerged as a radical functionalization paradigm with the potential to overcome the challenges faced by other strategies (Scheme 1). At its core, RLT involves the outer sphere transfer of an anionic, X-type ligand coordinated to a redox-active metal to a radical intermediate, resulting in formation of a new C–ligand bond with concomitant single electron reduction of the metal center.

Subsequent reoxidation of the metal with coordination of a new equivalent of anionic ligand allows for the RLT complex to be regenerated, making this strategy inherently compatible with catalysis.

Building on this, one of the most important examples of catalytic RLT can be found in the human body's own cytochrome P450 enzymes. These catalysts exhibit unique “radical rebound” reactivity at their heme active sites (Scheme 1) [12], a mechanism proposed by Groves and co-workers and heavily explored beginning in the 1970s [13,14]. This two-step functionalization sequence begins with HAT from an alkyl C–H bond to a high valent iron oxo species, resulting in formation of iron hydroxo and alkyl radical intermediates [15]. Subsequent RLT of the hydroxo ligand to the alkyl radical produces a hydroxylated

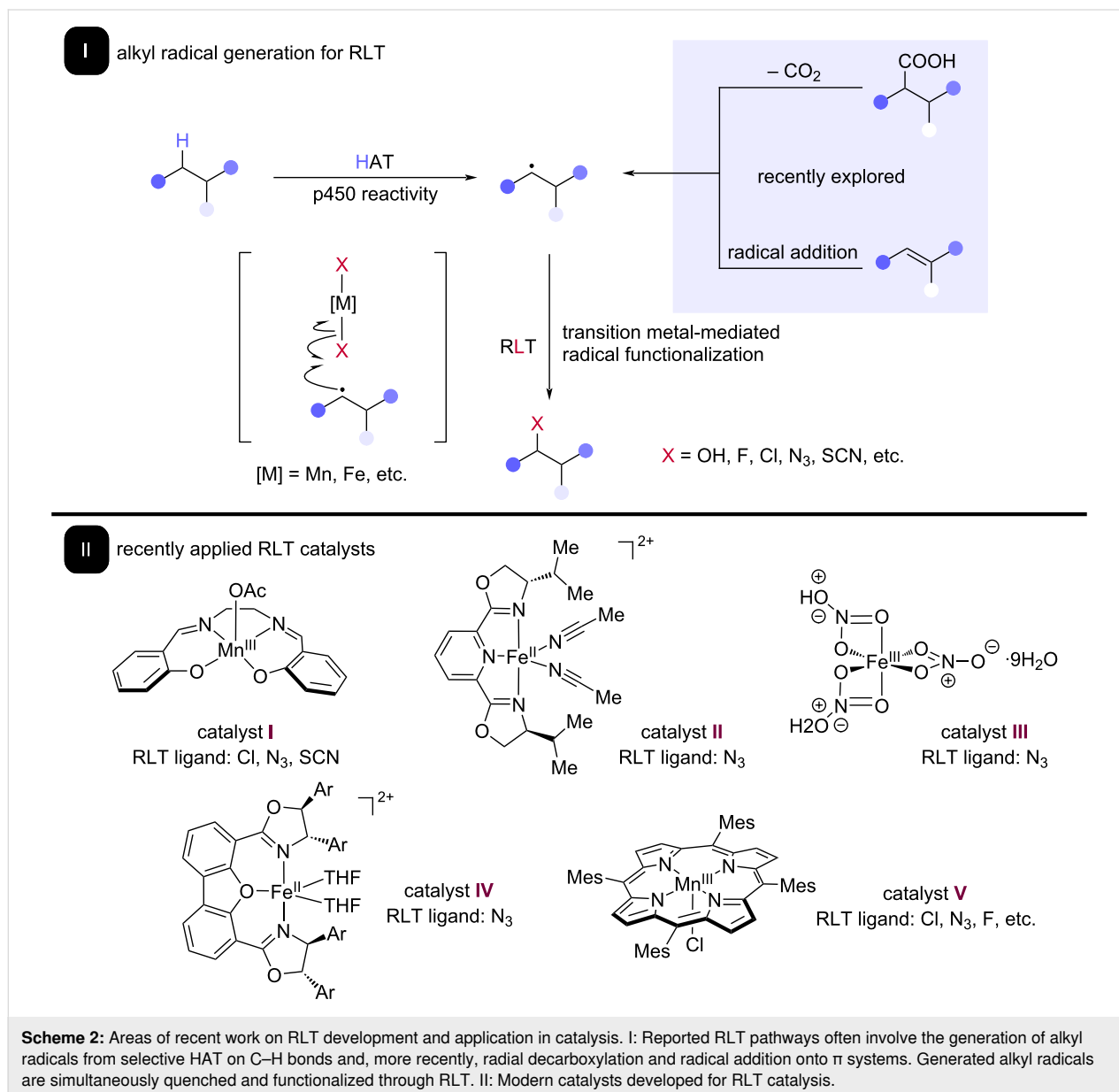


product, allowing for metabolism and excretion of previously diverse bioactive compounds. Similar RLT “rebound” steps have been implicated in non-heme oxygenase and halogenase enzymes as well [16–19], hinting that this strategy might be general; however, enzymatic examples outside of hydroxo and halide ligand transfer are scarce.

Groves’ initial discovery of the radical rebound behavior of P450 oxygenases encouraged early work on site-selective C–H functionalization [20]. Throughout their studies, it was found that manganese could perform the same HAT and RLT steps as iron at heme active sites. Groves developed the manganese tetramesitylporphine catalyst **V** (Scheme 2), which was found to be capable of functionalizing specific C–H bonds to numerous

functionalities, including C–F [21,22], C–N₃ [23], and C–Cl bonds [24,25]. Upon these remarkable observations, methodologies involving manganese–porphyrin catalysts have been developed over the years. These methods take advantage of the power of RLT to install a variety of medically relevant groups, largely mirroring the selectivity of CYP450s. Intriguingly, studies by Groves have revealed earth abundant iron and manganese to be particularly privileged for this application of RLT, a major advantage for sustainable method development.

Outside of bioinorganic chemistry, the concept of radical ligand transfer was investigated in early work by Jay Kochi in purely synthetic systems (Scheme 1) [26,27]. Studies on the oxidation of alkyl radicals with earth abundant cupric salts uncovered the



ability of simple Cu(II) chloride to form new C–Cl bonds in the presence of transient alkyl radicals, with mechanistic studies implicating homolytic abstraction of a chlorine ligand from the intermediate copper complex. Outside of the substitution products which could be generated from the RLT pathway, alkyl radicals could also undergo an elimination-like pathway to afford unsaturated C=C bonds in the presence of copper(II) sulfate, presumably via competitive RPC to the carbocation followed by E₁ olefination.

Kochi also demonstrated that RLT can be combined with other radical generation strategies to enable new, non-biomimetic reactions to be achieved (Scheme 1), showing that photolysis of stoichiometric Cu(II) chloride in the presence of unactivated alkenes allows for direct formation of vicinal dichloride products. The mechanistic study implicated initial formation of a chlorine radical through homolysis of a Cu–Cl bond via ligand-to-metal charge transfer (LMCT) which, following cage escape, could add to the alkene to generate an alkyl radical. This alkyl radical could then be chlorinated via RLT from a second Cu(II) chloride species, furnishing the dichlorinated product. While copper was unable to be used catalytically in this early report, it augured the potential of RLT to be a general strategy in synthetic method development, with modern examples including new alkene addition reactions and decarboxylative functionalizations (Scheme 2).

Recent applications of RLT in catalysis

Upon the discovery and initial exploration of the RLT paradigm by Groves and Kochi, many groups have adopted and characterized new ways of using RLT to form valuable carbon–heteroatom bonds from a diverse pool of simple starting materials. RLT has been especially present in modern catalysis, where complexes of earth abundant iron and manganese have been demonstrated to be particularly privileged in delivery of various ligands to alkyl radicals (Scheme 2). These developments have been supported by discovery of the compatibility of RLT with many different reaction paradigms leading to alkyl radical intermediates under catalytic conditions, including radical addition to alkenes and radical decarboxylation, with many of these being driven by light energy.

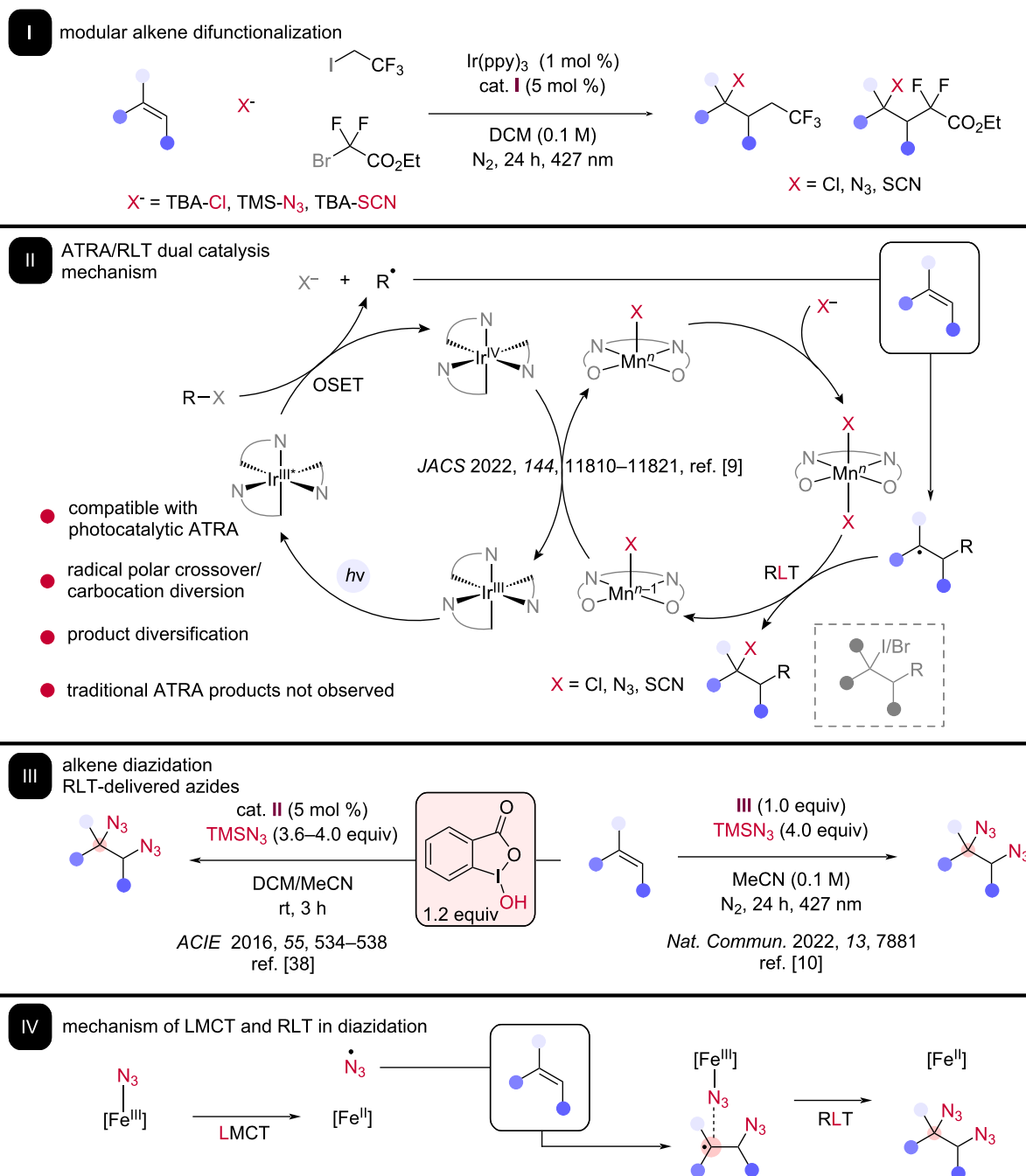
RLT in alkene functionalization

Outside of the realm of C–H activation, RLT has been leveraged to afford complex medicinal scaffolds in alkene difunctionalization. A recent example can be found in the merger of RLT with photoredox-catalyzed atom transfer radical addition (ATRA) (Scheme 3). ATRA results in the net addition of a C–X bond across an alkene, forming both valuable C–C and C–X bonds in a single reaction. While ATRA-type reactions were first reported in the 1940s by Kharasch [28], interest in the area

was revitalized the early 2010s with the advent of Stephenson's photoredox catalytic methods which dramatically simplified reaction conditions [29,30], driving ongoing interest in this mechanistic approach [31].

Our group recently devised a dual catalytic method which combines the RLT paradigm with photocatalytic ATRA to enable the modular difunctionalization of alkenes under reagent control (Scheme 3). In Stephenson's photocatalytic ATRA reports, the C–X bond in the product was proposed to be formed through both direct quenching of a transient alkyl radical by halogen atom transfer (XAT) from the alkyl halide reagent and further oxidation of the transient radical to a carbocation by radical polar crossover (RPC), providing two mechanistic pathways to form the ATRA products [32]. While powerful, this approach is inherently incompatible with introducing alternative functionality instead of the halide included in the alkyl halide reagent, limiting the ability to form different difunctionalization products. Taking inspiration from Groves' bio-inspired manganese tetradentate manganese catalysts, we found we could instead functionalize the transient alkyl radical via RLT from a simplified manganese salen complex **I**, allowing for the identity of the carbon–heteroatom bond to be controlled based on added nucleophile and enabling C–Cl, C–N, and C–S bonds to be formed directly while completely suppressing traditional ATRA products [9]. In mechanistic studies, rearrangement products indicative of a carbocationic pathway are not observed, suggesting that RPC does not occur. Further, the inability of ATRA products to undergo S_N2 with the added nucleophiles under our reaction conditions is inconsistent with a tandem ATRA/nucleophilic displacement alternative mechanism. Finally, a functionalization via the canonical organometallic steps of oxidative addition/reductive elimination was ruled out via catalytic reaction of the macrocyclic Groves-type porphyrin catalyst **V**, a species that is unable to accommodate the mutual cis-orientation of ligands for metal-centered reductive elimination. The system was found to be compatible with unactivated alkenes bearing a wide range of functionalities, including more-substituted alkenes, and a wide range of alkyl halide reagents, permitting a library of difunctionalized products to be prepared from a single alkene.

RLT can also be used to deliver valuable homodifunctionalized products using unactivated alkenes. Vicinal diazides (and to a lesser extent dihalides) have been popular targets for modern method development. Both photochemical [33] and electrochemical [34–36] methods have been effective in delivering products containing these molecular motifs. Intriguingly, several recent alkene diazidation methods have made RLT a key design criterion, with both thermal and photochemical driving forces [37].



Scheme 3: The incorporation of RLT catalysis in ATRA photocatalysis. I: The reported method is compatible with nucleophilic sources of chlorine groups, azide groups, and thioisocyanate groups. II: The proposed mechanism for the dual catalytic ATRA-RLT cycle. III: Our lab and Xu reported photochemical diazidation of alkenes carried out using iron and trimethylsilyl azide. IV: The proposed mechanism for photoinduced LMCT between iron and azide ligands as well as RLT on azidoalkyl radical intermediates.

Recent interest in alkene diazidation was accelerated by a 2016 report from Xu detailing alkene diazidation using low loadings of a molecular iron catalyst **II** and stoichiometric hydroxyiodine as a terminal oxidant [38]. It is proposed that an azidoiodine is generated in situ and serves as the radical initiator, generating an azido radical which adds to the less substituted

position on the alkene. The resultant transient radical is captured via RLT from an in-situ generated iron–azide complex, resulting in net reduction of iron. The competent RLT species can then be regenerated through oxidation by the iodine species and coordination of another equivalent of azide. This reaction was particularly notable for the wide alkene

scope, including terminal aliphatic alkenes, internal (cyclic) styrenes, and one example of a nonconjugated diene, suggesting RLT to be compatible with many functionalities. The diastereoselectivity of the reaction varies, with high anti-selectivity being achieved with cyclic styrenes and low diastereoselectivity in linear internal alkenes.

Building on this key iron catalysis result, our group and that of Shi contemporaneously reported the photochemical diazidation of alkenes using stoichiometric iron and no external oxidant or ancillary ligand, providing a simple protocol for the preparation of vicinal diamines with excellent functional group compatibility (Scheme 3) [10,39]. In both reports, it is proposed that photoinduced LMCT of an in-situ generated Fe(III) azide species furnishes an azido radical, compatible with unactivated alkene addition. These steps provide the reactive carbon-centered radical intermediate. RLT to this radical from another azide ligand leads to a diazidated product. The overall scope of both reports suggests that the diazidation of simple to complex drugs/natural product-derived alkene substrates is readily achievable, including highly substituted and cyclic aliphatic alkenes. Further, we demonstrated that diazidation could be rendered catalytic using Fe(III) nitrate hydrate **III** as the iron source and performing the reaction under continuous flow conditions. Interestingly, this mechanism bears some similarity to Lin's electrocatalytic diazidation, where azido radical generation is proposed via thermal homolysis of a Mn(III) azide species and RLT from a second equivalent of Mn(III) azide furnishes the desired organic diazide, providing a strong demonstration of the applicability of RLT to not only photochemical but electrochemical conditions as well [35].

RLT in decarboxylative functionalization

Aside from its strategic application in alkene difunctionalization methods, RLT has also found synthetic utility in radical decarboxylative reactions. Radical decarboxylative functionalization reactions to form C–X bonds have been demonstrated, with bond construction being proposed to follow one of two pathways: formation of a carbocation through RPC followed by nucleophilic attack or direct RLT from a redox-active metal complex.

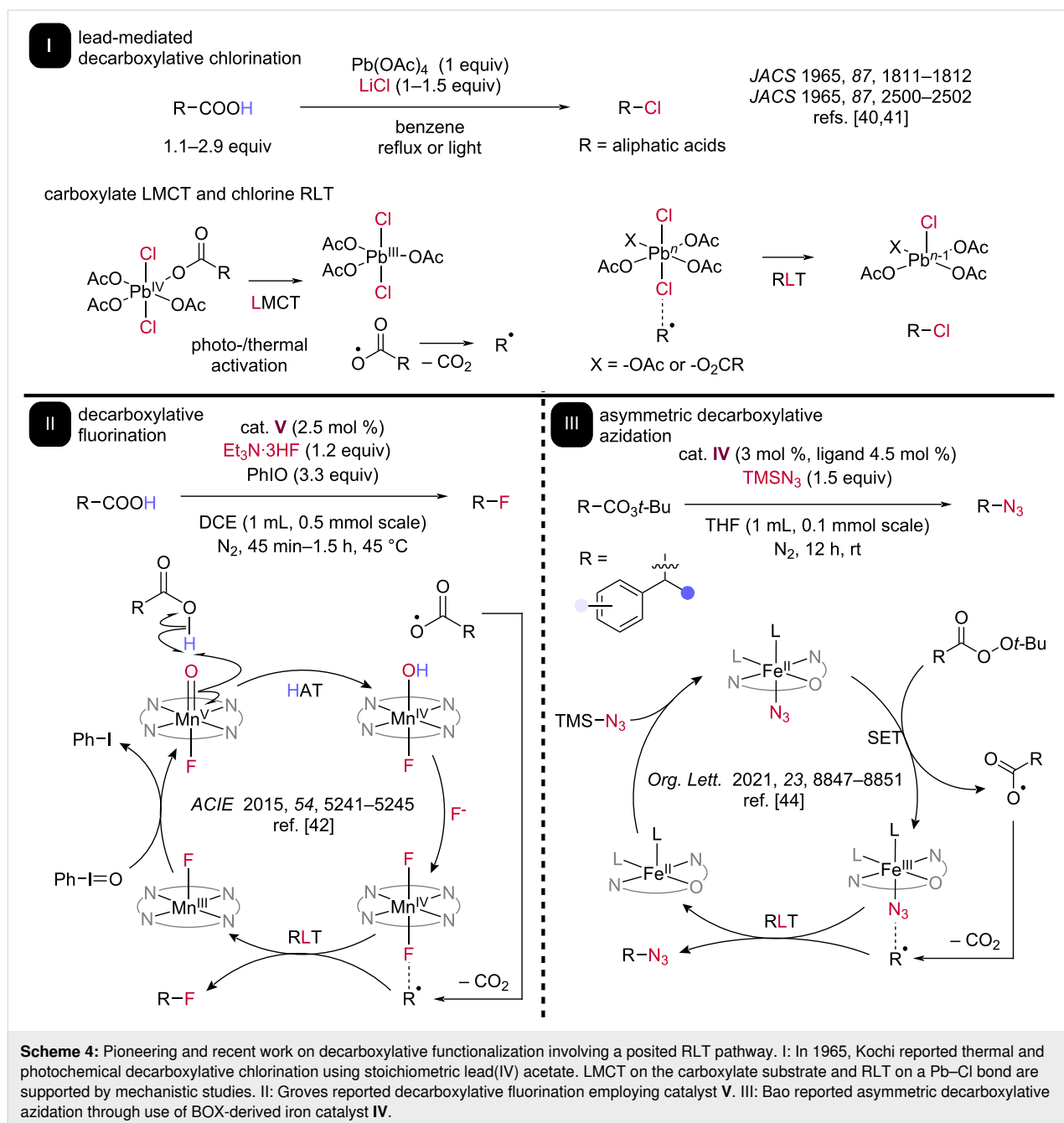
Preliminary evidence for a radical decarboxylation/RLT cascade was reported in 1965, when Kochi demonstrated decarboxylative chlorination of various acids with lead(IV) tetraacetate in the presence of lithium chloride (Scheme 4) [40,41]. Nucleophilic lithium chloride was used as the chlorine atom source for this transformation. In the representative scope of this transformation, primary and secondary chlorides could be formed in relatively high yields from their respective acids, a result incompatible with a carbocation RPC mechanism. This

Kochi decarboxylative chlorination separated itself from other pioneering methods of decarboxylative functionalization (i.e., Barton and Hunsdiecker) because of its inclusion of RLT as a key element of the mechanism.

In 2015, the Groves group reported their manganese porphyrin-based catalyst **V** and related species being capable of participating in decarboxylation reactions (Scheme 4) [42]. The activated Mn(V) species is proposed to perform HAT carboxylic acid O–H bond, directly forming a carboxyl radical and Mn(IV) species which can exchange its hydroxo ligand for a fluoride from triethylamine tris(hydrofluoride) (Scheme 4). Rapid decarboxylation of this intermediate produces the alkyl radical species which could be fluorinated via RLT from the Mn(IV)–F complex, generating a Mn(III) intermediate. To close the cycle and reform the oxo ligand on the Mn(V) species, a stoichiometric amount of iodosylbenzene is used in the reaction.

While initial development of this reaction focused on incorporating the stable ^{19}F , subsequent study expanded the scope to RLT of the unstable ^{18}F radioisotope, an important medical radioisotope used for positron emission tomography (PET) [43]. Optimized conditions of both isotopes included fast reaction times of under two hours; in the case of the ^{18}F radioisotope, reactions were carried out in 10 minutes and resulted in moderate to high yields, demonstrating the potential of RLT reactions to be rapid and efficient. In both cases, benzylic carboxylic acids were most amenable as substrates, with alkyl carboxylic acids such as adamantane and dicyclohexylmethane providing fluorinated aliphatic products in low to moderate yields.

Asymmetric RLT catalysis has also been of recent interest, with exciting preliminary decarboxylative azidation results obtained under thermal conditions by Hongli Bao and co-workers [44]. An asymmetric iron (NON) pincer catalyst **IV** was employed to decarboxylate benzylic peroxyesters and form enantiomerically enriched benzylic azides. An Fe(II/III) cycle is proposed, where a single electron transfer from Fe(II) reduces the peroxyester and produces a carboxyl radical and Fe(III), which can coordinate an azide ligand. Rapid decarboxylation produces the transient alkyl radical which can be asymmetrically azidated by RLT from an Fe(III) azide complex, reducing the iron catalyst back to the starting Fe(II) state. Organic azides can be formed in moderate to high enantioselectivity using this approach; however, the scope is largely limited to benzylic products, a result in line with Groves' finding that benzylic acid substrates perform much more efficiently in decarboxylative RLT reactions than aliphatic acids [42]. Outside of decarboxylation, X. Peter Zhang recently reported the enantioselective synthesis of allylic amines through coupled HAT and RLT on allylic C–H bonds [45],

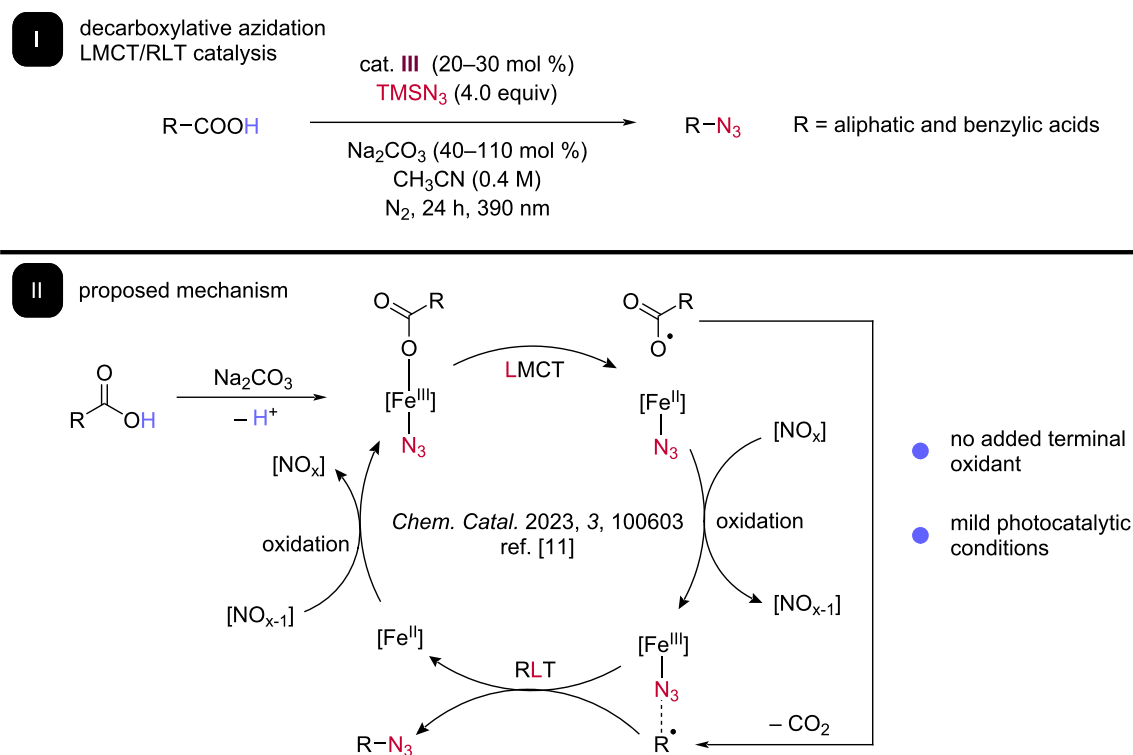


using a bulky cobalt porphyrin complex developed and utilized to perform both HAT and RLT. While many challenges remain for achieving general asymmetric induction in RLT catalysis, this advance represents an important step toward this aspirational goal with many lessons to build upon.

Our group has recently leveraged iron photochemistry to build on these beautiful decarboxylative azidation examples, combining iron-mediated photodecarboxylation via LMCT and azide RLT (Scheme 5) [11]. Irradiating a substoichiometric amount of iron(III) nitrate hydrate **III** in the presence of carboxylic acid,

TMS azide, and sodium carbonate allows for direct synthesis of alkyl azides for a wide range of both activated (benzylic) and unactivated carboxylic acids. Control reactions support the intermediacy of alkyl radicals and the absence of carbocation rearrangements in a variety of probe substrates disfavor the reaction proceeding via RPC.

Intriguingly, no additional oxidant is required for this process, implicating the nitrate counterion functioning as an internal oxidant to regenerate the active Fe(III) species capable of LMCT and RLT. This result is consistent with our finding that



Scheme 5: Our lab reported decarboxylative azidation of aliphatic and benzylic acids. I: The reaction proceeds via LMCT and RLT catalysis without the addition of terminal oxidant. II: The proposed mechanism includes reoxidation of the iron catalyst through inner-sphere electron transfer by anionic nitrate.

iron nitrate can catalytically diazidate alkenes in flow with no additional oxidant and literature examples of nitrate oxidation of different transition metals, such as palladium. Control reactions further supported this proposal, including the inability of alternative Fe(III) salts (e.g., FeCl_3) to form more than stoichiometric azide product in the absence of added nitrate. We believe this adventitious discovery of nitrate functioning as a mild and selective oxidant in RLT catalytic systems presents many opportunities for future method development and are avidly pursuing this area of research.

Outlook

After scant exploration following its elucidation in early mechanistic studies of bioinorganic and synthetic systems, radical ligand transfer (RLT) has reemerged as a powerful tool in the design of catalytic radical reactions. This development has been fueled by the unique aspects of RLT, with its ability to functionalize radicals with diverse nucleophilic reagents and inherent compatibility with different elementary steps, including hydrogen atom transfer (HAT) and ligand-to-metal charge transfer (LMCT), enabling new transformations to be unlocked with unprecedented modularity. Further, the privileged position of earth abundant elements such as iron and manganese in RLT has made reactions using this step appealing from a sustain-

ability standpoint. While exciting progress has been made, many opportunities remain using this mechanistic approach. Two key areas that could yield exciting advances are combining RLT with new radical-generating elementary steps and the further development of asymmetric RLT processes. We hope that this perspective provides a useful framework for understanding RLT reactivity and inspires new advances using this versatile and intriguing elementary step.

Funding

J.G.W. acknowledges financial support from CPRIT (RR190025), NIH NIGMS (R35GM142738), Research Corporation for Science Advancement (CS-CSA-2023-007), and the Welch Foundation (C-2085).

ORCID® iDs

David T. Nemoto Jr - <https://orcid.org/0000-0002-8596-6909>

Julian G. West - <https://orcid.org/0000-0002-3715-7883>

References

- Yan, M.; Kawamata, Y.; Baran, P. S. *Chem. Rev.* **2017**, *117*, 13230–13319. doi:10.1021/acs.chemrev.7b00397
- Yan, M.; Lo, J. C.; Edwards, J. T.; Baran, P. S. *J. Am. Chem. Soc.* **2016**, *138*, 12692–12714. doi:10.1021/jacs.6b08856

3. Crespi, S.; Fagnoni, M. *Chem. Rev.* **2020**, *120*, 9790–9833. doi:10.1021/acs.chemrev.0c00278
4. Corcé, V.; Ollivier, C.; Fensterbank, L. *Chem. Soc. Rev.* **2022**, *51*, 1470–1510. doi:10.1039/d1cs01084k
5. Capaldo, L.; Ravelli, D.; Fagnoni, M. *Chem. Rev.* **2022**, *122*, 1875–1924. doi:10.1021/acs.chemrev.1c00263
6. Yao, H.; Hu, W.; Zhang, W. *Molecules* **2021**, *26*, 105. doi:10.3390/molecules26010105
7. Chen, H.; Liu, Y. A.; Liao, X. *Synthesis* **2021**, *53*, 1–29. doi:10.1055/s-0040-1707273
8. Sharma, S.; Singh, J.; Sharma, A. *Adv. Synth. Catal.* **2021**, *363*, 3146–3169. doi:10.1002/adsc.202100205
9. Bian, K.-J.; Nemoto, D., Jr.; Kao, S.-C.; He, Y.; Li, Y.; Wang, X.-S.; West, J. G. *J. Am. Chem. Soc.* **2022**, *144*, 11810–11821. doi:10.1021/jacs.2c04188
10. Bian, K.-J.; Kao, S.-C.; Nemoto, D., Jr.; Chen, X.-W.; West, J. G. *Nat. Commun.* **2022**, *13*, 7881. doi:10.1038/s41467-022-35560-3
11. Kao, S.-C.; Bian, K.-J.; Chen, X.-W.; Chen, Y.; Martí, A. A.; West, J. G. *Chem Catal.* **2023**, *3*, 100603. doi:10.1016/j.cheecat.2023.100603
12. Meunier, B.; de Visser, S. P.; Shaik, S. *Chem. Rev.* **2004**, *104*, 3947–3980. doi:10.1021/cr020443g
13. Groves, J. T.; Van Der Puy, M. *J. Am. Chem. Soc.* **1976**, *98*, 5290–5297. doi:10.1021/ja00433a039
14. Groves, J. T.; McClusky, G. A. *J. Am. Chem. Soc.* **1976**, *98*, 859–861. doi:10.1021/ja00419a049
15. Groves, J. T. *Nat. Chem.* **2014**, *6*, 89–91. doi:10.1038/nchem.1855
16. Krebs, C.; Galonić Fujimori, D.; Walsh, C. T.; Bollinger, J. M., Jr. *Acc. Chem. Res.* **2007**, *40*, 484–492. doi:10.1021/ar700066p
17. Vaillancourt, F. H.; Yeh, E.; Vosburg, D. A.; Garneau-Tsodikova, S.; Walsh, C. T. *Chem. Rev.* **2006**, *106*, 3364–3378. doi:10.1021/cr050313i
18. Kojima, T.; Leising, R. A.; Yan, S.; Que, L., Jr. *J. Am. Chem. Soc.* **1993**, *115*, 11328–11335. doi:10.1021/ja00077a035
19. Costas, M.; Mehn, M. P.; Jensen, M. P.; Que, L. *Chem. Rev.* **2004**, *104*, 939–986. doi:10.1021/cr020628n
20. Huang, X.; Groves, J. T. *J. Biol. Inorg. Chem.* **2017**, *22*, 185–207. doi:10.1007/s00775-016-1414-3
21. Liu, W.; Huang, X.; Cheng, M.-J.; Nielsen, R. J.; Goddard, W. A., III; Groves, J. T. *Science* **2012**, *337*, 1322–1325. doi:10.1126/science.1222327
22. Liu, W.; Huang, X.; Placzek, M. S.; Krska, S. W.; McQuade, P.; Hooker, J. M.; Groves, J. T. *Chem. Sci.* **2018**, *9*, 1168–1172. doi:10.1039/c7sc04545j
23. Huang, X.; Bergsten, T. M.; Groves, J. T. *J. Am. Chem. Soc.* **2015**, *137*, 5300–5303. doi:10.1021/jacs.5b01983
24. Liu, W.; Groves, J. T. *J. Am. Chem. Soc.* **2010**, *132*, 12847–12849. doi:10.1021/ja105548x
25. Liu, W.; Groves, J. T. *Acc. Chem. Res.* **2015**, *48*, 1727–1735. doi:10.1021/acs.accounts.5b00062
26. Kochi, J. K. *J. Am. Chem. Soc.* **1962**, *84*, 2121–2127. doi:10.1021/ja00870a025
27. Kochi, J. K. *Science* **1967**, *155*, 415–424. doi:10.1126/science.155.3761.415
28. Kharasch, M. S.; Jensen, E. V.; Urry, W. H. *Science* **1945**, *102*, 128. doi:10.1126/science.102.2640.128.a
29. Nguyen, J. D.; Tucker, J. W.; Konieczynska, M. D.; Stephenson, C. R. J. *J. Am. Chem. Soc.* **2011**, *133*, 4160–4163. doi:10.1021/ja108560e
30. Wallentin, C.-J.; Nguyen, J. D.; Finkbeiner, P.; Stephenson, C. R. J. *J. Am. Chem. Soc.* **2012**, *134*, 8875–8884. doi:10.1021/ja300798k
31. Courant, T.; Masson, G. *J. Org. Chem.* **2016**, *81*, 6945–6952. doi:10.1021/acs.joc.6b01058
32. Williams, T. M.; Stephenson, C. R. J. Atom Transfer Radical Addition using Photoredox Catalysis. In *Visible Light Photocatalysis in Organic Chemistry*; Stephenson, C. R. J.; Yoon, T. P.; MacMillan, D. W. C., Eds.; Wiley-VCH: Weinheim, Germany, 2018; pp 73–92. doi:10.1002/9783527674145.ch3
33. Lian, P.; Long, W.; Li, J.; Zheng, Y.; Wan, X. *Angew. Chem., Int. Ed.* **2020**, *59*, 23603–23608. doi:10.1002/anie.202010801
34. Fu, N.; Sauer, G. S.; Lin, S. *J. Am. Chem. Soc.* **2017**, *139*, 15548–15553. doi:10.1021/jacs.7b09388
35. Fu, N.; Sauer, G. S.; Saha, A.; Loo, A.; Lin, S. *Science* **2017**, *357*, 575–579. doi:10.1126/science.aan6206
36. Dong, X.; Roeckl, J. L.; Waldvogel, S. R.; Morandi, B. *Science* **2021**, *371*, 507–514. doi:10.1126/science.abf2974
37. Ge, L.; Chiou, M.-F.; Li, Y.; Bao, H. *Green Synth. Catal.* **2020**, *1*, 86–120. doi:10.1016/j.gresc.2020.07.001
38. Yuan, Y.-A.; Lu, D.-F.; Chen, Y.-R.; Xu, H. *Angew. Chem., Int. Ed.* **2016**, *55*, 534–538. doi:10.1002/anie.201507550
39. Zhang, M.; Zhang, J.; Li, Q.; Shi, Y. *Nat. Commun.* **2022**, *13*, 7880. doi:10.1038/s41467-022-35344-9
40. Kochi, J. K. *J. Am. Chem. Soc.* **1965**, *87*, 2500–2502. doi:10.1021/ja01089a041
41. Kochi, J. K. *J. Am. Chem. Soc.* **1965**, *87*, 1811–1812. doi:10.1021/ja01086a046
42. Huang, X.; Liu, W.; Hooker, J. M.; Groves, J. T. *Angew. Chem., Int. Ed.* **2015**, *54*, 5241–5245. doi:10.1002/anie.201500399
43. Shields, A. F.; Grierson, J. R.; Dohmen, B. M.; Machulla, H.-J.; Stayanoff, J. C.; Lawhorn-Crews, J. M.; Obradovich, J. E.; Muzik, O.; Mangner, T. J. *Nat. Med.* **1998**, *4*, 1334–1336. doi:10.1038/3337
44. Wang, K.; Li, Y.; Li, X.; Li, D.; Bao, H. *Org. Lett.* **2021**, *23*, 8847–8851. doi:10.1021/acs.orglett.1c03355
45. Xu, P.; Xie, J.; Wang, D.-S.; Zhang, X. P. *Nat. Chem.* **2023**, *15*, 498–507. doi:10.1038/s41557-022-01119-4

License and Terms

This is an open access article licensed under the terms of the Beilstein-Institut Open Access License Agreement (<https://www.beilstein-journals.org/bjoc/terms>), which is identical to the Creative Commons Attribution 4.0 International License (<https://creativecommons.org/licenses/by/4.0>). The reuse of material under this license requires that the author(s), source and license are credited. Third-party material in this article could be subject to other licenses (typically indicated in the credit line), and in this case, users are required to obtain permission from the license holder to reuse the material.

The definitive version of this article is the electronic one which can be found at:
<https://doi.org/10.3762/bjoc.19.90>

α -(Aminomethyl)acrylates as acceptors in radical–polar crossover 1,4-additions of dialkylzincs: insights into enolate formation and trapping

Angel Palillero-Cisneros^{1,2}, Paola G. Gordillo-Guerra^{1,2,3}, Fernando García-Alvarez^{1,2}, Olivier Jackowski¹, Franck Ferreira¹, Fabrice Chemla¹, Joel L. Terán^{*2} and Alejandro Perez-Luna^{*1}

Full Research Paper

[Open Access](#)

Address:

¹Sorbonne Université, CNRS, Institut Parisien de Chimie Moléculaire, IPCM. 4 place Jussieu, 75005 Paris, France, ²Benemérita Universidad Autónoma de Puebla, Instituto de Ciencias, ICUAP, Edificio IC-9, Complejo de Ciencias, C.U., 72570, Puebla, México and ³(current address) Universidad Autónoma Metropolitana, Unidad Xochimilco, Departamento de Sistemas Biológicos, Ciudad de México, C.P., 04690, México

Email:

Joel L. Terán^{*} - joel.teran@correo.buap.mx; Alejandro Perez-Luna^{*} - alejandro.perez_luna@sorbonne-universite.fr

^{*} Corresponding author

Keywords:

β -amino acids; tandem reactions; radical–polar crossover; *tert*-butanesulfinamide; zinc radical transfer

Beilstein J. Org. Chem. **2023**, *19*, 1443–1451.

<https://doi.org/10.3762/bjoc.19.103>

Received: 27 July 2023

Accepted: 12 September 2023

Published: 21 September 2023

This article is part of the thematic issue "Modern radical chemistry".

Guest Editor: H.-M. Huang



© 2023 Palillero-Cisneros et al.; licensee Beilstein-Institut.

License and terms: see end of document.

Abstract

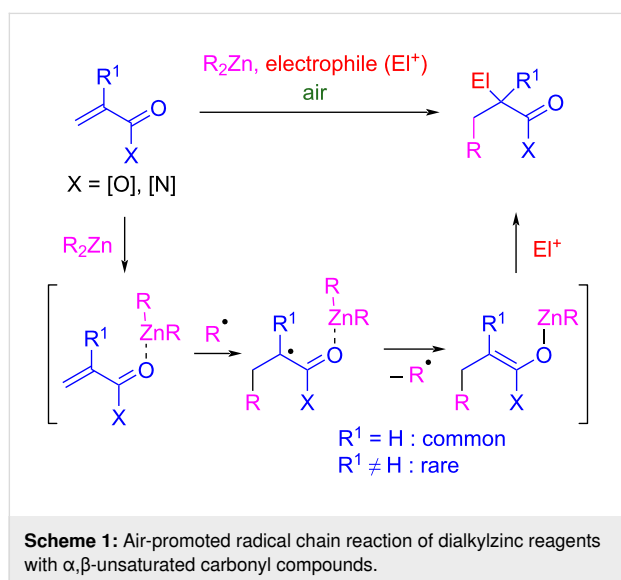
We demonstrate that α -(aminomethyl)acrylates are suitable acceptors for 1,4-additions of dialkylzincs in aerobic conditions. The air-promoted radical–polar crossover process involves the 1,4-addition of an alkyl radical followed by homolytic substitution at the zinc atom of dialkylzinc. Coordination of the nitrogen atom to zinc enables this S_H2 process which represents a rare example of alkylzinc-group transfer to a tertiary α -carbonyl radical. The zinc enolate thus formed readily undergoes β -fragmentation unless it is trapped by electrophiles in situ. Enolates of substrates having free N–H bonds undergo protodemetalation to provide ultimately the 1,4-addition adduct. In the presence of carbonyl acceptors, aldol condensation occurs providing overall a tandem 1,4-addition–aldol process. When a *tert*-butanesulfinyl moiety is present on the nitrogen atom, these electrophilic substitution reactions occur with good levels of chiral induction, paving the way to enantioenriched β^2 -amino acids and $\beta^{2,2}$ -amino acids.

Introduction

Dialkylzinc reagents react in aerobic medium with a range of α,β -unsaturated carbonyl compounds to provide the corresponding zinc enolates (Scheme 1) [1,2]. While simple, this reaction

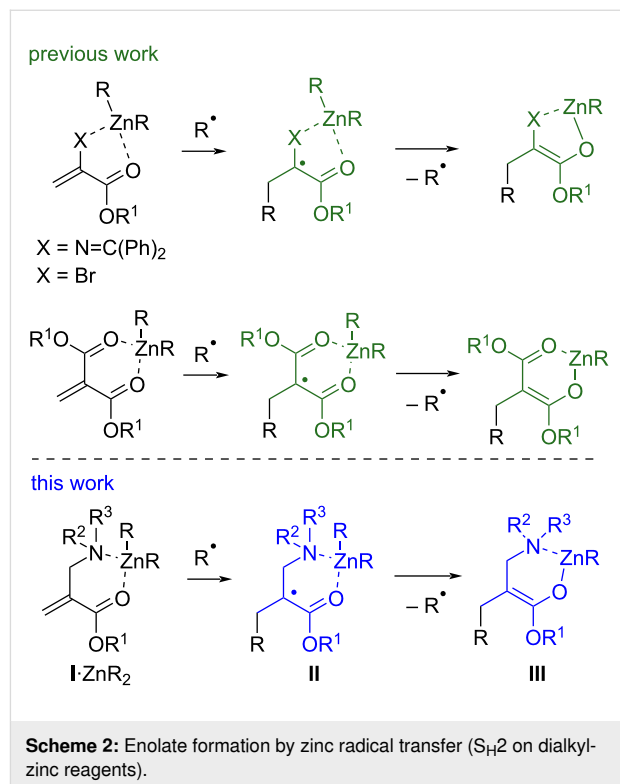
offers attractive features: 1) it proceeds under mild conditions in the absence of any transition-metal catalyst; 2) the 1,4-addition step can be combined with condensation reactions of the zinc

enolate with electrophiles in protocols wherein all the reactive partners can be introduced from the start, given that dialkylzinc reagents offer a large functional group tolerance; and 3) the radical character of the process allows for the use of alkyl iodides as alkyl source in multicomponent reactions. Trialkylboranes can react in a similar way with enones [3] whereas, distinctively, suitable acceptors for the reaction with dialkylzinc reagents also include α,β -unsaturated carboxylic acid derivatives such as α,β -unsaturated (di)esters [4,5], *N*-enoyloxazolidinones [6,7], *N*-enoyloxazolidines [8], or alkylidenemalonates [9–11]. These reactions follow a free-radical chain process wherein alkyl radicals (R^\bullet) add across the C–C double bond of the 1,4-acceptor, activated by complexation with the dialkylzinc, to deliver an enoxyl radical that undergoes homolytic substitution at zinc (S_H2) to produce a zinc enolate and a new R^\bullet that propagates the radical chain (Scheme 1). Initiation occurs upon oxidation of the dialkylzinc reagent by oxygen.



The feasibility of such 1,4-addition reactions is fully reliant on the ease of the intermediate enoxyl radical to undergo alkylzinc-group transfer. Secondary α -carbonyl radicals (Scheme 1, $R^1 = H$) undergo readily homolytic substitution. By contrast, tertiary α -carbonyl radicals (Scheme 1, $R^1 \neq H$) are less prone, making additions to α -substituted 1,4-acceptors more challenging. Typically, ethyl methacrylate does not react with dialkylzinc reagents [12]. Notwithstanding, 1,4-additions of dialkylzinc reagents have been reported with dehydroamino ester derivatives [13,14] and α -bromoacrylates [15], which both involve an S_H2 at zinc of tertiary α -alkoxycarbonyl radicals (Scheme 2, top). Here, the key to unlock the reactivity is the presence of a Lewis-basic substituent coordinated to the zinc atom: this offers a gain in enthalpy associated to the formation of zinc enolates stabilized by chelation and increases the spin

density delocalized at the oxygen atom involved in the chelate. Note that the reported 1,4-additions of dialkylzinc reagents to alkylidenemalonates could benefit from a similar effect, even though in this case, the direct formation of an intermediate enolate remains uncertain [11].



With this context in mind, we surmised that β -aminoenones **I** could be suitable 1,4-acceptors (Scheme 2, bottom). We previously reported tandem reactions of such substrates wherein the intermediate enoxyl radical **II** arising from the addition step evolves via intramolecular addition to tethered alkenes [16,17] or alkynes [18]. We wondered if, in the absence of the pending radical acceptor, the presence of the β -nitrogen atom could nevertheless promote zinc enolate formation. Trapping of this enolate would lead to β -amino acid units, a class of compounds that has attracted a great deal of attention [19–24]. An obvious possible shortcoming that had to be considered was still that the generated zinc enolate **III** having a β -amino group could undergo β -elimination, thereby precluding its synthetic exploitation.

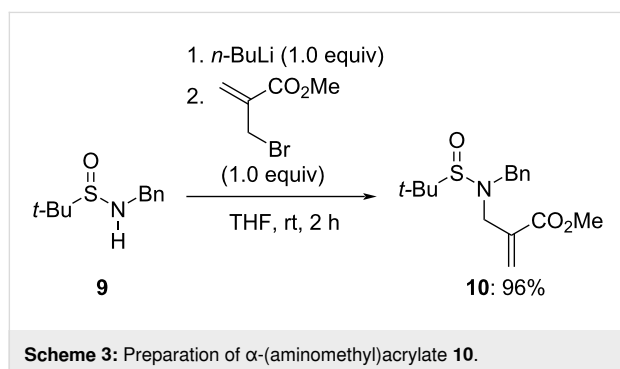
Results and Discussion

Preparation of α -(aminomethyl)acrylates

We commenced our study by preparing a selection of α -(aminomethyl)acrylates with variations of the nitrogen protecting group and the ester substituent. Towards this end, the direct allylation of primary amines **1–3** with methyl α -(bromo-

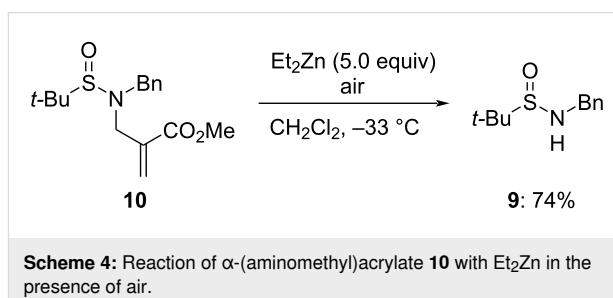
methyl)acrylate was contemplated first under several typical conditions that all afforded non-synthetically useful mixtures of mono- and diallylation, even if excess of the nitrogen nucleophiles was used. An alternative strategy was thus developed relying on the allylation of lithium (trimethylsilyl)amides prepared in situ from the parent amines by a lithiation/silylation/lithiation sequence (Table 1). Using this protocol, α -(aminomethyl)acrylates **5** and **6** derived from benzhydramine and aniline were prepared in high yields (Table 1, entries 1 and 2). The procedure was poorly efficient with tosylamine, leading to product **7** in low 20% yield [25].

With the aim to develop asymmetric variants, we also considered the synthesis of *N*-(*tert*-butanesulfinyl) α -(aminomethyl)acrylates **8a–c**. For this purpose, the application of the same protocol with (\pm)-*tert*-butanesulfinamide (**4**) and the requisite α -(bromomethyl)acrylates gave satisfactory yields as well. Finally, *N*-benzyl-*N*-(*tert*-butanesulfinyl) α -(aminomethyl)acrylate **10** was prepared by allylation of lithiated *N*-benzyl *tert*-butanesulfinamide **9** (Scheme 3).



1,4-Addition reactions

Having the requisite α -(aminomethyl)acrylates in hands, we carried out an initial survey of their reaction with Et_2Zn in CH_2Cl_2 at -33°C on addition of air. In these conditions, acrylate **10** led to the recovery (following aqueous work-up) of sulfinamide **9** without traces of formation of the 1,4-adduct (Scheme 4).



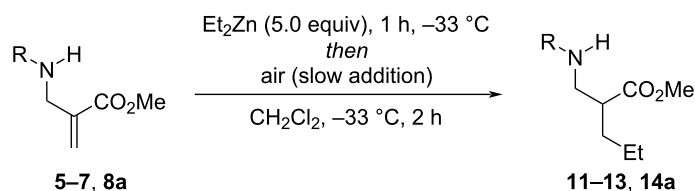
By contrast, 1,4-addition without subsequent fragmentation was observed starting from α -(aminomethyl)acrylates having free N–H bonds (Table 2). The reaction of Et_2Zn with acrylates **5–7** afforded the desired 1,4-addition products **11–13** in 42–55% yield. Better results were obtained starting from **8a**, which delivered adduct **14a** in 79% yield and 70:30 dr. We also noted that in the absence of deliberately added air, these reactions proceeded only with low conversion. For instance, starting from **8a**, product **14a** was obtained in only 25% yield along with $\approx 70\%$ of starting material recovery.

These results are relevant in the sense that not only they demonstrate that the oxygen-promoted 1,4-addition of α -(aminomethyl)acrylates with free N–H bonds is a productive process,

Table 1: Preparation of α -(aminomethyl)acrylates with free N–H bonds.

Entry	Substrate (R)	R ¹	Product	Yield ^a
1	1 (CH(Ph) ₂)	Me	5	81
2	2 (Ph)	Me	6	80
3	3 (Ts)	Me	7	20
4	4 (S(O) <i>t</i> -Bu)	Me	8a	69
5	4 (S(O) <i>t</i> -Bu)	<i>t</i> -Bu	8b	50
6	4 (S(O) <i>t</i> -Bu)	Bn	8c	36

^aIsolated yield.

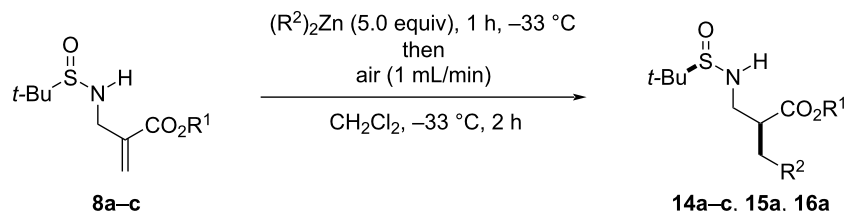
Table 2: Air-promoted 1,4-addition of Et₂Zn onto α-(aminomethyl)acrylates having free N–H bonds.^a

Entry	Substrate (R)	Product	Yield ^b	dr ^c
1	5 (CH(Ph) ₂)	11	42	
2	6 (Ph)	12	55	
3	7 (Ts)	13	55	
4	8a (S(O) <i>t</i> -Bu)	14a	76	70:30
5	8a (S(O) <i>t</i> -Bu)	14a	25 ^d	50:50

^aGeneral conditions: α-(aminomethyl)acrylate (0.2 mmol), Et₂Zn (1.0 mmol), CH₂Cl₂ (6 mL), air (20 mL introduced via syringe at 0.5 mL·min^{−1} rate).^bIsolated yield. ^cRatio of diastereomers measured by ¹H NMR spectroscopy prior to purification. ^dNo air was added.

but also that the *tert*-butanesulfinyl moiety is well tolerated and that 1,4-stereoselection can be achieved. Hence, in order to improve the levels of diastereoselectivity, we investigated further the reaction conditions starting with enoate **8a** as model substrate (Table 3).

Carrying out the reaction at −78 °C instead of −33 °C was deleterious both for the yield and the selectivity (Table 3, entry 2). By contrast, we rapidly learned that leaving diethylzinc in contact with the starting acrylate for 1 h prior to the addition of air had a significant impact on the stereoselectivity. When air was

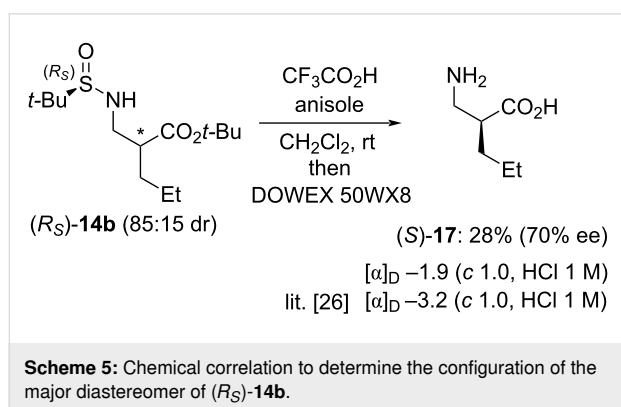
Table 3: Optimization of the air-promoted 1,4-addition of dialkylzinc reagents onto *N*-(*tert*-butanesulfinyl) α-(aminomethyl)acrylates.

Entry	Substrate (R ¹)	R ²	Product	Variation of conditions ^a	Yield ^b	dr ^{c,d}
1	8a (Me)	Et	14a	none	76	70:30
2	8a (Me)	Et	14a	−78 °C instead of −33 °C	60	57:43
3	8a (Me)	Et	14a	oxygen (5 mL) was added at once immediately after Et ₂ Zn	83	59:41
4	8a (Me)	Et	14a	toluene instead of CH ₂ Cl ₂	82	75:25
5	8a (Me)	Et	14a	hexane instead of CH ₂ Cl ₂	82	85:15
6	8b (<i>t</i> -Bu)	Et	14b	hexane instead of CH ₂ Cl ₂	88	85:15
7	8c (Bn)	Et	14c	none	76	70:30
8	8a (Me)	Bu	15a	none	71	67:33
9	8a (Me)	Me	16a	none	n.r. ^e	
10	8a (Me)	Me	16a	hexane instead of CH ₂ Cl ₂	n.r. ^e	

^aAll reactions were conducted at a 0.2 mmol scale using 20 mL of air. ^bIsolated yield (mixture of diastereoisomers). ^cMeasured by ¹H or ¹³C NMR spectroscopy prior to purification. ^dThe relative configuration of the major diastereomer is shown in the scheme; it was determined by chemical correlation for **14b** (see below) and inferred by analogy for **14a** and **14c**. ^eNo reaction.

introduced directly after Et_2Zn (Table 3, entry 3) a much lower 59:41 dr was observed. This behavior was suggestive of the need for coordination of diethylzinc both to the carbonyl and sulfinyl unit to achieve good levels of selectivity. Hence, to reinforce Lewis pair formation, the reaction was also carried out in apolar solvents such as toluene and hexane (entries 4 and 5 in Table 3). In hexane, an 88% yield with 85:15 dr was obtained, which constituted the best conditions. Importantly, the protocol was found to be similarly applicable with enoates **8b** (Table 3, entry 6) and **8c** (entry 7) having *tert*-butyl and benzyl ester groups, which, as the methyl ester unit, are typical in the context of amino acid synthesis. ZnBu_2 was also amenable to 1,4-addition (Table 3, entry 8), but not ZnMe_2 (entries 9 and 10). This difference can be ascribed to a less favorable homolytic substitution reaction of ZnMe_2 in relation to its higher analogues and is in line with previous literature observations [11].

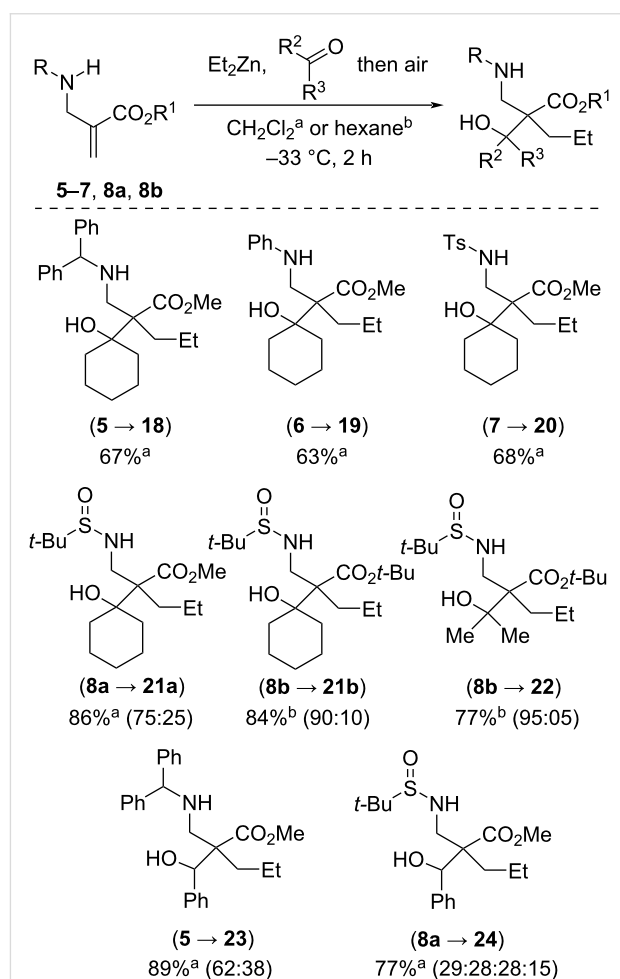
The configuration of the major diastereomer was determined by chemical correlation (Scheme 5). Product (*R_S*)-**14b** (85:15 dr), i.e., a mixture of two enantiomerically pure diastereomers, was obtained from (*R_S*)-*tert*-butylsulfinamide upon allylation with *tert*-butyl α -(bromomethyl)acrylate followed by 1,4-addition with Et_2Zn . It was then converted into the known β^2 -amino acid **17** by TFA-promoted concomitant deprotection of the nitrogen and the ester groups. The sample was found to have a negative optical rotation, thereby indicating that the major enantiomer present had *S* configuration [26]. This allowed to establish that the configuration of the major diastereomer present in (*R_S*)-**14b** was (*R_{S,S}*), and thus the sense of chiral induction for the 1,4-addition reactions reported in Table 2.



Tandem 1,4-addition–aldol condensation reactions

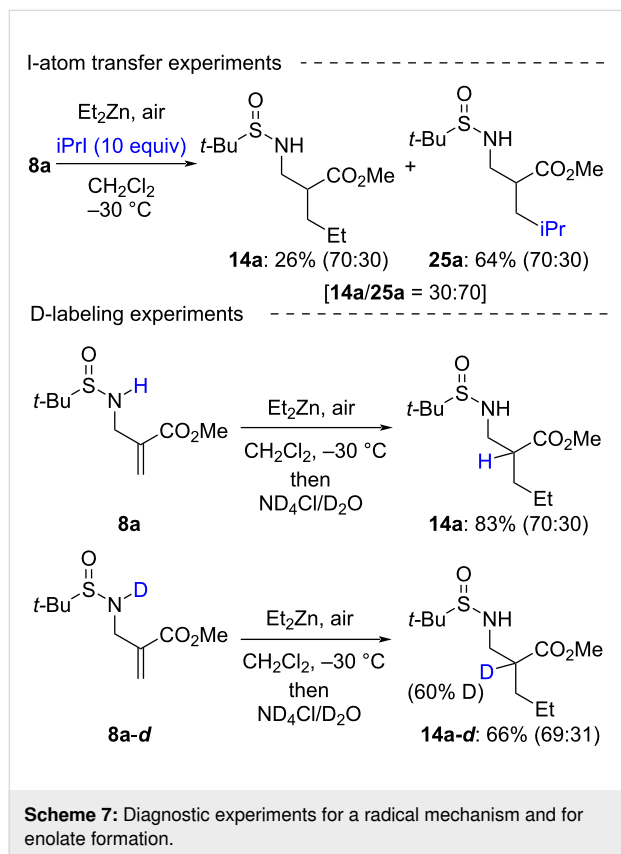
We then went on to consider tandem 1,4-addition–aldol condensation reactions (Scheme 6), which offer the interesting prospect of generating an all-carbon quaternary stereocenter. α -(Aminomethyl)acrylates **5–7** reacted smoothly at -33°C

within 2 h with Et_2Zn in the presence of cyclohexanone to afford amino alcohols **18–20** in quite good yields (63–68%). Even better yields were obtained with enoates **8a** and **8b** both with cyclohexanone and acetone as carbonyl partners. Starting from **8a** and carrying out the reaction in CH_2Cl_2 , product **21a** was obtained in 86% yield with 75:25 dr. Alike for the 1,4-addition protocol, better stereoselection was obtained by performing the reaction in hexane: **8b** was converted into **21b** and **22** in 77–84% yield with higher than 90:10 dr. It is also interesting to note that the levels of induction for the 1,4-addition–aldol condensations are somewhat higher than those obtained for the 1,4-additions. Aldehydes also proved competent terminal electrophiles for the tandem sequence. Illustratively, adducts **23** and **24** were obtained from α -(aminomethyl)acrylates **5** and **8a** in 77–88% yields, albeit as poorly selective mixtures of diastereoisomers. This lack of stereocontrol is not surprising, given the well-known difficulty to control the relative configuration between the two adjacent stereocenters created during aldol condensations with zinc enolates.



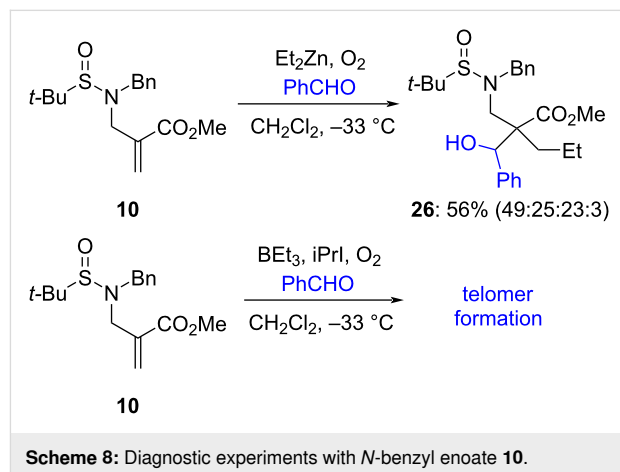
Mechanistic insights

The last part of our work was devoted to gain mechanistic insight for the developed reaction protocols through several diagnostic experiments. Regarding the 1,4-addition process, the lower reactivity noted in the absence of air (Table 2, entry 5) represents already a strong indication for a radical addition mechanism. This is further supported by the result of an I-atom transfer experiment (Scheme 7, top). In the presence of two equivalents of *i*PrI, the reaction of **8a** with Et₂Zn leads to a mixture of product **14a** and product **25a**, incorporating an *i*Pr moiety, in a **14a/25a** 30:70 mixture. Product **25a** is formed on addition of an *i*Pr radical generated by I-atom transfer from *i*PrI to the Et radical, and is diagnostic for the formation of the latter in the reaction medium.



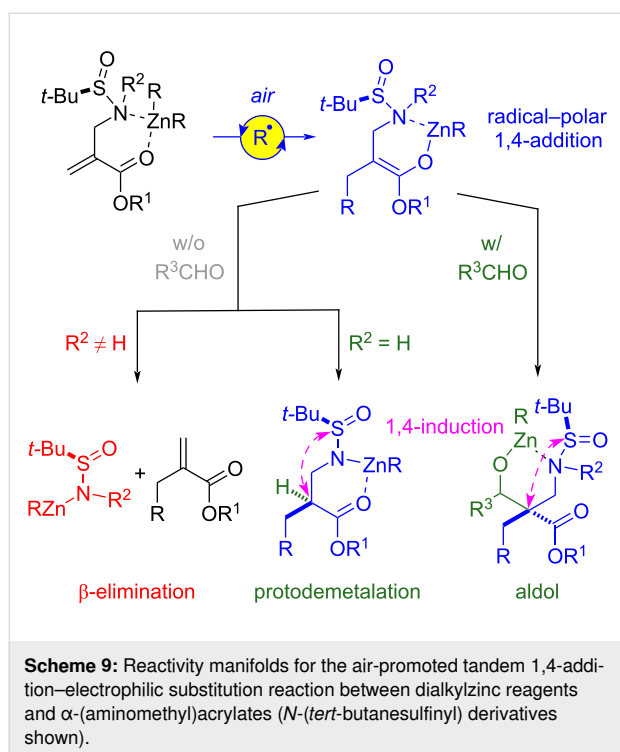
Deuterium labeling experiments were then performed to substantiate the formation of a zinc enolate following radical addition (Scheme 7, bottom). Much to our surprise however, no deuterium incorporation is observed on quenching with ND₄Cl/D₂O the reaction between **8a** and Et₂Zn. By contrast, a significant deuterium incorporation is obtained when deuterated starting material (**8a-d**) is engaged. The combination of these two results is in agreement with the formation of a zinc enolate that undergoes proto- (or deuterio)demetalation with the N–H (or N–D) as proton (or deuterium) source.

To further analyze the influence of the presence of an N–H function, we performed other reactions with *N*-benzyl enoate **10** which proved highly informative. As discussed previously (Scheme 4), application of the developed protocol for 1,4-addition to **10** only yields *N*-benzyl-*N*-*tert*-butylsulfonamide following β-elimination. By contrast, in the presence of benzaldehyde, 1,4-addition–aldol condensation is predominant, yielding **26** in 56% yield as a 49:25:23:3 diastereomeric mixture (Scheme 8). When **10** is exposed to Et₃B in the presence of *i*PrI, benzaldehyde, and O₂, which are conditions known to promote radical 1,4-addition, only formation of telomers [7] is noted. This lends clear evidence that the intermediate enoxyl radical does not intervene neither in the β-fragmentation (Scheme 4) nor in the addition across the carbonyl bonds.



Overall, the mechanistic investigations support the scenario depicted in Scheme 9. Oxygen (in air) triggers a free-radical chain reaction between α-(aminomethyl)acrylates and dialkylzinc reagents that entails 1,4-addition and S_H2 of the formed enoxyl radical facilitated by coordination of nitrogen to zinc. The zinc enolate thus formed evolves following different pathways according to the type of substrate and reaction conditions. In the absence of a carbonyl electrophile, enolates of substrates with trisubstituted nitrogen groups undergo β-fragmentation. By contrast, those derived from substrates having N–H bonds undergo protodemetalation to provide ultimately the 1,4-addition adduct. In the presence of carbonyl acceptors, these two competitive reactions are superseded and the enolate engages in aldol condensation regardless of its nitrogen substitution; the outcome of the reaction is a tandem 1,4-addition–aldol process. When the *tert*-butanesulfinyl moiety is present on the nitrogen atom, electrophilic substitution of the intermediate enolates (protodemetalation or aldol condensation) occurs with decent levels of chiral induction. It should be mentioned here that our attempts to trap the intermediate enolate with a carbon electrophile other than carbonyl acceptors (i.e., iodomethane) were not

successful and protodemetalation of the enolate outcompeted methylation.



Conclusion

In conclusion, we have demonstrated that α -(aminomethyl)acrylates are suitable acceptors for 1,4-additions with dialkylzincs in aerobic conditions. Coordination of the nitrogen atom to zinc is crucial to enable the $\text{S}_{\text{H}}2$ step of the tertiary α -carbonyl radical that follows radical 1,4-addition in order to deliver a zinc enolate. The latter is poised to undergo β -fragmentation, but this process can be outcompeted by in situ electrophilic substitution reactions which offer synthetically useful procedures: 1,4-addition (for substrates having N–H bonds) or tandem 1,4-addition–aldol reactions (in the presence of carbonyl electrophiles). Asymmetric variants of these transformations are possible using the *tert*-butanesulfinyl chiral auxiliary on the nitrogen atom. The levels of 1,4-stereoinduction are significant but a convincing model to account for it cannot be put forward at this point. Nonetheless, from a synthetic methodology point of view, the reported protocols are relevant as they offer a new, direct and modular route to enantioenriched α -mono- and α,α -disubstituted β -amino acids (β^2 -amino acids and $\beta^{2,2}$ -amino acids), with, for the latter, the noteworthy stereocontrolled construction of an all-carbon quaternary stereocenter. Furthermore, our protocol provides a complement to existing literature, as none of the previously reported methods to convert α -(aminomethyl)acrylates into enantioenriched β -amino acids is applicable for the preparation of $\beta^{2,2}$ -amino acids [27–31].

Experimental

1. Procedure for the monoallylation of primary amines and *tert*-butylsulfonamide (preparation of compounds 5–7 and 8a–c). In a round-bottomed flask under argon, *n*-BuLi (1.0 equiv, soln. in heptane) was added dropwise to a THF (0.2 mol·L^{−1}) solution of the appropriate primary amine or *tert*-butylsulfonamide (1.0 equiv) at −55 °C. The mixture was then stirred at rt for 30 min, cooled to −55 °C, and trimethylsilyl chloride (1.0 equiv) was added. The mixture was then stirred at rt for 30 min, cooled to −55 °C, and *n*-BuLi (1.0 equiv, soln. in heptane) was added dropwise. The mixture was stirred at rt for 30 min, cooled to −78 °C, and the corresponding α -(bromo-methyl)acrylate (1.0 equiv) was added. The reaction mixture was then stirred for 2 h letting the temperature rise to rt and quenched with aq 1 M NH₄Cl. The aqueous layer was extracted with EtOAc (3×) and the combined organic layer was washed (brine), dried (MgSO₄), and concentrated under reduced pressure to provide the crude product which was then purified by column chromatography on silica gel.

2. Procedure for the air-promoted 1,4-addition of dialkyl-zinc reagents to α -(aminomethyl)acrylates (preparation of compounds 11–13, 14a–c, and 15a). In a Schlenk-tube under argon, the appropriate α -(aminomethyl)acrylate (0.2 mmol) was dissolved in the indicated reaction solvent (3 mL) and the solution was cooled to −33 °C. Then, Et₂Zn (1 M in hexanes, 1.0 mL, 1.0 mmol) was added dropwise and the solution was stirred for 1 h. Air (20 mL) was introduced directly into the solution via a syringe fitted with a CaCl₂ pad at a 0.5 mL/min rate (syringe pump). After the end of the air addition, the mixture was stirred for an additional 80 min at −33 °C and then quenched with aq NH₄Cl (5 mL) at 0 °C. The aqueous layer was extracted with CH₂Cl₂ (2×). The combined organic layer was washed (brine), dried (MgSO₄), and concentrated under reduced pressure to provide the crude product which was then purified by column chromatography on silica gel.

3. Procedure for the air-promoted tandem 1,4-addition–aldol reaction between dialkylzinc reagents, α -(aminomethyl)acrylates and carbonyl derivatives (preparation of compounds 18–20, 21a–b, 22–24). In a Schlenk-tube under argon, the appropriate α -(aminomethyl)acrylate (0.2 mmol) was dissolved in the indicated reaction solvent (3 mL) and the solution was cooled to −33 °C. The carbonyl electrophile (1.0 mmol) and then Et₂Zn (1 M in hexanes, 1.0 mL, 1.0 mmol) were added dropwise and the solution was stirred for 1 h. Air (20 mL) was introduced directly into the solution via a syringe fitted with a CaCl₂ pad at a 0.5 mL/min rate (syringe pump). After the end of the air addition, the mixture was stirred for an additional 80 min at −33 °C and then quenched with aq NH₄Cl (5 mL) at 0 °C. The aqueous layer was extracted with CH₂Cl₂

(2×). The combined organic layer was washed (brine), dried (MgSO₄), and concentrated under reduced pressure to provide the crude product which was then purified by column chromatography on silica gel.

Supporting Information

Supporting Information File 1

General information, characterization data, chemical correlation, and copies of NMR spectra.

[<https://www.beilstein-journals.org/bjoc/content/supplementary/1860-5397-19-103-S1.pdf>]

Acknowledgements

The authors acknowledge MS3U of Sorbonne Université for HRMS analysis.

Funding

A. P.-C. (207839), P. G.-G. (226571) and F. G.-A. (360237) are thankful to CONACyT for scholarships.

ORCID® iDs

Fernando García-Alvarez - <https://orcid.org/0000-0002-4833-9420>

Olivier Jackowski - <https://orcid.org/0000-0001-9162-3294>

Franck Ferreira - <https://orcid.org/0000-0002-7571-1830>

Joel L. Terán - <https://orcid.org/0000-0002-4055-4353>

Alejandro Perez-Luna - <https://orcid.org/0000-0002-5578-9024>

References

- Bazin, S.; Feray, L.; Bertrand, M. P. *Chimia* **2006**, *60*, 260–265. doi:10.2533/000942906777674679
- Chemla, F.; Pérez-Luna, A. Radical-Polar Crossover Reactions. In *Free Radicals: Fundamentals and Applications in Organic Synthesis 2*; Fensterbank, L.; Ollivier, C., Eds.; *Science of Synthesis*; Thieme: Stuttgart, Germany, 2021; pp 209–357. doi:10.1055/sos-sd-233-00075
- Brown, H. C.; Midland, M. M. *Angew. Chem., Int. Ed. Engl.* **1972**, *11*, 692–700. doi:10.1002/anie.197206921
- Bazin, S.; Feray, L.; Vanthuyne, N.; Siri, D.; Bertrand, M. P. *Tetrahedron* **2007**, *63*, 77–85. doi:10.1016/j.tet.2006.10.049
- Maury, J.; Mouysset, D.; Feray, L.; Marque, S. R. A.; Siri, D.; Bertrand, M. P. *Chem. – Eur. J.* **2012**, *18*, 3241–3247. doi:10.1002/chem.201102366
- Bazin, S.; Feray, L.; Vanthuyne, N.; Bertrand, M. P. *Tetrahedron* **2005**, *61*, 4261–4274. doi:10.1016/j.tet.2005.02.042
- Bazin, S.; Feray, L.; Siri, D.; Naubron, J.-V.; Bertrand, M. P. *Chem. Commun.* **2002**, 2506–2507. doi:10.1039/b206695e
- Zelocualtecatl-Montiel, I.; García-Álvarez, F.; Juárez, J. R.; Orea, L.; Gnecco, D.; Mendoza, A.; Chemla, F.; Ferreira, F.; Jackowski, O.; Aparicio, D. M.; Perez-Luna, A.; Terán, J. L. *Asian J. Org. Chem.* **2017**, *6*, 67–70. doi:10.1002/ajoc.201600501
- Yamada, K.-i.; Konishi, T.; Nakano, M.; Fujii, S.; Cadou, R.; Yamamoto, Y.; Tomioka, K. *J. Org. Chem.* **2012**, *77*, 5775–5780. doi:10.1021/jo300944f
- Yamada, K.-i.; Matsumoto, Y.; Fujii, S.; Konishi, T.; Yamaoka, Y.; Takasu, K. *J. Org. Chem.* **2016**, *81*, 3809–3817. doi:10.1021/acs.joc.6b00485
- Lingua, H.; Dwadnia, N.; Siri, D.; Bertrand, M. P.; Feray, L. *Tetrahedron* **2018**, *74*, 7507–7515. doi:10.1016/j.tet.2018.11.029
- Bertrand, M. P.; Feray, L.; Nougier, R.; Perfetti, P. J. *J. Org. Chem.* **1999**, *64*, 9189–9193. doi:10.1021/jo9912404
- Miyabe, H.; Asada, R.; Yoshida, K.; Takemoto, Y. *Synlett* **2004**, 540–542. doi:10.1055/s-2004-815407
- Miyabe, H.; Asada, R.; Takemoto, Y. *Tetrahedron* **2005**, *61*, 385–393. doi:10.1016/j.tet.2004.10.104
- Vibert, F.; Maury, J.; Lingua, H.; Besson, E.; Siri, D.; Bertrand, M. P.; Feray, L. *Tetrahedron* **2015**, *71*, 8991–9002. doi:10.1016/j.tet.2015.09.045
- Denes, F.; Chemla, F.; Normant, J. F. *Angew. Chem., Int. Ed.* **2003**, *42*, 4043–4046. doi:10.1002/anie.200250474
- Denes, F.; Cutri, S.; Pérez-Luna, A.; Chemla, F. *Chem. – Eur. J.* **2006**, *12*, 6506–6513. doi:10.1002/chem.200600334
- Beniazza, R.; Romain, E.; Chemla, F.; Ferreira, F.; Jackowski, O.; Perez-Luna, A. *Eur. J. Org. Chem.* **2015**, 7661–7665. doi:10.1002/ejoc.201501173
- Cheng, R. P.; Gellman, S. H.; DeGrado, W. F. *Chem. Rev.* **2001**, *101*, 3219–3232. doi:10.1021/cr000045i
- Liu, M.; Sibi, M. P. *Tetrahedron* **2002**, *58*, 7991–8035. doi:10.1016/s0040-4020(02)00991-2
- Lelais, G.; Seebach, D. *Biopolymers* **2004**, *76*, 206–243. doi:10.1002/bip.20088
- Seebach, D.; Gardiner, J. *Acc. Chem. Res.* **2008**, *41*, 1366–1375. doi:10.1021/ar700263g
- Seebach, D.; Beck, A. K.; Capone, S.; Deniau, G.; Groselj, U.; Zass, E. *Synthesis* **2009**, 1–32. doi:10.1055/s-0028-1087490
- Noda, H.; Shibasaki, M. *Eur. J. Org. Chem.* **2020**, 2350–2361. doi:10.1002/ejoc.201901596
- Xuan, J.; Daniliuc, C. G.; Studer, A. *Org. Lett.* **2016**, *18*, 6372–6375. doi:10.1021/acs.orglett.6b03267
- Gutiérrez-García, V. M.; Reyes-Rangel, G.; Muñoz-Muñoz, O.; Juaristi, E. *Helv. Chim. Acta* **2002**, *85*, 4189–4199. doi:10.1002/hlca.200290004
- Sibi, M. P.; Tatamidani, H.; Patil, K. *Org. Lett.* **2005**, *7*, 2571–2573. doi:10.1021/ol050630b
- Qiu, L.; Prashad, M.; Hu, B.; Prasad, K.; Repič, O.; Blacklock, T. J.; Kwong, F. Y.; Kok, S. H. L.; Lee, H. W.; Chan, A. S. C. *Proc. Natl. Acad. Sci. U. S. A.* **2007**, *104*, 16787–16792. doi:10.1073/pnas.0704461104
- Guo, Y.; Shao, G.; Li, L.; Wu, W.; Li, R.; Li, J.; Song, J.; Qiu, L.; Prashad, M.; Kwong, F. Y. *Adv. Synth. Catal.* **2010**, *352*, 1539–1553. doi:10.1002/adsc.201000122
- Li, L.; Chen, B.; Ke, Y.; Li, Q.; Zhuang, Y.; Duan, K.; Huang, Y.; Pang, J.; Qiu, L. *Chem. – Asian J.* **2013**, *8*, 2167–2174. doi:10.1002/asia.201300339
- Sibi, M. P.; Patil, K. *Angew. Chem., Int. Ed.* **2004**, *43*, 1235–1238. doi:10.1002/anie.200353000

License and Terms

This is an open access article licensed under the terms of the Beilstein-Institut Open Access License Agreement (<https://www.beilstein-journals.org/bjoc/terms>), which is identical to the Creative Commons Attribution 4.0 International License (<https://creativecommons.org/licenses/by/4.0>). The reuse of material under this license requires that the author(s), source and license are credited. Third-party material in this article could be subject to other licenses (typically indicated in the credit line), and in this case, users are required to obtain permission from the license holder to reuse the material.

The definitive version of this article is the electronic one which can be found at:
<https://doi.org/10.3762/bjoc.19.103>



Radical chemistry in polymer science: an overview and recent advances

Zixiao Wang, Feichen Cui, Yang Sui and Jiajun Yan*

Review

Open Access

Address:
School of Physical Science and Technology, ShanghaiTech
University, 393 Middle Huaxia Rd., Shanghai, 201210, China

Email:
Jiajun Yan* - yanjj@shanghaitech.edu.cn

* Corresponding author

Keywords:
crosslinking; polymer surface modification; post-polymerization
modification; radical chemistry; radical polymerization

Beilstein J. Org. Chem. **2023**, *19*, 1580–1603.
<https://doi.org/10.3762/bjoc.19.116>

Received: 09 June 2023
Accepted: 05 October 2023
Published: 18 October 2023

This article is part of the thematic issue "Modern radical chemistry".

Guest Editor: H.-M. Huang



© 2023 Wang et al.; licensee Beilstein-Institut.
License and terms: see end of document.

Abstract

Radical chemistry is one of the most important methods used in modern polymer science and industry. Over the past century, new knowledge on radical chemistry has both promoted and been generated from the emergence of polymer synthesis and modification techniques. In this review, we discuss radical chemistry in polymer science from four interconnected aspects. We begin with radical polymerization, the most employed technique for industrial production of polymeric materials, and other polymer synthesis involving a radical process. Post-polymerization modification, including polymer crosslinking and polymer surface modification, is the key process that introduces functionality and practicality to polymeric materials. Radical depolymerization, an efficient approach to destroy polymers, finds applications in two distinct fields, semiconductor industry and environmental protection. Polymer chemistry has largely diverged from organic chemistry with the fine division of modern science but polymer chemists constantly acquire new inspirations from organic chemists. Dialogues on radical chemistry between the two communities will deepen the understanding of the two fields and benefit the humanity.

Introduction

Early last century, with the groundbreaking macromolecular hypothesis by Hermann Staudinger [1], polymer science was born out of organic chemistry. Since then, polymer science has evolved into an important branch of physical science and a fundament of the modern life. Like many other organic methodologies, radical chemistry was applied to polymer science and nowadays, radical chemistry plays a critical role in both the pro-

duction of a major portion of industrial polymers and the research on novel materials [2]. In this minireview, we discuss several aspects of radical chemistry found in polymer science.

Section 1 focuses on the best-established radical chemistry – radical polymerization, including radical polymerization in nature, conventional radical polymerization, and a new class of

radical polymerization, reversible deactivation radical polymerization, which emerged late last century. To continue with the discussion on polymer construction, section 2 explores some emergent polymer synthesis techniques via a radical process but other than a chain-growth mechanism by addition of radical species to vinyl monomers. In section 3, we cover radical chemistry approaches used in post-polymerization modification, including chemical crosslinking of polymers and polymer surface modification. Radicals are powerful tools for post-polymerization processes because of their exceptional reactivity. In contrast to the previous sections, we set the topic of section 4 on the radical degradation of polymers, both in nanofabrication and polymer upcycling.

Review

1 Radical polymerization

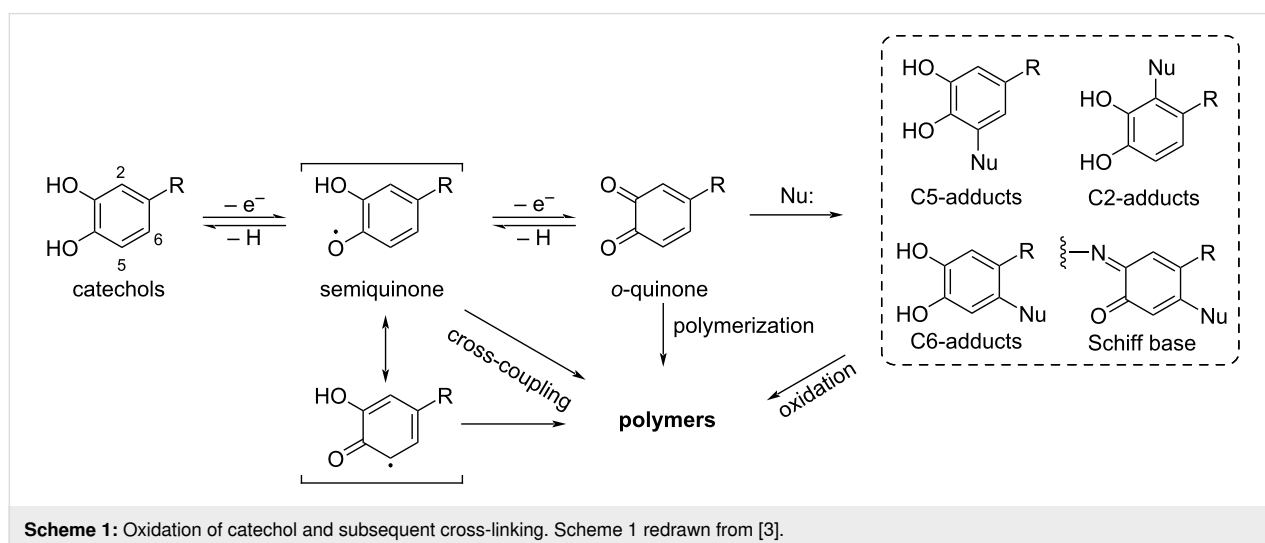
Radical polymerization has long been an effective and inexpensive method in the synthesis of polymers since it was invented, making it the most important industrial polymerization technique. Polymers produced by radical polymerization represent a major fraction of all industrial polymers.

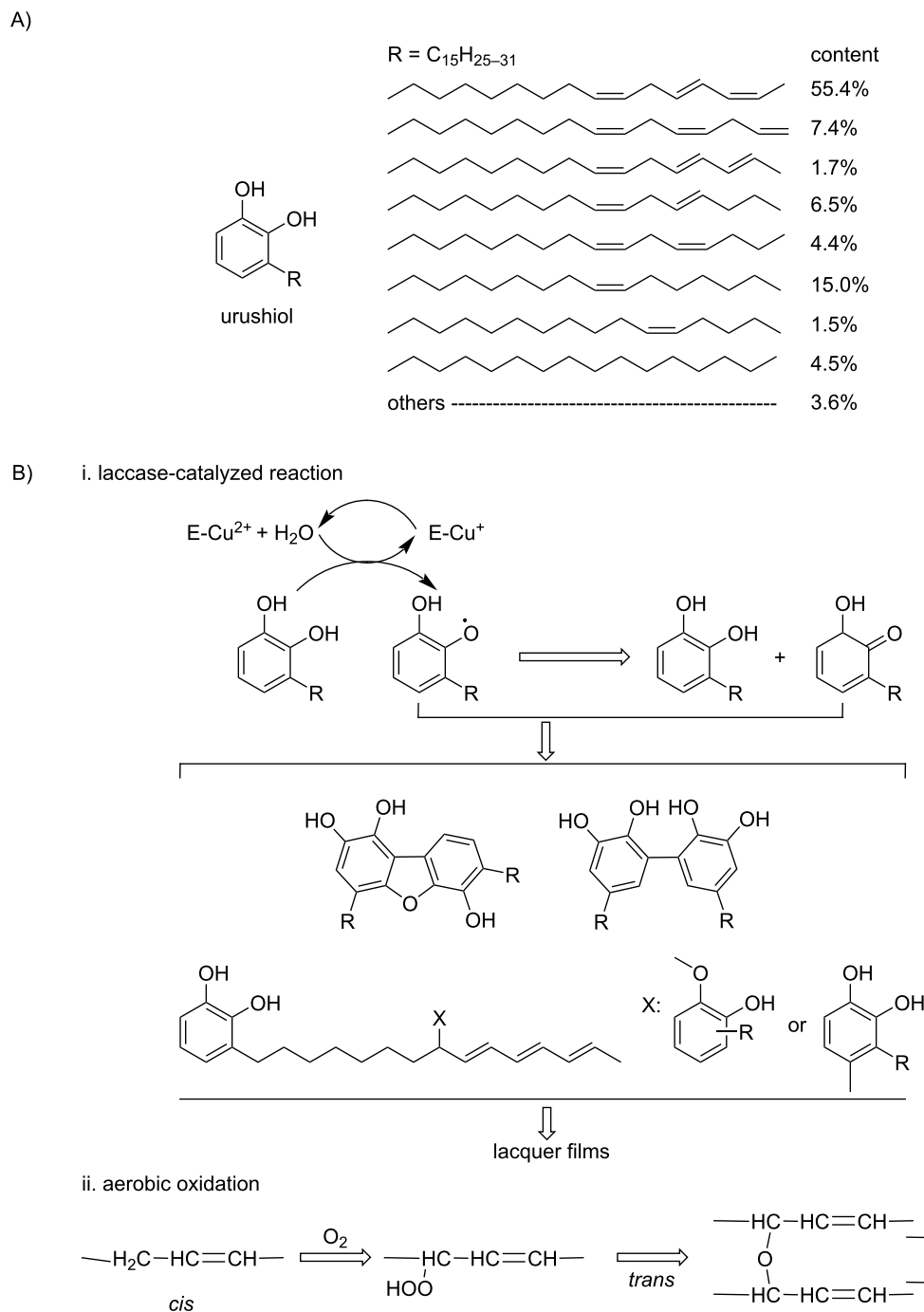
1.1 Radical polymerization in nature

In addition to well-established processes in modern industry, examples of radical polymerization exist in nature. The principle of the two cases in the following text is based on the radical polymerization of catechol derivatives. Catechols are known as easily oxidizable compounds and are prone to undergo oxidation by losing one or two electrons [3]. This way, either semiquinone radicals or *o*-quinones are formed by single or double-electron oxidation, respectively [4]. The semiquinone radicals formed during the oxidation of catechol can undergo a cross-coupling reaction to form polymers (Scheme 1).

One example is the radical polymerization of urushiol. The earliest recorded application of natural radical polymerization can be traced back to the manufacture of lacquerwares several thousand years ago [5]. The surface coating of lacquerwares was made up of a sap from a lacquer tree growing in Asia. The lacquer sap obtained from *Rhus vernicifera* lacquer tree mainly consists of urushiol (60–65%), water (20–30%), lacquer polysaccharide (3–7%), water-insoluble glycoprotein (≈ 1 –2%), laccase ($\approx 0.2\%$), and stellacyanin ($\approx 0.02\%$) [6,7]. Urushiol is the main active coating-forming ingredient of the resin. A typical urushiol is shown in Scheme 2. In a humid and warm environment, urushiol absorbs oxygen from air and is oxidized to a phenolic oxygen free radical under the action of laccase enzymes [5]. The radical then rearranges to form a semiquinone radical and reacts rapidly with a neighboring urushiol molecule to produce a biphenyl dimer. The dimers further polymerize to form the polymer [8].

Radical processes also occur in oceans. The mussel attachment system consists of a bundle of disc-tipped acellular thread called *byssus*, which connect the mussel to the surfaces of substrates [10]. A family of proteins called mussel foot proteins (mfp's) distribute throughout the whole length of *byssus* while there is an extremely high concentration of mfp's at the plaque–substrate interface. The mfp's contain up to 27 mol % of DOPA (L-3,4-dihydroxyphenylalanine), which plays a crucial role on mussel adhesion [11]. Although the crucial role of DOPA in mussel adhesion is not fully understood, a prevailing view suggests that DOPA can be oxidized to *o*-quinones at an acidic pH and the quinones react with unoxidized catechols to form *o*-semiquinone radicals afterwards [12]. The semiquinone radicals can help DOPA adhere onto organic surfaces. At a basic pH, the system is cured and mechanically stabilized through the formation of DOPA-metal coordination bonds. The





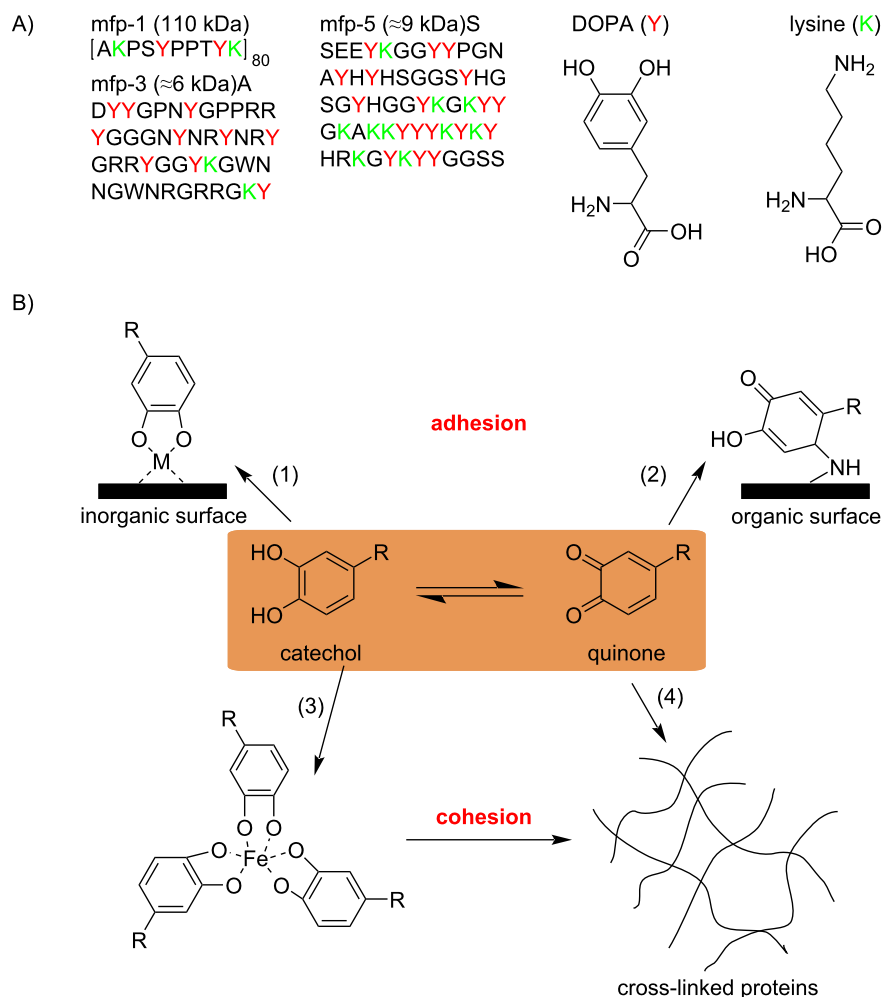
Scheme 2: (A) Structure of typical urushiol in Chinese lacquer, and (B) schematic process of laccase-catalyzed oxidation polymerization of Chinese lacquer and autoxidation reaction on the long aliphatic unsaturated side chain. Scheme 2 redrawn from [9].

cohesion of the DOPA-metal complex helps mussel adhere onto inorganic surfaces (Scheme 3).

1.2 Conventional radical polymerization

Radical polymerization, which IUPAC defines as ‘A chain polymerization in which the kinetic-chain carriers are radicals’

[13], is the most widely used reaction in polymer industry. As far back as the 1950s, the basic theory and comprehension of radical polymerization was established. In the past decades, radical polymerization was introduced to be an efficient industrial synthesis method to produce numerous chemicals such as low-density polyethylene (LDPE), polystyrene (PS), and



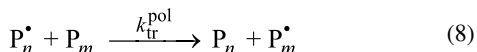
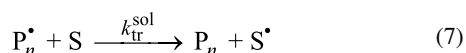
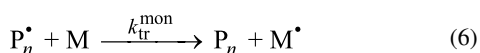
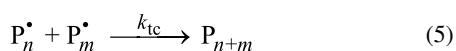
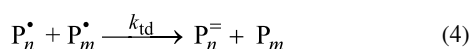
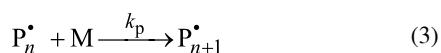
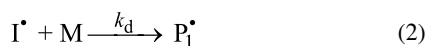
Scheme 3: A) Primary amino acid sequence of mfp-1, mfp-3, and mfp-5 (Y: DOPA, K: lysine). B) Scheme showing examples of the adhesive and cohesive properties of catechol-containing proteins. R represents the remainder of the mfp's. Scheme 3 redrawn from [10].

poly(vinyl chloride) (PVC) [14]. About half of the industrial polymers manufactured worldwide are produced by radical polymerization [15,16].

1.2.1 Key features of radical polymerization: Radical polymerization, which has a classical chain reaction process, usually analyzed kinetically on the assumption of a steady state with respect to the concentration of chain carriers (radicals) [17]. Radical polymerization is a complex mechanism. The basic reactions have been known for quite some time now. They can be simply described by 8 equations (Equations 1–8) as follows. In the equations, I_2 represents an initiator molecule; M represents a monomer molecule; P_i represents a polymer chain with i repeating units; S represents a solvent molecule; and a dot indicates free radical species. These reactions are classified into four elementary steps: initiation, propagation, termination, and

transfer. The initiation step includes Equation 1 and Equation 2, when the thermal initiator decomposes into two small-molecule radical species and the first monomer adds to the growing chain to form the first repeating unit. The propagation step is depicted in Equation 3 when monomers take turns to undergo radical addition. The termination step occurs by either disproportionation (radical β -elimination, Equation 4) or biradical coupling (Equation 5). Chain transfer (Equations 6–8) is usually considered as a type of side effect in radical polymerization [18]. It occurs between the growing chain and a transfer agent, which can be the monomer (Equation 6), the solvent (Equation 7), the polymer itself (Equation 8), or a chain-transfer agent intentionally added to tune the molecular weight or to introduce chain-end functionalities. When chain transfer happens, the originally growing chain halts while a new chain launches from the radical species formed from the chain transfer agent. In the case when a

growing chain-end radical transfers to its own backbone, i.e., backbiting occurs, a branching point forms as propagation continues in the middle of the backbone.



Radical polymerization is applicable to a large number of vinylic monomers and is tolerant toward many solvents, functional groups, and impurities common in industrial systems, which makes it an ideal choice for industrial production [19]. Vinylic monomers should be thermodynamically and kinetically polymerizable. The former requires a sufficiently negative free energy of polymerization and the latter an adequate reactivity of the monomer, stability of the derived free radical, and a low proportion of side reactions.

A slow rate of chain initiation, a fast rate of chain propagation, and a rapid rate of chain termination are key features of conven-

tional radical polymerization. Most free radicals have an extremely short lifetime due to a diffusion-controlled termination process between two free radicals. The inevitable termination between radicals makes the synthesis of well-defined polymers and co-polymers very difficult. In addition, polymers obtained from conventional radical polymerization are commonly linear polymers, though transfer to polymer may induce branching.

1.2.2 Radical polymerization in modern industry: In the commercial production of high-molecular-weight polymers, radical polymerization is a widely used method. Its main advantages are (i) the universality to a wide range of monomers such as (meth)acrylates, (meth)acrylamides, dienes, vinyl ethers/esters, etc.; (ii) tolerance to unprotected functionalities in monomers and the solvent including –OH, –COOH, –SO₃H, etc.; (iii) different reaction conditions, including bulk, solution, emulsion, and suspension; and (iv) inexpensive and facile set-ups compared to other polymerization techniques [20].

There are four common industrial methods of radical polymerization [2] as shown in Table 1.

The only components of a bulk polymerization mixture are monomers, the initiator, and optionally, a chain-transfer agent [21]. Products obtained from bulk polymerization have high optical clarity and are usually very pure [2]. The mechanism and equipment are relatively simple for a large-scale production in a short time. However, heat and mass transfer become difficult as the viscosity of the reaction mixture increases. This may lead to autoacceleration, also known as the Trommsdorff–Norrish effect, or even a violent explosive polymerization. At the same time, heat acquisition may cause a broad molecular weight distribution.

Solution polymerization can effectively mitigate problems of bulk polymerization. The use of a solvent can lower the viscosity of the polymerization system, leading to better mass and heat transfer. Good heat transfer can reduce the Trommsdorff–Norrish effect [22]. Meanwhile, the inhibited

Table 1: Common ways of radical polymerization in industry.

method	contains	where polymerization happens
bulk polymerization	monomer, initiator	in bulk
solution polymerization	monomer, initiator, solvent	in solution
suspension polymerization	hydrophobic monomer, hydrophilic initiator, water, suspending agents	in monomer droplet
emulsion polymerization	hydrophobic monomer, hydrophilic initiator, water, surfactants	in latex/colloid particles

termination reactions cause a significant increase in the overall yield.

Polyacrylonitrile (PAN), polyacrylic acid (PAA), and polyacrylamide (PAM), for instance, are obtained by solution polymerization in the polymer industry [23–25]. In addition to the reduced reaction rate due to lower monomer and initiator concentrations, one of the major disadvantages of solution polymerization is that it is difficult to completely rule out chain transfer to the solvent. Therefore, obtaining very high molecular weight product through solution polymerization is tough.

Suspension polymerization is a heterogeneous process and requires the use of a mechanical agitation to mix monomers and dissolved initiators in the liquid phase during the process. A suspending agent, e.g., polyvinyl alcohol (PVA), is added to the system to prevent coalescence. The viscosity in suspension polymerization is low throughout the process which brings good heat transfer and temperature control, and therefore well-defined and high-molecular-weight polymers. PVC, PS, and poly(methyl methacrylate) (PMMA) are industrially produced through suspension polymerization [2]. Nonetheless, the Trommsdorff–Norrish effect exists in suspension polymerization processes, and the residual suspending agent becomes an impurity.

Emulsion polymerization is also a widely-used method in radical polymerization. It is applied to produce several commercially important polymers such as acrylic rubber, nitrile rubber, and polytetrafluoroethylene (PTFE). Polymerization happens in latex or colloid particles that are formed under the action of surfactants, which are also called emulsifiers within the first few minutes [26]. Emulsifiers such as sodium lauryl sulfate, sodium or potassium salts of fatty acids (soaps), salts of alkylbenzene sulfonates, and *O*-polyoxyethylenated long-chain alcohols are used to change the two incompatible water phase and oil phase into an emulsion phase. The simultaneous presence of a hydrophobic head and a hydrophilic tail on emulsifiers provides the ability to combine water and oil phase into an emulsion. In emulsion polymerization, high molecular weights can be achieved at fast polymerization rates, because both the rate of polymerization and the molecular weight depends on the number of particles. A small latex particle only rooms a single propagating radical at a time. Thus, the chain keeps growing until another radical enters to terminate it. Due to the enormous number of particles, the overall radical concentration in the latex is greatly higher than in a typical bulk polymerization. Meanwhile, the polymerization rate is higher in emulsion polymerization compared to bulk or suspension polymerization. Radicals are divided in different particles also allows for longer lifetimes, which results in a higher degree of polymerization. As the fre-

quency of radical entry decreases with the particle number at a certain initiator concentration, the rate of polymerization and molecular weight can be boosted by raising the number of particles, e.g. by tuning the monomer to surfactant ratio.

The final product can be used as is and does not generally need to be altered or processed. Drawbacks of emulsion polymerization include residual surfactants, significant chain transfer to polymer, and difficulty to dry polymers.

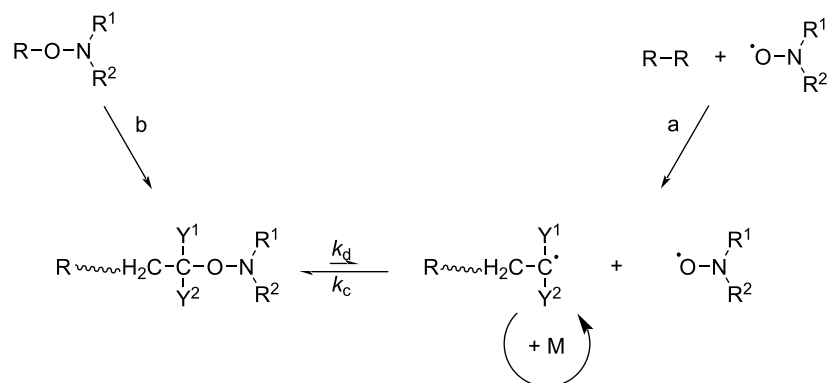
1.3 Reversible deactivation radical polymerization

A key drawback of conventional radical polymerization is that a limited control of molecular weights and architectures can be achieved due to the slow initiation and rapid termination. In 1956, Szwarc coined the term “living polymerization” in an anionic system [27]. Since then, polymer chemists have been in pursuit for a comparable “living radical polymerization”. Despite the fact that radical polymerization is never as “living” as the anionic counterpart, RDRP as per the IUPAC definition, or more commonly named controlled radical polymerization (CRP) has made a booming progress and attracted great attention in the past three decades [28].

1.3.1 Deactivation by reversible coupling: In 1982, Otsu and Yoshida [29] successfully polymerized styrene and MMA using dithiocarbamate compounds, and in 1986, Solomon et al. [30] published a patent entitled “Polymerization Processes and Polymers Produced Thereby”, which led to the successful nitroxide-mediated polymerization (NMP). In 1993, Georges et al. used benzoyl peroxide (BPO) as the initiator and 2,2,6,6-tetramethyl-1-piperidinyloxy (TEMPO) as the control agent. It was called a bicomponent initiating system containing both stable free nitroxide and a conventional thermal initiator. Polystyrene of different molecular weights was obtained with low M_w/M_n and active chain ends [31].

Although a bicomponent initiating system is economical and practical, the traditional initiators have many problems such as the poor initiation efficiency. It is difficult to control the molecular weight and polymerization rate precisely. In order to solve these problems, Hawker et al. [32–34] proposed the concept of the unimolecular initiation system. In this system, an alkoxyamine compound is used instead of the original nitroxide radical/initiator combination. These unimolecular initiators can decompose to produce a stoichiometric pair of the primary initiating radical and a nitroxide radical, thus combining the roles of a conventional initiator and a control agent. The mechanism is shown in Scheme 4 [35].

Due to the steric effect of TEMPO, the dissociation rate constant, k_d , of the corresponding alkoxyamine is very low and it



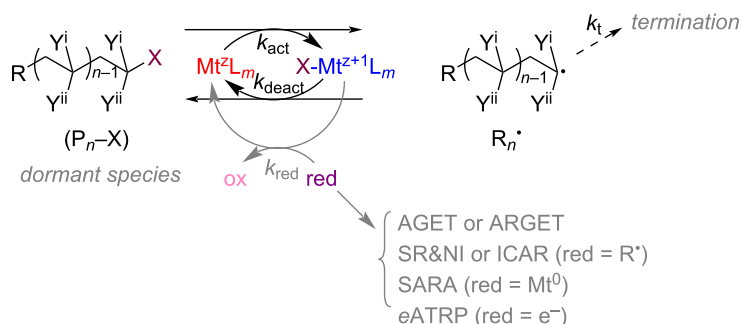
Scheme 4: Activation–deactivation equilibrium in nitroxide-mediated polymerizations. Bicomponent initiating system (a) and unicomponent initiating system (b). Scheme 4 redrawn from [35].

tends to undergo β -elimination in acrylic systems. Thus, TEMPO is only suitable for the polymerization of styrenic monomers at a high temperature and for long time [36]. Functionalized TEMPO was therefore developed for the polymerization of other monomers, such as acrylates, under milder conditions [37–39]. Grimaldi et al. [40] achieved NMP of styrene and *n*-butyl acrylate using SG1-type nitroxide radical (*N*-*tert*-butyl-*N*-(1-diethylphosphono-2,2-dimethylpropyl)nitroxide). Compared with TEMPO, SG1 was considered that it initiated the truly “living”/controlled polymerization at that time and the rate of propagation was much faster than with TEMPO under the same conditions.

1.3.2 Deactivation by atom transfer: Atom transfer radical polymerization (ATRP) was independently reported by the teams of Matyjaszewski [41] and Sawamoto [42] in 1995. The efficient conduct of ATRP relies on the establishment of a reversible activation/deactivation equilibrium reaction between an alkyl halide or halide-like initiator (RX) and a radical species (R^\cdot) [43]. During the activation process, the organohalides quickly lose their terminal halogen atoms in the presence of the

liganded low-valent metal complex (activator, Mt^z/L , typically Cu^I/L) to form the active radical species (R^\cdot), which in turn initiates polymerization to form the active polymer chain species (P_n^\cdot). On the other hand, the termination reactions always present in the system causing the liganded high-valent metal complex (deactivator, $X-Mt^{z+1}/L$, typically $X-Cu^{II}/L$) to accumulate. When the accumulation reaches a certain level, the deactivator interacts with the active radical chain species (P_n^\cdot), so that the radical chain species gets into the dormant state (P_nX) via a halogen atom transfer process. This is the deactivation process. Activation and deactivation reactions are always present throughout the process, and the rate of deactivation must be sufficiently high in order to maintain a low radical concentration to effectively inhibit the termination [44]. The mechanism of ATRP is shown in Scheme 5 [14].

Compared with the earlier ATRP techniques (normal ATRP [41], reverse ATRP [45], SR&NI ATRP [46], and AGET ATRP [47]), the recently proposed ATRP techniques (ICAR ATRP [48], ARGET ATRP [49], SARA ATRP [50], *e*ATRP [51,52], photoATRP [53,54], and ultrasonic ATRP [55]) require a much



Scheme 5: Mechanism of a transition metal complex-mediated ATRP. Scheme 5 redrawn from [14].

lower catalyst dosage, even down to 10 ppm [56], which to some extent, solves the problem of metal impurities. Meanwhile, the presence of external stimuli in *e*ATRP, photoATRP, and ultrasonic ATRP, allows spatial and temporal control over the polymerization [57]. Hawker et al. proposed a metal-free ATRP in 2014 using an organic photoredox catalyst mediated by light to overcome the challenge of metal contamination in the precipitated polymers [58]. After the ATRP reaction, a reactive chain end retains as a stable alkyl halide moiety. Therefore, ATRP is particularly suitable for the synthesis of polymers with complex architectures [59,60].

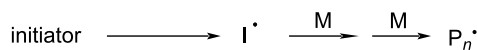
1.3.3 Deactivation by degenerative transfer: Reversible addition-fragmentation chain transfer (RAFT) polymerization is one of the most well-established RDRP technique. It was first proposed in 1998 by Commonwealth Scientific and Industrial Research Organization (CSIRO) researchers Chiefari et al. [61]. Due to the presence of chain-transfer agents (CTAs), such as thiocarbonylthio compounds, in RAFT polymerizations, the chain propagating radical species can add to CTAs to form intermediate radical species. RAFT can rely on reversible chain-transfer reactions between the propagating radical species and

the dormant chains to achieve controlled polymerization of the monomers, allowing all polymer chains to grow nearly simultaneously.

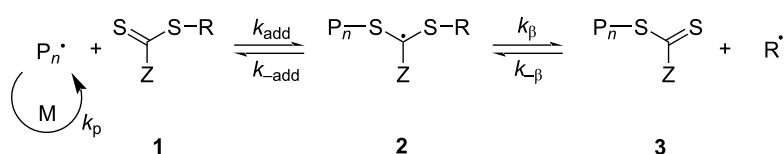
The product of RAFT polymerization has a preserved thiocarbonylthio chain end. The polymerization reaction can be continued by adding more monomers. Therefore, RAFT is often used to perform chain expansion reactions or to synthesize functionalized multi-block copolymers [62–64]. Boyer and co-workers developed a photocatalytically mediated RAFT polymerization, PET-RAFT, which removes the requirement for conventional radical initiators. The reaction is oxygen tolerant and can be carried out in a milder environment [65,66]. Pan and co-workers recently further advanced the RAFT techniques by allowing them to be fueled by oxygen [67]. The mechanism of a RAFT polymerization is shown in Scheme 6 [68].

Organometallic-mediated radical polymerization (OMRP) is also a commonly used polymerization method, which uses transition-metal complexes such as titanium and vanadium for coordination polymerization [69]. However, due to the high cost of these complexes and their post-processing, OMRP is not widely

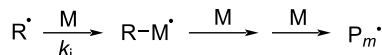
initiation:



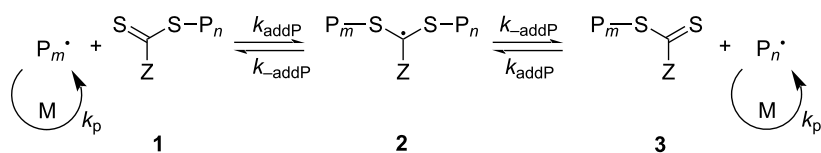
reversible chain transfer/propagation:



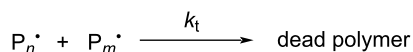
reinitiation:



chain equilibration/propagation:

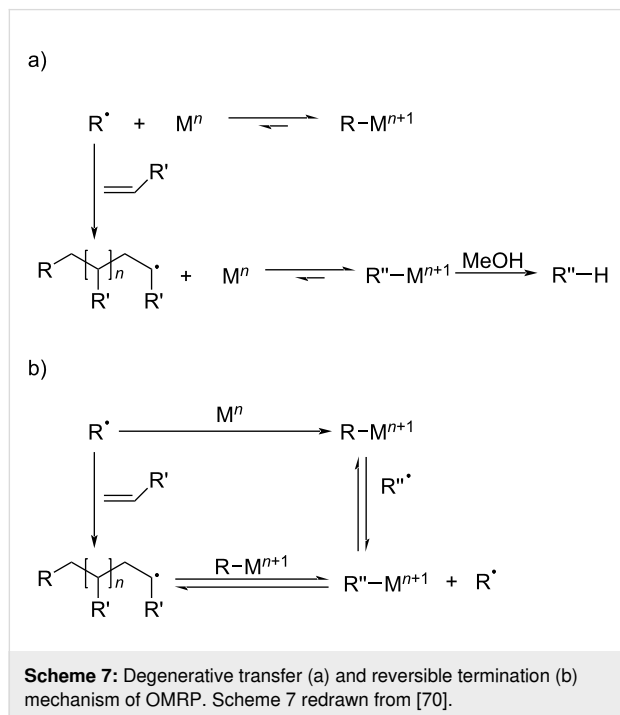


termination:



Scheme 6: Mechanism of RAFT polymerization. Scheme 6 redrawn from [68].

used. The chain termination reaction of OMRP is considered to have two mechanisms, degenerative transfer and reversible termination, which are comparable to RAFT and NMP, respectively (Scheme 7) [70].



Iodine transfer polymerization (ITP) is also a commonly used degenerate chain-transfer method. Its origin can be traced back to the 1970s [71] and it is mostly used for the polymerization of fluorinated olefins. However, the C–I bond of iodoalkyl compounds used as chain-transfer agents is weak and unstable during storage [21]. Therefore, Lacroix-Desmazes et al. [72]

used iodine molecules to synthesize iodine chain transfer agents in situ, a process known as reverse iodine transfer polymerization (RITP), which is similar to reverse ATRP. The mechanism of the RITP is shown in Scheme 8.

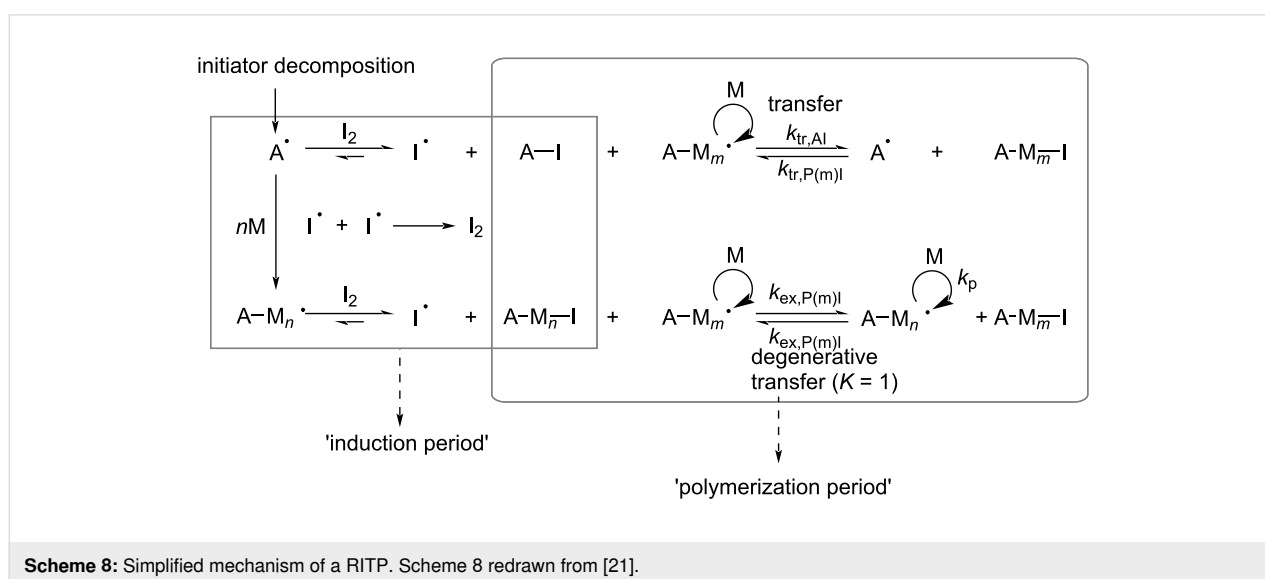
RDRP is applicable to a wide range of monomers and the reaction conditions become milder and more versatile with emerging techniques, such as oxygen tolerance or even oxygen initiation [73]. Compared with the conventional radical polymerization, RDRP has shown fascinating advantage in complex polymer polymerization. However, RDRP is currently less applied in industry due to cost and process obstacles. It is expected that future technical innovation will allow RDRP to be more widely employed.

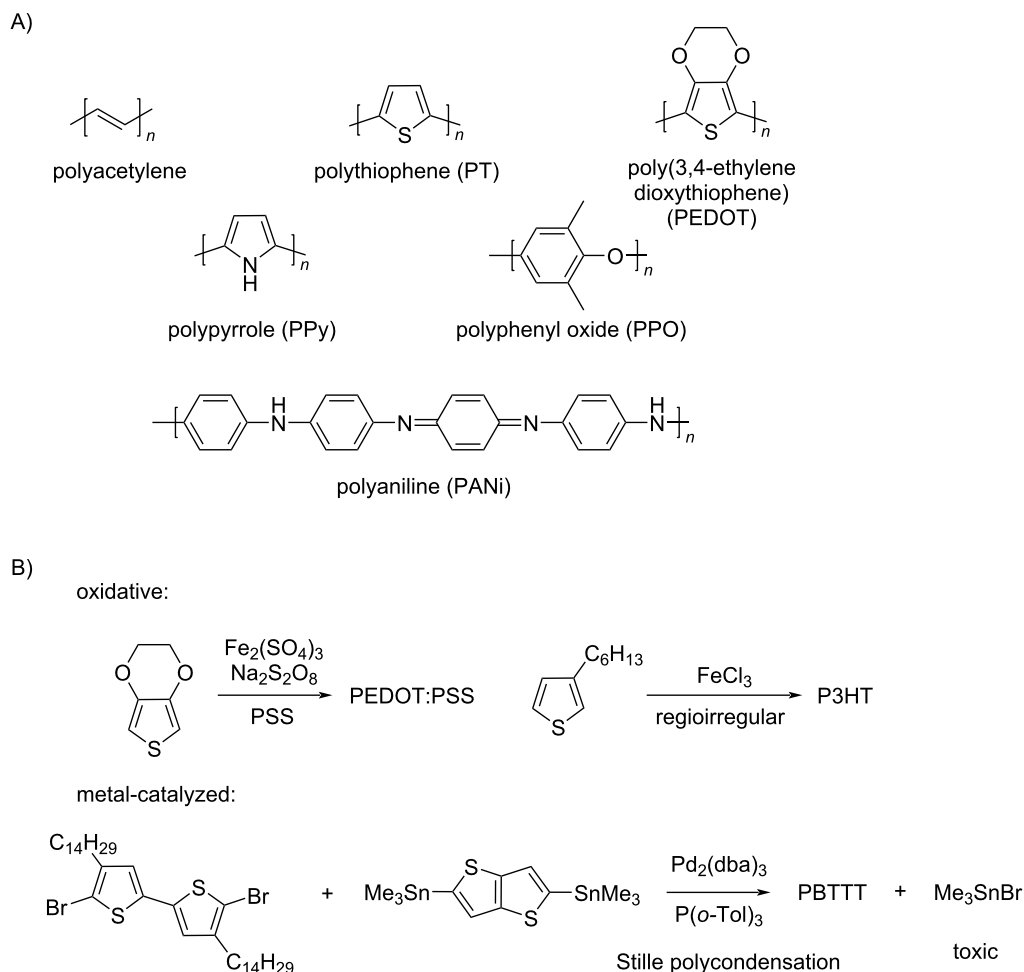
2 Other polymerization techniques involving radical chemistry

As discussed in section 1, chain-growth polymerization via radical addition to vinyl monomers is the most broadly applied polymerization technique. However, radical chemistry is used in other polymerization systems. In this section, we cover these techniques excluded from our previous discussion.

2.1 Oxidative synthesis of conductive polymers

The breaking accomplishments of Shirakawa, MacDiarmid, and Heeger have changed our view of organic polymers, from insulating polymers to electrically (semi)conducting materials [74]. In 2000, they received the Nobel Prize in Chemistry. Typical conductive polymer structures have π -conjugation (Scheme 9A) [75]. They can be synthesized by various methods such as electrochemical and chemical methods. Oxidative polymerization and chain-growth polymerization are also good ways to produce conductive polymers (Scheme 9B) [76].





Scheme 9: (A) Structures of π -conjugated conductive polymers. (B) Examples of conductive polymer synthesis via chain-growth polymerization. Scheme 9 redrawn from [76].

Nowadays, most conductive polymers are prepared via metal-catalyzed cross-coupling reactions [77]. However, radical polymerization is also an effective way to synthesize conductive polymers at a relatively low cost. Niemi et al. [78] used FeCl_3 as catalyst to produce radicals at the 2- and 5-positions of thiophene and synthesized four types of poly(3-alkylthiophene)s (PATs) with different linking ways (Scheme 10).

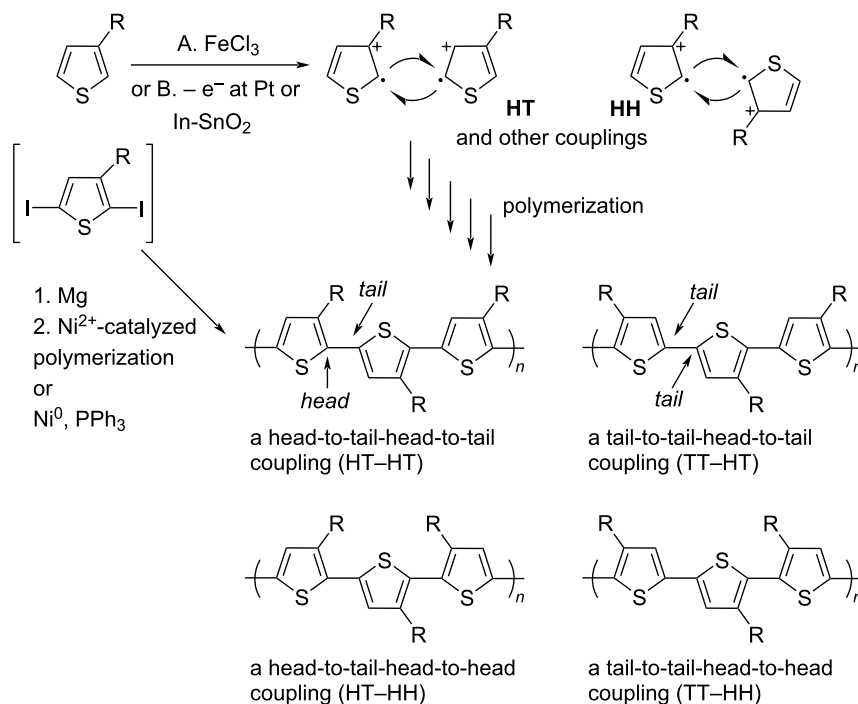
2.2 Polymerization by thiol–ene chemistry

The thiol–ene reaction (also called alkene hydrothiolation) is the anti-Markovnikov addition of a thiol to a C–C double bond and was first reported in 1905 [80]. It is considered as a click chemistry reaction due to its high yield, stereoselectivity, rate, and thermodynamic driving force.

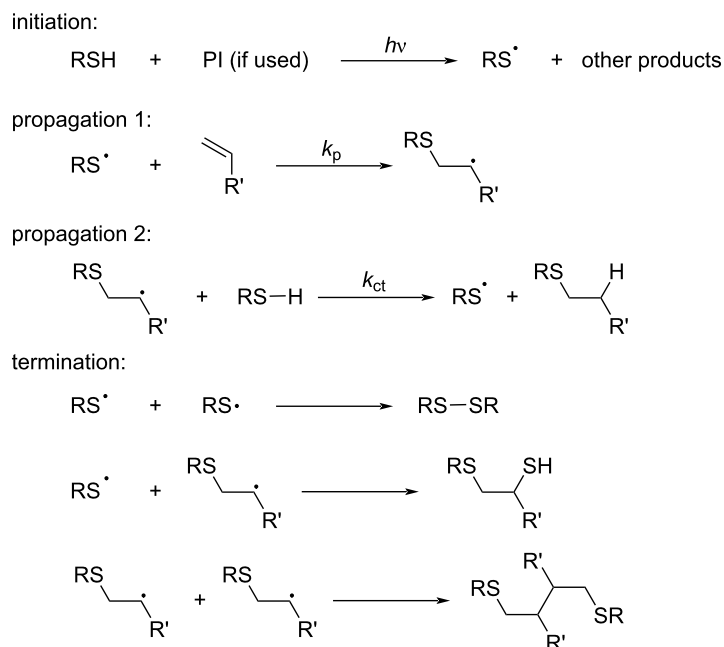
Generally, the thiol–ene reaction is conducted under radical conditions, often photochemically induced [81]. In a typical thiol–ene system, the polymerization undergoes a free-radical

chain mechanism, involving an initiation step from a thiol group via radical transfer or homolysis (Scheme 11, initiation), radical addition of the thiyl radical to the ene functionality (propagation 1), transfer from the carbon-centered radical to another thiol group (propagation 2), and biradical termination between either carbon-centered or thiyl radicals (termination).

Polymerization by thiol–ene coupling is a step-growth polymerization, which means it can produce polymers with no theoretical upper-limited molecular weight. The simple setup, mild conditions, absence of unfavored byproducts, orthogonality with other reactions, and high yields (nearly full conversion) [82] made thiol–ene polymerizations an ideal way to produce high-molecular-weight cross-linked polymers, optical polymers, biomacromolecules, and materials used in additive manufacturing. It is also compatible to a photopolymerization process. For example, it can be applied to the photo-3D-printing of silicone resin [83]. The refractive index is one of the most impor-



Scheme 10: Possible regiochemical couplings in PATs. Scheme 10 redrawn from [79].



Scheme 11: General thiol-ene photopolymerization process. Scheme 11 redrawn from [81].

tant optical properties and researchers have invested plenty of effort to develop high refractive-index polymers. A common approach is to incorporate atoms or groups with high polariz-

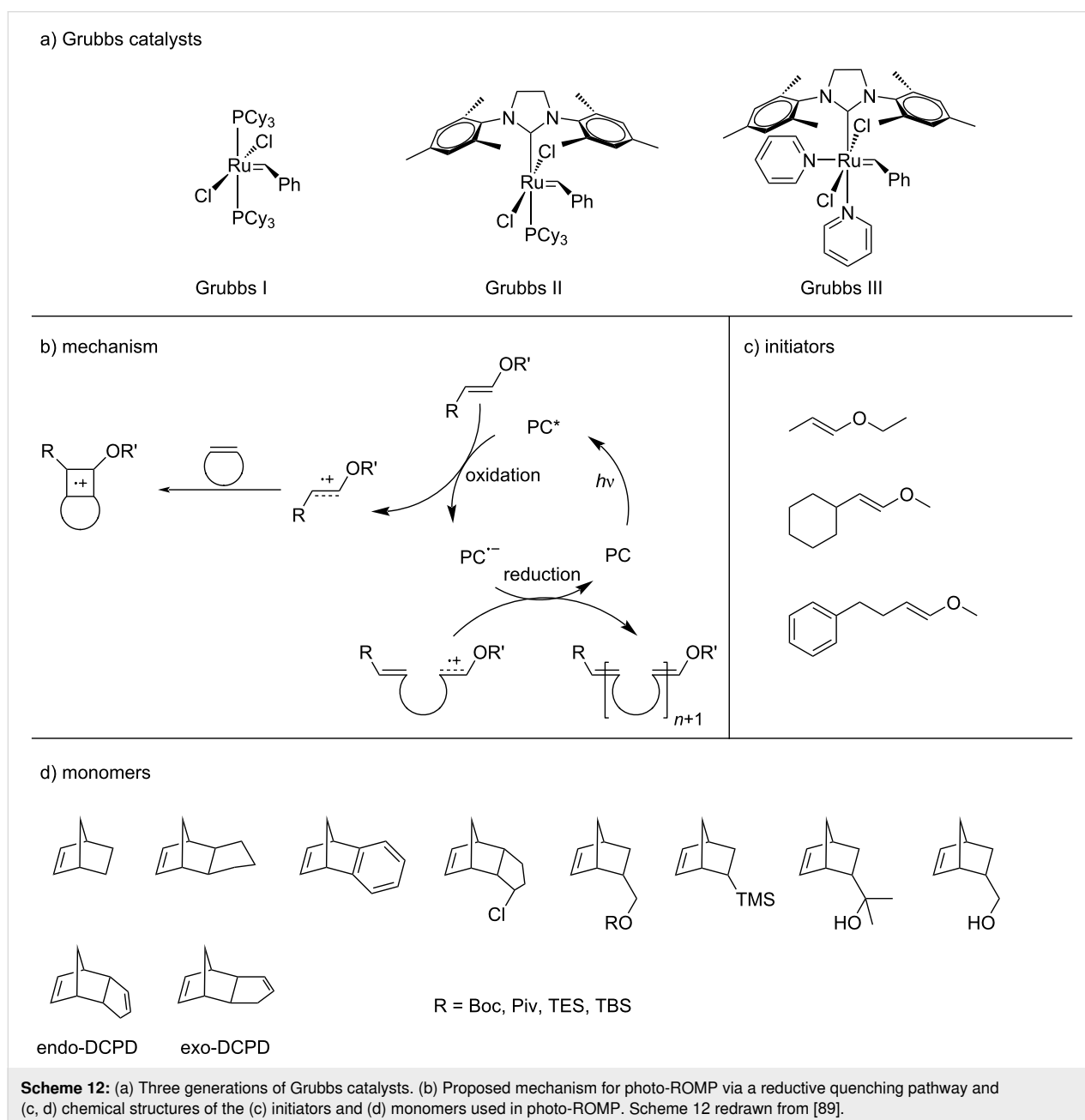
ability and sulfur is a typical constituent with high molar refractivity and is widely used in optical polymers. For example, Bhagat et al. [84] produced polymers with high cross-linking

density and refractive index from tetravinylsilane, ethanedithiol, and benzenedithiol. Polymers made by thiol–ene polymerization usually have well-ordered molecular networks. This character gives thiol–ene polymers highly tunable mechanical response hence it shows great application potential in additive manufacturing. Cook et al. [85] presented the first report of volumetric additive manufacturing-printed thiol–ene resins and showed the potential of the thiol–ene system.

In addition to thiol–ene chemistry, radical hydrosilylation was also used to prepare linear, branched, or cross-linked polymers via a step-growth mechanism (cf. section 3.2) [86].

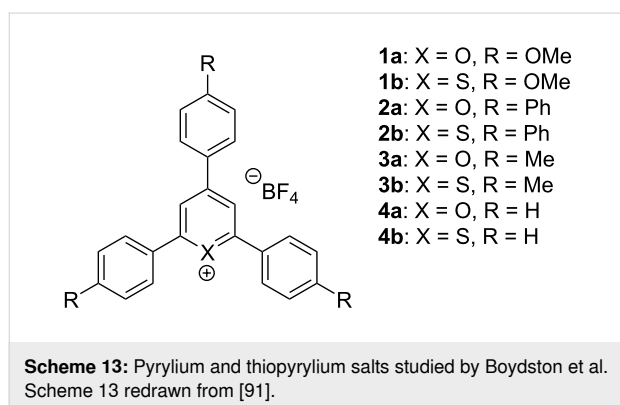
2.3 Metal-free ring opening metathesis polymerization (MF-ROMP)

ROMP is a powerful and broadly applicable technique for synthesizing polymers. Traditional ROMP systems are initiated by transition-metal complexes and Ru-based alkylidene complexes, which are also known as Grubbs catalysts (Scheme 12A), are the most popular ones [87]. However, Ru-based catalysts are expensive making them less attractive for industrial applications. Living ROMP is commonly terminated by adding a special chemical which can remove the transition metal from the chain end and deactivate it from propagation. However, removing this residue from the product by tradi-



tional chromatographic methods can be a challenging task and limits the application of ROMP-produced polymers in biomedical and microelectronic fields [88]. To avoid such drawbacks, the development of a metal-free (MF) procedures is necessary.

MF-ROMP, also termed photo-ROMP, is a novel technique to polymerize cyclic olefins. It begins with the reductive quenching of an photoexcited photocatalyst (PC) at an enol ether initiator to produce a radical cation carrier [90]. Then, the carrier undergoes cyclic addition with a cyclic olefin monomer to generate a cyclobutene radical cation intermediate. The thermodynamically instable intermediate subsequently forms the propagating radical cation species via a ring-opening process. The reduced PC^{•−} terminates the catalytic loop by reducing the propagating species to provide a polymer chain (Scheme 12B). Boydston and co-workers [91], systematically studied various pyrylium and thiopyrylium PCs (Scheme 13). It is necessary for these PCs having a high excited-state redox potential to oxidize the enol ether initiators. A range of enol ether initiators that has been successfully applied in metal-free ROMP are shown in Scheme 12C.



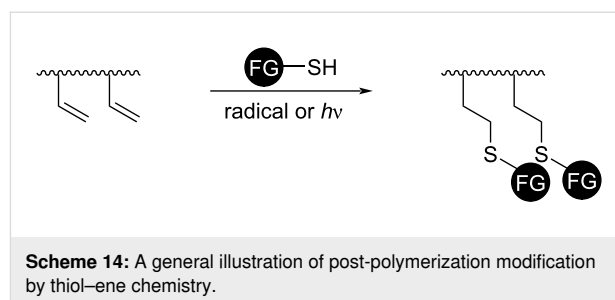
Meanwhile, metal-free ROMP is applied to monomers like functionalized norbornenes and dicyclopentadienes (DCPD) (Scheme 12D) to synthesize polymers and block copolymers [88,92,93].

3 Post-polymerization radical chemistry

Post-polymerization modification is a chemical process that introduces functionalities to backbones or side-groups of pre-synthesized polymers [94,95]. It typically takes place in polymer solutions. On the other hand, surface modification of polymers is a special case of post-polymerization on polymeric solids. Radical chemistry is overwhelmingly more common in the latter because there are other more selective and efficient solution chemistry methods for post-polymerization modification, such as nucleophilic substitution [94,96]. In this section, we discuss the radical chemistry used in both processes.

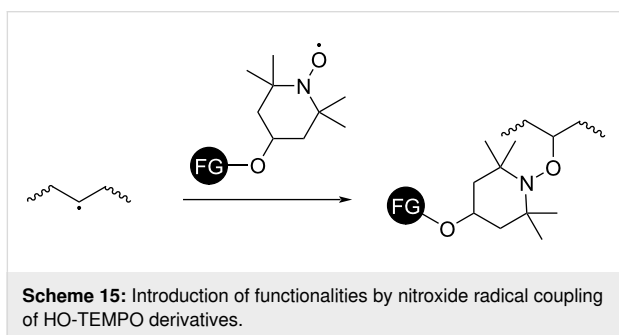
3.1 Post-polymerization modification

Radical addition is a popular technique for post-polymerization modification of double-bond-containing polymers (Scheme 14). Thiol–ene and thiol–yne “click chemistry” are highly efficient radical processes well-adopted in synthetic chemistry, material fabrication, and chemical biology (cf. section 2.2) [97,98]. The S[•] radical is typically generated using a thermal initiator or a photochemical process [99,100]. 1,3-Diene polymers are most commonly modified via thiol–ene chemistry through the pendant vinyl after the polymerization [101] and this technique can be traced back to 1948 [102]. The excellent temporal and spatial control of the available photochemical approach makes the technique especially viable for non-solution processes [103]. When a multifunctional thiol is used with diene-functionalized polymers, the approach becomes suitable for chemical cross-linking [103,104], *vide infra*. It has been used to cure a liquid isoprene polymer in precise digital light processing 3D printing [105]. Recently, Kanbayashi et al. reported that thiol–ene chemistry would not cause racemization of an asymmetric center linked to a pendant vinyl group, which can be particularly valuable for functionalization of optically active polymers [106]. Theato and co-workers introduced vinyl/alkyne-bearing poly(vinyl ether)s [107], poly(vinylcyclopropanes) [108], and poly(allyl 2-ylideneacetate) [109] as promising new platforms compatible to thiol–ene chemistry. Atom transfer radical addition (ATRA) is another process that usually qualifies for a definition of “click chemistry” [44]. A similar radical addition to vinyl groups takes place in ATRA despite the halogen atom transfer is mediated by a metal complex. Post-polymerization modification by ATRA was pioneered by Jérôme and co-workers [110,111]. In 2014, Xu et al. demonstrated that it can be extended to a milder photochemical process as well [112].



Radical coupling may also be used to introduce functional groups into polymer backbones. In this context, rapid radical trapping with stable nitroxide radicals is an efficient way [113]. However, this technique requires radical generation on the polymer backbone. A typical approach involves hydrogen abstraction by organic oxidants such as oxygen radicals from peroxide initiators [114], which is similar to the radical cross-

linking process, vide infra. Radicals may also be generated thermally, through photoinduction, or by ATRP initiators incorporated in the polymer backbones [115–117]. TEMPO and its derivatives have a long history of application as radical trapping agents. Commercially available HO-TEMPO is a particularly useful platform for post-polymerization modification via radical coupling because of the chemical versatility of the hydroxy moiety (Scheme 15). Site-selective radical C–H activation has been proven to be a useful tool to functionalize relatively inert polymer backbones and upcycling of polymer waste (cf. section 4) [118,119]. Radical chain-end modification as a highly specific type of post-polymerization modification introduces or removes functionalities at polymer chain ends [120].



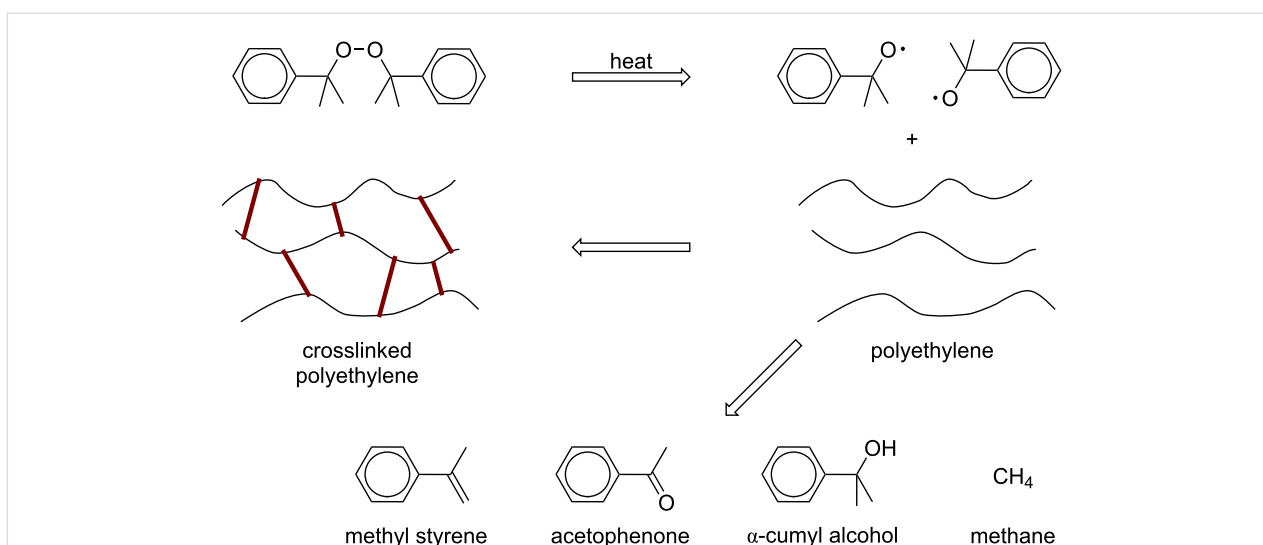
3.2 Chemical crosslinking of polymers

Chemical crosslinking is a suitable approach to increase chemical resistance [121], mechanical strength [122], and other properties [123] of polymers. In 1830s, Charles Goodyear invented vulcanized rubber. By heating natural rubber with lead oxide and sulfur, the temperature-sensitive rubber became a more stable material, even at high and low temperatures, while

keeping the elasticity, plasticity, insulation, and other excellent characteristics [124]. During the vulcanization of natural rubber, elemental sulfur was heated to form sulfur radicals which then react with natural rubber crosslinking two independent polymer molecules [125]. This is a typical example of polymer crosslinking by a radical mechanism.

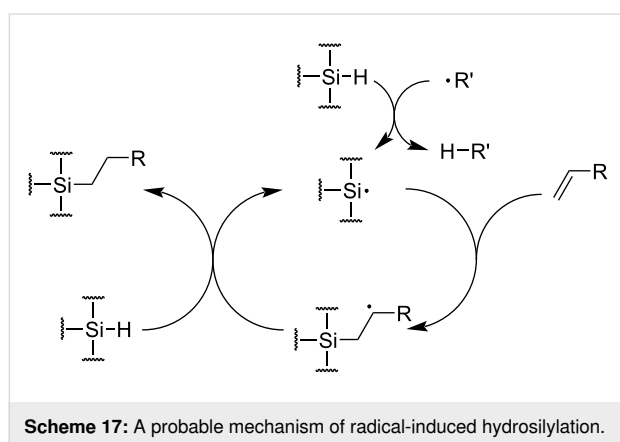
As the traditional vulcanization process, an initiator is needed to start the radical crosslinking. Besides sulfur, peroxides such as di-*tert*-butylcumyl peroxide (BCUP) and dicumyl peroxide (DCP) are often used in radical crosslinking. Free radicals are generated at the peroxides' decomposition temperature and attack the polymer chains to achieve crosslinking (Scheme 16). In dry crosslinking processing of crosslinked polyethylene (XLPE) used in power delivery system, a blend of DCP in low-density polyethylene (LDPE) is extruded at its melting point. In comparison to LDPE, the operational temperature and the short-circuit permissible temperature of XLPE cables are increased from 70 °C to 90 °C and 150 °C to 230 °C, respectively. Besides that, XLPE shows a more rubber-like behavior [126]. As the peroxide crosslinking process is industrially important, multiple kinetic models have been established to understand the reaction between polymers, peroxides, and monomers [127–129].

Polysiloxanes are another class of crosslinkable polymers. Modern silicone industry typically uses Pt-catalyzed hydrosilylation to crosslink multi-vinyl polysiloxane with silicon hydride compounds to manufacture silicone rubbers [130]. However, hydrosilylation may also be achieved via a radical mechanism (Scheme 17). In comparison to the Pt-catalyzed system, the radical-induced hydrosilylation has a lower cost, better toler-



Scheme 16: Chemical reaction process scheme of DCP-induced crosslinking of LDPE. Scheme 16 redrawn from [126].

ance to coordinating functionalities, and yields products without metal residues, but its efficiency is inferior to transition-metal catalyzed methods. Silicone rubber was prepared in such a process [131]. Pan and co-workers recently reported a photo-redox hydrosilylation process compatible to both electron-sufficient and -deficient vinyl species [86], and applicable to both post-polymerization modification and crosslinking of polymers bearing pendant vinyl groups [132], demonstrating a promising new orientation of radical hydrosilylation. It is noteworthy, that since the 1940s, polysiloxanes were crosslinked via hydrogen abstraction from Si-CH₃ and a radical coupling mechanism like polyolefins, *vide supra* [133].



Irradiation can also lead to the crosslinking of polymers. Polymeric materials may become brittle or colored after being exposed to sunlight for a long time, which was called 'photo-ageing' [134]. In fact, the light sensitivity of many polymers results from some impurities or additives remaining in polymer materials, which can form radical species through irradiation. This photooxidation process can lead to the generation of some small molecules or chain scissoring. At the same time, the photooxidation process can also result in crosslinking of polymer backbones [135]. Bousquet and Fouassier [135] investigated the photooxidation and crosslinking of photosensitized elastomers. Samples of an EPDM (ethylene-propenebutadiene) terpolymer were prepared with different additives. Observable crosslinking products were obtained through irradiation of different wavelengths. Besides the side reactions induced during photoageing, rational photocrosslinking of polymers is also feasible in the presence of photoinitiators or photoresponsive moieties [136–138]. Sophisticatedly designed photocrosslinking of polymers finds broad applications in modern 3D printing/additive manufacturing [139–142].

Radical chemistry has been demonstrated as a powerful tool for polymer crosslinking and preparation of materials with enhanced properties.

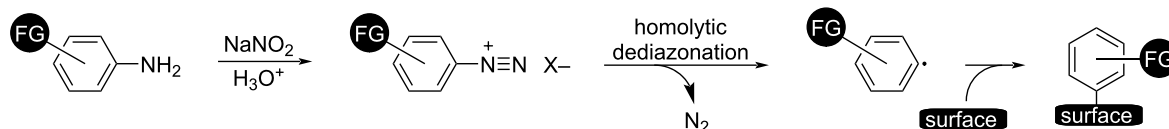
3.3 Polymer surface modification

When modifying the surface of polymers, chemical selectivity typically plays a minor role, while harsh reaction conditions are useful for the modification of chemically inert substrates. Here, radical chemistry comes into play. When polymer surfaces are modified by radical chemistry, radicals are either generated directly on the polymers or on modifiers. In the latter case, a radical addition, substitution, or coupling reaction takes place to complete the modification. Radicals can be generated by a broader selection of homogeneous and heterogeneous approaches, including hydrogen atom abstraction, decomposition of immobilized initiators, electrochemical redox reaction, or irradiation because the reactions only need to take place at the surface.

Small-molecule oxidants, such as organic peroxides, hydrogen peroxide, persulfates undergo homolysis of O–O bonds generating radicals that can break C–H bonds followed by a hydrogen abstraction reaction. Phenolic compounds can be oxidized by molecular oxygen in the presence of laccase, and the resulting phenolic radical reacts with poly(ethersulfone) [143]. Highly reactive gaseous species may also generate radicals on polymer surfaces. For example, atomic oxygen radical anions emitted from 12CaO·7Al₂O₃ crystals [144] were used to modify PVC and polystyrene [145,146]. Plasma is also a powerful gas-phase tool for polymer surface modification and radical generation [147,148]. It can even generate radicals on otherwise inert fluoropolymer surfaces [149].

Electrochemical reactions are another approach to generate radicals at polymer surfaces. Hydroxyl radicals generated via the electro-Fenton reaction from H₂O₂ in the presence of the Fe³⁺ were used to functionalize polypropylene surfaces [150,151]. Using a scanning electrochemical microscope, highly oxidative Ag(II) and NO₃[•] species were generated at a polymer surface [152], and oxidized the organic surface via a radical process. The homolytic dediazonation of diazonium salts produces highly reactive aryl radicals (Scheme 18) [153]. The chemical conversion can be initiated by electrochemical reduction [154], a reducing agent [155–157], a base [158], heating [159], or photochemically [160]. Aryl radicals may act as a halogen abstractor for alkyl halides and generate alkyl radicals for surface modification [161]. Electrochemical surface modification also works for inert PTFE surfaces in the presence of a 2,2'-dipyridyl redox mediator [162].

Photons and high-energy charged particles can transfer their energy to bound electrons in atoms, exciting the electron to a higher energy level or even the vacuum, generating radical species. The energy of UV photons is comparable to the energy of chemical bonds [163], and therefore photons are particularly

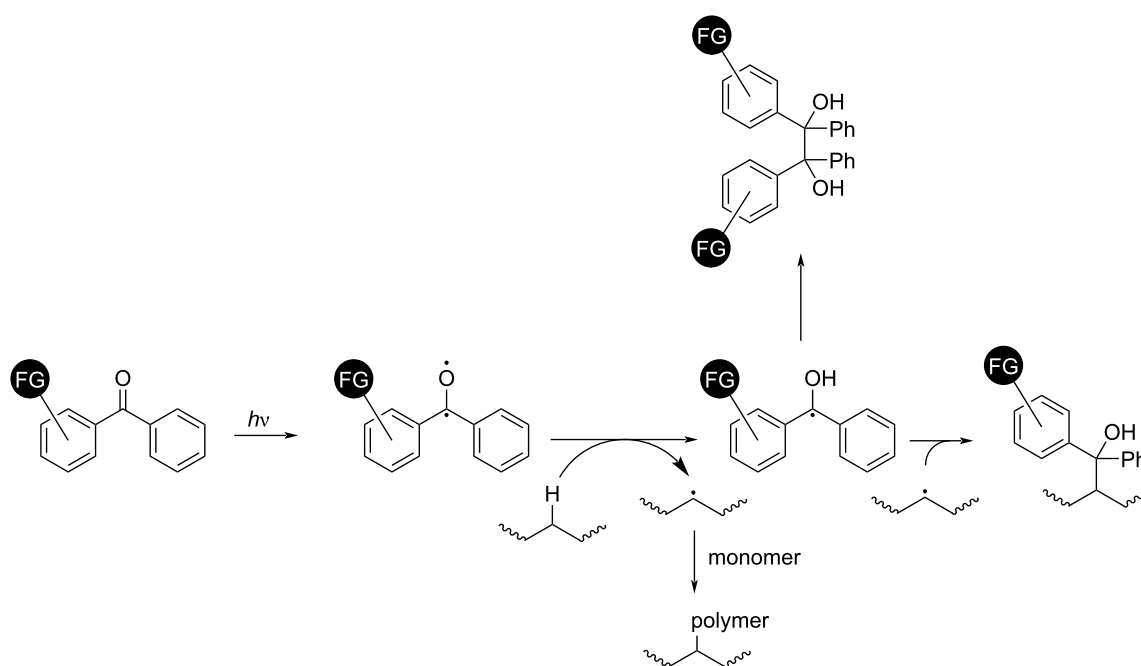


Scheme 18: Polymer surface modification by homolytic dediazonation of diazonium salts.

suitable for driving chemical reactions on polymer surfaces. Benzophenone is the best-established source of radicals on polymer surfaces. Its photoexcitation and subsequent reaction with polymers have been studied for decades [164–166]. When irradiated at around 360 nm, benzophenone undergoes excitation to a triplet state with biradical behavior. It then abstracts a hydrogen atom from the polymer resulting in a $\text{Ph}_2\text{C}^\bullet$ species and a radical on the polymer (Scheme 19). This reaction may complete in radical coupling or proceed with radical polymerization from the surface [167–169], resulting in crosslinked polymers, surface-functionalized polymers, or surface-grafted polymers. RDRP was used to graft well-defined polymer brushes from polymer surfaces [170,171]. Photoinduced processes, including photoATRP and PET-RAFT were used [172–175]. Poly(aryl ether ketone)s such as poly(ether ether ketone), bearing a diaryl ketone moiety resembling that of benzophenone, can generate biradicals upon UV irradiation without a photoinitiator [176,177]. Grafted polymers and untethered polymers are generated simultaneously in the presence of a monomer.

Ionizing radiation including high-energy photons (X-rays and γ -rays) and charged α - or β -particles generate charged particles, especially electrons, emitted from the surface of polymers [178]. When a high-energy photon impacts an atomic electron, part of the photon energy is transferred to the electron leading to excitation or ionization and radical formation, and a deflected photon with lower energy is emitted, ready to impact another electron. This process is called Compton scattering [179]. One of the major purposes of radiation modification of polymer surfaces is grafting. The surface grafting can be simply tuned by the dose of radiation [180]. Radiation grafting on polymer surfaces is also compatible with RDRP for high density and well-defined polymer grafts [181–184]. Polymer surfaces can also be modified using electron and ion beams [185,186]. Komatsu et al. reported surface-initiated ATRP from electron-beam irradiated polymer surfaces [187].

The radical chemistry used for post-polymerization modification, crosslinking, and polymer surface modification has many



Scheme 19: Photoinduced polymer surface modification or surface grafting using benzophenone.

aspects in common. The key is to activate chemically unreactive polymer backbones with highly reactive radical species to construct new chemical bonds.

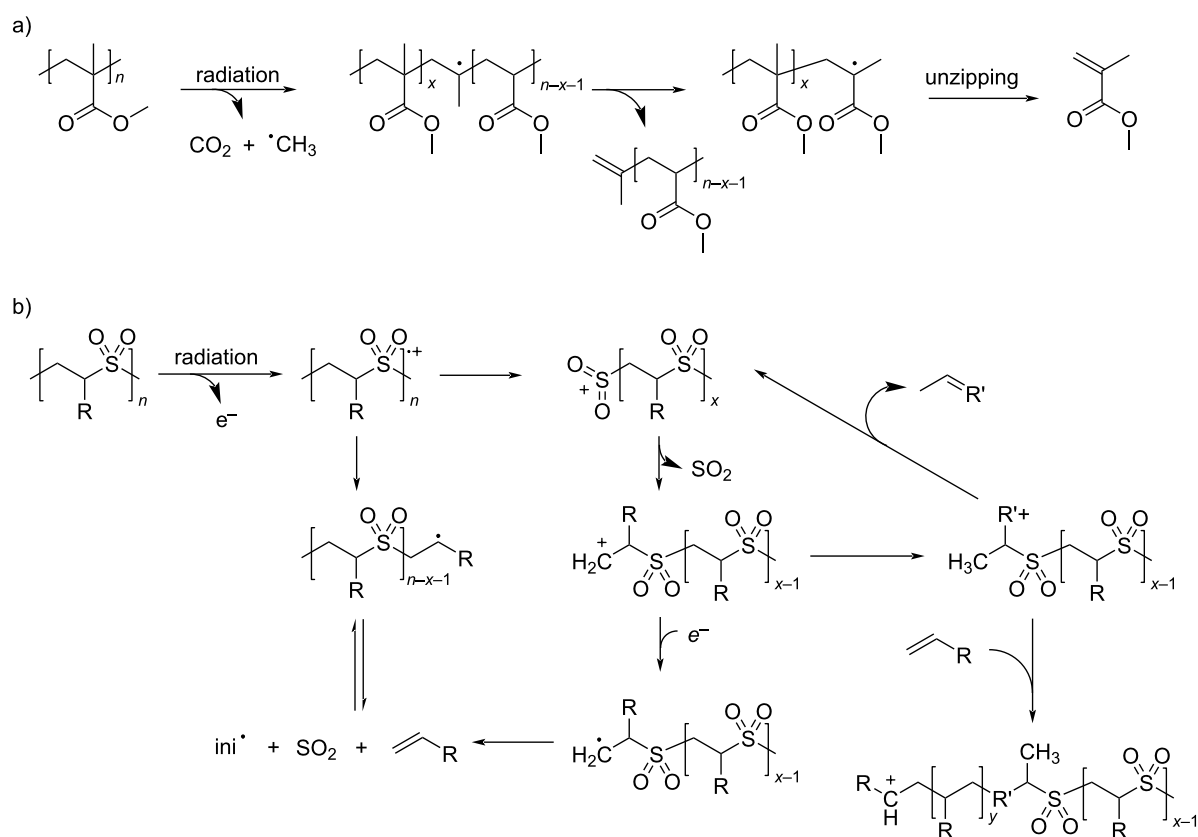
4 Radical depolymerization

Radical destruction of polymer chains is an undesirable side reaction sometimes observed in the post-polymerization modification. However, it is also an important chemical process in several circumstances.

Photoresist is one of the bedrocks of the semiconductor industry [188,189]. There are two types of photoresists, positive and negative photoresists, and they become more or less soluble upon radiation, respectively. Some early negative photoresists undergo a photochemical crosslinking process of 1,3-diene cyclic polymers [190] (cf. section 3.2), but such systems are no longer studied due to the poor resolution and sensitivity. On the other hand, positive resists based on decomposition of polymers, especially upon radiation with an electron beam, because of its narrow wavelengths, are still regarded as a promising alternative. Poly(methyl methacrylate) has a long history of being used as a positive resist [191,192]. It undergoes a scission by a

Norrish-type I reaction followed by radical unzipping depolymerization under photon or β -irradiation (Scheme 20a). Similarly, poly(olefin sulfone) undergoes depolymerization upon irradiation of light or electron beams [193,194]. It is an alternating copolymer of 1-olefins and SO_2 , and therefore the decomposition products are mostly gaseous [195]. While the depolymerization in both systems has a thermodynamic origin [196], the mechanism of poly(olefin sulfone) depolymerization is much more complex. Bowmer et al. proposed a simultaneous radical/cationic process (Scheme 20b) [197]. Meanwhile, an anionic process is also possible in the presence of a photogenerated base [198].

Thanks to their low cost, light weight, and durability, polymeric materials are ubiquitous in modern life. However, over the past decades, people have become aware of the environmental impact of polymeric wastes [199]. One of the approaches to tackle this crisis is upcycling of polymeric wastes, i.e., chemical conversion of polymeric wastes into high-value raw materials [200]. Upcycling of polyesters has been extensively studied in recent years [201]. Nevertheless, upcycling of vinyl polymers, which comprise a major portion of commercial



Scheme 20: Depolymerization mechanism of common photoresists. (a) A possible mechanism of radiation decomposition of poly(methyl methacrylate). (b) A proposed mechanism of simultaneous radical/cationic decomposition of poly(olefin sulfone) upon radiation [197].

polymers, remains a great challenge because of their relatively unreactive backbones. Pyrolysis of such polymers is currently experimented by the industry to recover a variety of small molecules. Researchers have introduced radical depolymerization of vinyl polymers as a promising candidate for this task. Oh and Stache reported the photooxidation of polystyrene in the presence of FeCl_3 as a radical source (Scheme 21a) [202]. A molar yield of 23% benzoyl small molecules was achieved. Reisner and co-workers employed a similar approach but using aromatic ketones as photocatalyst (Scheme 21b) [203]. Benzoic acid and other aromatic small molecules were recovered at a yield of $\approx 40\%$ and $\approx 20\%$, respectively. Both processes were carried out under relatively mild conditions, paving a route toward a greener future of vinyl polymer upcycling. However, the yield and value of the small molecules produced in photooxidative depolymerization are still relatively low. Thermodynamics dominates the depolymerization of methacrylates [204,205]. Therefore, pyrolysis of PMMA gives a relatively high conversion to its monomer and the purification is straightforward [206,207].

Polyethylene and polypropylene make up a major fraction of commercial polymers. However, their upcycling is much more challenging. Uncontrolled radical depolymerization of these polymers in thermal processes typically gives low-value fuels and wax [208–210]. Kong et al. recently demonstrated a photothermal radical process for the conversion of polyethylene and polypropylene into blending compatibilizers [211].

Radical depolymerization capability can be incorporated at synthesis. Wang et al. introduced photodegradability to polyolefins by copolymerization of carbon monoxide [212]. Nevertheless, radical depolymerization is an essential tool to tackle the problem of polymer wastes.

Conclusion

Radical chemistry has been deeply intertwined with the development of polymer science. Conventional free radical polymerization contributes to a major portion of modern polymer industry while novel polymerization techniques involving radicals emerged in the past decades to enable a rich selection of precisely controlled, high-value polymeric materials. The extremely high reactivity of radical species enabled efficient polymer modifications and depolymerizations with applications in many aspects essential to the advancement of the human society. Since the dawn of polymer science, it has been inextricably linked to organic chemistry. However, the two fields took divergent paths over the past century. Many emergent radical chemistries in the organic chemistry community has not yet found a place in the polymer science. We believe this gap will narrow with a broader use of chemical informatics tools and in-depth dialogs between the organic and polymer communities. Therefore, future opportunities for polymer science evolution lie in the collaboration of radical chemists in both communities.

Used abbreviations in the text and their explanations are collected in Table 2.

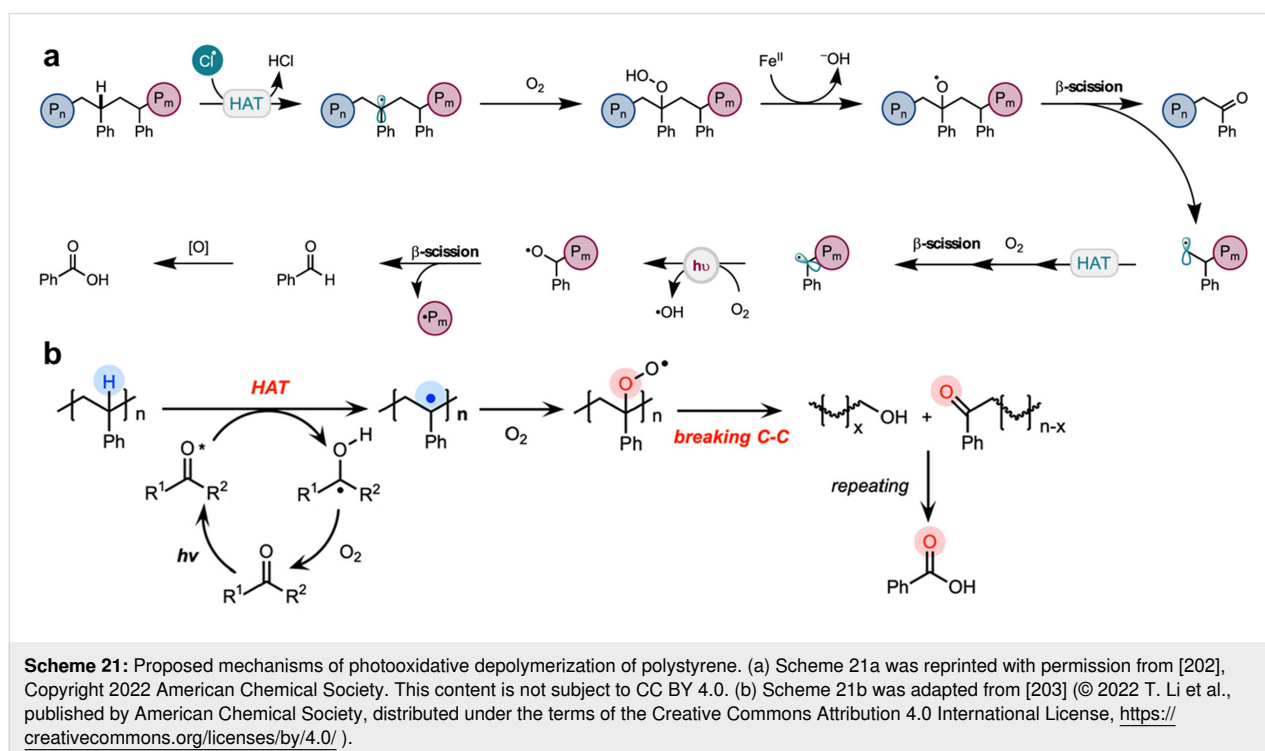


Table 2: Abbreviations used.

Abbreviation	Explanation
ATRA	atom transfer radical addition
ATRP	atom transfer radical polymerization
BCUP	di- <i>tert</i> -butylcumyl peroxide
BPO	benzoyl peroxide
CRP	controlled radical polymerization
CSIRO	Commonwealth Scientific and Industrial Research Organization
CTAs	chain transfer agents
DCP	dicumyl peroxide
DCPD	dicyclopentadiene
DOPA	L-3,4-dihydroxyphenylalanine
HO-TEMPO	4-hydroxy-2,2,6,6-tetramethylpiperidine-1-oxyl
ITP	iodine transfer polymerization
IUPAC	International Union of Pure and Applied Chemistry
LDPE	low-density polyethylene
mfp	mussel foot protein
MMA	methyl methacrylate
MF-ROMP	metal-free ring opening metathesis polymerization
NMP	nitroxide-mediated polymerization
OMRP	organometallic-mediated radical polymerization
PAA	polyacrylic acid
PAN	polyacrylonitrile
PAM	polyacrylamide
PAT	poly(3-alkylthiophene)
PC	photocatalyst
PET-RAFT	photoinduced electron/energy transfer reversible addition–fragmentation chain transfer (polymerization)
PMMA	poly(methyl methacrylate)
PS	polystyrene
PTFE	polytetrafluoroethylene
PVA	poly(vinyl alcohol)
PVC	poly(vinyl chloride)
RAFT	reversible addition-fragmentation chain transfer
RDRP	reversible deactivation radical polymerization
RITP	reverse iodine transfer polymerization
ROMP	ring opening metathesis polymerization
TEMPO	2,2,6,6-tetramethylpiperidine-1-oxyl
UV	ultraviolet
XLPE	crosslinked polyethylene

Funding

This work is sponsored by Science and Technology Commission of Shanghai Municipality (Grant No. 22YF1428200) and the start-up fund at ShanghaiTech University.

Acknowledgements

We thank Prof. Yifan Li for his constructive discussions.

ORCID® iDs

Zixiao Wang - <https://orcid.org/0000-0003-2627-6630>

Feichen Cui - <https://orcid.org/0009-0001-0763-7536>

Yang Sui - <https://orcid.org/0009-0009-5396-6769>

Jiajun Yan - <https://orcid.org/0000-0003-3286-3268>

References

1. Staudinger, H. *Ber. Dtsch. Chem. Ges.* **1920**, *53*, 1073–1085. doi:10.1002/cber.19200530627
2. Nesvadba, P. Radical Polymerization in Industry. In *Encyclopedia of Radicals in Chemistry, Biology and Materials*; Chatgililoglu, C.; Studer, A., Eds.; John Wiley & Sons, 2012. doi:10.1002/9781119953678.rad080
3. Lyu, Q.; Hsueh, N.; Chai, C. L. *ACS Biomater. Sci. Eng.* **2019**, *5*, 2708–2724. doi:10.1021/acsbomaterials.9b00281
4. Yang, J.; Cohen Stuart, M. A.; Kamperman, M. *Chem. Soc. Rev.* **2014**, *43*, 8271–8298. doi:10.1039/c4cs00185k
5. Yang, J.; Chen, N.; Zhu, J.; Cai, J.; Deng, J.; Pan, F.; Gao, L.; Jiang, Z.; Shen, F. *Sci. Rep.* **2020**, *10*, 12867. doi:10.1038/s41598-020-69823-0
6. Kumanotani, J. *Prog. Org. Coat.* **1995**, *26*, 163–195. doi:10.1016/0300-9440(95)00559-5
7. Snyder, D. M. *J. Chem. Educ.* **1989**, *66*, 977. doi:10.1021/ed066p977
8. Kumanotani, J. *Prog. Org. Coat.* **1998**, *34*, 135–146. doi:10.1016/s0300-9440(97)00115-x
9. Xia, J.; Lin, J.; Xu, Y.; Chen, Q. *ACS Appl. Mater. Interfaces* **2011**, *3*, 482–489. doi:10.1021/am1010578
10. Krogsgaard, M.; Nue, V.; Birkedal, H. *Chem. – Eur. J.* **2016**, *22*, 844–857. doi:10.1002/chem.201503380
11. Priemel, T.; Palia, G.; Förste, F.; Jehle, F.; Sviben, S.; Mantouvalou, I.; Zaslansky, P.; Bertinetti, L.; Harrington, M. *J. Science* **2021**, *374*, 206–211. doi:10.1126/science.abi9702
12. Yu, M.; Hwang, J.; Deming, T. J. *J. Am. Chem. Soc.* **1999**, *121*, 5825–5826. doi:10.1021/ja990469y
13. Jenkins, A. D.; Kratochvíl, P.; Stepto, R. F. T.; Suter, U. W. *Pure Appl. Chem.* **1996**, *68*, 2287–2311. doi:10.1351/pac199668122287
14. Matyjaszewski, K.; Tsarevsky, N. V. *J. Am. Chem. Soc.* **2014**, *136*, 6513–6533. doi:10.1021/ja408069v
15. Sugihara, S. *Polym. J.* **2022**, *54*, 1407–1418. doi:10.1038/s41428-022-00698-w
16. Abreu, C. M. R.; Fonseca, A. C.; Rocha, N. M. P.; Guthrie, J. T.; Serra, A. C.; Coelho, J. F. J. *Prog. Polym. Sci.* **2018**, *87*, 34–69. doi:10.1016/j.progpolymsci.2018.06.007
17. Jenkins, A. D.; Jones, R. G.; Moad, G. *Pure Appl. Chem.* **2009**, *82*, 483–491. doi:10.1351/pac-rep-08-04-03
18. Pirman, T.; Ocepek, M.; Likozar, B. *Ind. Eng. Chem. Res.* **2021**, *60*, 9347–9367. doi:10.1021/acs.iecr.1c01649
19. Tsarevsky, N. V.; Matyjaszewski, K. *Chem. Rev.* **2007**, *107*, 2270–2299. doi:10.1021/cr050947p
20. Moad, G.; Rizzardo, E.; Thang, S. H. *Acc. Chem. Res.* **2008**, *41*, 1133–1142. doi:10.1021/ar800075n

21. Lacroix-Desmazes, P.; Tonnar, J. Degenerative Transfer with Alkyl Iodide. In *Polymer Science: A Comprehensive Reference*; Matyjaszewski, K.; Möller, M., Eds.; Elsevier: Amsterdam, Netherlands, 2012; pp 159–180. doi:10.1016/b978-0-444-53349-4.00065-0
22. Norrish, R. G. W.; Smith, R. R. *Nature* **1942**, *150*, 336–337. doi:10.1038/150336a0
23. Dong, H.; Tang, W.; Matyjaszewski, K. *Macromolecules* **2007**, *40*, 2974–2977. doi:10.1021/ma070424e
24. Odell, P. G.; Veregin, R. P. N.; Michalak, L. M.; Brousmiche, D.; Georges, M. K. *Macromolecules* **1995**, *28*, 8453–8455. doi:10.1021/ma00128a073
25. Jones, G. R.; Li, Z.; Anastasaki, A.; Lloyd, D. J.; Wilson, P.; Zhang, Q.; Haddleton, D. M. *Macromolecules* **2016**, *49*, 483–489. doi:10.1021/acs.macromol.5b01994
26. Slomkowski, S.; Alemán, J. V.; Gilbert, R. G.; Hess, M.; Horie, K.; Jones, R. G.; Kubisa, P.; Meisel, I.; Mormann, W.; Penczek, S.; Stepto, R. F. T. *Pure Appl. Chem.* **2011**, *83*, 2229–2259. doi:10.1351/pac-rec-10-06-03
27. Szwarc, M.; Levy, M.; Milkovich, R. *J. Am. Chem. Soc.* **1956**, *78*, 2656–2657. doi:10.1021/ja01592a101
28. Parkatzidis, K.; Wang, H. S.; Truong, N. P.; Anastasaki, A. *Chem* **2020**, *6*, 1575–1588. doi:10.1016/j.chempr.2020.06.014
29. Otsu, T.; Yoshida, M. *Makromol. Chem., Rapid Commun.* **1982**, *3*, 127–132. doi:10.1002/marc.1982.030030208
30. Solomon, D. H.; Rizzardo, E.; Cacioli, P. Polymerization process and polymers produced thereby. U.S. Patent US4581429, July 11, 1986.
31. Georges, M. K.; Veregin, R. P. N.; Kazmaier, P. M.; Hamer, G. K. *Macromolecules* **1993**, *26*, 2987–2988. doi:10.1021/ma00063a054
32. Hawker, C. J.; Barclay, G. G.; Orellana, A.; Dao, J.; Devonport, W. *Macromolecules* **1996**, *29*, 5245–5254. doi:10.1021/ma951905d
33. Hawker, C. J. *J. Am. Chem. Soc.* **1994**, *116*, 11185–11186. doi:10.1021/ja00103a055
34. Hawker, C. J. *Angew. Chem., Int. Ed. Engl.* **1995**, *34*, 1456–1459. doi:10.1002/anie.199514561
35. Nicolas, J.; Guillaneuf, Y.; Lefay, C.; Bertin, D.; Gimes, D.; Charleux, B. *Prog. Polym. Sci.* **2013**, *38*, 63–235. doi:10.1016/j.progpolymsci.2012.06.002
36. Moad, G.; Rizzardo, E. *Macromolecules* **1995**, *28*, 8722–8728. doi:10.1021/ma00130a003
37. Chang, C.-C.; Siegenthaler, K. O.; Studer, A. *Helv. Chim. Acta* **2006**, *89*, 2200–2210. doi:10.1002/hlca.200690206
38. Siegenthaler, K. O.; Studer, A. *Macromolecules* **2006**, *39*, 1347–1352. doi:10.1021/ma0513463
39. Miura, Y.; Nakamura, N.; Taniguchi, I.; Ichikawa, A. *Polymer* **2003**, *44*, 3461–3467. doi:10.1016/s0032-3861(03)00275-1
40. Grimaldi, S.; Finet, J.-P.; Le Moigne, F.; Zeghdaoui, A.; Tordo, P.; Benoit, D.; Fontanille, M.; Gnanou, Y. *Macromolecules* **2000**, *33*, 1141–1147. doi:10.1021/ma9913414
41. Wang, J.-S.; Matyjaszewski, K. *J. Am. Chem. Soc.* **1995**, *117*, 5614–5615. doi:10.1021/ja00125a035
42. Kato, M.; Kamigaito, M.; Sawamoto, M.; Higashimura, T. *Macromolecules* **1995**, *28*, 1721–1723. doi:10.1021/ma00109a056
43. Matyjaszewski, K. *Macromolecules* **2012**, *45*, 4015–4039. doi:10.1021/ma3001719
44. Pintauer, T.; Matyjaszewski, K. *Chem. Soc. Rev.* **2008**, *37*, 1087–1097. doi:10.1039/b714578k
45. Xia, J.; Matyjaszewski, K. *Macromolecules* **1997**, *30*, 7692–7696. doi:10.1021/ma9710085
46. Gromada, J.; Matyjaszewski, K. *Macromolecules* **2001**, *34*, 7664–7671. doi:10.1021/ma010864k
47. Min, K.; Gao, H.; Matyjaszewski, K. *J. Am. Chem. Soc.* **2005**, *127*, 3825–3830. doi:10.1021/ja0429364
48. Matyjaszewski, K.; Jakubowski, W.; Min, K.; Tang, W.; Huang, J.; Braunecker, W. A.; Tsarevsky, N. V. *Proc. Natl. Acad. Sci. U. S. A.* **2006**, *103*, 15309–15314. doi:10.1073/pnas.0602675103
49. Jakubowski, W.; Matyjaszewski, K. *Angew. Chem., Int. Ed.* **2006**, *45*, 4482–4486. doi:10.1002/anie.200600272
50. Matyjaszewski, K.; Tsarevsky, N. V.; Braunecker, W. A.; Dong, H.; Huang, J.; Jakubowski, W.; Kwak, Y.; Nicolay, R.; Tang, W.; Yoon, J. A. *Macromolecules* **2007**, *40*, 7795–7806. doi:10.1021/ma0717800
51. Chmielarz, P.; Fantin, M.; Park, S.; Isse, A. A.; Gennaro, A.; Magenau, A. J. D.; Sobkowiak, A.; Matyjaszewski, K. *Prog. Polym. Sci.* **2017**, *69*, 47–78. doi:10.1016/j.progpolymsci.2017.02.005
52. Magenau, A. J. D.; Strandwitz, N. C.; Gennaro, A.; Matyjaszewski, K. *Science* **2011**, *332*, 81–84. doi:10.1126/science.1202357
53. Kwak, Y.; Matyjaszewski, K. *Macromolecules* **2010**, *43*, 5180–5183. doi:10.1021/ma100850a
54. Pan, X.; Tasdelen, M. A.; Laun, J.; Junkers, T.; Yagci, Y.; Matyjaszewski, K. *Prog. Polym. Sci.* **2016**, *62*, 73–125. doi:10.1016/j.progpolymsci.2016.06.005
55. Mohapatra, H.; Kleiman, M.; Esser-Kahn, A. P. *Nat. Chem.* **2017**, *9*, 135–139. doi:10.1038/nchem.2633
56. Schröder, K.; Mathers, R. T.; Buback, J.; Konkolewicz, D.; Magenau, A. J. D.; Matyjaszewski, K. *ACS Macro Lett.* **2012**, *1*, 1037–1040. doi:10.1021/mz3003787
57. Pan, X.; Fantin, M.; Yuan, F.; Matyjaszewski, K. *Chem. Soc. Rev.* **2018**, *47*, 5457–5490. doi:10.1039/c8cs00259b
58. Treat, N. J.; Sprafke, H.; Kramer, J. W.; Clark, P. G.; Barton, B. E.; Read de Alaniz, J.; Fors, B. P.; Hawker, C. J. *J. Am. Chem. Soc.* **2014**, *136*, 16096–16101. doi:10.1021/ja510389m
59. Matyjaszewski, K.; Tsarevsky, N. V. *Nat. Chem.* **2009**, *1*, 276–288. doi:10.1038/nchem.257
60. Matyjaszewski, K. *Adv. Mater. (Weinheim, Ger.)* **2018**, *30*, 1706441. doi:10.1002/adma.201706441
61. Chiefari, J.; Chong, Y. K.; Ercole, F.; Krstina, J.; Jeffery, J.; Le, T. P. T.; Mayadunne, R. T. A.; Meijs, G. F.; Moad, C. L.; Moad, G.; Rizzardo, E.; Thang, S. H. *Macromolecules* **1998**, *31*, 5559–5562. doi:10.1021/ma9804951
62. Mayadunne, R. T. A.; Rizzardo, E.; Chiefari, J.; Krstina, J.; Moad, G.; Postma, A.; Thang, S. H. *Macromolecules* **2000**, *33*, 243–245. doi:10.1021/ma991451a
63. Chong, Y. K.; Le, T. P. T.; Moad, G.; Rizzardo, E.; Thang, S. H. *Macromolecules* **1999**, *32*, 2071–2074. doi:10.1021/ma981472p
64. Barner-Kowollik, C.; Quinn, J. F.; Morsley, D. R.; Davis, T. P. *J. Polym. Sci., Part A: Polym. Chem.* **2001**, *39*, 1353–1365. doi:10.1002/pola.1112
65. Xu, J.; Jung, K.; Atme, A.; Shanmugam, S.; Boyer, C. *J. Am. Chem. Soc.* **2014**, *136*, 5508–5519. doi:10.1021/ja501745g
66. Allegrezza, M. L.; Konkolewicz, D. *ACS Macro Lett.* **2021**, *10*, 433–446. doi:10.1021/acsmacrolett.1c00046
67. Lv, C.; He, C.; Pan, X. *Angew. Chem., Int. Ed.* **2018**, *57*, 9430–9433. doi:10.1002/anie.201805212
68. Moad, G.; Rizzardo, E.; Thang, S. H. *Aust. J. Chem.* **2006**, *59*, 669–692. doi:10.1071/ch06250

69. Hurtgen, M.; Detrembleur, C.; Jerome, C.; Debuigne, A. *Polym. Rev. (Philadelphia, PA, U. S.)* **2011**, *51*, 188–213. doi:10.1080/15583724.2011.566401
70. Allan, L. E. N.; Perry, M. R.; Shaver, M. P. *Prog. Polym. Sci.* **2012**, *37*, 127–156. doi:10.1016/j.progpolymsci.2011.07.004
71. Tatemoto, M.; Suzuki, T.; Tomoda, M.; Furukawa, Y.; Ueta, Y. Cross linkable fluorine-containing polymer and its production. U.S. Patent US4,243,770, Jan 6, 1981.
72. Lacroix-Desmazes, P.; Severac, R.; Boutevin, B. *Macromolecules* **2005**, *38*, 6299–6309. doi:10.1021/ma050056j
73. Li, N.; Pan, X.-C. *Chin. J. Polym. Sci.* **2021**, *39*, 1084–1092. doi:10.1007/s10118-021-2597-9
74. *Chem. Commun.* **2003**, 1–4. doi:10.1039/b210718j
75. Nezakati, T.; Seifalian, A.; Tan, A.; Seifalian, A. M. *Chem. Rev.* **2018**, *118*, 6766–6843. doi:10.1021/acs.chemrev.6b00275
76. Guo, X.; Facchetti, A. *Nat. Mater.* **2020**, *19*, 922–928. doi:10.1038/s41563-020-0778-5
77. Xu, C.; Dong, J.; He, C.; Yun, J.; Pan, X. *Giant* **2023**, *14*, 100154. doi:10.1016/j.giant.2023.100154
78. Niemi, V. M.; Knuuttila, P.; Österholm, J.-E.; Korvola, J. *Polymer* **1992**, *33*, 1559–1562. doi:10.1016/0032-3861(92)90138-m
79. McCullough, R. D. *Adv. Mater. (Weinheim, Ger.)* **1998**, *10*, 93–116. doi:10.1002/(sici)1521-4095(199801)10:2<93::aid-adma93>3.0.co;2-f
80. Posner, T. *Ber. Dtsch. Chem. Ges.* **1905**, *38*, 646–657. doi:10.1002/cber.190503801106
81. Hoyle, C. E.; Lee, T. Y.; Roper, T. *J. Polym. Sci., Part A: Polym. Chem.* **2004**, *42*, 5301–5338. doi:10.1002/pola.20366
82. Sticker, D.; Geczy, R.; Häfeli, U. O.; Kutter, J. P. *ACS Appl. Mater. Interfaces* **2020**, *12*, 10080–10095. doi:10.1021/acsami.9b22050
83. Sirrine, J. M.; Meenakshisundaram, V.; Moon, N. G.; Scott, P. J.; Mondschein, R. J.; Weiseman, T. F.; Williams, C. B.; Long, T. E. *Polymer* **2018**, *152*, 25–34. doi:10.1016/j.polymer.2018.02.056
84. Bhagat, S. D.; Chatterjee, J.; Chen, B.; Stiegman, A. E. *Macromolecules* **2012**, *45*, 1174–1181. doi:10.1021/ma202467a
85. Cook, C. C.; Fong, E. J.; Schwartz, J. J.; Porcincula, D. H.; Kaczmarek, A. C.; Oakdale, J. S.; Moran, B. D.; Champley, K. M.; Rackson, C. M.; Muralidharan, A.; McLeod, R. R.; Shusteff, M. *Adv. Mater. (Weinheim, Ger.)* **2020**, *32*, 2003376. doi:10.1002/adma.202003376
86. Huang, Z.; Chen, Z.; Jiang, Y.; Li, N.; Yang, S.; Wang, G.; Pan, X. *J. Am. Chem. Soc.* **2021**, *143*, 19167–19177. doi:10.1021/jacs.1c09263
87. Grubbs, R. H.; Carr, D. D.; Hoppin, C.; Burk, P. L. *J. Am. Chem. Soc.* **1976**, *98*, 3478–3483. doi:10.1021/ja00428a015
88. Kensy, V. K.; Tritt, R. L.; Haque, F. M.; Murphy, L. M.; Knorr, D. B., Jr.; Grayson, S. M.; Boydston, A. J. *Angew. Chem., Int. Ed.* **2020**, *59*, 9074–9079. doi:10.1002/anie.202000434
89. Wu, C.; Corrigan, N.; Lim, C.-H.; Liu, W.; Miyake, G.; Boyer, C. *Chem. Rev.* **2022**, *122*, 5476–5518. doi:10.1021/acs.chemrev.1c00409
90. Ogawa, K. A.; Goetz, A. E.; Boydston, A. J. *J. Am. Chem. Soc.* **2015**, *137*, 1400–1403. doi:10.1021/ja512073m
91. Pascual, L. M. M.; Dunford, D. G.; Goetz, A. E.; Ogawa, K. A.; Boydston, A. J. *Synlett* **2016**, *27*, 759–762. doi:10.1055/s-0035-1561330
92. Goetz, A. E.; Boydston, A. J. *J. Am. Chem. Soc.* **2015**, *137*, 7572–7575. doi:10.1021/jacs.5b03665
93. Goetz, A. E.; Pascual, L. M. M.; Dunford, D. G.; Ogawa, K. A.; Knorr, D. B., Jr.; Boydston, A. J. *ACS Macro Lett.* **2016**, *5*, 579–582. doi:10.1021/acsmacrolett.6b00131
94. Gauthier, M. A.; Gibson, M. I.; Klok, H.-A. *Angew. Chem., Int. Ed.* **2009**, *48*, 48–58. doi:10.1002/anie.200801951
95. Günay, K. A.; Theato, P.; Klok, H.-A. *J. Polym. Sci., Part A: Polym. Chem.* **2013**, *51*, 1–28. doi:10.1002/pola.26333
96. Larsen, M. B.; Herzog, S. E.; Quilter, H. C.; Hillmyer, M. A. *ACS Macro Lett.* **2018**, *7*, 122–126. doi:10.1021/acsmacrolett.7b00896
97. Hoyle, C. E.; Bowman, C. N. *Angew. Chem., Int. Ed.* **2010**, *49*, 1540–1573. doi:10.1002/anie.200903924
98. Fairbanks, B. D.; Scott, T. F.; Kloxin, C. J.; Anseth, K. S.; Bowman, C. N. *Macromolecules* **2009**, *42*, 211–217. doi:10.1021/ma801903w
99. Cramer, N. B.; Scott, J. P.; Bowman, C. N. *Macromolecules* **2002**, *35*, 5361–5365. doi:10.1021/ma0200672
100. Xu, J.; Boyer, C. *Macromolecules* **2015**, *48*, 520–529. doi:10.1021/ma502460t
101. Soares, F. A.; Steinbüchel, A. *Macromol. Biosci.* **2021**, *21*, 2100261. doi:10.1002/mabi.202100261
102. Serniuk, G. E.; Baner, F. W.; Swaney, M. W. *J. Am. Chem. Soc.* **1948**, *70*, 1804–1808. doi:10.1021/ja01185a046
103. Decker, C.; Viet, T. N. T. *Macromol. Chem. Phys.* **1999**, *200*, 1965–1974. doi:10.1002/(sici)1521-3935(19990801)200:8<1965::aid-macp1965>3.0.co;2-w
104. Thielke, M. W.; Bruckner, E. P.; Wong, D. L.; Theato, P. *Polymer* **2014**, *55*, 5596–5599. doi:10.1016/j.polymer.2014.09.002
105. Strohmeier, L.; Frommwald, H.; Schlögl, S. *RSC Adv.* **2020**, *10*, 23607–23614. doi:10.1039/d0ra04186f
106. Kanbayashi, N.; Miyamoto, S.; Ishido, Y.; Okamura, T.-a.; Onitsuka, K. *Polym. Chem.* **2017**, *8*, 985–994. doi:10.1039/c6py01946c
107. Butzelaar, A. J.; Schneider, S.; Molle, E.; Theato, P. *Macromol. Rapid Commun.* **2021**, *42*, 2100133. doi:10.1002/marc.202100133
108. Ntoukam, D. H. S.; Mutlu, H.; Theato, P. *Eur. Polym. J.* **2020**, *122*, 109319. doi:10.1016/j.eurpolymj.2019.109319
109. Krappitz, T.; Brauer, D.; Theato, P. *Polym. Chem.* **2016**, *7*, 4525–4530. doi:10.1039/c6py00818f
110. Riva, R.; Rieger, J.; Jérôme, R.; Lecomte, P. *J. Polym. Sci., Part A: Polym. Chem.* **2006**, *44*, 6015–6024. doi:10.1002/pola.21674
111. Riva, R.; Lenoir, S.; Jérôme, R.; Lecomte, P. *Polymer* **2005**, *46*, 8511–8518. doi:10.1016/j.polymer.2005.03.105
112. Xu, J.; Atme, A.; Marques Martins, A. F.; Jung, K.; Boyer, C. *Polym. Chem.* **2014**, *5*, 3321–3325. doi:10.1039/c4py00193a
113. Coiai, S.; Passaglia, E.; Cicogna, F. *Polym. Int.* **2019**, *68*, 27–63. doi:10.1002/pi.5664
114. Miller, J. L.; Lawrence, J.-M. I. A.; Rodriguez del Rey, F. O.; Floreancig, P. E. *Chem. Soc. Rev.* **2022**, *51*, 5660–5690. doi:10.1039/d1cs01169c
115. Mardyukov, A.; Studer, A. *Macromol. Rapid Commun.* **2013**, *34*, 94–101. doi:10.1002/marc.201200595
116. Wang, G.; Zhang, Y.; Huang, J. J. *J. Polym. Sci., Part A: Polym. Chem.* **2010**, *48*, 1633–1640. doi:10.1002/pola.23929
117. Amamoto, Y.; Higaki, Y.; Matsuda, Y.; Otsuka, H.; Takahara, A. *J. Am. Chem. Soc.* **2007**, *129*, 13298–13304. doi:10.1021/ja075447n

118. Hodges, M. N.; Elardo, M. J.; Seo, J.; Dohoda, A. F.; Michael, F. E.; Golder, M. R. *Angew. Chem., Int. Ed.* **2023**, *62*, e202303115. doi:10.1002/anie.202303115
119. Zhang, Z.; Li, X.; Zhou, D.; Ding, S.; Wang, M.; Zeng, R. *J. Am. Chem. Soc.* **2023**, *145*, 7612–7620. doi:10.1021/jacs.3c01100
120. Li, N.; Yang, S.; Huang, Z.; Pan, X. *Macromolecules* **2021**, *54*, 6000–6005. doi:10.1021/acs.macromol.1c00996
121. Gardel, M. L.; Shin, J. H.; MacKintosh, F. C.; Mahadevan, L.; Matsudaira, P.; Weitz, D. A. *Science* **2004**, *304*, 1301–1305. doi:10.1126/science.1095087
122. Zhang, X.; Wang, S.; Jiang, Z.; Li, Y.; Jing, X. *J. Am. Chem. Soc.* **2020**, *142*, 21852–21860. doi:10.1021/jacs.0c10244
123. Chen, J.; Garcia, E. S.; Zimmerman, S. C. *Acc. Chem. Res.* **2020**, *53*, 1244–1256. doi:10.1021/acs.accounts.0c00178
124. Fisher, H. L. *Ind. Eng. Chem.* **1939**, *31*, 1381–1389. doi:10.1021/ie50359a015
125. Coran, A. Y. Vulcanization. In *The Science and Technology of Rubber*, 4th ed.; Mark, J. E.; Erman, B.; Roland, C. M., Eds.; Academic Press: Boston, MA, USA, 2013; pp 337–381. doi:10.1016/b978-0-12-394584-6.00007-8
126. Huang, X. *High Voltage* **2020**, *5*, 229–230. doi:10.1049/hve.2020.0196
127. Likoza, B. *React. Funct. Polym.* **2011**, *71*, 11–22. doi:10.1016/j.reactfunctpolym.2010.11.004
128. Likoza, B.; Krajnc, M. *Polym. Eng. Sci.* **2009**, *49*, 60–72. doi:10.1002/pen.21218
129. Likoza, B.; Krajnc, M. *Chem. Eng. Process.* **2011**, *50*, 200–210. doi:10.1016/j.ccep.2010.12.007
130. Hofmann, R. J.; Vlatković, M.; Wiesbrock, F. *Polymers (Basel, Switz.)* **2017**, *9*, 534. doi:10.3390/polym9100534
131. Deriabina, K. V.; Dobrynina, M. V.; Islamova, R. M. *Dalton Trans.* **2020**, *49*, 8855–8858. doi:10.1039/d0dt01061h
132. Huang, Z.; Liu, K.; Liu, M.; Yun, J.; Dong, J.; Chen, Z.; Xie, Z.; Pan, X. *Chin. J. Chem.* **2023**, *41*, 2275–2281. doi:10.1002/cjoc.202300158
133. Wang, D.; Klein, J.; Mejía, E. *Chem. – Asian J.* **2017**, *12*, 1180–1197. doi:10.1002/asia.201700304
134. Rånby, B. G.; Rabek, J. F. *Photodegradation, Photo-oxidation, and Photostabilization of Polymers: Principles and Applications*; John Wiley & Sons: New York, NY, USA, 1975.
135. Bousquet, J. A.; Fouassier, J. P. *Polym. Degrad. Stab.* **1987**, *18*, 163–185. doi:10.1016/0141-3910(87)90029-2
136. Decker, C. *Prog. Polym. Sci.* **1996**, *21*, 593–650. doi:10.1016/0079-6700(95)00027-5
137. Lai, H.; Peng, X.; Li, L.; Zhu, D.; Xiao, P. *Prog. Polym. Sci.* **2022**, *128*, 101529. doi:10.1016/j.progpolymsci.2022.101529
138. Decker, C. *Macromol. Rapid Commun.* **2002**, *23*, 1067–1093. doi:10.1002/marc.200290014
139. Li, J.; Boyer, C.; Zhang, X. *Macromol. Mater. Eng.* **2022**, *307*, 2200010. doi:10.1002/mame.202200010
140. Bagheri, A.; Jin, J. *ACS Appl. Polym. Mater.* **2019**, *1*, 593–611. doi:10.1021/acsapm.8b00165
141. Zhang, J.; Xiao, P. *Polym. Chem.* **2018**, *9*, 1530–1540. doi:10.1039/c8py00157j
142. Bao, Y. *Macromol. Rapid Commun.* **2022**, *43*, 2200202. doi:10.1002/marc.202200202
143. Nady, N.; Schroën, K.; Franssen, M. C. R.; Lagen, B. v.; Murali, S.; Boom, R. M.; Mohyeldin, M. S.; Zuilhof, H. *ACS Appl. Mater. Interfaces* **2011**, *3*, 801–810. doi:10.1021/am101155e
144. Li, Q. X.; Hayashi, K.; Nishioka, M.; Kashiwagi, H.; Hirano, M.; Torimoto, Y.; Hosono, H.; Sadakata, M. *Appl. Phys. Lett.* **2002**, *80*, 4259–4261. doi:10.1063/1.1476958
145. Wang, L.; Yan, L.; Zhao, P.; Torimoto, Y.; Sadakata, M.; Li, Q. *Appl. Surf. Sci.* **2008**, *254*, 4191–4200. doi:10.1016/j.apsusc.2008.01.035
146. Zhao, E.; Wang, L.; Yan, L.; Torimoto, Y.; Li, Q. *J. Appl. Polym. Sci.* **2008**, *110*, 39–48. doi:10.1002/app.28464
147. Felix, T.; Trigueiro, J. S.; Bundaleski, N.; Teodoro, O. M. N. D.; Sério, S.; Debacher, N. A. *Appl. Surf. Sci.* **2018**, *428*, 730–738. doi:10.1016/j.apsusc.2017.09.147
148. Förster, F. *Plasma Processes Polym.* **2022**, *19*, 2100240. doi:10.1002/ppap.202100240
149. Okubo, M.; Tahara, M.; Saeki, N.; Yamamoto, T. *Thin Solid Films* **2008**, *516*, 6592–6597. doi:10.1016/j.tsf.2007.11.033
150. Brillas, E.; Sirés, I.; Oturan, M. A. *Chem. Rev.* **2009**, *109*, 6570–6631. doi:10.1021/cr900136g
151. Bureau, C.; Pinson, J. Method for the modification of polymer surfaces, such as the hydroxylation of polymer surfaces, and products thus obtained. Eur. Pat. Appl. EP1937759 A1, July 2, 2008.
152. Ktari, N.; Poncet, P.; Sénéchal, H.; Malaquin, L.; Kanoufi, F.; Combellas, C. *Langmuir* **2010**, *26*, 17348–17356. doi:10.1021/la1028564
153. Zollinger, H. Applications of Heterolytic and Homolytic Diazoniations in Organic Syntheses: Sections 10.1–10.9. *Diazo Chemistry I*; Wiley-VCH: Weinheim, Germany, 1994; pp 221–253. doi:10.1002/3527601724.ch10a
154. Santos, L. M.; Ghilane, J.; Fave, C.; Lacaze, P.-C.; Randriamahazaka, H.; Abrantes, L. M.; Lacroix, J.-C. *J. Phys. Chem. C* **2008**, *112*, 16103–16109. doi:10.1021/jp8042818
155. Liu, X.; Wang, M.; Jia, Y.-x. *Sep. Sci. Technol.* **2016**, *51*, 2823–2832. doi:10.1080/01496395.2016.1210643
156. Chehimi, M. M.; Lamouri, A.; Picot, M.; Pinson, J. *J. Mater. Chem. C* **2014**, *2*, 356–363. doi:10.1039/c3tc31492h
157. Bastekova, K.; Guselnikova, O.; Postnikov, P.; Elashnikov, R.; Kunes, M.; Kolska, Z.; Švorčík, V.; Lyutakov, O. *Appl. Surf. Sci.* **2017**, *397*, 226–234. doi:10.1016/j.apsusc.2016.11.062
158. Troian-Gautier, L.; Martínez-Tong, D. E.; Hubert, J.; Reniers, F.; Sferrazza, M.; Mattiuzzi, A.; Lagrost, C.; Jabin, I. *J. Phys. Chem. C* **2016**, *120*, 22936–22945. doi:10.1021/acs.jpcc.6b06143
159. Benoit, C.; Demeter, D.; Bélanger, D.; Cougnon, C. *Angew. Chem., Int. Ed.* **2016**, *55*, 5318–5321. doi:10.1002/anie.201601395
160. Bouriga, M.; Chehimi, M. M.; Combellas, C.; Decorse, P.; Kanoufi, F.; Deronzier, A.; Pinson, J. *Chem. Mater.* **2013**, *25*, 90–97. doi:10.1021/cm3032994
161. Hetemi, D.; Kanoufi, F.; Combellas, C.; Pinson, J.; Podvorica, F. I. *Langmuir* **2014**, *30*, 13907–13913. doi:10.1021/la503833j
162. Combellas, C.; Kanoufi, F.; Nunige, S. *Chem. Mater.* **2007**, *19*, 3830–3839. doi:10.1021/cm070438z
163. Blanksby, S. J.; Ellison, G. B. *Acc. Chem. Res.* **2003**, *36*, 255–263. doi:10.1021/ar020230d
164. Horie, K.; Mita, I. *Chem. Phys. Lett.* **1982**, *93*, 61–65. doi:10.1016/0009-2614(82)85056-2
165. Kinstle, J. F.; Watson, S. L., Jr. Photoassisted Modification of and Grafting to Polyethylene. In *Polymer Alloys. Polymer Science and Technology*; Klempner, D.; Frisch, K. C., Eds.; Springer: Boston, MA, USA, 1977; Vol. 10, pp 461–478. doi:10.1007/978-1-4684-0874-4_33
166. Williams, J. L. R.; Daly, R. C. *Prog. Polym. Sci.* **1977**, *5*, 61–93. doi:10.1016/0079-6700(77)90005-3

167. Lin, X.; Fukazawa, K.; Ishihara, K. *ACS Appl. Mater. Interfaces* **2015**, *7*, 17489–17498. doi:10.1021/acsami.5b05193
168. Kato, K.; Uchida, E.; Kang, E.-T.; Uyama, Y.; Ikada, Y. *Prog. Polym. Sci.* **2003**, *28*, 209–259. doi:10.1016/s0079-6700(02)00032-1
169. Chen, Y. L.; Rånby, B. *Polym. Adv. Technol.* **1990**, *1*, 103–107. doi:10.1002/pat.1990.220010112
170. Barbey, R.; Lavanant, L.; Paripovic, D.; Schüwer, N.; Sugnaux, C.; Tugulu, S.; Klok, H.-A. *Chem. Rev.* **2009**, *109*, 5437–5527. doi:10.1021/cr900045a
171. Zoppe, J. O.; Ataman, N. C.; Mocny, P.; Wang, J.; Moraes, J.; Klok, H.-A. *Chem. Rev.* **2017**, *117*, 1105–1318. doi:10.1021/acs.chemrev.6b00314
172. Zhou, J.; Huang, Z.; Sun, Y.; Cui, M.; Luo, Z.; Yu, B.; Zou, X.; Hu, H. *Colloids Surf., B* **2021**, *203*, 111718. doi:10.1016/j.colsurfb.2021.111718
173. Zain, G.; Bučková, M.; Mosnáčková, K.; Doháňšová, J.; Opálková Šíšková, A.; Mičušík, M.; Kleinová, A.; Matúš, P.; Mosnáček, J. *Polym. Chem.* **2021**, *12*, 7073–7084. doi:10.1039/d1py01322j
174. Ng, G.; Li, M.; Yeow, J.; Jung, K.; Pester, C. W.; Boyer, C. *ACS Appl. Mater. Interfaces* **2020**, *12*, 55243–55254. doi:10.1021/acsami.0c15221
175. Rong, L.-H.; Cheng, X.; Ge, J.; Krebs, O. K.; Capadona, J. R.; Caldon, E. B.; Advincula, R. C. *ACS Appl. Polym. Mater.* **2022**, *4*, 6449–6457. doi:10.1021/acsapm.2c00868
176. Kyomoto, M.; Ishihara, K. *ACS Appl. Mater. Interfaces* **2009**, *1*, 537–542. doi:10.1021/am800260t
177. Kyomoto, M.; Moro, T.; Takatori, Y.; Kawaguchi, H.; Nakamura, K.; Ishihara, K. *Biomaterials* **2010**, *31*, 1017–1024. doi:10.1016/j.biomaterials.2009.10.055
178. Kabanov, V. Y.; Feldman, V. I.; Ershov, B. G.; Polikarpov, A. I.; Kiryukhin, D. P.; Apel', P. Y. *High Energy Chem.* **2009**, *43*, 1–18. doi:10.1134/s0018143909010019
179. Tsoulfanidis, N.; Landsberger, S. *Measurement & Detection of Radiation*, 5th ed.; CRC Press: Boca Raton, FL, USA, 2021. doi:10.1201/9781003009849
180. Flores-Rojas, G. G.; Bucio, E. *Radiat. Phys. Chem.* **2016**, *127*, 21–26. doi:10.1016/j.radphyschem.2016.05.015
181. Barner, L.; Quinn, J. F.; Barner-Kowollik, C.; Vana, P.; Davis, T. P. *Eur. Polym. J.* **2003**, *39*, 449–459. doi:10.1016/s0014-3057(02)00247-1
182. Barsbay, M.; Güven, O. *Radiat. Phys. Chem.* **2020**, *169*, 107816. doi:10.1016/j.radphyschem.2018.04.009
183. Sawada, S.-i.; Hasegawa, S.; Zhao, Y.; Maekawa, Y. *J. Membr. Sci.* **2017**, *532*, 105–114. doi:10.1016/j.memsci.2017.03.016
184. Chen, Q.; Zhang, Z.; Zhou, N.; Cheng, Z.; Zhu, J.; Zhang, W.; Zhu, X. *J. Polym. Sci., Part A: Polym. Chem.* **2011**, *49*, 3588–3594. doi:10.1002/pola.24797
185. Dong, H.; Bell, T. *Surf. Coat. Technol.* **1999**, *111*, 29–40. doi:10.1016/s0257-8972(98)00698-7
186. Burkert, S.; Kuntzsch, M.; Bellmann, C.; Uhlmann, P.; Stamm, M. *Appl. Surf. Sci.* **2009**, *255*, 6256–6261. doi:10.1016/j.apsusc.2009.01.096
187. Komatsu, M.; Kawakami, T.; Kanno, J.-i.; Sasaki, T. *J. Appl. Polym. Sci.* **2011**, *119*, 2533–2538. doi:10.1002/app.33071
188. Xu, H.; Kosma, V.; Giannelis, E. P.; Ober, C. K. *Polym. J.* **2018**, *50*, 45–55. doi:10.1038/pj.2017.64
189. Inoue, S.; Amano, T.; Itani, T.; Watanabe, H.; Mori, I.; Watanabe, T.; Kinoshita, H.; Miyai, H.; Hatakeyama, M. *Adv. Opt. Technol.* **2012**, *1*, 269–278. doi:10.1515/aot-2012-0029
190. Clecak, N. J.; Cox, R. J.; Moreau, W. M. *Polym. Eng. Sci.* **1974**, *14*, 491–493. doi:10.1002/pen.760140705
191. Lin, B. J. *J. Vac. Sci. Technol. (N. Y., NY, U. S.)* **1975**, *12*, 1317–1320. doi:10.1116/1.568527
192. Emoto, F.; Gamo, K.; Namba, S.; Samoto, N.; Shimizu, R. *Jpn. J. Appl. Phys., Part 1* **1985**, *24*, L809. doi:10.1143/jjap.24.L809
193. Pacansky, J.; Waltman, R. J.; Pacansky, G. *Chem. Mater.* **1993**, *5*, 1526–1532. doi:10.1021/cm00034a024
194. Lawrie, K.; Blakey, I.; Blinco, J.; Gronheid, R.; Jack, K.; Pollentier, I.; Leeson, M. J.; Younkin, T. R.; Whittaker, A. K. *Radiat. Phys. Chem.* **2011**, *80*, 236–241. doi:10.1016/j.radphyschem.2010.07.038
195. Bowmer, T. N.; O'Donnell, J. H. *J. Polym. Sci., Polym. Chem. Ed.* **1981**, *19*, 45–50. doi:10.1002/pol.1981.170190105
196. Dainton, F. S.; Ivin, K. J. *Q. Rev., Chem. Soc.* **1958**, *12*, 61–92. doi:10.1039/qr9581200061
197. Bowmer, T. N.; O'Donnell, J. H.; Wells, P. R. *Makromol. Chem., Rapid Commun.* **1980**, *1*, 1–6. doi:10.1002/marc.1980.030010101
198. Sasaki, T.; Yaguchi, H. *J. Polym. Sci., Part A: Polym. Chem.* **2009**, *47*, 602–613. doi:10.1002/pola.23179
199. Borrelle, S. B.; Ringma, J.; Law, K. L.; Monnahan, C. C.; Lebreton, L.; McGivern, A.; Murphy, E.; Jambeck, J.; Leonard, G. H.; Hilleary, M. A.; Eriksen, M.; Possingham, H. P.; De Frond, H.; Gerber, L. R.; Polidoro, B.; Tahir, A.; Bernard, M.; Mallos, N.; Barnes, M.; Rochman, C. M. *Science* **2020**, *369*, 1515–1518. doi:10.1126/science.aba3656
200. Stadler, B. M.; de Vries, J. G. *Philos. Trans. R. Soc., A* **2021**, *379*, 20200341. doi:10.1098/rsta.2020.0341
201. Payne, J.; Jones, M. D. *ChemSusChem* **2021**, *14*, 4041–4070. doi:10.1002/cssc.202100400
202. Oh, S.; Stache, E. E. *J. Am. Chem. Soc.* **2022**, *144*, 5745–5749. doi:10.1021/jacs.2c01411
203. Li, T.; Vijeta, A.; Casadevall, C.; Gentleman, A. S.; Euser, T.; Reisner, E. *ACS Catal.* **2022**, *12*, 8155–8163. doi:10.1021/acscatal.2c02292
204. Wang, H. S.; Truong, N. P.; Pei, Z.; Coote, M. L.; Anastasaki, A. *J. Am. Chem. Soc.* **2022**, *144*, 4678–4684. doi:10.1021/jacs.2c00963
205. Martinez, M. R.; De Luca Bossa, F.; Olszewski, M.; Matyjaszewski, K. *Macromolecules* **2022**, *55*, 78–87. doi:10.1021/acs.macromol.1c02246
206. Godiya, C. B.; Gabrielli, S.; Materazzi, S.; Pianesi, M. S.; Stefanini, N.; Marcantoni, E. *J. Environ. Manage.* **2019**, *231*, 1012–1020. doi:10.1016/j.jenvman.2018.10.116
207. Braidó, R. S.; Borges, L. E. P.; Pinto, J. C. *J. Anal. Appl. Pyrolysis* **2018**, *132*, 47–55. doi:10.1016/j.jaap.2018.03.017
208. Shabtai, J.; Xiao, X.; Zmierczak, W. *Energy Fuels* **1997**, *11*, 76–87. doi:10.1021/ef960076+
209. Liu, Y.; Chandra Akula, K.; Phani Raj Dandamudi, K.; Liu, Y.; Xu, M.; Sanchez, A.; Zhu, D.; Deng, S. *Chem. Eng. J.* **2022**, *446*, 137238. doi:10.1016/j.cej.2022.137238
210. Lal, S.; Anisia, K. S.; Jhansi, M.; Kishore, L.; Kumar, A. *J. Mol. Catal. A: Chem.* **2007**, *265*, 15–24. doi:10.1016/j.molcata.2006.09.027
211. Kong, S.; He, C.; Dong, J.; Li, N.; Xu, C.; Pan, X. *Macromol. Chem. Phys.* **2022**, *223*, 2100322. doi:10.1002/macp.202100322

212. Wang, C.; Xia, J.; Zhang, Y.; Hu, X.; Jian, Z. *Natl. Sci. Rev.* **2023**, *10*, nwad039. doi:10.1093/nsr/nwad039

License and Terms

This is an open access article licensed under the terms of the Beilstein-Institut Open Access License Agreement (<https://www.beilstein-journals.org/bjoc/terms>), which is identical to the Creative Commons Attribution 4.0 International License (<https://creativecommons.org/licenses/by/4.0>). The reuse of material under this license requires that the author(s), source and license are credited. Third-party material in this article could be subject to other licenses (typically indicated in the credit line), and in this case, users are required to obtain permission from the license holder to reuse the material.

The definitive version of this article is the electronic one which can be found at:
<https://doi.org/10.3762/bjoc.19.116>



Mechanisms for radical reactions initiating from *N*-hydroxyphthalimide esters

Carlos R. Azpilcueta-Nicolas and Jean-Philip Lumb*

Perspective

Open Access

Address:
Department of Chemistry, McGill University, 801 Sherbrooke Street
West, Montreal, Quebec H3A 0B8, Canada

Email:
Jean-Philip Lumb* - jean-philip.lumb@mcgill.ca

* Corresponding author

Keywords:
decarboxylative couplings; mechanisms; NHPI-esters; radical
reactions

Beilstein J. Org. Chem. **2024**, *20*, 346–378.
<https://doi.org/10.3762/bjoc.20.35>

Received: 11 September 2023

Accepted: 29 January 2024

Published: 21 February 2024

This article is part of the thematic issue "Modern radical chemistry".

Guest Editor: H.-M. Huang



© 2024 Azpilcueta-Nicolas and Lumb; licensee
Beilstein-Institut.
License and terms: see end of document.

Abstract

Due to their ease of preparation, stability, and diverse reactivity, *N*-hydroxyphthalimide (NHPI) esters have found many applications as radical precursors. Mechanistically, NHPI esters undergo a reductive decarboxylative fragmentation to provide a substrate radical capable of engaging in diverse transformations. Their reduction via single-electron transfer (SET) can occur under thermal, photochemical, or electrochemical conditions and can be influenced by a number of factors, including the nature of the electron donor, the use of Brønsted and Lewis acids, and the possibility of forming charge-transfer complexes. Such versatility creates many opportunities to influence the reaction conditions, providing a number of parameters with which to control reactivity. In this perspective, we provide an overview of the different mechanisms for radical reactions involving NHPI esters, with an emphasis on recent applications in radical additions, cyclizations and decarboxylative cross-coupling reactions. Within these reaction classes, we discuss the utility of the NHPI esters, with an eye towards their continued development in complexity-generating transformations.

Introduction

The historical challenges of using radicals in synthetic chemistry is well documented [1,2]. Traditional approaches for radical generation relied on hazardous reagents and harsh conditions, resulting in low reaction efficiency and undesired byproduct formation [3-6]. As a consequence, the utility of radicals in organic synthesis remained limited for many years and in the past, they were perceived as fleeting reaction intermediates.

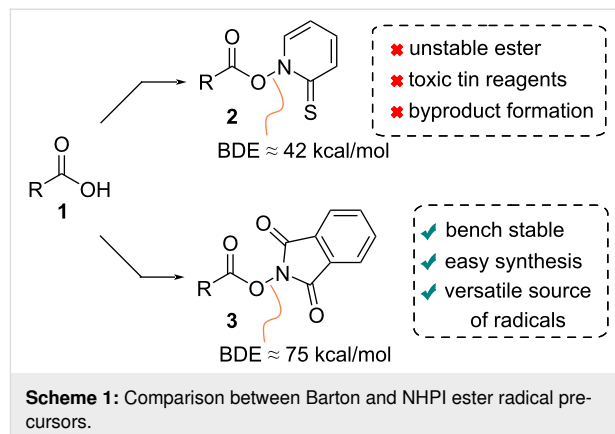
Recent progress in photoredox catalysis [6-8], electrochemistry [9,10], and the use of transition-metal (TM) catalysts in radical cross-coupling reactions [11] have dramatically expanded the use of radicals in synthesis, leading to their strategic incorporation as "synthons" in modern organic chemistry, with complementary reactivity to more common polar reaction manifolds [12-15]. The utility of radicals has also been expanded through the recent development of transformations involving radical-

polar crossover, which incorporate both radical and ionic bond-forming steps into a single synthetic operation [16,17].

The success of radical reactions is intimately linked to the mechanisms of their initiation and the radical progenitor employed. Amongst the many progenitors that are available, carboxylic acids are one of the most extensively used, owing to their structural diversity and widespread commercial availability [18,19]. Carboxylic acids **1** can generate radicals under oxidative conditions, as in classical decarboxylative halogenation reactions (Hunsdiecker reaction) that proceed via a radical mechanism [20,21]. More recent approaches have leveraged photoinduced ligand-to-metal charge transfer to generate radicals from aliphatic [22] and aromatic [23,24] carboxylic acids.

However, more broadly used approaches involve carefully designed activated esters. Barton esters **2** emerged in the early 1980s [25,26] (Scheme 1) and have found applications in a number of functional group interconversions mediated by radical chain decarboxylation [27]. However, their widespread use in synthesis, especially in complex molecular settings, suffers from significant disadvantages. These include thermal and photochemical instability, as evidenced by their low N–O bond dissociation energy (BDE \approx 42 kcal/mol) [28], the reliance on toxic tin hydrides as reductants and the undesired radical recombination with reactive 2-pyridylthiyl radicals that leads to (alkylthio)pyridine byproducts [26]. More recently, *N*-hydroxyphthalimide (NHPI) esters (**3**) have emerged as convenient alternatives to Barton esters (Scheme 1) due in part to their ease of synthesis and greater stability (N–O BDE \approx 75 kcal/mol) [28]. Their use as radical precursors was first described by Okada and colleagues in 1988 [29], who showed that C(sp³)-centered radicals were successfully generated by subjecting NHPI esters to light irradiation in the presence of the photoreductant 1,6-bis(dimethylamino)pyrene (BDMAP). Following their initial discovery, multiple studies have shown their versatility as radical progenitors under thermal, photochemical, and electrochemical conditions [30,31].

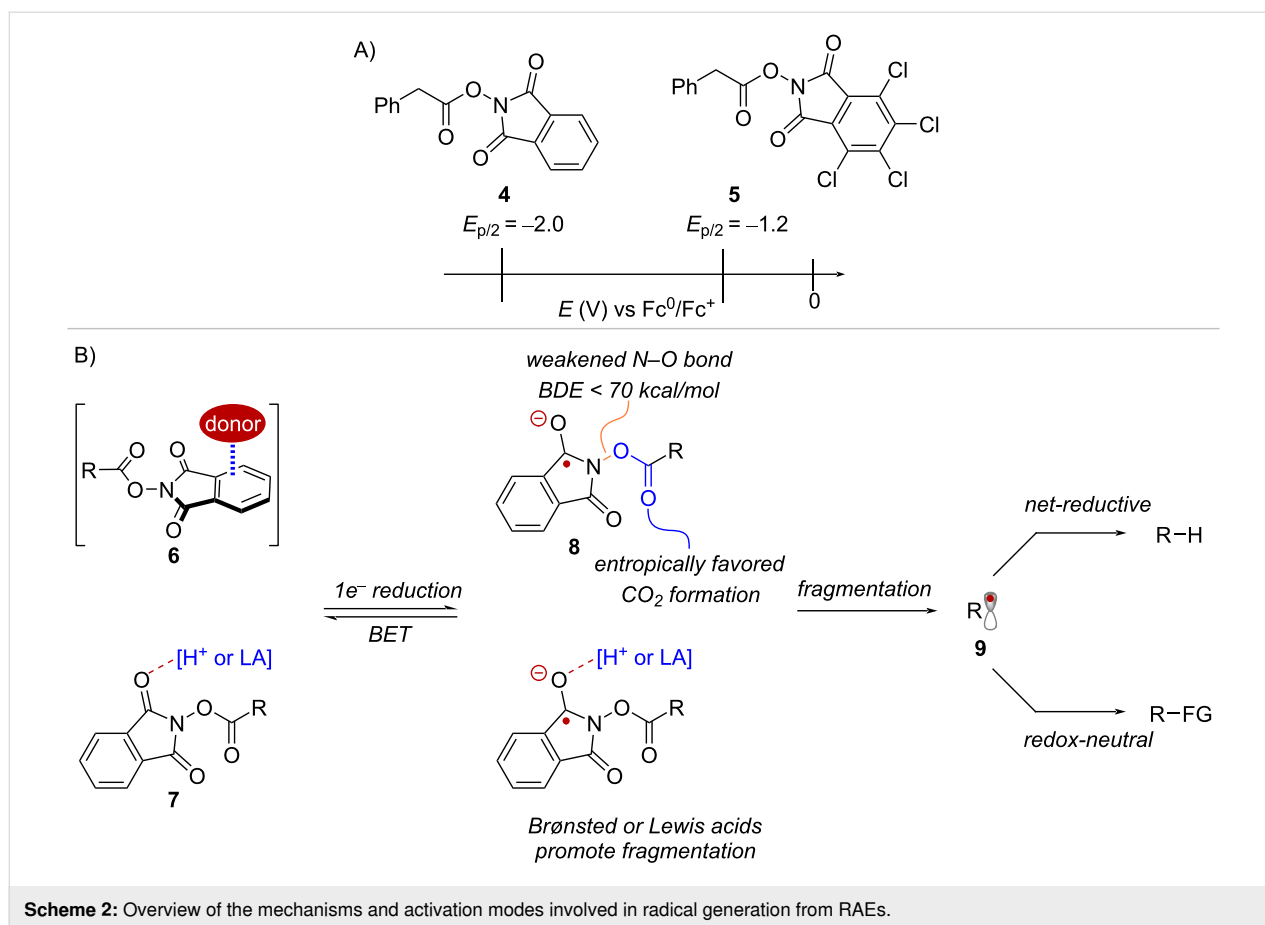
Due to their propensity towards single-electron reduction, NHPI esters, and similar derivatives such as *N*-hydroxytetrachlorophthalimide (TCNHPI) esters, are collectively referred to as "redox-active esters" (RAEs). The versatility of RAEs stems, in part, to the sensitivity of their reduction half peak potentials ($E_{p/2}$) to their environment. For instance, a recent study by Cornella and co-workers, showed that RAEs derived from phenylacetic acid exhibited varying reduction half peak potentials ($E_{p/2}$) ranging from -2.0 V for the NHPI ester **4** to -1.2 V for the corresponding TCNHPI ester **5** (measured in MeCN vs Fc^0/Fc^+ , see Scheme 2A) [32]. Based solely on their redox potentials, single-electron reduction of RAEs is only possible in



the presence of a sufficiently strong reducing agent. However, the reduction of RAEs can also be facilitated through the formation of charge transfer complexes with a donor species **6** or via LUMO lowering activation with Brønsted and Lewis acids **7** (Scheme 2B), collectively offering a number of variables to influence their reactivity.

Upon reduction, RAEs give rise to a radical anion **8** with a weakened N–O bond (BDE < 70 kcal/mol) [33]. While fragmentation of **8** affords a radical species **9** in a constructive step towards initiating the radical reaction, a principal competing step is back-electron transfer (BET) to return the closed shell starting materials (Scheme 2B). A recent study showed comparable rates for fragmentation ($8 \pm 5 \times 10^5 \text{ s}^{-1}$) and BET (3.15 to $2.06 \times 10^5 \text{ s}^{-1}$) [34] when employing catalytic Ir^{III} excited state reductants with moderate reducing potentials ($E_{1/2}^{\text{red}}[\text{Ir}^{\text{IV}}/\text{Ir}^{\text{III}}] \approx -1.13 \text{ V}$ vs Fc^0/Fc^+ in MeCN) [35]. This suggests that in the absence of a sufficiently strong driving force, BET and fragmentation compete to influence the resulting concentration of radicals. In such instances, opting for a stronger catalytic reductant or utilizing a stoichiometric electron donor can greatly improve the efficiency of radical generation. On the other hand, additional factors such as the ability of Brønsted and Lewis acid additives to promote the fragmentation step can be considered. Importantly, the diverse mechanisms in which RAEs engage in radical reactions can be exploited to modulate the reactivity of the resulting substrate radicals. For example, under net-reductive conditions, the radical intermediates are typically terminated via hydrogen atom transfer (HAT) or sequential electron transfer and proton transfer (ET/PT) steps. Alternatively, redox-neutral transformations can be envisioned using catalytic reductants, which can enable a complementary scope of downstream functionalizations (Scheme 2B).

In this perspective, we present an overview of the diverse mechanisms that have been proposed for radical based transformat-



ions initiating from NHPI esters. The discussion is organized into four sections: (i) mechanisms under photochemical conditions, (ii) initiation by metal catalysis and stoichiometric reductants, (iii) *N*-heterocyclic carbene (NHC)-catalyzed radical relay, and (iv) mechanisms under electrochemical activation.

By discussing selected literature examples, we illustrate how the activation mode of NHPI esters, and the reactivity of the resulting radical species, can vary depending upon the choice of catalytic or stoichiometric electron donors, the presence of a TM catalyst, the formation of a charge-transfer complex, and the overall reaction conditions. While we hope that this discussion will spur the continued development of NHPI esters in complexity-generating transformations, it is not comprehensive, and we refer readers to recently published review articles for additional discussion [30,31].

Discussion

Mechanism under photochemical conditions

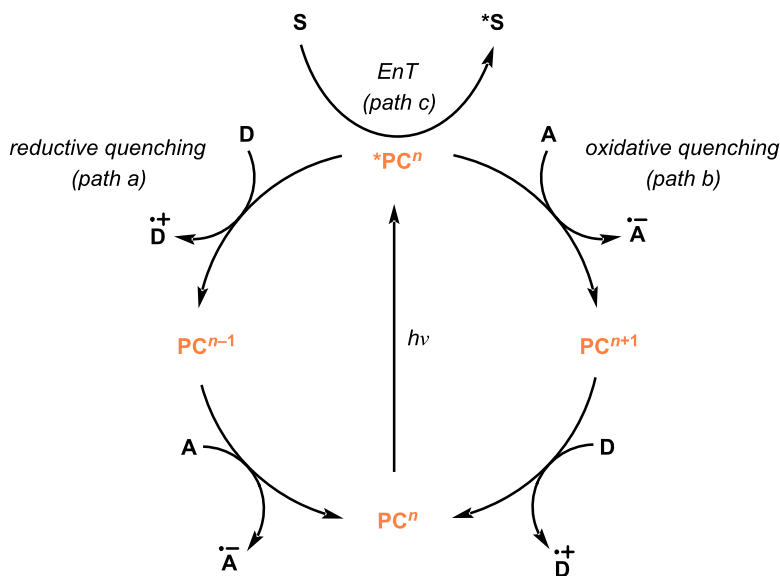
In this section we provide a summary of the various conditions and activation modes employed in radical reactions of NHPI esters using visible-light irradiation. Upon absorption of light, an excited photocatalyst ($^*\text{PC}$) engages in single-electron

transfer (SET) with either donor (**D**) or acceptor (**A**) molecules (Scheme 3) [8,36]. Accordingly, a reductive quenching mechanism (path a) will operate when an excited photocatalyst effects the one-electron oxidation of a sacrificial donor giving rise to a strongly reducing catalytic species (PC^{n-1}). On the other hand, in an oxidative quenching mechanism (path b) the excited photocatalyst directly induces the one-electron reduction of an acceptor substrate. Alternatively, the photocatalyst can mediate the formation of an electronically excited substrate ($^*\text{S}$) through an energy transfer (EnT) mechanism (path c).

In addition to these mechanistic blueprints, the formation of charge-transfer complexes involving NHPI esters, as well as examples of photoinduced transition metal-catalyzed activation will be discussed. Depending on the specific activation mechanism, both net reductive and redox neutral transformations can be implemented.

Photocatalytic reductive quenching mechanism

Among the most common reactions of NHPI esters are radical additions to electron-deficient olefins under net-reductive conditions, often referred to as Giese type addition reactions



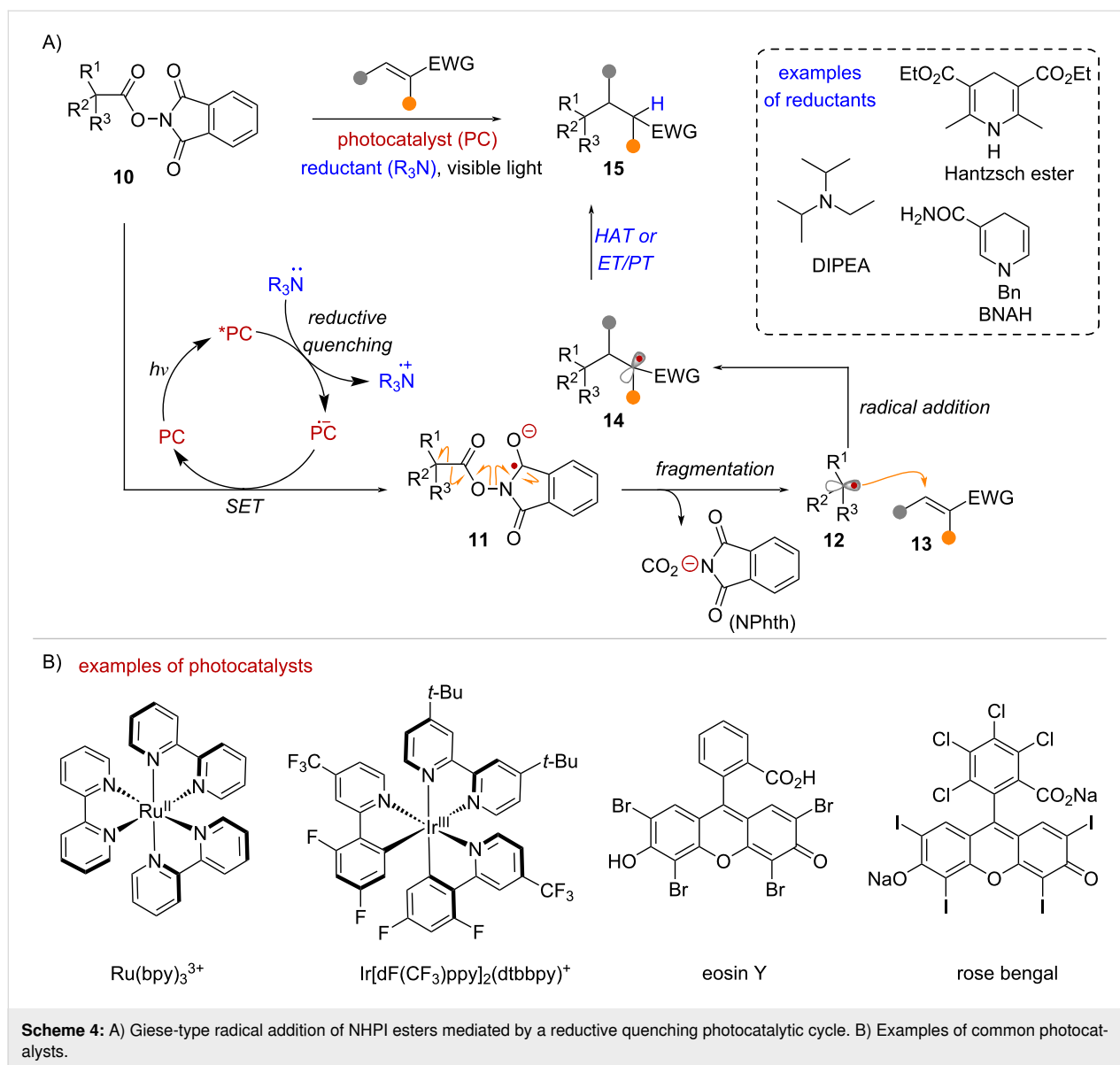
Scheme 3: Common mechanisms in photocatalysis.

(Scheme 4A). In 1991, Okada and co-workers reported the addition of alkyl radicals to α,β -unsaturated ketones, by subjecting NHPI esters to visible-light irradiation in the presence of the photocatalyst $[\text{Ru}(\text{bpy})_3]\text{Cl}_2$ and the reductant 1-benzyl-1,4-dihydronicotinamide (BNAH) [37]. Two decades later, in 2012 the Overman group demonstrated the utility of this transformation in the total synthesis of (–)-aplyvioline, involving the diastereoselective coupling of a tertiary radical and an enone acceptor [38]. Further developments of this chemistry resulted in the general use of NHPI esters for the construction of quaternary carbons via conjugate addition of 3° radicals [39,40]. In general, this transformation operates under a reductive quenching photocatalytic cycle, requiring a stoichiometric reductant (Scheme 4A). Both TM complexes, and organic dyes such as eosin Y [41–43], have been employed as suitable photocatalysts (Scheme 4B). Under visible light irradiation the photocatalyst (PC) is excited into its corresponding excited state ($^*\text{PC}$), where it can be reduced by a suitable electron donor such as DIPEA or Hantzsch ester to generate the reduced form of the photocatalyst ($\text{PC}^{\bullet-}$) (Scheme 4A). This strong reducing agent mediates the one-electron reduction of the NHPI ester **10**, forming radical anion intermediate **11**. Fragmentation of **11** via N–O bond homolysis and decarboxylation forms the key tertiary radical **12** with concomitant formation of phthalimidyl anion ($^-\text{Nphth}$) and CO_2 . Radical **12** undergoes intermolecular addition to the olefin acceptor **13** to form radical intermediate **14**. Finally, under reductive conditions radical **14** can undergo hydrogen atom transfer (HAT) or sequential electron transfer and proton transfer (ET/PT) to form the conjugate addition product **15**.

With this mechanistic blueprint as a backdrop, Phipps and co-workers developed an enantioselective Minisci-type addition, under dual photoredox and chiral Brønsted acid catalysis [44] (Scheme 5A). In their proposed mechanism, the activation of the NHPI ester radical precursor was proposed to occur via a reductive quenching mechanism. However, since the overall transformation is redox-neutral, no stoichiometric reductant was employed. Instead, fluorescence-quenching studies suggested that the reductive quenching of the iridium excited state ($^*\text{Ir}^{\text{III}}$) was taking place "off-cycle" via oxidation of the chiral phosphate co-catalyst (Scheme 5B). This event leads to the generation of a potent Ir^{II} reductant that begins the photocatalytic cycle by reducing **16** into radical anion **17** while regenerating the ground state of the Ir^{III} photocatalyst. After fragmentation, α -amino radical **18** was proposed to undergo addition to the heterocyclic radical acceptor **19** through a ternary transition state **20** involving hydrogen bonding interactions with the chiral phosphate co-catalyst. Notably, a follow-up report revealed that the radical addition is reversible, and that the selectivity determining step involves the deprotonation of **21** to provide radical intermediate **22** [45]. Finally, the iridium excited state ($^*\text{Ir}^{\text{III}}$) formed under blue light irradiation oxidizes **22** to form product **23** and the corresponding reduced Ir^{II} complex, beginning a new photocatalytic cycle.

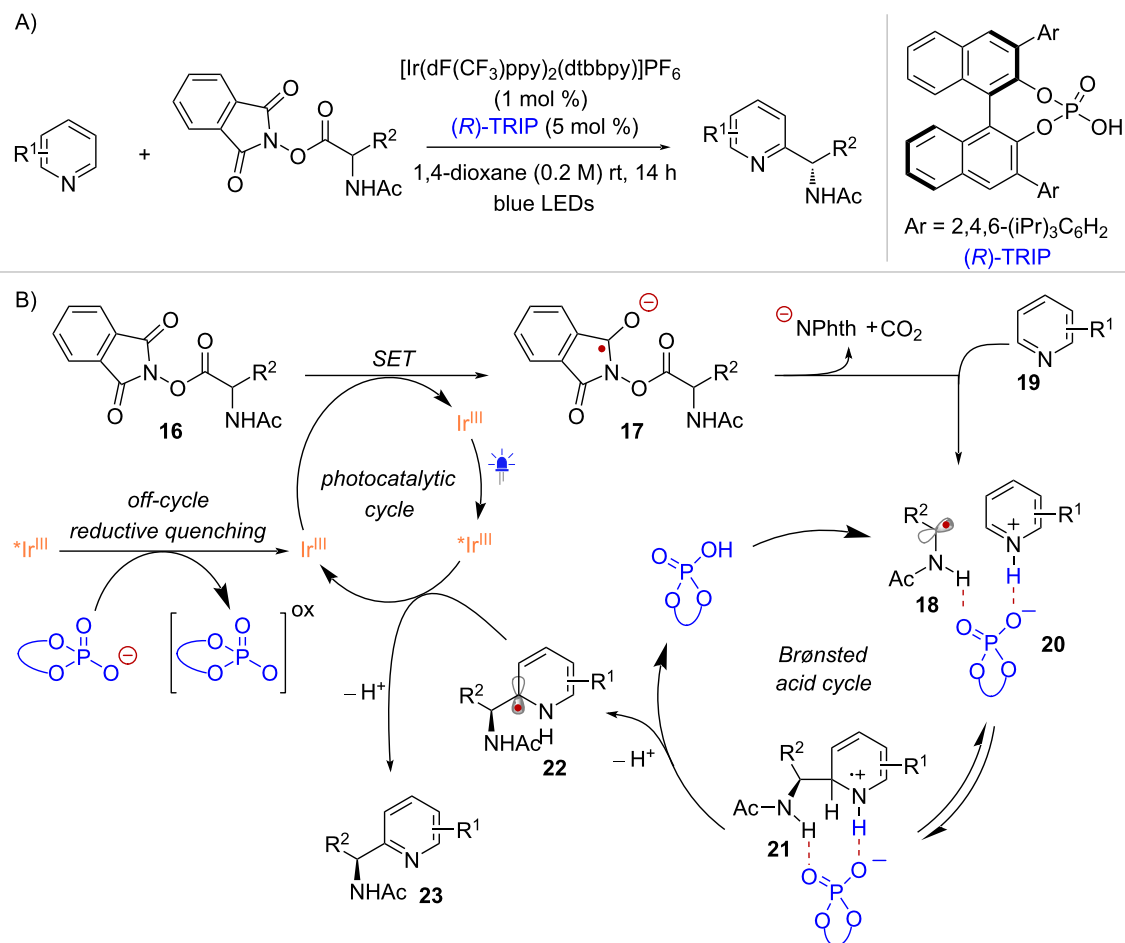
Photocatalytic oxidative quenching mechanism

The activation of NHPI esters under a photocatalytic oxidative quenching mechanism was reported for the first time by Glorius and co-workers in 2017 [46]. This activation mode was applied



in the functionalization of styrenes using an Ir-photocatalyst and a diverse range of nucleophiles that are H-bond donors (Scheme 6A). Stern–Volmer analysis revealed that quenching of the photocatalyst's excited state by the NHPI ester occurred only in presence of a hydrogen bond donor such as water (H_2O) or methanol (MeOH). This supported the hypothesis that activation of NHPI esters towards photoinduced electron transfer can occur through hydrogen bonding. In the proposed mechanism (Scheme 6B), hydrogen bonded complex **24** undergoes single electron reduction via oxidative quenching of the excited state $^*Ir^{III}$, resulting in the formation of radical anion **25** (presumably H-bonded to H_2O) and the corresponding Ir^{IV} complex. Radical intermediate **9** formed upon fragmentation of **25**, adds to the styrene acceptor forming radical **26**. Finally, a radical-polar crossover event between **26** and the Ir^{IV} complex regenerates the Ir^{III} ground state while delivering cation **27** that is then trapped by the oxygen-nucleophile to form the oxyalkylation product **28**.

Li and co-workers described the activation of NHPI esters towards SET using a Lewis acid catalyst, allowing for the functionalization of styrene radical acceptors with nucleophiles that do not necessarily engage in hydrogen-bonding interactions, such as electron-rich (hetero)arenes [47] (Scheme 7A). Cyclic voltammetry measurements of a model NHPI ester showed a shift in its reduction potential from -1.79 V to -1.51 V (vs SCE in MeCN) in the presence of $In(OTf)_3$. As such, it was hypothesized that the Lewis acid lowers the LUMO of the NHPI ester via interaction with the oxygen lone pair in the phthalimide moiety (Scheme 7B). Thus, the excited state reductant $^*Ir^{III}$

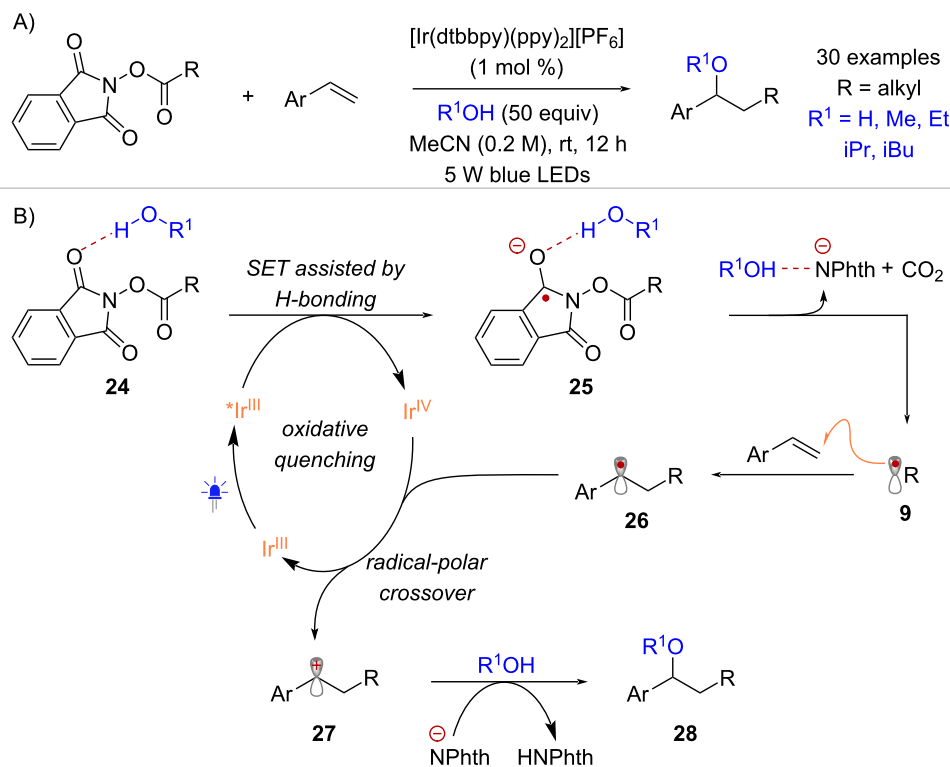


Scheme 5: A) Minisci-type radical addition of NHPI esters. B) Reaction mechanism involving an “off-cycle” reductive quenching.

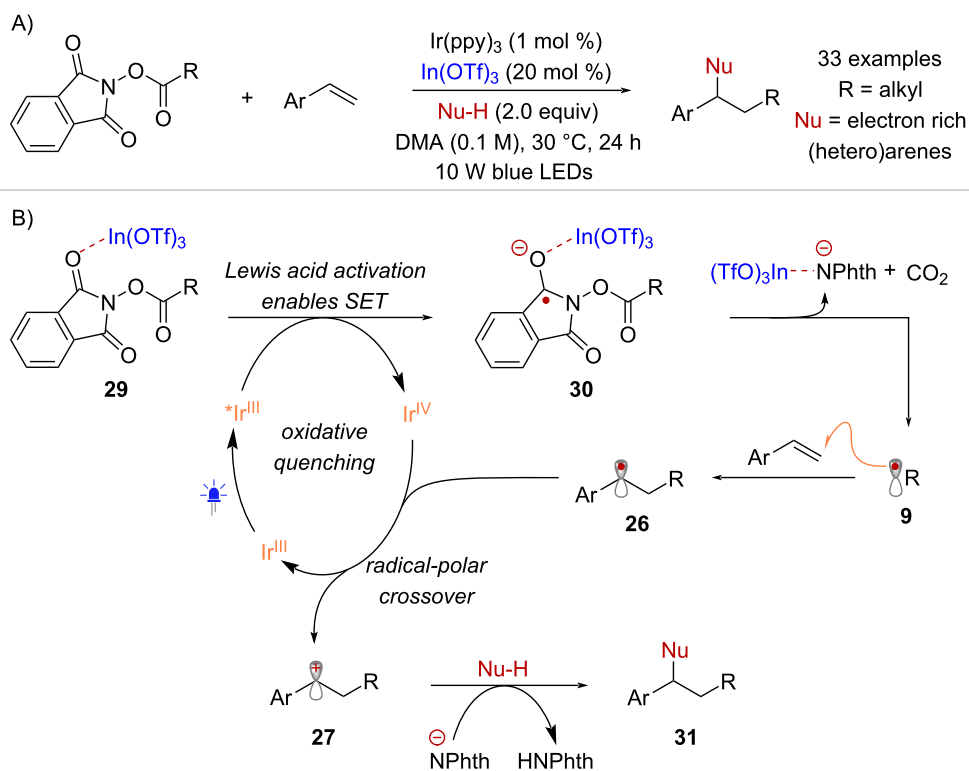
reduces the activated substrate **29** to form the stabilized radical anion **30**. Fragmentation into radical **9**, followed by radical addition to styrene gives benzyl radical intermediate **26**. Turn-over of the catalytic cycle through radical-polar crossover affords cation **27** that delivers functionalized product **31** upon nucleophilic addition.

The Doyle and Knowles groups reported the use of NHPI esters as radical precursors in the context of a radical redox annulation method [48] (Scheme 8A). This transformation occurs through an oxidative quenching photocatalytic cycle employing Ir-based photoreductants and a Brønsted acid additive. While the interaction between the RAE **32** and diphenyl phosphoric acid involves hydrogen bonding, in analogy to the Glorius proposal, it is thought that the substrate activation occurs through proton-coupled electron transfer (PCET), forming neutral radical species **33** and the corresponding phosphate conjugate base (Scheme 8B). The hypothesis is supported by an observed increase in the luminescence quenching of $^*\text{Ir}(\text{p-CF}_3\text{-}$

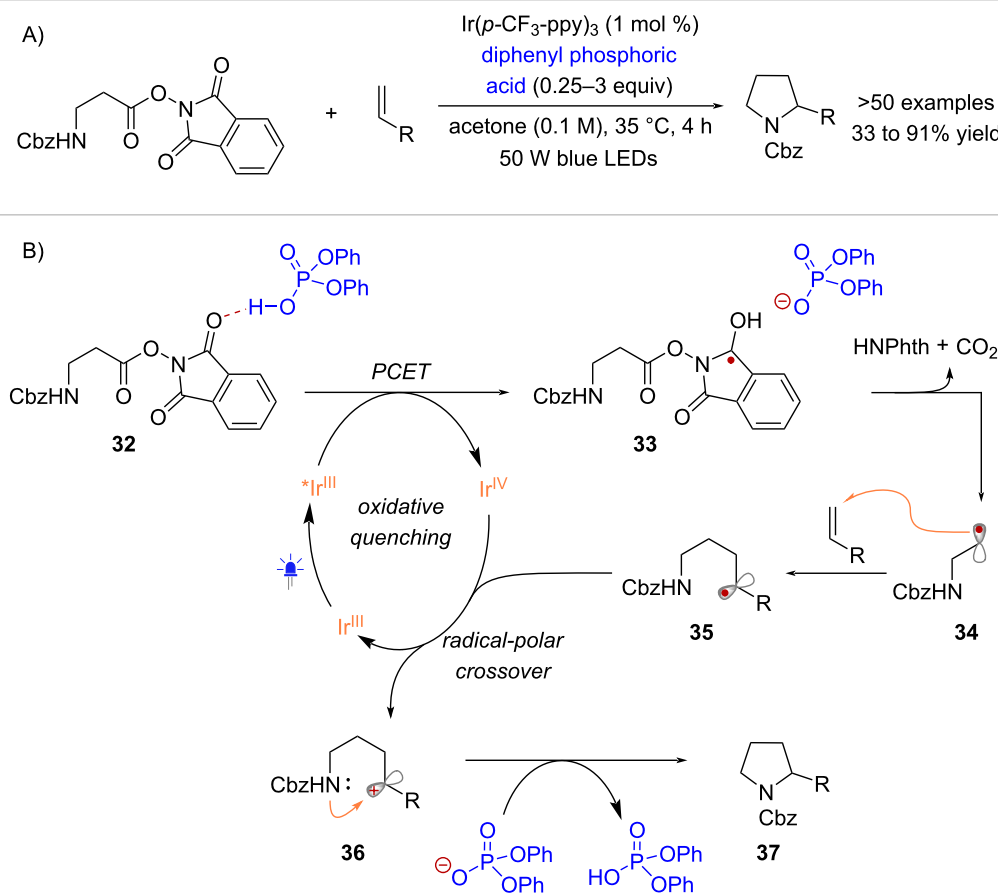
$\text{ppy})_3$ by **32** in the presence of diphenyl phosphoric acid, as quantified by the Stern–Volmer constant ($K_{\text{SV}} = 1146 \text{ M}^{-1}$ with acid vs $K_{\text{SV}} = 603 \text{ M}^{-1}$ without acid). The reaction mechanism continues with the fragmentation of **33** into radical **34**. From radical **34** the annulation reaction initiates via intermolecular radical addition, resulting in the formation of intermediate **35**. After oxidation of **35** to **36**, the photocatalyst is regenerated and product **37** is formed through intramolecular nucleophilic cyclization facilitated by the phosphate base. Importantly, the activation of NHPI esters through PCET may also play a role in transformations mediated by the cyanoarene-based donor–acceptor photocatalyst 4CzIPN, which typically requires the use of strong H^+ donors such as trifluoroacetic acid [49–52]. While many reports, including Okada’s original work, have suggested that a proton donor can accelerate the fragmentation rate of RAEs [29,49,53], specific values comparing the fragmentation rate constants or the N–O bond dissociation energies of radical anions and neutral radicals derived from RAEs are not available in the literature.



Scheme 6: Activation of NHPI esters through hydrogen-bonding in an oxidative quenching photocatalytic cycle.



Scheme 7: SET activation of RAE facilitated by a Lewis acid catalyst.



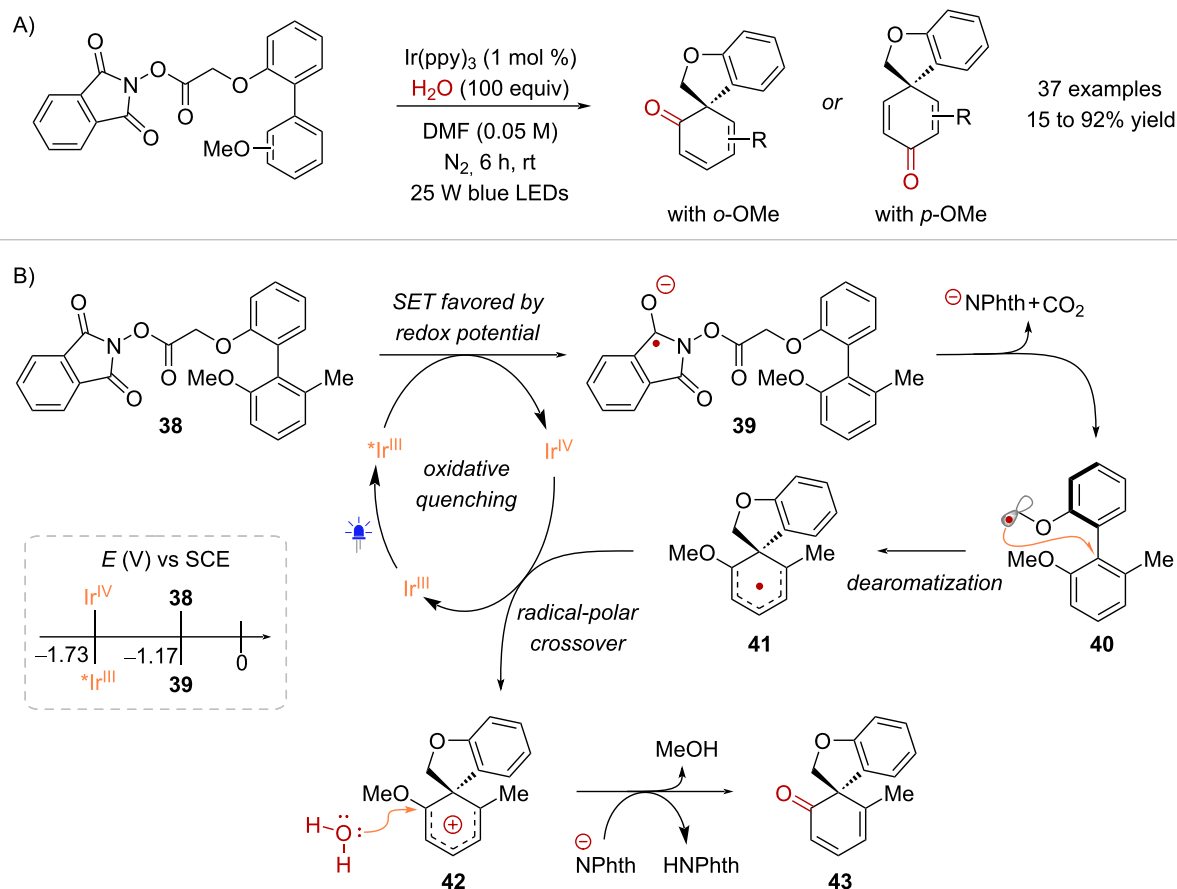
Scheme 8: PCET activation of NHPI esters in the context of a radical-redox annulation.

Lumb and co-workers recently published a study on the conversion of biaryl-derived NHPI esters into spirocyclic cyclohexadienones through a photocatalytic radical-mediated dearomatization, with H_2O serving as the nucleophile [54] (Scheme 9A). Despite the presence of H_2O in the reaction, the reduction of **38** to its corresponding radical anion **39** could occur without the need for hydrogen-bonding (Scheme 9B). Cyclic voltammetry measurements of NHPI ester **38** displayed a reduction half peak potential ($E_{p/2}$) of -1.17 V (vs SCE in MeCN) indicating that the single-electron reduction of **38** by a suitably strong reductant, such as $^*\text{Ir}(\text{ppy})_3$ ($E_{1/2}^{\text{red}}[\text{Ir}^{\text{IV}}/^*\text{Ir}^{\text{III}}] = -1.73$ V vs SCE in MeCN) would be thermodynamically favorable. Indeed, Stern–Volmer photoquenching experiments confirmed that **38** effectively quenched $^*\text{Ir}(\text{ppy})_3$ under anhydrous conditions. Consequently, the SET reduction of **38**, followed by fragmentation of **39** yielded α -oxy radical intermediate **40**. Subsequently, the spirocyclization of **40** induced the dearomatization of the methoxy-substituted aromatic ring, forming intermediate **41**, which was then oxidized to cation **42**, thereby completing the photocatalytic cycle. The reaction proceeded by regioselective nucleophilic addition of H_2O , accompanied by the loss of MeOH to deliver spirocycle **43**. Notably, the dearomative spiro-

cyclization of biaryl-derived NHPI esters has found application in the total synthesis of natural products, including the plant metabolite denobilone A and the highly oxidized dibenzocyclooctadiene lignans heteroclitin J and kadsulignan E [55].

Activation via charge-transfer complex formation

Under conditions where oxidative quenching is not thermodynamically favorable, the single electron reduction of RAEs can proceed via an alternative mechanism. For example, in the transformation of NHPI ester **44** into spirocycle **45** catalyzed by $[\text{Ir}(\text{ppy})_2(\text{dtbbpy})][\text{PF}_6]_6$, Reiser and co-workers observed that the excited state of this Ir-catalyst ($E_{1/2}^{\text{red}}[\text{Ir}^{\text{IV}}/^*\text{Ir}^{\text{III}}] = -0.96$ V vs SCE) would not promote the reduction of **44** (-1.25 V vs SCE) [56] (Scheme 10). Interestingly, the role of H-bonding in substrate activation was not considered. To explain the observed transformation, it was suggested that the Ir^{III} -photocatalyst acted as a photosensitizer in an energy-transfer (EnT) mechanism. This proposal was supported by fluorescence quenching measurements, as well as the direct excitation of **44** by UV irradiation, resulting in the formation of **45** in a 45% yield. According to this hypothesis, NHPI ester **44** would adopt



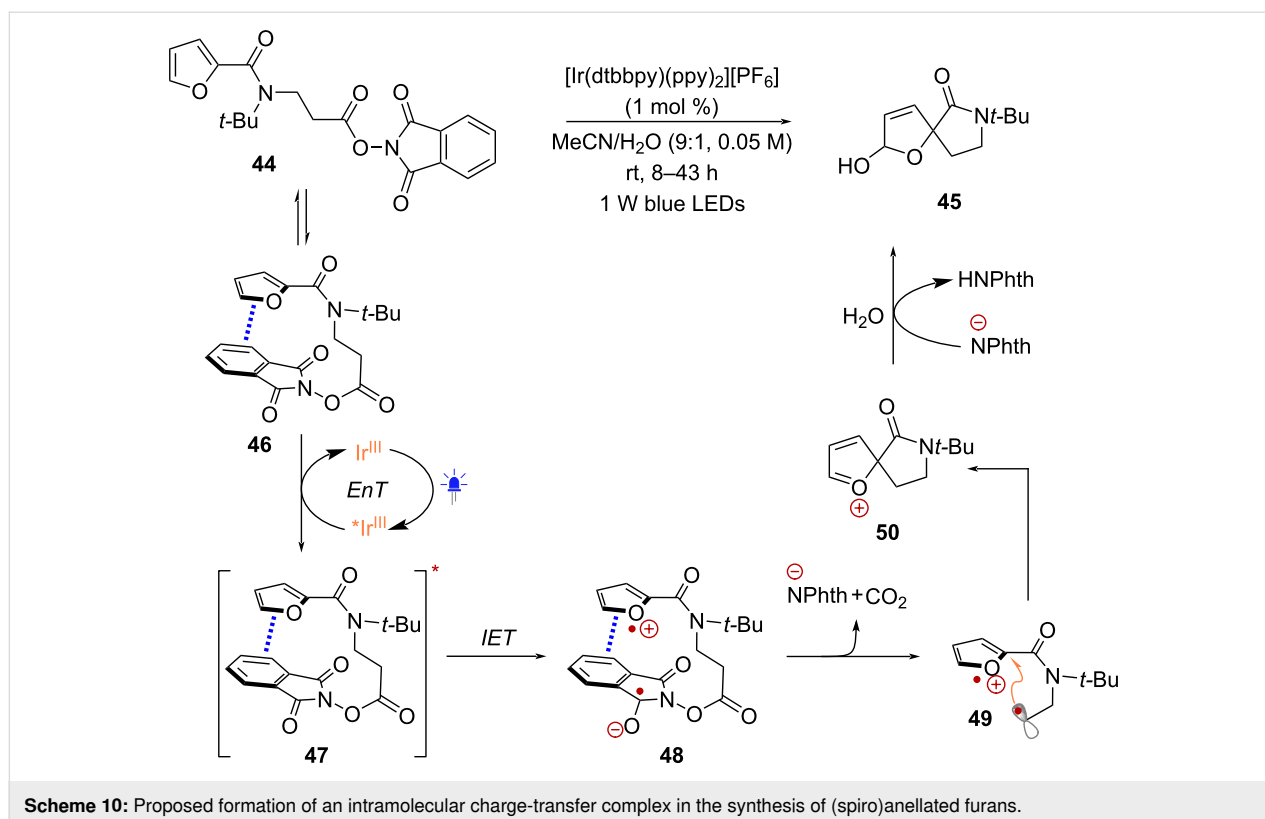
Scheme 9: Activation enabled by a strong excited-state reductant catalyst and its application in the dearomative spirocyclization of biaryls.

a favorable conformation (**46**) for π -stacking between the furan and phthalimide rings, before EnT from $^*\text{Ir}^{\text{III}}$ leads to the formation of an excited charge-transfer complex **47**. This species would undergo intramolecular electron transfer (IET) giving rise to intermediate **48**, which upon fragmentation would form radical **49**. Intramolecular radical addition into the radical cation of the furan ring would then form cation **50** before nucleophilic capture by H₂O leads to product **45**.

In 2020, the Wang group reported the functionalization of enamides employing radicals derived from NHPI esters in combination with indole nucleophiles [57] (Scheme 11A). This transformation occurred under light irradiation either in the presence or absence of a Ru^{II} photoredox catalyst. It was found that the chiral lithium phosphate catalyst (*R*)-TRIP-Li played a crucial role in accelerating the reaction rate. Following an in-depth analysis of the mechanism, the authors proposed that (*R*)-TRIP-Li has the capability to engage enamide **51** through H-bonding and NHPI ester **3** through Li-promoted Lewis acid activation, acting as a pocket that facilitates the formation of charge-transfer complex **52** (Scheme 11B). This complex can

be excited either by direct irradiation at 390 nm or through Ru^{II}-mediated EnT under blue light irradiation (456 nm). Following excitation, SET from the enamide to the active ester forms intermediate **53**, which undergoes fragmentation and radical recombination to afford intermediate **54**. At this stage, the indole nucleophile substitutes the phthalimidyl anion within the chiral pocket of the phosphate catalyst to form complex **55**, before enantioselective addition to the iminium ion affords product **56**.

NHPI esters can also engage in π - π interactions with electron-rich species to generate charge-transfer complexes that can absorb light in the visible region. These species are referred to in the literature as electron donor-acceptor (EDA) complexes [58,59] and undergo photoexcitation in the absence of an exogenous photoredox catalyst. When excited by visible light, an intra-complex SET from the donor substrate **D** to the NHPI ester acceptor takes place, generating radical ion pair **57**. Subsequently, this ion pair undergoes fragmentation, forming the corresponding substrate radical **9**, which can participate in diverse chemical transformations (Scheme 12).

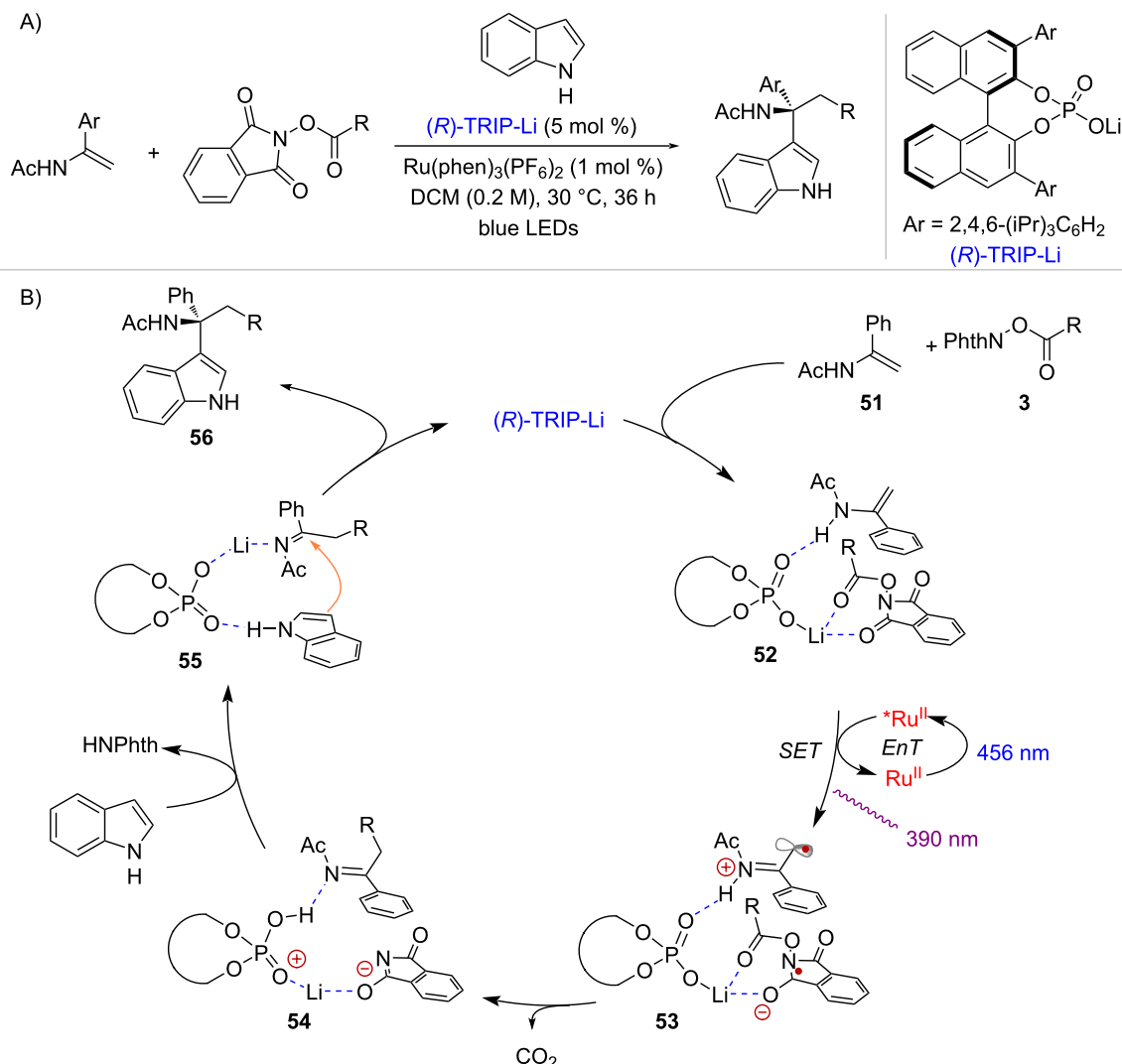


Different donor molecules are known to form EDA complexes with NHPI esters. For example, the NHPI ester derived from pivalic acid **58** and Hantzsch ester **HE** form EDA complex **59** which participates in radical mediated hydroalkylation reactions [60,61] (Scheme 13A). In the presence of electron deficient olefin **60**, classic Giese-type addition takes place under photocatalyst-free conditions, affording product **61** [60]. On the other hand, reaction with 1,7-enyne **62** affords dihydroquinoline product **63** via a cascade radical addition/cyclization process [61]. In both transformations, **HE** serves a dual role by activating the NHPI ester through EDA complex formation and providing a hydrogen atom to terminate the radical reaction. The proposed mechanism of the hydroalkylation cascade is depicted in Scheme 13B. Upon excitation of complex **59** with blue light, intra-complex SET takes place from the **HE** to the NHPI ester, leading to the formation of *tert*-butyl radical **64** and radical cation **65**. Addition of radical **64** to enyne **62** followed by 6-*exo-dig* cyclization yields radical intermediate **66**. Finally, species **65** acts as a hydrogen atom donor, delivering product **63** while forming pyridine **67** as a byproduct.

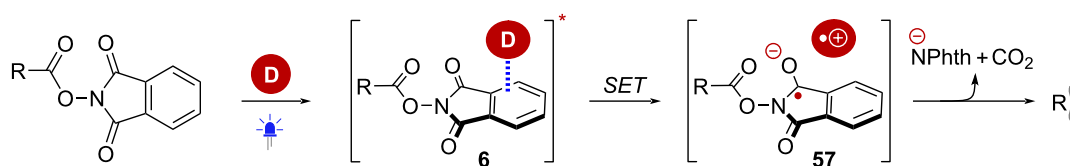
A similar mechanism would in principle account for EDA-complex-mediated Giese-type additions. However, an alternative radical chain mechanism has been discussed in the literature [62] (Scheme 14). In this instance, chain initiation takes place through photoinduced SET, enabled by EDA complex forma-

tion between the reductant *N*-(*n*-butyl)-1,4-dihydronicotinamide (**BuNAH**) and an NHPI ester (complex **68**). This process delivers substrate radical **9** and nicotinyl radical **69** following proton transfer to the phthalimidy anion. Then, addition of **9** to α,β -unsaturated ester **70** yields radical intermediate **71**. At this stage, HAT mediated by another equivalent of **BuNAH** delivers product **72**, with concomitant formation of radical **69**. Finally, aromatization of **69** via SET to NHPI ester **3**, generates pyridinium **73** as a byproduct, while propagating the radical chain reaction.

Aggarwal and co-workers discovered the photoinduced decarboxylative borylation of NHPI esters mediated by bis(catecholato)diboron (B_2cat_2) [63] (Scheme 15A). UV-vis absorption measurements showed that a mixture of a model NHPI ester with B_2cat_2 in dimethylacetamide (DMA) formed a new charge-transfer band in the visible region (>390 nm), which was attributed to the formation of EDA complex **74** (Scheme 15B). Under blue light irradiation, EDA complex **74** triggered a radical chain process initiated by B–B bond cleavage, forming boryl-NHPI ester radical **75** and boryl radical **76**. Subsequent decarboxylation of **75** yields carbon-centered radical **9** and boryl-phthalimide byproduct **77**. Meanwhile DMA-ligated B_2cat_2 **78** is formed upon dimerization of radical **76**. Reaction between radical **9** and species **78** affords boronic ester **79** while returning boryl radical **76**. Finally, chain propa-



Scheme 11: Formation of a charge-transfer complex between enamides and NHPI esters enabled by a chiral phosphate catalyst.

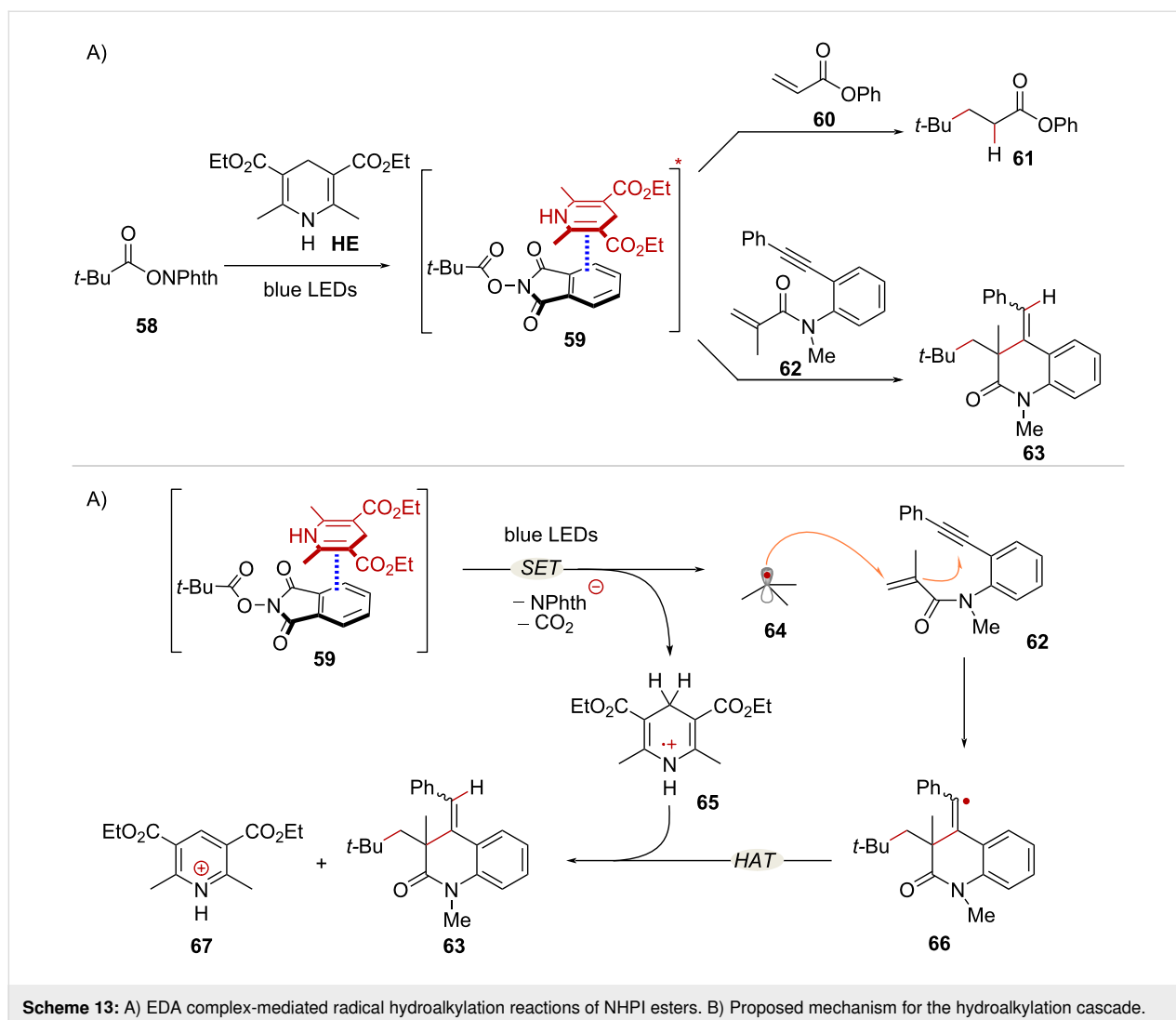


Scheme 12: Activation of NHPI ester through the formation of photoactive EDA-complexes.

gation takes place via reaction of **76** with another equivalent of the NHPI ester **3**.

The Baran lab has recently published a complementary electrochemical method, wherein the activation of complex **74** takes place through SET under constant current electrolysis [64]. The

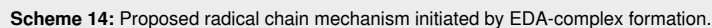
Glorius and Y. Fu groups have independently proposed the formation of analogous charge-transfer complexes involving NHPI esters, bis(pinacolato)diboron (B_2pin_2), and Lewis bases (pyridine or isonicotinate *tert*-butyl ester) in $C(sp^2)$ -borylation methods under photochemical and thermal conditions, respectively [65,66].



The activation of NHPI esters through EDA complex formation is also possible by employing a catalytic donor species, which enables a range of redox neutral transformations. In 2019, Shang and Fu initially demonstrated this approach by utilizing catalytic amounts of triphenylphosphine (PPh₃) and sodium iodide (NaI) [67]. Upon formation of EDA complex **80**, radical addition to silyl enol ether **81** was promoted under blue light irradiation, affording acetophenone product **82** (Scheme 16A). Additionally, Minisci-type additions were carried out in the presence of protonated quinoline radical acceptor **83**, affording product **84** (Scheme 16A). Mechanistically, this activation mode involves an intra-complex SET that forms the Ph₃P–NaI radical cation species **85** and the corresponding radical anion **86**. Decarboxylative fragmentation of **86** forms radical **9**, which upon radical addition to **84** and deprotonation yields radical **87**. Finally, oxidation of **87** mediated by **85** delivers the Minisci addition product **84** while regenerating PPh₃ and NaI (Scheme 16B).

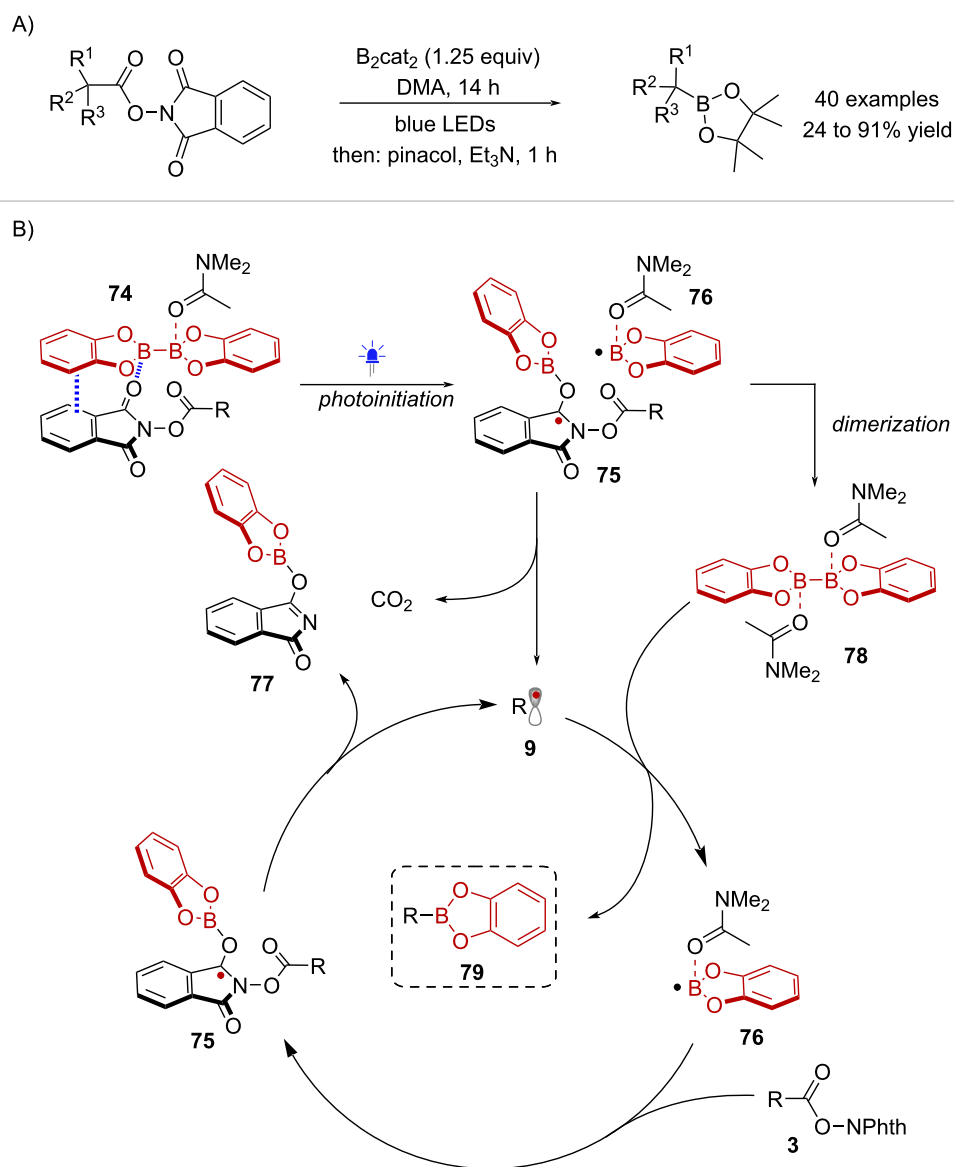
The Ohmiya group has developed a series of light-mediated decarboxylative transformations of NHPI esters using a phenothiazine-based organophotoredox catalyst **PTH1**. This type of catalyst is believed to facilitate SET to NHPI esters through the formation of EDA complexes. Interestingly, upon addition of RAE **58** to a solution of **PTH1**, a noticeable red shift in the UV–vis absorption spectra of **PTH1** was observed, suggesting the formation of a charge transfer complex of the type **88** [68] (Scheme 17A). *tert*-Butyl radical (**64**), along with additional 2° and 3° alkyl radicals, resulting from these EDA complexes were harnessed in C(sp³)-heteroatom bond forming reactions [69], and in the difunctionalization of styrenes [68] (Scheme 17B).

The catalytic cycle for the styrene difunctionalization reaction is depicted in Scheme 18. First, EDA complex **88** consisting of RAE **58** and the **PTH1** catalyst is formed. Under blue light irradiation, intra-complex SET leads to the formation of PTH



H. Fu and co-workers reported that the combination of NHPI esters and cesium carbonate (Cs_2CO_3) gave rise to a new absorption band in the visible region, suggesting the formation of a photoactive charge-transfer complex [70]. This activation mode was initially employed in a decarboxylative coupling reaction with aryl thiols [70]. Further studies showed that 4-(trifluoromethyl)thiophenol (**97**) could act as a catalytic reductant in the aminodecarboxylation reaction of NHPI esters derived

Bosque and Bach reported the use of 3-acetoxyquinuclidine (**q-Ac**) as a catalytic donor for the activation of TCNHPI esters derived from α -amino acids [72] (Scheme 20). Treatment of *N*-Boc-proline-derived TCNHPI ester **104** with **q-OAc** in MeCN resulted in the formation of a yellow solution, which upon blue light irradiation provided the aminodecarboxylation product **105** in 69% yield. It was hypothesized that the reaction involved the formation of EDA complex **106** that led to the formation of α -amino radical **107** through photoinduced SET followed by fragmentation. Subsequent oxidation of **107** by radical cation **q-Ac^{•+}** afforded iminium ion **108** before nucleophilic addition of the in situ-generated tetrachlorophthalimyl anion ([−]TCPhth) led to the formation of a final product **105**. Of note,



Scheme 15: A) Photoinduced decarboxylative borylation. B) Proposed radical chain mechanism.

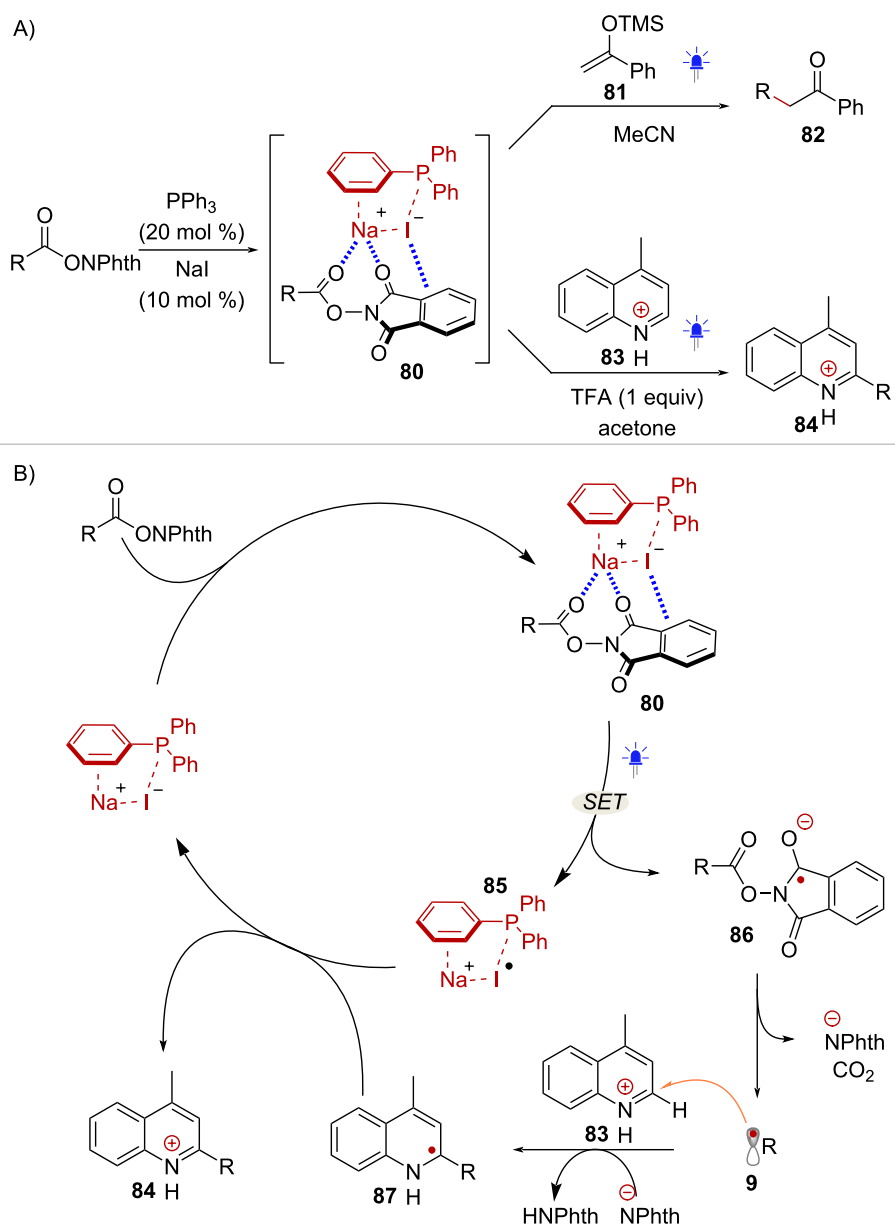
the amino-decarboxylation reaction proved unsuccessful when employing alternative photocatalysts such as Ru(bpy)₃Cl₂ or eosin Y, underscoring the distinctive ability of **q-OAc** to activate TCNHPI esters via EDA complex formation.

Photoinduced transition metal-catalyzed mechanisms

The in situ formation of photoactive catalysts can be achieved by combining simple transition metal (TM) salts with suitable ligands. These TM catalysts are fundamentally distinct from traditional Ru- and Ir-based photoredox catalysts, as they play a dual role, by engaging in photoinduced electron transfer processes with the substrate and participating in the key bond-

forming/breaking steps via substrate–TM interactions [73,74]. This paradigm has been employed in the activation of NHPI esters under photoinduced copper (Cu) and palladium (Pd) catalysis.

In 2017, Peters and Fu reported a Cu-catalyzed decarboxylative C(sp³)–N coupling employing NHPI esters as dual reagents [75] (Scheme 21A). The combination of CuCN and the ligands xantphos and neocuproine in a 2:3:1 ratio resulted in the formation of a light absorbing species with an absorption band in the 380–460 nm range. Thus, it was hypothesized that Cu^I catalytic species **109** would give rise to photoexcited complex **110** under blue light irradiation (Scheme 21B). Complex **110** and NHPI

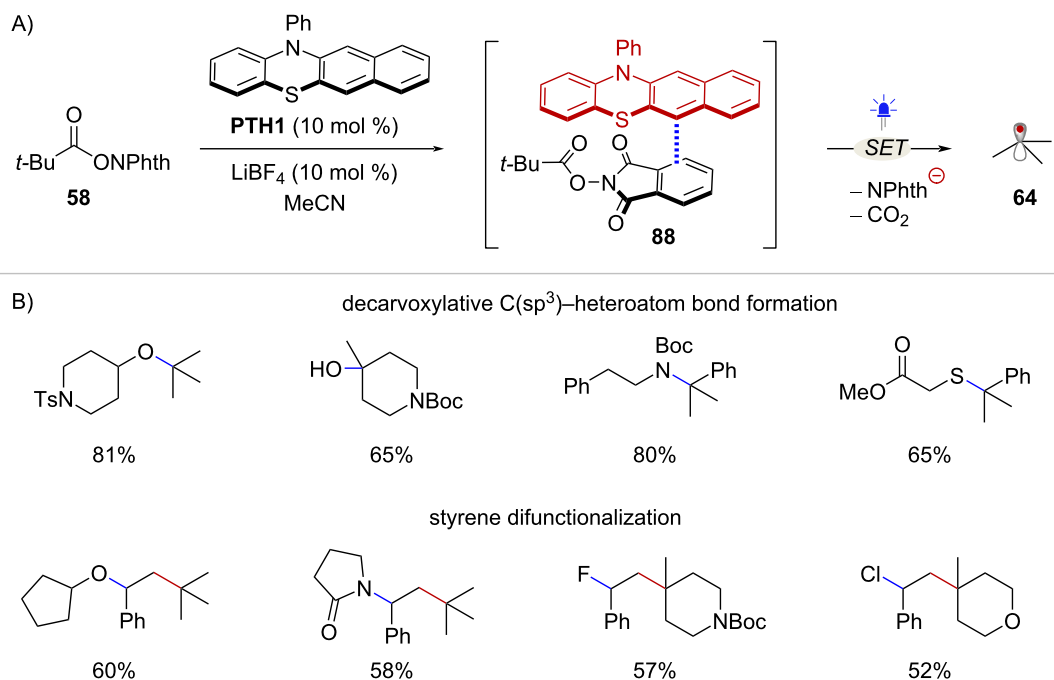


Scheme 16: A) Activation of NHPI esters mediated by PPh_3/NaI . B) Proposed catalytic cycle involving EDA-complex formation.

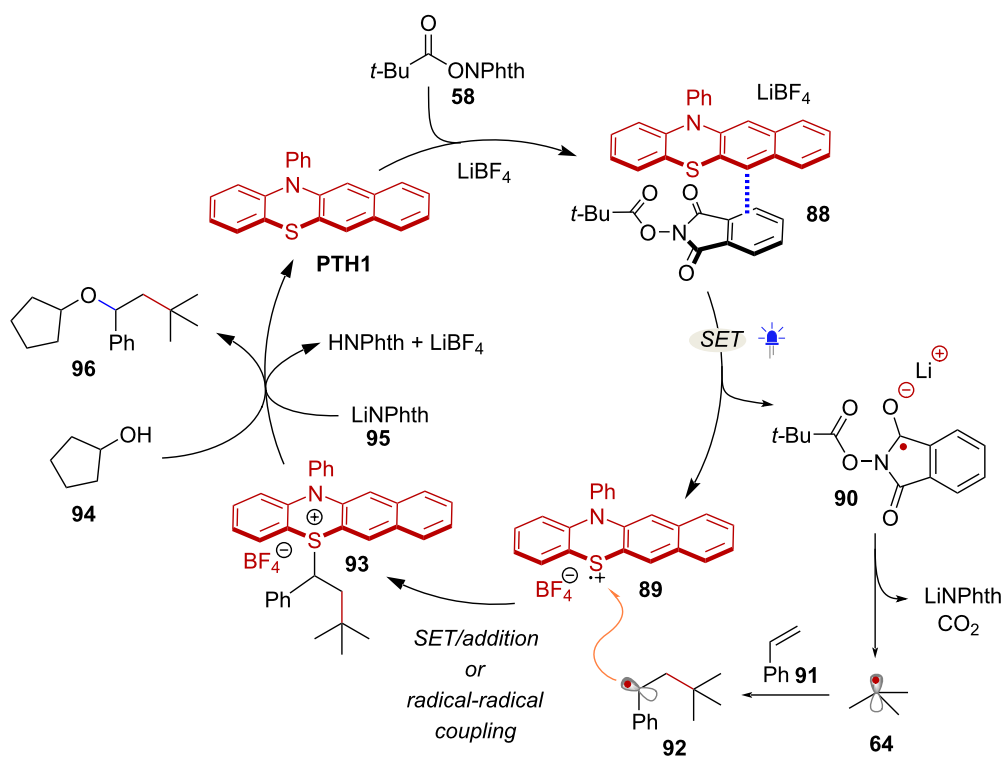
ester **3** would then engage in SET likely through an inner sphere mechanism, providing phthalimide ligated Cu^{II} intermediate **111** and carboxyl radical **112**. At this stage, the resulting radical species **9** would recombine with **111** to form Cu^{III} complex **113**. Alternatively, reaction of **3** with the photoexcited Cu^{I} complex through oxidative addition (OA) followed by decarboxylation could directly lead to intermediate **113** (Scheme 21B, blue arrow). However, radical clock experiments support the intermediacy of free radicals, indicating the involvement of the SET pathway (Scheme 21C). Eventually, reductive elimination of **113** afforded product **114** while regenerating the catalytic species **109**. It is worth nothing that further transformations of

NHPI esters under photoinduced Cu catalysis have been reported in recent years, including decarboxylative alkynylations [76–78] and the $\text{C}(\text{sp}^3)\text{--H}$ alkylation of α -amino acids [79].

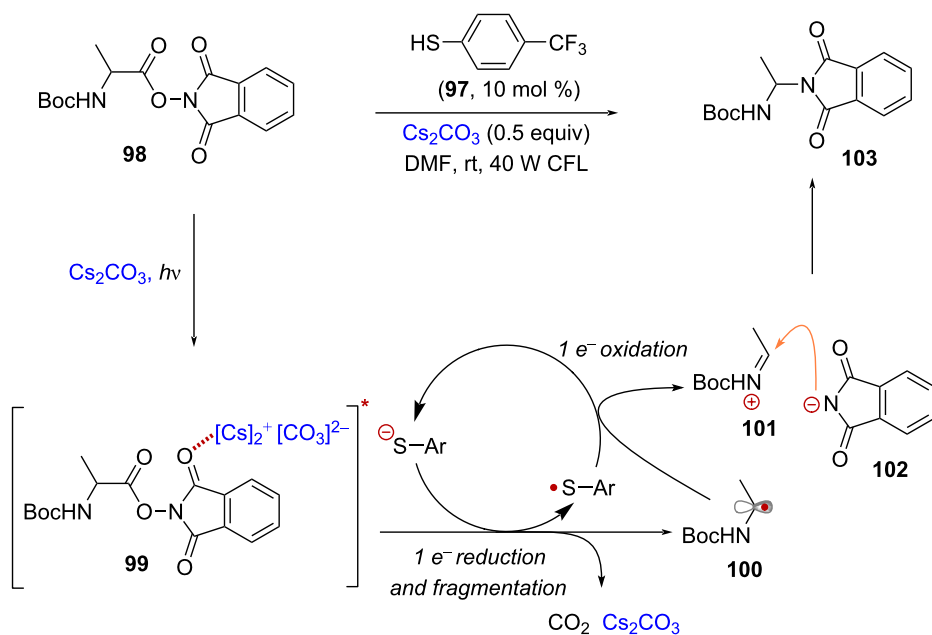
The ability of NHPI esters to act as dual reagents was also investigated by Glorius and co-workers in the context of a photo-induced Pd-catalyzed aminoalkylation of 1,4-dienes [80] (Scheme 22A). The study showed that a photoexcited Pd^0 species formed upon blue-light irradiation of $\text{Pd}(\text{Ph}_3)_4$, was able to promote the activation of NHPI esters via SET (Scheme 22B). The photoinduced electron transfer process between the Pd-photocatalyst and RAE **58** was proposed to form a



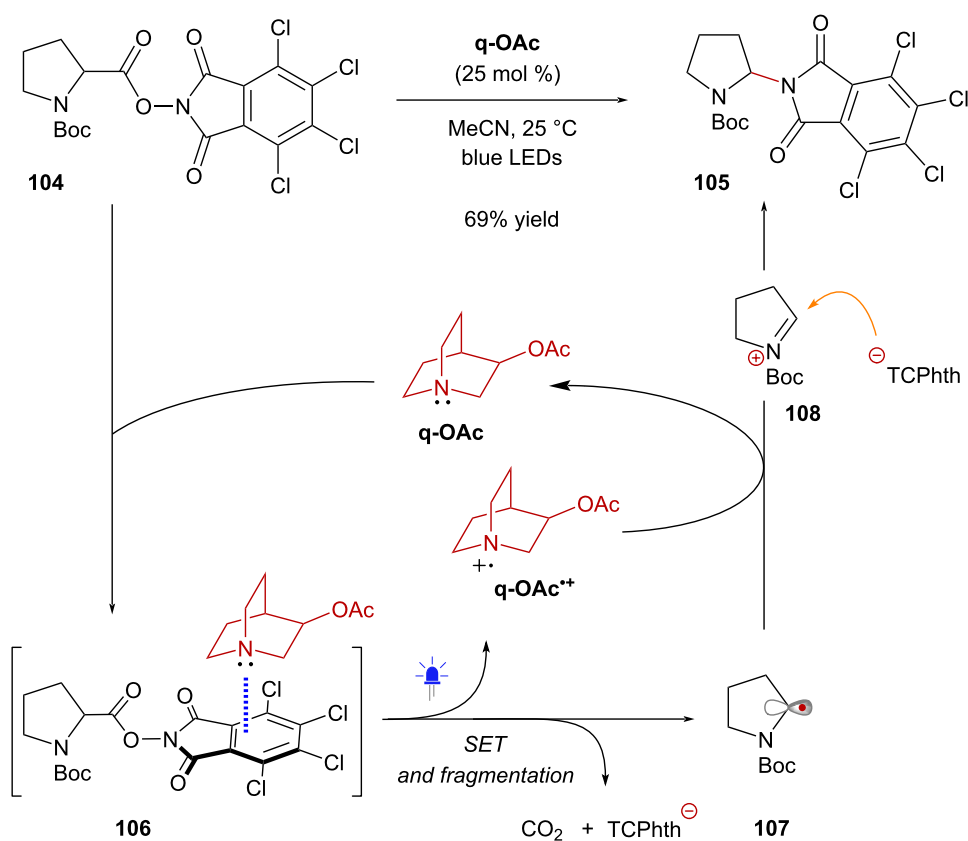
Scheme 17: A) Radical generation facilitated by EDA complex formation between **PTH1** catalyst and NHPI esters. B) Selected scope of **PTH1**-catalyzed decarboxylative transformations.



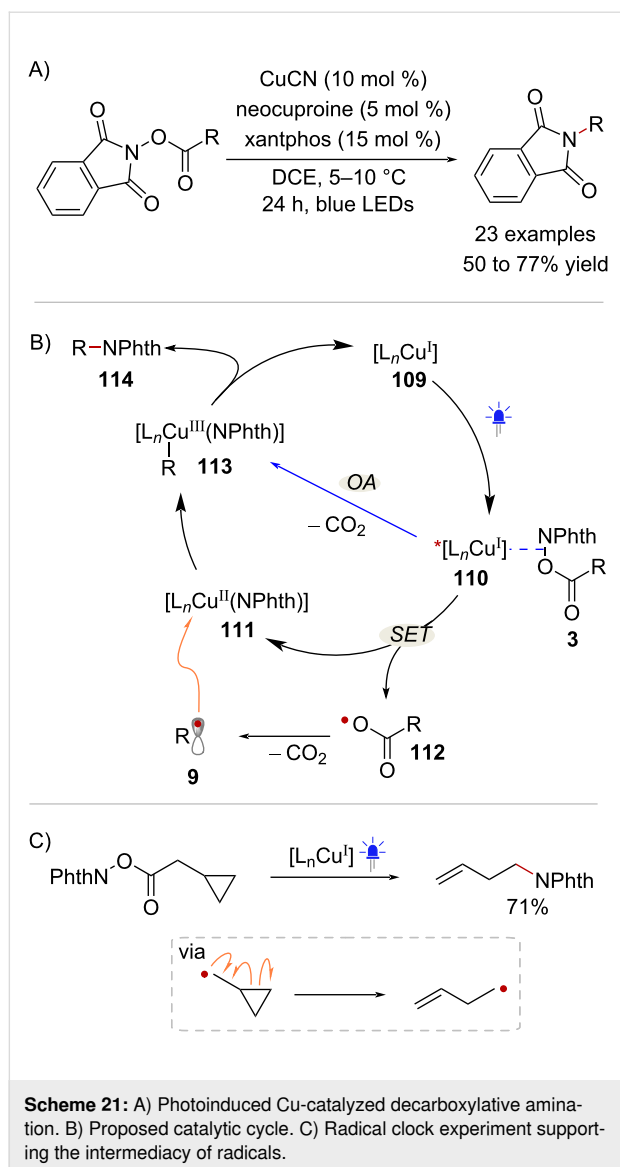
Scheme 18: Proposed catalytic cycle for the difunctionalization of styrenes.



Scheme 19: Formation of a charge-transfer complex between NHPI esters and Cs_2CO_3 enables decarboxylative amination.



Scheme 20: 3-Acetoxyquinuclidine as catalytic donor in the activation of TCNHPI esters.



hybrid alkyl Pd^I-radical species **115** which could then react with 1,4-butadiene (**116**) to form hybrid allyl Pd^I complex **117**. Subsequently, it was suggested that the species **117** would lead to the formation of a π -allylpalladium intermediate **118** through radical recombination. Ultimately, nucleophilic attack by the phthalimidyl anion would generate the aminoalkylation product **119**, completing the catalytic cycle. In addition to this aminoalkylation method, the synthetic utility of radical intermediates derived from NHPI esters under photoinduced Pd-catalysis has been demonstrated in Heck-type couplings [81,82] and in the desaturation of aliphatic carboxylic acids [83].

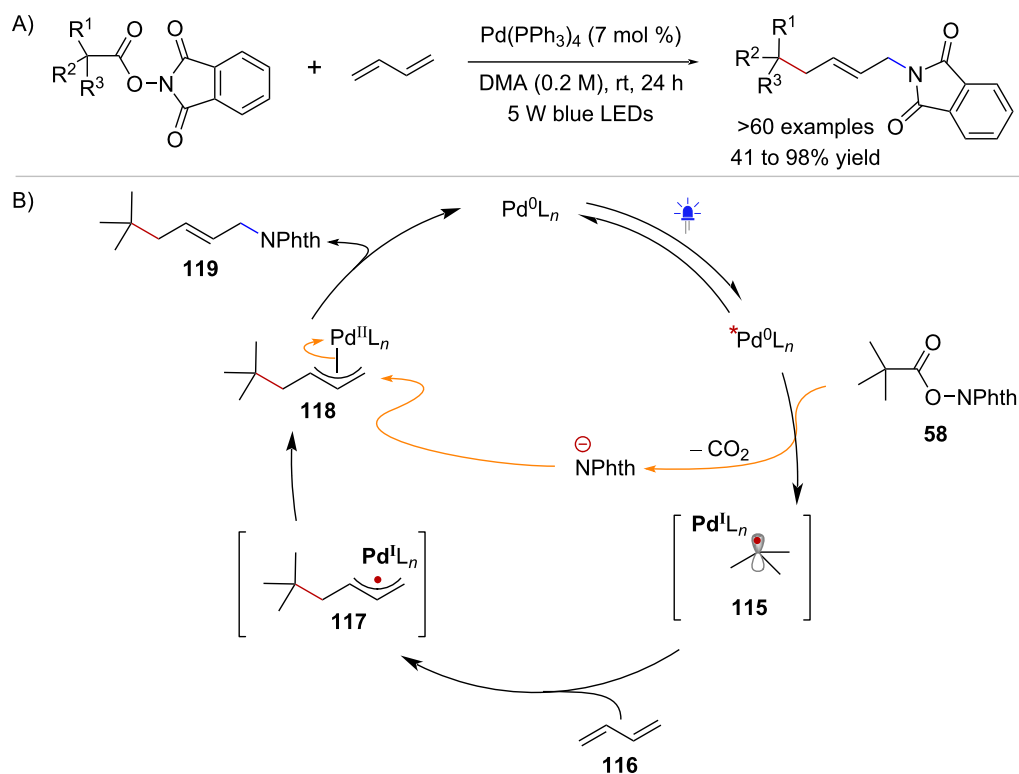
Initiation by metal catalysts and stoichiometric reductants

The activation of NHPI esters under transition metal catalysis without the need of light is also feasible, and generally, two

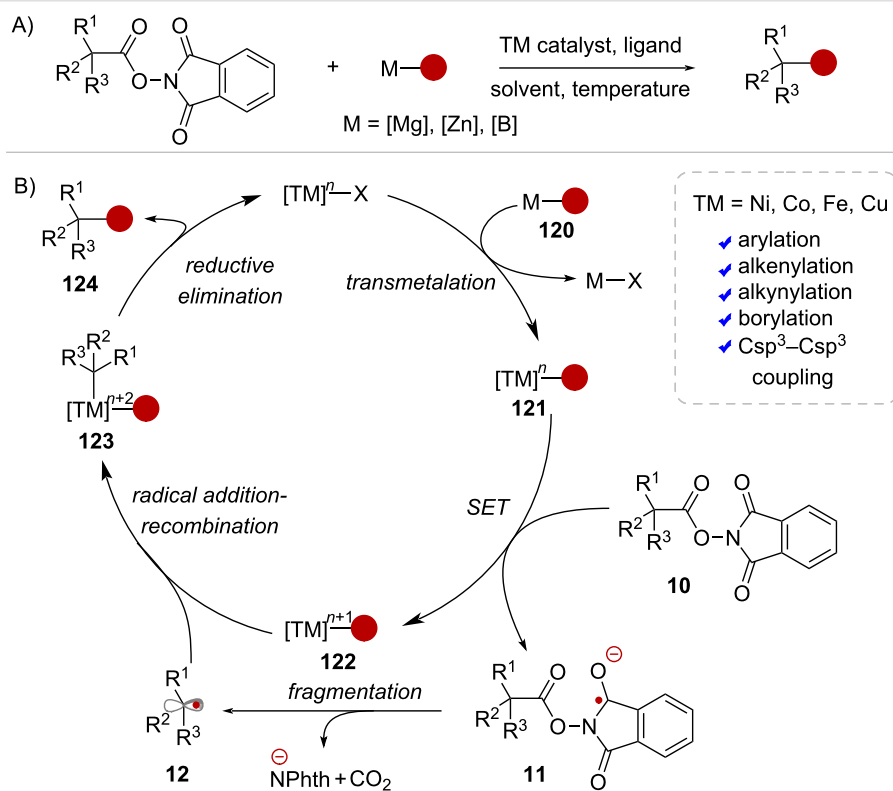
types of coupling reactions can be envisioned. On one hand, the decarboxylative cross-coupling (DCC) of NHPI esters with organometallic reagents, resembling classic Kumada, Negishi, and Suzuki couplings, has been enabled by nickel (Ni), cobalt (Co), iron (Fe), and copper (Cu) catalysts [84–91] (Scheme 23A). The typical mechanism begins by transmetalation of the organometallic coupling partner **120** to the TM catalyst (Scheme 23B). The resulting organometallic intermediate **121** can act as a reducing agent, transferring an electron to RAE **10** to form radical anion **11** and the corresponding oxidized metal complex **122**. Following fragmentation, the ensuing alkyl radical **12** is captured by intermediate **122**, resulting in the formation of complex **123**. At this point, the metal center has undergone a two-electron oxidation, making it well-suited for reductive elimination yielding the cross-coupling product **124**.

Under these catalytic conditions, various TM-catalyzed decarboxylative functionalizations employing RAEs have been established (Scheme 24). Baran and co-workers have reported arylation protocols (Scheme 24A) using arylzinc reagents [84,85], Grignard reagents [85] and arylboronic acids [86], as well as decarboxylative alkenylation [87] (Scheme 24B), alkynylation [88] (Scheme 24C) and C(sp³)–C(sp³) cross-coupling [89] (Scheme 24D). Finally, similar chemistry has been extended to the decarboxylative borylation of RAEs under Ni [90] and Cu [91] catalysis (Scheme 24E). Importantly, the Wang group has independently studied the decarboxylative Negishi coupling of RAEs with organozinc reagents under Co-catalysis, effecting diverse arylation, alkenylation, and alkynylation reactions [92].

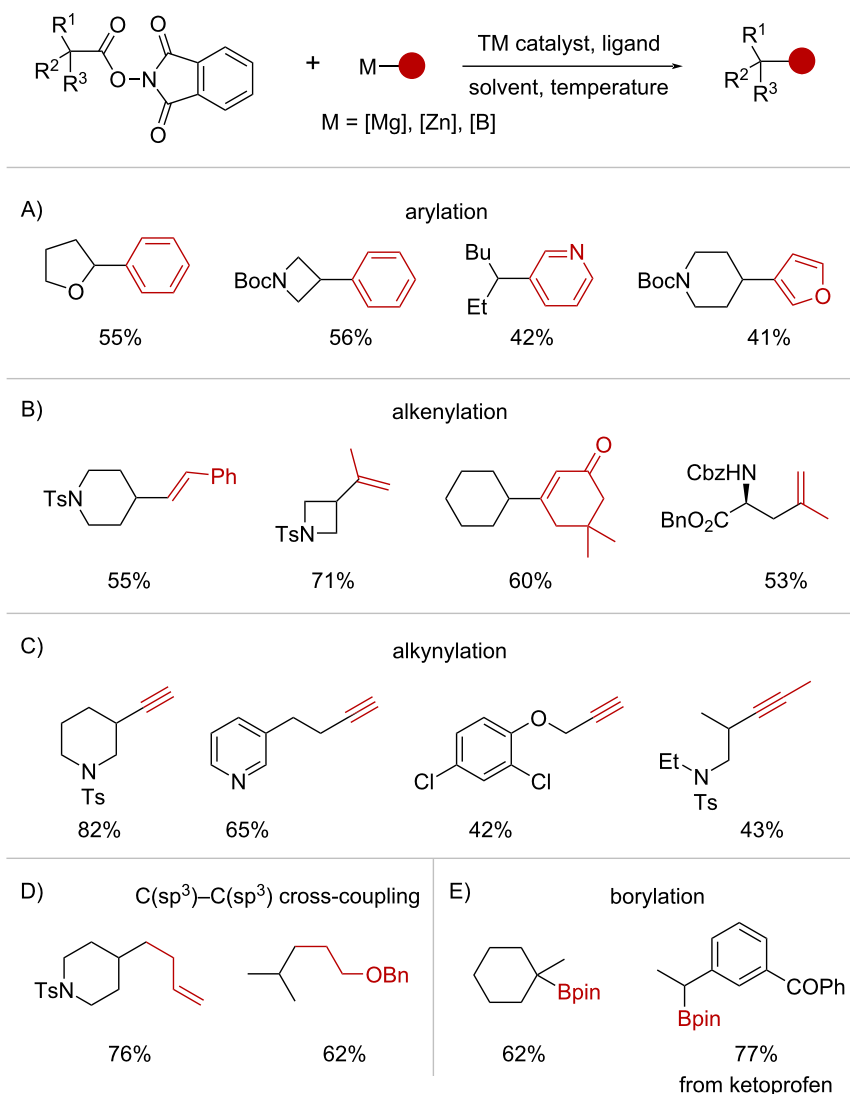
The second type of reaction is referred to as cross-electrophile coupling and involves the Ni-catalyzed reaction of NHPI esters with aryl- and vinyl halides under reducing conditions (Scheme 25A). The general catalytic cycle begins with oxidative addition of an organohalide into a Ni⁰ catalyst yielding Ni^{II} complex **125** (Scheme 25B). In parallel, the initial SET activation of RAE **10**, leading to the formation of radical anion **11**, takes place in the presence of a stoichiometric reductant, which can be an organic reductant, such as tetrakis(*N,N*-dimethylamino)ethylene (TDAE) or Hantzsch ester (HE), or a metal such as zinc (Zn⁰) or manganese (Mn⁰). Upon fragmentation, radical species **12** is captured by the oxidative addition complex **125**, giving rise to Ni^{III} complex **126**. The cross-coupling product **127** is then formed via reductive elimination of **126** which gives Ni^I intermediate **128**. At this stage, it is proposed that the Ni^I complex **128** can participate in a SET event with another equivalent of substrate **10**, generating another equivalent of radical **12**, that propagates into the next catalytic cycle. Finally, the corresponding Ni^{II} complex **129** is reduced back to



Scheme 22: A) Photoinduced Pd-catalyzed aminoalkylation of 1,4-dienes. B) Proposed catalytic cycle.



Scheme 23: A) TM-catalyzed decarboxylative coupling of NHPi esters and organometallic reagents. B) Representative catalytic cycle.



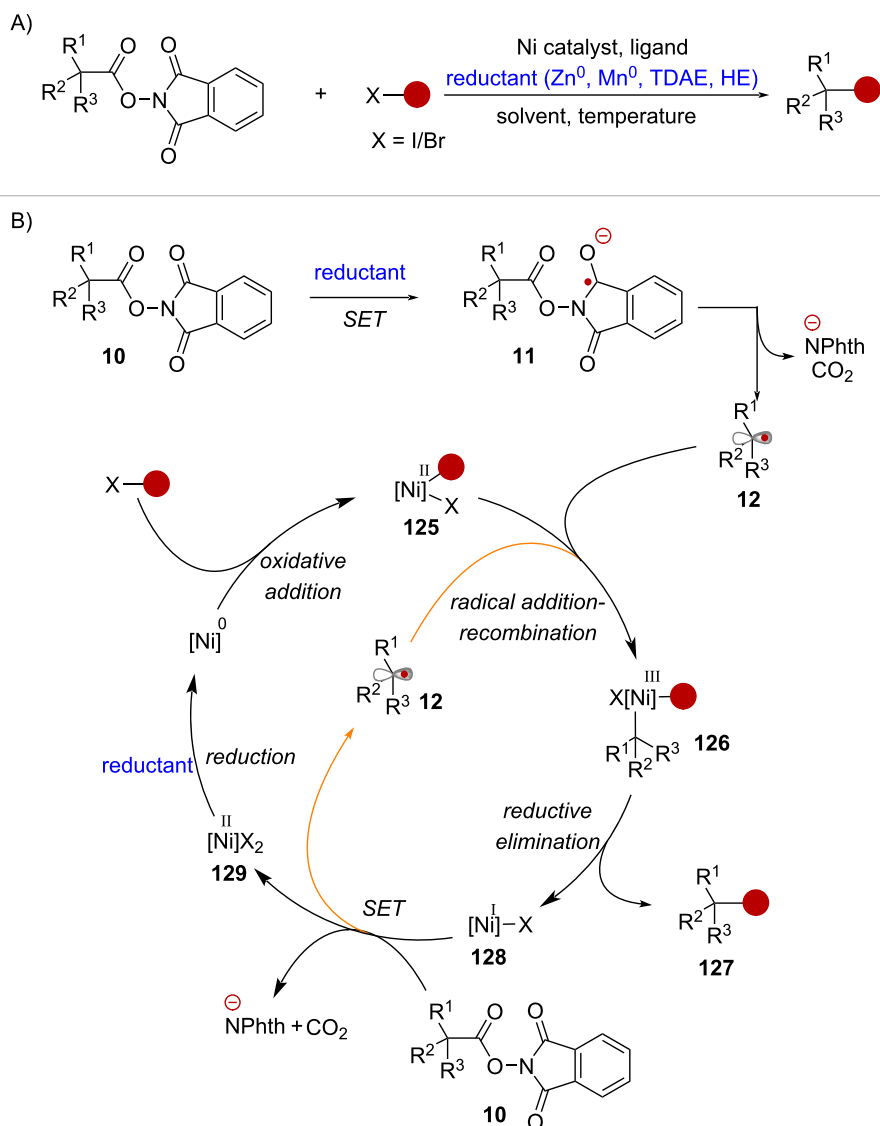
Scheme 24: Synthetic applications of the TM-catalyzed decarboxylative coupling of NHPI esters and organometallic reagents.

the corresponding Ni⁰ species by the stoichiometric reductant, initiating a new catalytic cycle.

Weix and co-workers have developed a series of Ni-catalyzed couplings of NHPI esters with different electrophiles, including aryl halides [93,94], bromoalkynes [95], bromoalkanes [96], and pyridyl thioesters [97] (Scheme 26A). Likewise, the Rousseaux group has recently documented the arylation of NHPI esters obtained from cyclopropanecarboxylic acids [98] and malonic acid half amides [99], while the Reisman lab has pioneered an enantioselective cross-electrophile coupling between NHPI esters and alkenyl bromides [100] (Scheme 26A). In addition, Jolit and Molander disclosed the decarboxylative arylation of NHPI esters derived from bicyclo[1.1.1]pentanes

(BCPs) by combining Ni-catalysis and photoinduced EDA complex activation [101] (Scheme 26B).

A novel approach for the activation of redox-active esters was recently reported by Cornella and co-workers [32]. In this study, low valent bismuth (Bi) complex **Bi-1** was found to exhibit redox properties similar to those of first row-transition metal catalysts, enabling the activation of tetrachlorophthalimide (TCPhth) active esters towards C(sp³)-N cross-couplings with nitrogen heterocycles (Scheme 27). The catalytic reaction was proposed to begin by oxidative addition of RAE **104** to catalyst **Bi-1**, forming an in cage radical pair consisting of Bi^{III} species **130** and α -amino radical **107** (Scheme 27B). Importantly, electron paramagnetic resonance (EPR) spectroscopy at



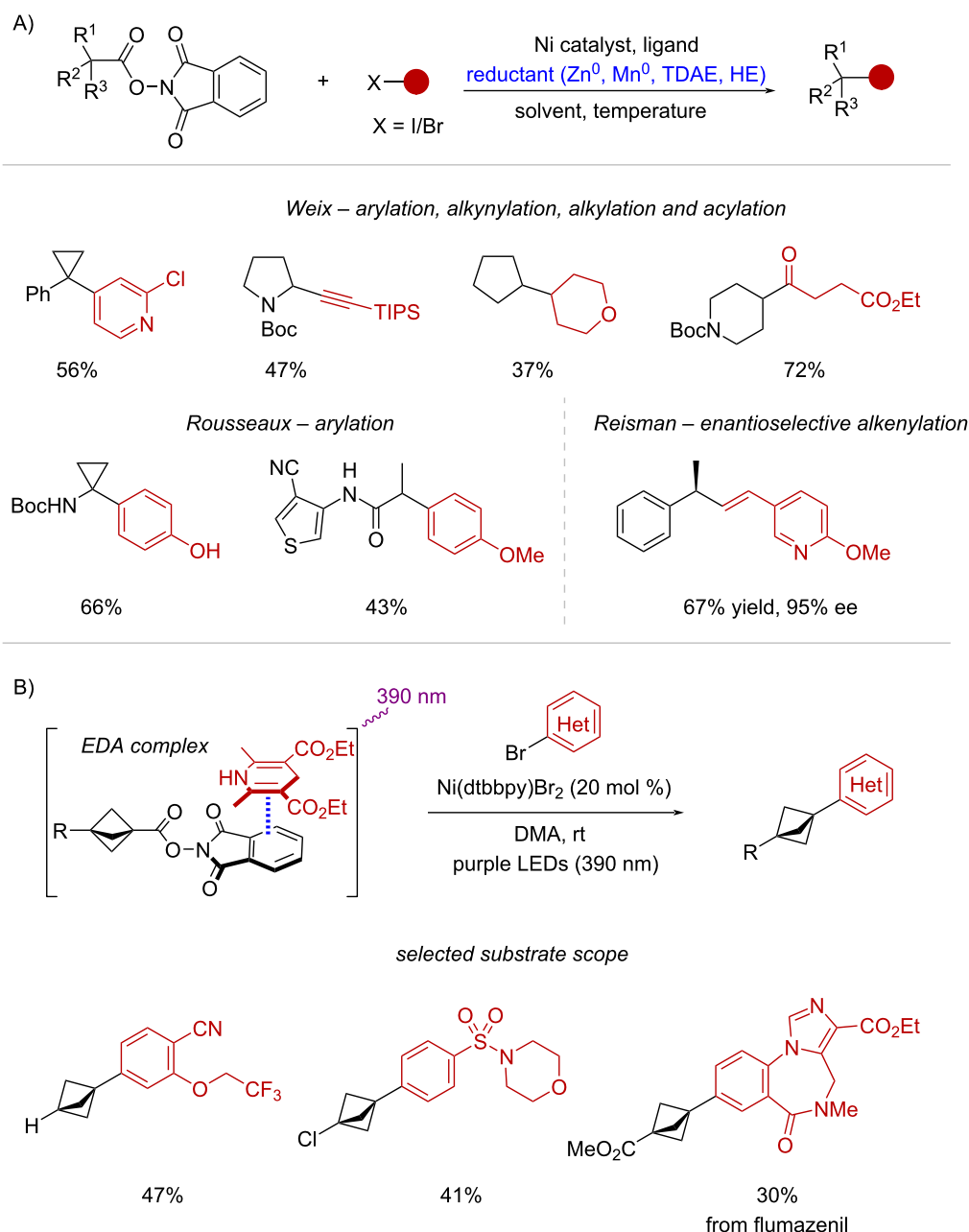
Scheme 25: A) Ni-catalyzed cross-electrophile coupling of NHPI esters. B) Representative catalytic cycle.

25 °C supported the formation of species **107**. However, NMR measurements at –40 °C showed the accumulation of Bi^{III} complex **131**, which can be prepared separately in a stoichiometric experiment. As such, two different pathways may lead to the C(sp³)–N cross-coupling products. On one hand, in-cage electron transfer from radical **107** to Bi^{III} complex **130** can generate iminium ion **108**. Alternatively, intermediate **108** could arise from complex **131** by reductive elimination. Ultimately, the iminium ion can be trapped by the nitrogen nucleophile to form product **132** or by the in-situ-generated tetrachlorophthalimyl anion (–TCPhth) affording product **105**.

Stoichiometric reductants can facilitate certain radical-mediated transformations that involve NHPI esters, even without the presence of metal catalysts. Larionov and Sun have indepen-

dently reported notable examples of these transformations, involving the Zn⁰-mediated cross-coupling of redox-active esters with chlorophosphines [102] and *gem*-difluoroalkenes [103], respectively. In the report by Sun and co-workers, it was proposed that the activation of RAE **10** occurs upon reduction with Zn powder to give radical anion **11** (Scheme 28). Following fragmentation, radical intermediate **12** would then attack *gem*-difluoroalkene **133**, affording intermediate **134**. Reduction of this radical species by another equivalent of Zn⁰ would then form anionic intermediate **135**. Finally, the selective formation of *Z*-monofluoroalkene product **136** is achieved through anti-coplanar elimination of fluoride.

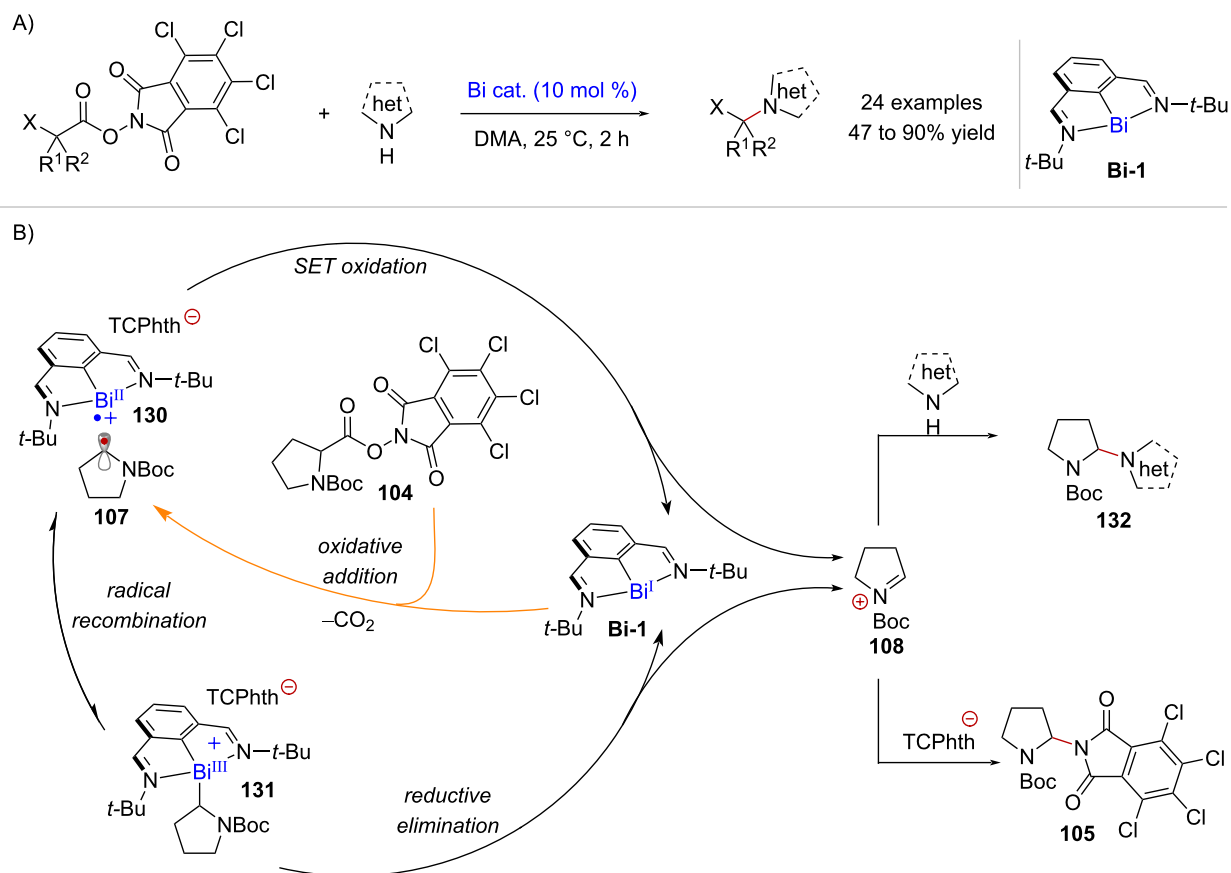
Shuhua Li and co-workers reported the generation of alkyl radicals from NHPI esters, mediated by a pyridine-boryl radical



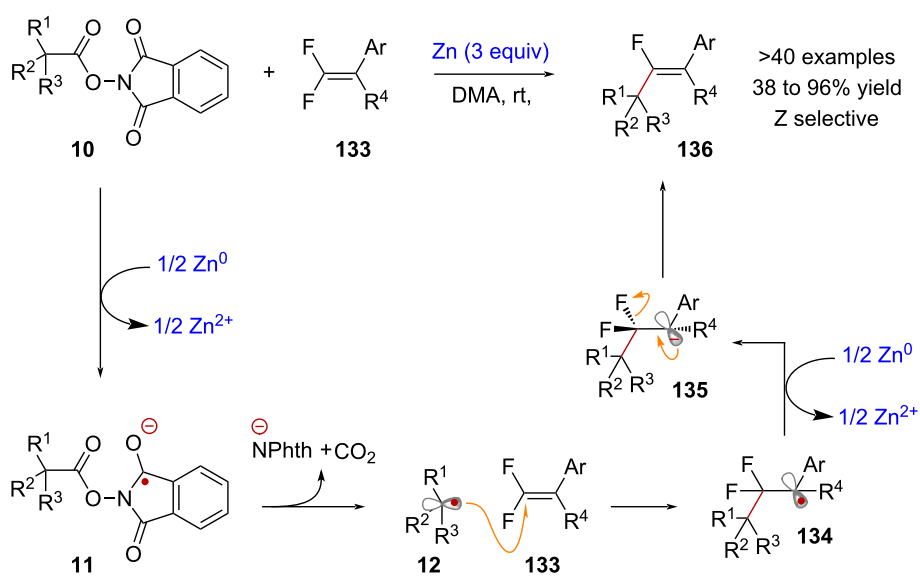
Scheme 26: A) Synthetic applications of decarboxylative cross-electrophile couplings. B) Decarboxylative arylation of BCP-redox active esters enabled by EDA complex activation and Ni catalysis.

reductant species in the context of alkene hydroalkylation [104] and cross-decarboxylative couplings with 4-cyanopyridines [105] (Scheme 29A). In the mechanism of the latter transformation, pyridine **137** also serves as a catalyst, generating the crucial pyridine-boryl radical **138** via reaction with B_2pin_2 (Scheme 29B). The proposed species **138** induces the reductive fragmentation of active ester **10**, regenerating pyridine **137** while forming alkyl radical **12**, CO_2 and phthalimide-B(pin)

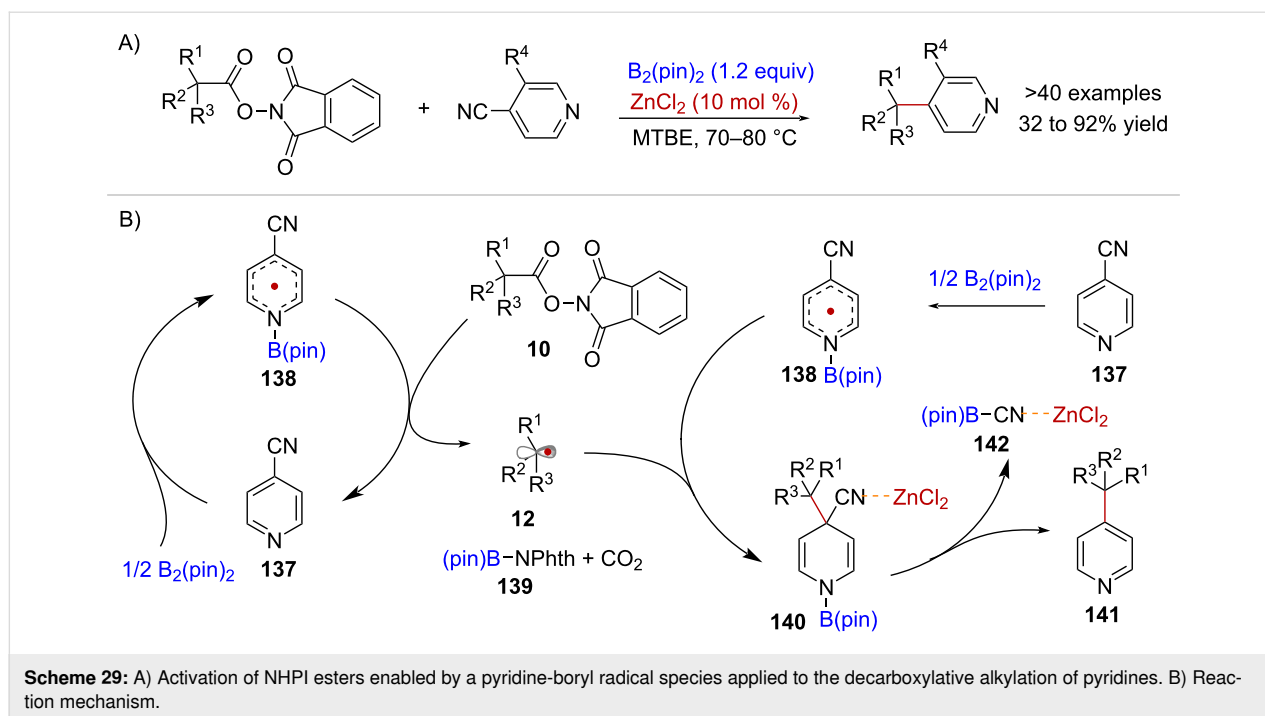
adduct **139**. Subsequently, radical–radical coupling between **12** and one equivalent of **138** affords dihydropyridine **140**, which upon re-aromatization, facilitated by ZnCl_2 acting as a Lewis acid, yields product **141**, accompanied by the formation of cyano-B(pin) **142**. Importantly, in the absence of ZnCl_2 , intermediate **140** could be detected by HRMS and ^{11}B NMR, highlighting the pivotal role of ZnCl_2 in promoting rearomatization.



Scheme 27: A) Activation of tetrachlorophthalimide redox-active esters enabled by a low-valency Bi complex. B) Proposed mechanism involving two plausible reaction pathways.



Scheme 28: Activation of NHPI esters mediated by Zn⁰ applied in a Z-selective alkenylation reaction.



N-Heterocyclic carbene (NHC) catalysis

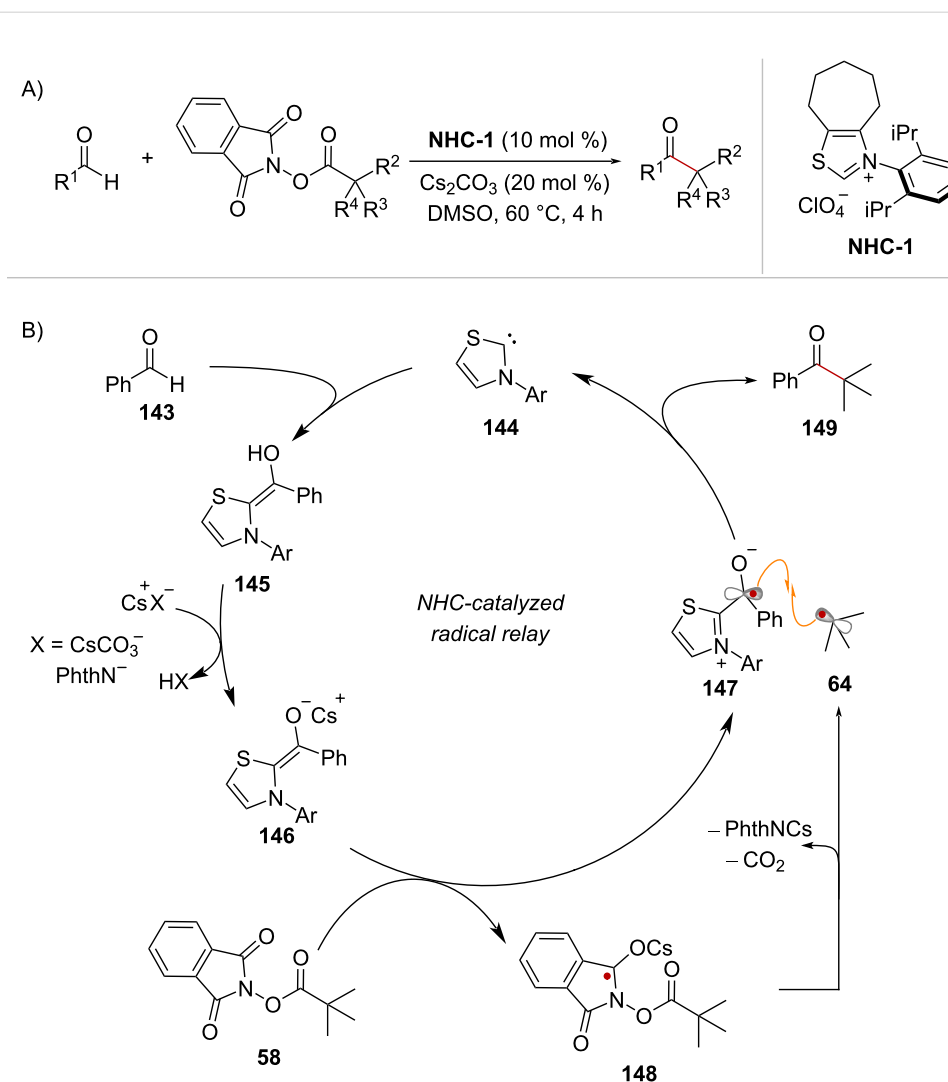
In 2019, Nagao and Ohmiya reported the decarboxylative coupling of NHPI esters with aldehydes enabled by NHC catalysis [106]. The reaction proceeds with the catalyst **NHC-1** at 60 °C and gives rise to ketones (Scheme 30A). The proposed mechanism begins with the reaction of benzaldehyde (**143**) and the NHC-catalyst **144** to form the neutral Breslow intermediate **145** (Scheme 30B). Then, cesium carbonate deprotonates the enol OH in **145**, to provide the enolate form of Breslow's intermediate **146**, which is a suitable reducing agent to trigger the fragmentation of NHPI ester **58** ($E^{\circ}_{\text{ox}} = -0.97$ V vs SCE in MeCN). Hence, it is proposed that enolate **146** induces the single electron reduction of **58**, generating the persistent radical **147** and the transient species **148**, which fragments into *tert*-butyl radical (**64**). Notably, the reduction of NHPI ester **58** could be facilitated by interaction of a cesium cation with the oxygen lone pair of the phthalimide, in analogy to the mechanism discussed in Scheme 7B. Lastly, radical–radical coupling between **64** and **147**, accompanied by elimination of the NHC catalyst, yields ketone product **149**. In subsequent studies, this NHC-catalyzed radical relay activation mode has been extended to the alkylation of aliphatic aldehydes [107] and to the three-component alkylacylation of olefins [108].

Alternatively, NHC catalysts can mediate the generation of radical intermediates from NHPI esters via the stabilization of a photoactive EDA complex. In 2020, Wang and Chen reported a photochemical C(sp³)-heteroatom coupling reaction of NHPI esters mediated by NaI and the catalyst **NHC-2** [109]

(Scheme 31A). Initial investigations showed that the reaction proceeded in the absence of the NHC catalyst, and it was reasoned that substrate **150** and NaI formed EDA complex **151** that would undergo light-mediated decarboxylation (Scheme 31B). However, upon addition of catalyst **NHC-2** an improvement of the reaction yield from 36% to 63% was observed. The authors proposed that the addition of the NHC catalyst facilitates the formation of EDA complex **151**. In addition, it is thought that the stabilization imparted by the NHC catalyst is crucial in the subsequent radical recombination between C(sp³) radical **152** and the corresponding iodine-centered radical which provides iodination product **153** (Scheme 31B). It is worth noting that the iodination product is formed exclusively when using acetone as the solvent (see compound **154** in scheme C) whereas in DMF a nucleophilic substitution takes place to afford products of the type **155** (Scheme 31B). Representative examples of the substrate scope are shown in Scheme 31C. The in situ-generated phthalimidyl anion (–Nphth) is a competent nucleophile and gives rise to primary protected amines such as **156**. Additionally, sodium phenolate and thiophenolate salts give rise to products **157** and **158**, respectively, while the chlorination product **159** was obtained upon the addition of tetrabutylammonium chloride (Scheme 31C).

Mechanisms under electrochemical activation

The electrochemical activation of NHPI esters provides significant advantages compared to other methods. It allows for single



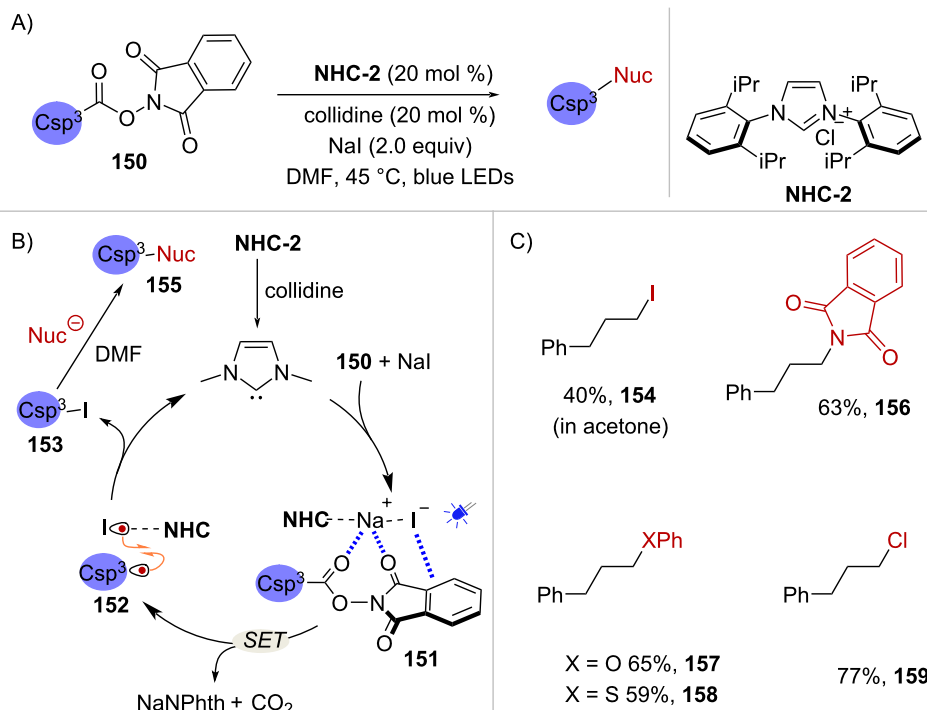
Scheme 30: A) Decarboxylative coupling of RAE and aldehydes enabled by NHC-catalyzed radical relay. B) Proposed reaction mechanism.

electron reduction to be facilitated by cost-effective carbon-based cathodes, eliminating the requirement for precious metal photocatalysts or exogenous reductants such as Zn^0 . In the final section of this perspective, we explore examples where NHPI esters have been utilized as radical precursors under electrochemical conditions.

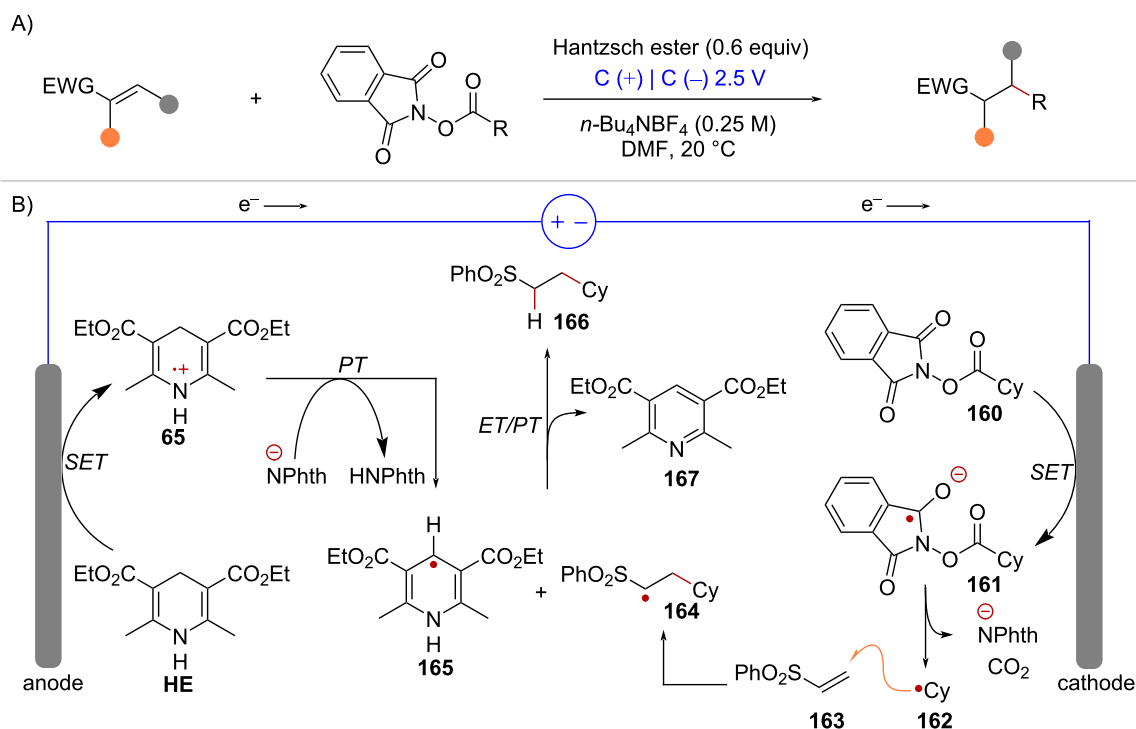
Giese-type radical additions, which are usually performed under conditions of photoredox-catalysis (see Scheme 4), can also be achieved under constant-potential electrolysis employing graphite electrodes [110] (Scheme 32A). Under these conditions, activation of NHPI ester **160** by SET occurs at the cathode's surface affording the corresponding radical anion **161** (Scheme 32B). Subsequent fragmentation leads to the cyclohexyl radical (**162**) which then adds to the terminal carbon of radical acceptor **163**, leading to radical intermediate **164**. In the

other redox half-reaction, Hantzsch ester (**HE**) undergoes anodic oxidation to form radical cation **65**, which then transfers a proton, likely to the phthalimidyl anion (N^-phth), resulting in the formation of radical species **165**. Finally, reaction between intermediates **164** and **165** through sequential electron transfer and proton transfer (ET/PT) leads to the hydroalkylation product **166** and the pyridine byproduct **167**.

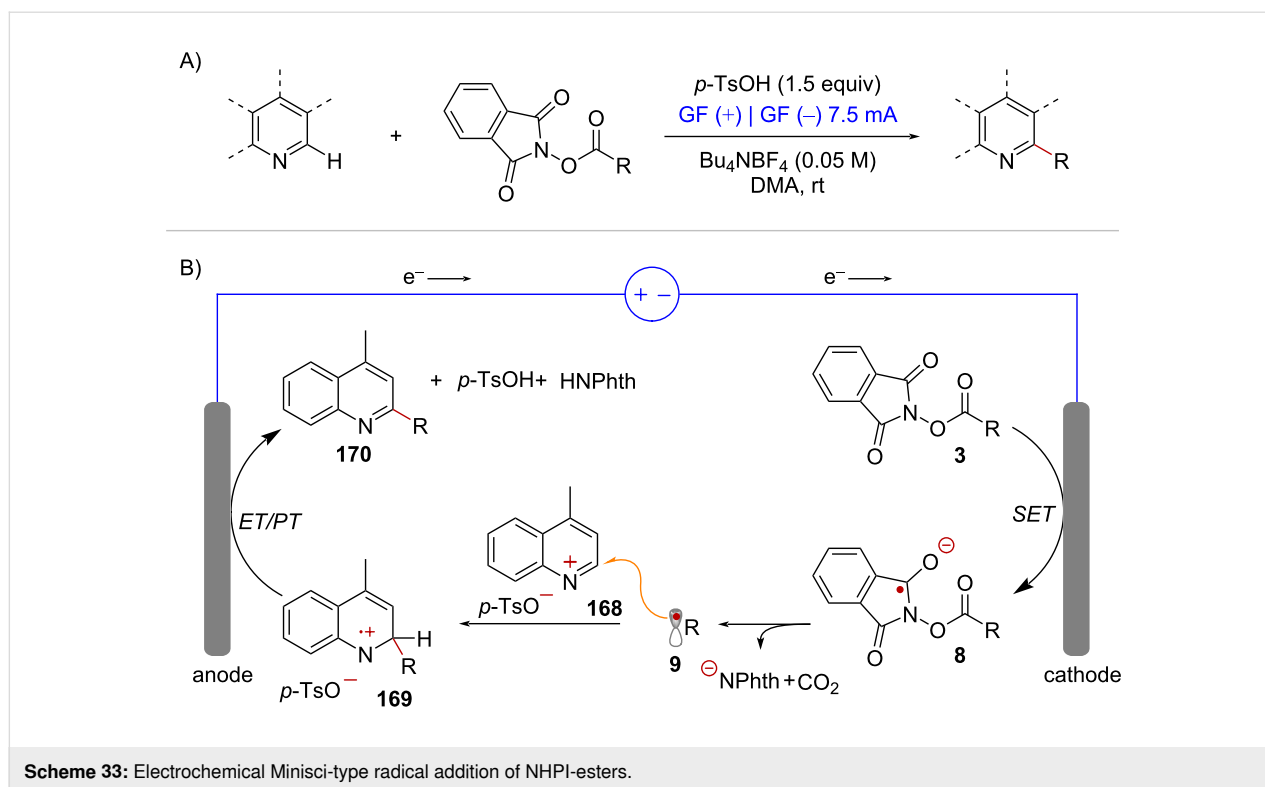
In addition, there have been reports of Minisci-type additions where radical intermediates are electrochemically generated from NHPI esters [111–113] (Scheme 33A). The mechanism of this redox neutral reaction involves reductive fragmentation of the radical precursor **3** mediated by the cathode under constant-current electrolysis (Scheme 33B). The resulting alkyl radical **9** attacks the protonated quinoline **168**, forming radical cation intermediate **169**. Finally, single electron oxidation of **169** at the



Scheme 31: A) Decarboxylative C(sp³)-heteroatom coupling reaction of NHPI esters under NHC catalysis B) The NHC catalyst improves reaction efficiency by EDA complex stabilization. C) Examples of substrate scope.



Scheme 32: A) Electrochemical Giese-type radical addition of NHPI esters. B) Reaction mechanism.



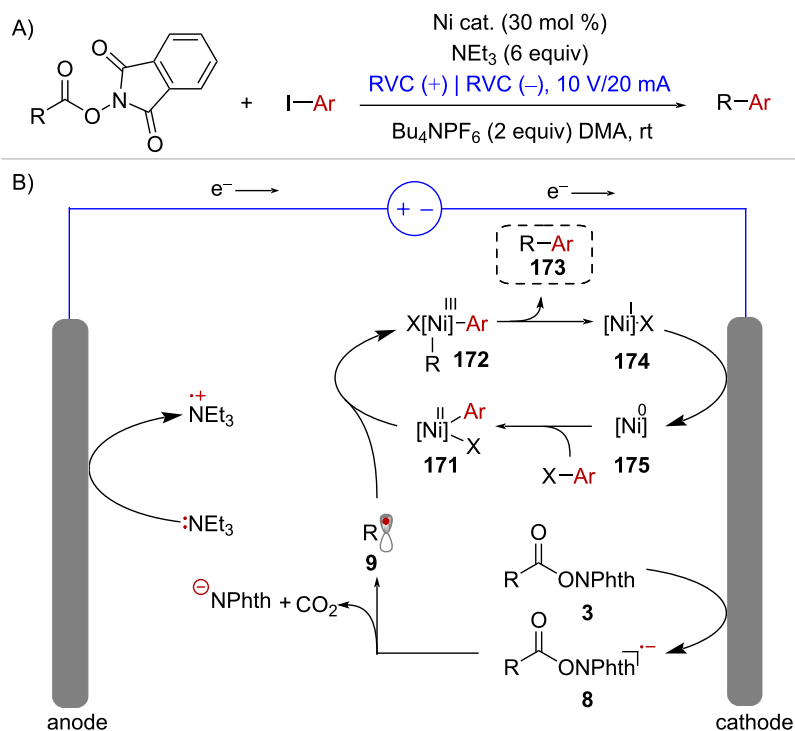
anode, followed by rearomatization via proton-transfer forms the alkylated heterocycle **170**.

As discussed in Scheme 25, the Ni-catalyzed cross-electrophile coupling between redox-active esters and aryl halides requires the addition of a stoichiometric reductant (typically Zn^0 or Mn^0) to both activate the NHPI ester and turn-over the catalytic cycle. However, the merger of Ni-catalysis and electrochemistry allows for the implementation of more convenient conditions in which these two crucial reductive steps can be mediated by the cathode (Scheme 34). In this context, Jamison and co-workers developed an electrochemically driven decarboxylative $\text{C}(\text{sp}^3)\text{--C}(\text{sp}^2)$ cross-coupling protocol that proceeds in a divided electrochemical cell with reticulated vitreous carbon (RVC) electrodes and triethylamine (NEt_3) as sacrificial reductant [114] (Scheme 34A). In the proposed mechanism, radical species **9**, which is generated upon cathodic reduction of active ester **3**, is captured by complex **171** (Scheme 34B). The resulting Ni^{III} complex **172** undergoes facile reductive elimination to form cross-coupling product **173** and Ni^{I} intermediate **174**. Finally, reduction of **174** at the cathode surface restores the Ni^0 species **175** giving rise to a new catalytic cycle.

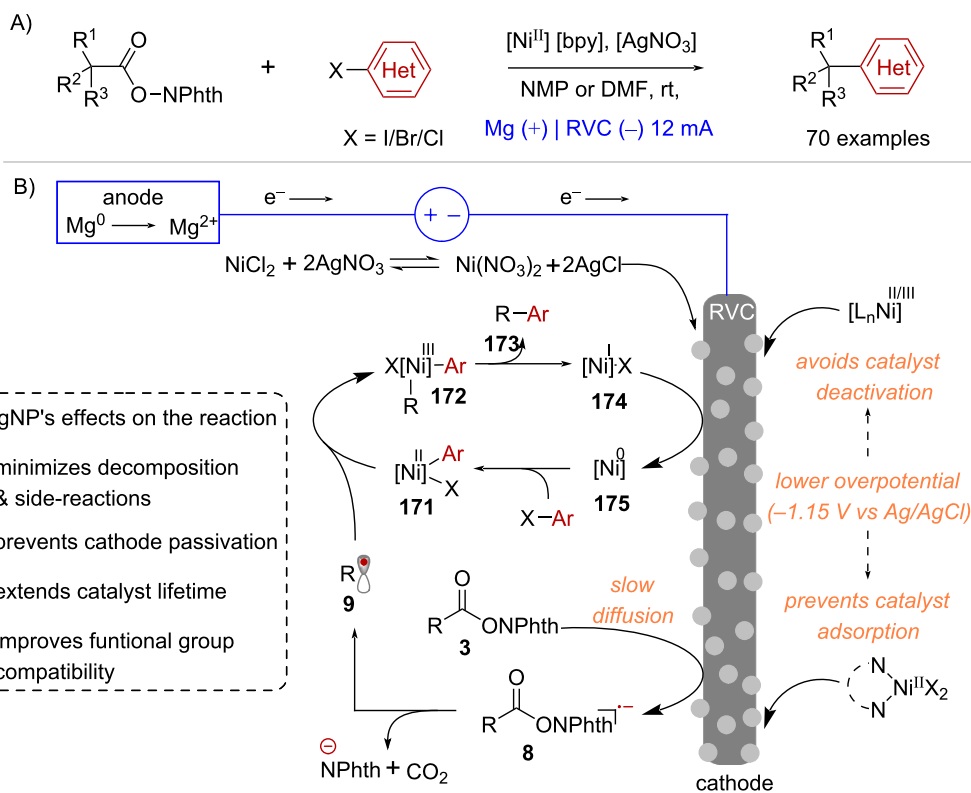
Reductive cross-electrophile couplings that incorporate redox-active esters and aryl halides have the potential to simplify the syntheses of drug-like compounds through $\text{C}(\text{sp}^3)\text{--C}(\text{sp}^2)$ bond formation. However, their synthetic utility is frequently

restricted due to various challenges, such as RAE decomposition and a limited aryl halide scope. In recent years, the Baran lab has made progress in enhancing the practicality and applicability of electrochemically driven decarboxylative couplings involving NHPI esters and aryl-halides [115]. Their optimized reaction conditions required a Ni^{II} precursor, 2,2'-bipyridine (bpy) as ligand, silver nitrate (AgNO_3) as an additive and the combination of a magnesium (Mg) sacrificial anode and a RVC cathode (Scheme 35A). A crucial discovery in advancing this methodology was the in situ formation of silver nanoparticles (AgNP) on the cathode's surface [116] (Scheme 35B). The use of this Ag-doped cathode led to slower mass transport and minimized side reactions caused by rapid reduction of RAEs, thereby avoiding substrate decomposition and enhancing reaction yields (Scheme 35B). Furthermore, the presence of the AgNP layer on the cathode caused a decrease of the reaction's overpotential from -1.66 V to -1.15 V (vs Ag/AgCl), which is thought to prevent catalyst deactivation via successive reduction of the various Ni species, while also avoiding electrode passivation caused by catalyst adsorption (Scheme 35B).

Baran and co-workers have demonstrated that these overall milder reaction conditions greatly improved the functional group compatibility of decarboxylative couplings under reducing conditions. For example, the cross-coupling between NHPI esters and both electron-poor and electron-rich



Scheme 34: Ni-electrocatalytic cross-electrophile coupling of NHPI esters with aryl iodides.



Scheme 35: A) Decarboxylative arylation of NHPI esters under Ag-Ni electrocatalysis B) Formation of AgNP on the cathode's surface and its effect on the reaction.

(hetero)aryl halides was equally effective (Scheme 36). In addition, the preparation of unnatural amino acids in multigram scale [115], along with the syntheses of complex terpenes [116] and (+)-calcipotriol [117] have showcased the vast synthetic potential and broad applicability of NHPI esters activated under these electrochemical conditions (Scheme 36).

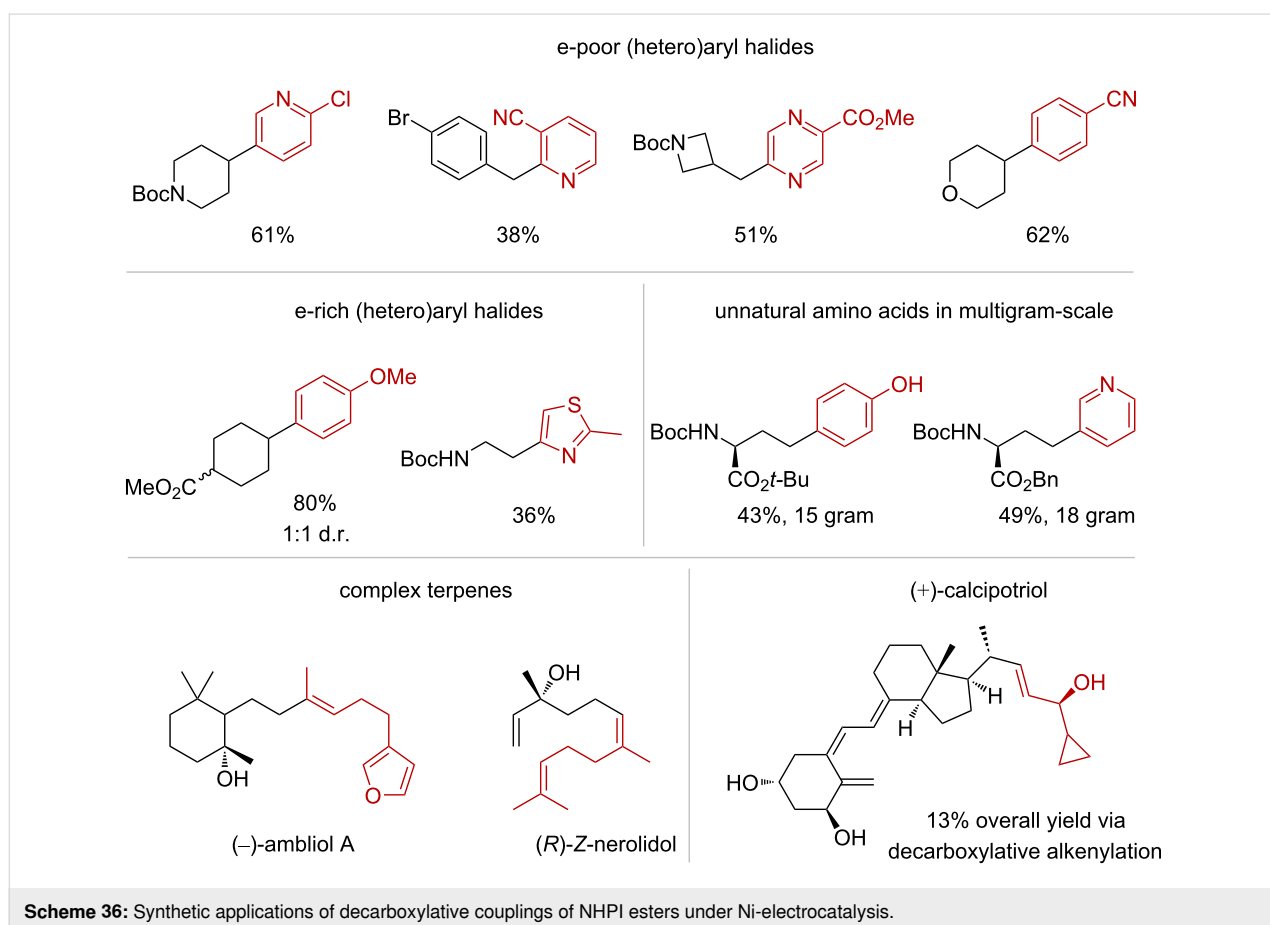
Conclusion

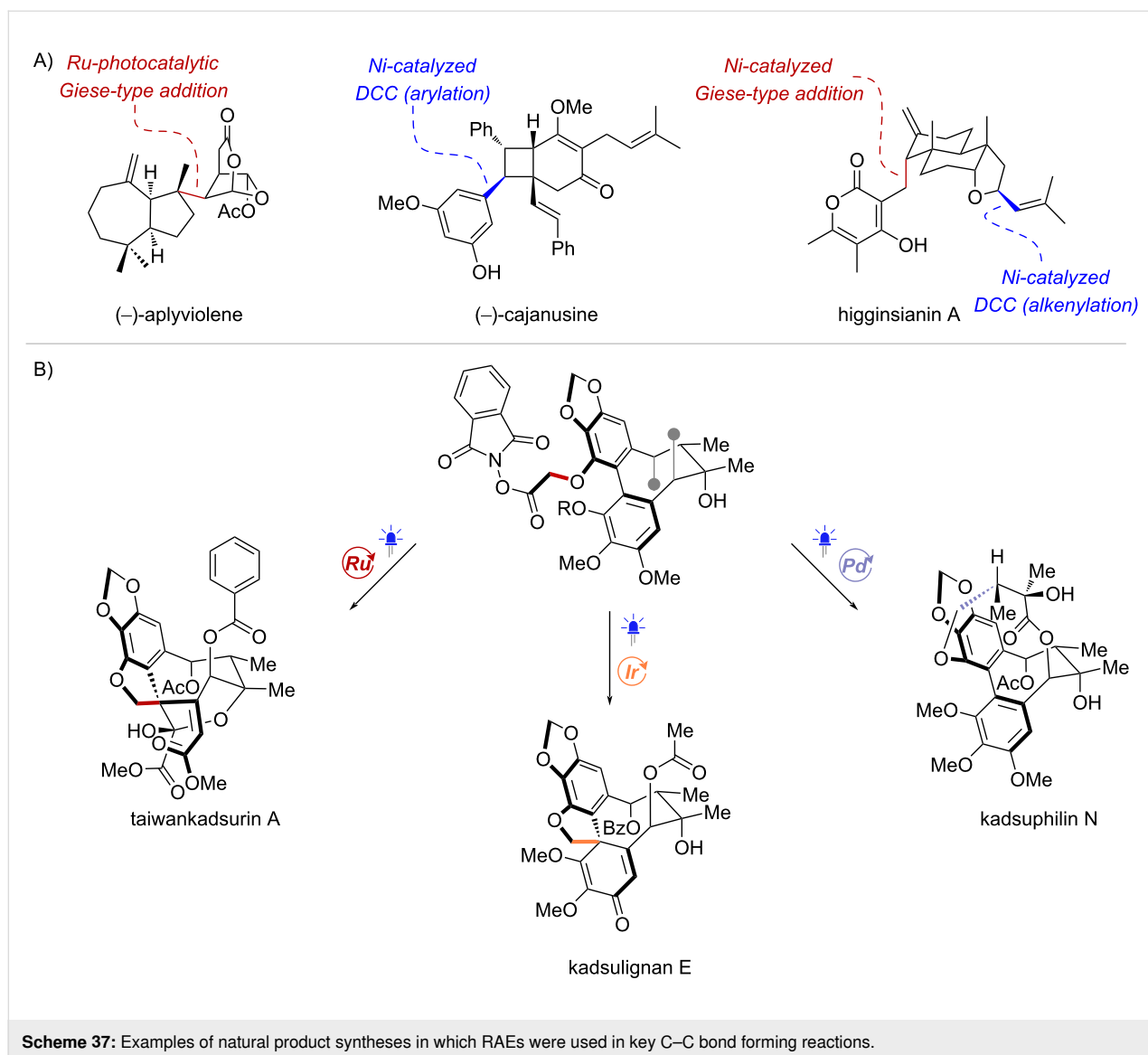
Given their rich history and their continued use in diverse methodologies, *N*-hydroxyphthalimide esters have been and will remain to be important tools in synthetic organic chemistry. In this perspective, we have surveyed recent advancements in photochemistry, TM catalysis, NHC catalysis, and electrochemistry to show the generality of these RAEs in diverse mechanistic paradigms. Their application as radical progenitors continues to broaden the scope of radical-mediated reactions, especially in complex molecular settings, where issues of chemoselectivity can benefit from the multitude of mechanisms for their activation.

Particularly, the use of RAEs in natural product total synthesis enables the assembly of strategic C–C bonds through radical coupling reactions that can draw from a wide range of reaction

conditions (Scheme 37). Pioneering work by Schnermann and Overman demonstrated the early potential of photocatalytic Giese-type additions, successfully coupling two complex ring fragments and creating adjacent stereocenters, which effectively solved major challenges in the synthesis of (–)-aplyvioline [38] (Scheme 37A). Brown and co-workers devised a diastereoselective Ni-catalyzed decarboxylative arylation as a crucial step in the synthesis of (–)-cajanusine [118] (Scheme 37A). Likewise, the Baran lab employed Ni-catalyzed decarboxylative couplings of RAEs to form two strategic C–C bonds in the synthesis of higginsianin A [119] (Scheme 37A). Recently, Lumb and co-workers showcased the use of NHPI esters in key radical cyclizations, allowing the synthesis of diverse dibenzocyclooctadiene lignans [55] (Scheme 37B). A Ru-catalyzed cyclization was employed to construct the quaternary stereocenter in taiwankadsurin A, whereas the corresponding spirocycle in kadsulignan E was formed under Ir photocatalysis. In addition, photoinduced Pd catalysis was applied in the key macrocyclization step to complete the synthesis of kadsuphilin N.

These applications in total synthesis serve as a testament to the synthetic versatility of radical reactions facilitated by the use of





RAEs. In the years to come, we anticipate that the continued development of new catalysts and the implementation of increasingly mild reaction conditions will open new possibilities for further applications of NHPI esters in radical reactions. Expanding the mechanisms and reactivity discussed herein will continue to improve our understanding of radical chemistry toward exploring novel chemical space.

Funding

Financial support was provided by the Natural Sciences and Engineering Research Council of Canada (Discovery Grant to J.-P.L.) and the FRQNT Center for Green Chemistry and Catalysis. C.R.A.N. is grateful to Mitacs (Globalink), FRQNT (PBEEE), and CONACyT (Mexican National Council of Science and Technology) for the doctoral scholarships awarded.

ORCID® iDs

Carlos R. Azpilcueta-Nicolas - <https://orcid.org/0000-0002-8839-3501>

Jean-Philip Lumb - <https://orcid.org/0000-0002-9283-1199>

References

- Yan, M.; Lo, J. C.; Edwards, J. T.; Baran, P. S. *J. Am. Chem. Soc.* **2016**, *138*, 12692–12714. doi:10.1021/jacs.6b08856
- Zard, S. Z. *Org. Lett.* **2017**, *19*, 1257–1269. doi:10.1021/acs.orglett.7b00531
- Kuivila, H. G. *Acc. Chem. Res.* **1968**, *1*, 299–305. doi:10.1021/ar50010a002
- Gallher, M. S.; Roldan, B. J.; Stephenson, C. R. J. *Chem. Soc. Rev.* **2021**, *50*, 10044–10057. doi:10.1039/d1cs00411e
- Kvasovs, N.; Gevorgyan, V. *Chem. Soc. Rev.* **2021**, *50*, 2244–2259. doi:10.1039/d0cs00589d
- Crespi, S.; Fagnoni, M. *Chem. Rev.* **2020**, *120*, 9790–9833. doi:10.1021/acs.chemrev.0c00278

7. Matsui, J. K.; Lang, S. B.; Heitz, D. R.; Molander, G. A. *ACS Catal.* **2017**, *7*, 2563–2575. doi:10.1021/acscatal.7b00094
8. Prier, C. K.; Rankic, D. A.; MacMillan, D. W. C. *Chem. Rev.* **2013**, *113*, 5322–5363. doi:10.1021/cr300503r
9. Yan, M.; Kawamata, Y.; Baran, P. S. *Chem. Rev.* **2017**, *117*, 13230–13319. doi:10.1021/acs.chemrev.7b00397
10. Siu, J. C.; Fu, N.; Lin, S. *Acc. Chem. Res.* **2020**, *53*, 547–560. doi:10.1021/acs.accounts.9b00529
11. Kaga, A.; Chiba, S. *ACS Catal.* **2017**, *7*, 4697–4706. doi:10.1021/acscatal.7b01405
12. Smith, J. M.; Harwood, S. J.; Baran, P. S. *Acc. Chem. Res.* **2018**, *51*, 1807–1817. doi:10.1021/acs.accounts.8b00209
13. Gennaiou, K.; Kelesidis, A.; Kourgiantaki, M.; Zografos, A. L. *Beilstein J. Org. Chem.* **2023**, *19*, 1–26. doi:10.3762/bjoc.19.1
14. Laudadio, G.; Palkowitz, M. D.; El-Hayek Ewing, T.; Baran, P. S. *ACS Med. Chem. Lett.* **2022**, *13*, 1413–1420. doi:10.1021/acsmmedchemlett.2c00286
15. Ni, S.; Padial, N. M.; Kingston, C.; Vantourout, J. C.; Schmitt, D. C.; Edwards, J. T.; Kruszyk, M. M.; Merchant, R. R.; Mykhailiuk, P. K.; Sanchez, B. B.; Yang, S.; Perry, M. A.; Gallego, G. M.; Mousseau, J. J.; Collins, M. R.; Cherney, R. J.; Lebed, P. S.; Chen, J. S.; Qin, T.; Baran, P. S. *J. Am. Chem. Soc.* **2019**, *141*, 6726–6739. doi:10.1021/jacs.9b02238
16. Wiles, R. J.; Molander, G. A. *Isr. J. Chem.* **2020**, *60*, 281–293. doi:10.1002/ijch.201900166
17. Pitzer, L.; Schwarz, J. L.; Glorius, F. *Chem. Sci.* **2019**, *10*, 8285–8291. doi:10.1039/c9sc03359a
18. Gooßen, L. J.; Rodríguez, N.; Gooßen, K. *Angew. Chem., Int. Ed.* **2008**, *47*, 3100–3120. doi:10.1002/anie.200704782
19. Xuan, J.; Zhang, Z.-G.; Xiao, W.-J. *Angew. Chem., Int. Ed.* **2015**, *54*, 15632–15641. doi:10.1002/anie.201505731
20. Wang, Z.; Zhu, L.; Yin, F.; Su, Z.; Li, Z.; Li, C. *J. Am. Chem. Soc.* **2012**, *134*, 4258–4263. doi:10.1021/ja210361z
21. Concepcion, J. I.; Francisco, C. G.; Freire, R.; Hernandez, R.; Salazar, J. A.; Suarez, E. *J. Org. Chem.* **1986**, *51*, 402–404. doi:10.1021/jo00353a026
22. Li, Q. Y.; Gockel, S. N.; Lutovsky, G. A.; DeGlopper, K. S.; Baldwin, N. J.; Bundesmann, M. W.; Tucker, J. W.; Bagley, S. W.; Yoon, T. P. *Nat. Chem.* **2022**, *14*, 94–99. doi:10.1038/s41557-021-00834-8
23. Su, W.; Xu, P.; Ritter, T. *Angew. Chem., Int. Ed.* **2021**, *60*, 24012–24017. doi:10.1002/anie.202108971
24. Chen, T. Q.; Pedersen, P. S.; Dow, N. W.; Fayad, R.; Hauke, C. E.; Rosko, M. C.; Danilov, E. O.; Blakemore, D. C.; Dechert-Schmitt, A.-M.; Knauber, T.; Castellano, F. N.; MacMillan, D. W. C. *J. Am. Chem. Soc.* **2022**, *144*, 8296–8305. doi:10.1021/jacs.2c02392
25. Barton, D. H. R.; Crich, D.; Motherwell, W. B. *J. Chem. Soc., Chem. Commun.* **1983**, 939–941. doi:10.1039/c39830000939
26. Barton, D. H. R.; Crich, D.; Motherwell, W. B. *Tetrahedron* **1985**, *41*, 3901–3924. doi:10.1016/s0040-4020(01)97173-x
27. Saraiva, M. F.; Couri, M. R. C.; Le Hyaric, M.; de Almeida, M. V. *Tetrahedron* **2009**, *65*, 3563–3572. doi:10.1016/j.tet.2009.01.103
28. St. John, P. C.; Guan, Y.; Kim, Y.; Kim, S.; Paton, R. S. *Nat. Commun.* **2020**, *11*, 2328. doi:10.1038/s41467-020-16201-z
BDE values were predicted using the ALFABET web server: <https://bde.ml.nrel.gov/>. More details can be found in this referenced article.
29. Okada, K.; Okamoto, K.; Oda, M. *J. Am. Chem. Soc.* **1988**, *110*, 8736–8738. doi:10.1021/ja00234a047
30. Parida, S. K.; Mandal, T.; Das, S.; Hota, S. K.; De Sarkar, S.; Murarka, S. *ACS Catal.* **2021**, *11*, 1640–1683. doi:10.1021/acscatal.0c04756
31. Murarka, S. *Adv. Synth. Catal.* **2018**, *360*, 1735–1753. doi:10.1002/adsc.201701615
32. Mato, M.; Spinnato, D.; Leutzsch, M.; Moon, H. W.; Reijerse, E. J.; Cornella, J. *Nat. Chem.* **2023**, *15*, 1138–1145. doi:10.1038/s41557-023-01229-7
33. Bach, R. D.; Schlegel, H. B. *J. Phys. Chem. A* **2021**, *125*, 5014–5021. doi:10.1021/acs.jpca.1c02741
34. Sayre, H.; Ripberger, H. H.; Odella, E.; Zieleniewska, A.; Heredia, D. A.; Rumbles, G.; Scholes, G. D.; Moore, T. A.; Moore, A. L.; Knowles, R. R. *J. Am. Chem. Soc.* **2021**, *143*, 13034–13043. doi:10.1021/jacs.1c01701
35. Tucker, J. W.; Stephenson, C. R. J. *J. Org. Chem.* **2012**, *77*, 1617–1622. doi:10.1021/jo202538x
The cyclic voltammetry and spectroscopic data reported by Knowles was used to approximate the $E_{1/2}^{\text{red}}[\text{Ir}^{\text{IV}}/\text{Ir}^{\text{III}}]$ value, following the procedure reported by Tucker and Stephenson.
36. Schultz, D. M.; Yoon, T. P. *Science* **2014**, *343*, 1239176. doi:10.1126/science.1239176
37. Okada, K.; Okamoto, K.; Morita, N.; Okubo, K.; Oda, M. *J. Am. Chem. Soc.* **1991**, *113*, 9401–9402. doi:10.1021/ja00024a074
38. Schnermann, M. J.; Overman, L. E. *Angew. Chem., Int. Ed.* **2012**, *51*, 9576–9580. doi:10.1002/anie.201204977
39. Müller, D. S.; Untiedt, N. L.; Dieskau, A. P.; Lackner, G. L.; Overman, L. E. *J. Am. Chem. Soc.* **2015**, *137*, 660–663. doi:10.1021/ja512527s
40. Pratsch, G.; Lackner, G. L.; Overman, L. E. *J. Org. Chem.* **2015**, *80*, 6025–6036. doi:10.1021/acs.joc.5b00795
41. Schwarz, J.; König, B. *Green Chem.* **2016**, *18*, 4743–4749. doi:10.1039/c6gc01101b
42. Xu, R.; Xu, T.; Yang, M.; Cao, T.; Liao, S. *Nat. Commun.* **2019**, *10*, 3752. doi:10.1038/s41467-019-11805-6
43. Shu, X.; Xu, R.; Ma, Q.; Liao, S. *Org. Chem. Front.* **2020**, *7*, 2003–2007. doi:10.1039/d0qo00440e
44. Proctor, R. S. J.; Davis, H. J.; Phipps, R. J. *Science* **2018**, *360*, 419–422. doi:10.1126/science.aar6376
45. Ermanis, K.; Colgan, A. C.; Proctor, R. S. J.; Hadrys, B. W.; Phipps, R. J.; Goodman, J. M. *J. Am. Chem. Soc.* **2020**, *142*, 21091–21101. doi:10.1021/jacs.0c09668
46. Tlahuext-Aca, A.; Garza-Sanchez, R. A.; Glorius, F. *Angew. Chem., Int. Ed.* **2017**, *56*, 3708–3711. doi:10.1002/anie.201700049
47. Wang, X.; Han, Y.-F.; Ouyang, X.-H.; Song, R.-J.; Li, J.-H. *Chem. Commun.* **2019**, 55, 14637–14640. doi:10.1039/c9cc07494e
48. Murray, P. R. D.; Leibler, I. N.-M.; Hell, S. M.; Villalona, E.; Doyle, A. G.; Knowles, R. R. *ACS Catal.* **2022**, *12*, 13732–13740. doi:10.1021/acscatal.2c04316
49. Sherwood, T. C.; Xiao, H.-Y.; Bhaskar, R. G.; Simmons, E. M.; Zaretsky, S.; Rauch, M. P.; Knowles, R. R.; Dhar, T. G. M. *J. Org. Chem.* **2019**, *84*, 8360–8379. doi:10.1021/acs.joc.9b00432
50. Sherwood, T. C.; Li, N.; Yazdani, A. N.; Dhar, T. G. M. *J. Org. Chem.* **2018**, *83*, 3000–3012. doi:10.1021/acs.joc.8b00205
51. He, J.; Chen, G.; Zhang, B.; Li, Y.; Chen, J.-R.; Xiao, W.-J.; Liu, F.; Li, C. *Chem* **2020**, *6*, 1149–1159. doi:10.1016/j.chempr.2020.02.003
52. Reich, D.; Noble, A.; Aggarwal, V. K. *Angew. Chem., Int. Ed.* **2022**, *61*, e202207063. doi:10.1002/anie.202207063

53. Williams, O. P.; Chmiel, A. F.; Mikhael, M.; Bates, D. M.; Yeung, C. S.; Wickens, Z. K. *Angew. Chem., Int. Ed.* **2023**, *62*, e202300178. doi:10.1002/anie.202300178
54. Azpilcueta-Nicolas, C. R.; Meng, D.; Edelmann, S.; Lumb, J.-P. *Angew. Chem., Int. Ed.* **2023**, *62*, e202215422. doi:10.1002/anie.202215422
55. Huang, Z.; Lumb, J.-P. *Nat. Chem.* **2021**, *13*, 24–32. doi:10.1038/s41557-020-00603-z
56. Kachkovskiy, G.; Faderl, C.; Reiser, O. *Adv. Synth. Catal.* **2013**, *355*, 2240–2248. doi:10.1002/adsc.201300221
57. Shen, Y.; Shen, M.-L.; Wang, P.-S. *ACS Catal.* **2020**, *10*, 8247–8253. doi:10.1021/acscatal.0c02660
58. Crisenza, G. E. M.; Mazzarella, D.; Melchiorre, P. *J. Am. Chem. Soc.* **2020**, *142*, 5461–5476. doi:10.1021/jacs.0c01416
59. Lima, C. G. S.; de M. Lima, T.; Duarte, M.; Jurberg, I. D.; Paixão, M. W. *ACS Catal.* **2016**, *6*, 1389–1407. doi:10.1021/acscatal.5b02386
60. Zheng, C.; Wang, G.-Z.; Shang, R. *Adv. Synth. Catal.* **2019**, *361*, 4500–4505. doi:10.1002/adsc.201900803
61. Correia, J. T. M.; Piva da Silva, G.; Kisukuri, C. M.; André, E.; Pires, B.; Carneiro, P. S.; Paixão, M. W. *J. Org. Chem.* **2020**, *85*, 9820–9834. doi:10.1021/acs.joc.0c01130
62. Chowdhury, R.; Yu, Z.; Tong, M. L.; Kohlhepp, S. V.; Yin, X.; Mendoza, A. J. *Am. Chem. Soc.* **2020**, *142*, 20143–20151. doi:10.1021/jacs.0c09678
63. Fawcett, A.; Pradeilles, J.; Wang, Y.; Mutsuga, T.; Myers, E. L.; Aggarwal, V. K. *Science* **2017**, *357*, 283–286. doi:10.1126/science.aan3679
64. Barton, L. M.; Chen, L.; Blackmond, D. G.; Baran, P. S. *Proc. Natl. Acad. Sci. U. S. A.* **2021**, *118*, e2109408118. doi:10.1073/pnas.2109408118
65. Candish, L.; Teders, M.; Glorius, F. *J. Am. Chem. Soc.* **2017**, *139*, 7440–7443. doi:10.1021/jacs.7b03127
66. Cheng, W.-M.; Shang, R.; Zhao, B.; Xing, W.-L.; Fu, Y. *Org. Lett.* **2017**, *19*, 4291–4294. doi:10.1021/acs.orglett.7b01950
67. Fu, M.-C.; Shang, R.; Zhao, B.; Wang, B.; Fu, Y. *Science* **2019**, *363*, 1429–1434. doi:10.1126/science.aav3200
68. Shibutani, S.; Nagao, K.; Ohmiya, H. *Org. Lett.* **2021**, *23*, 1798–1803. doi:10.1021/acs.orglett.1c00211
69. Shibutani, S.; Kodo, T.; Takeda, M.; Nagao, K.; Tokunaga, N.; Sasaki, Y.; Ohmiya, H. *J. Am. Chem. Soc.* **2020**, *142*, 1211–1216. doi:10.1021/jacs.9b12335
70. Jin, Y.; Yang, H.; Fu, H. *Chem. Commun.* **2016**, *52*, 12909–12912. doi:10.1039/c6cc06994k
71. Jin, Y.; Yang, H.; Fu, H. *Org. Lett.* **2016**, *18*, 6400–6403. doi:10.1021/acs.orglett.6b03300
72. Bosque, I.; Bach, T. *ACS Catal.* **2019**, *9*, 9103–9109. doi:10.1021/acscatal.9b01039
73. Parasram, M.; Gevorgyan, V. *Chem. Soc. Rev.* **2017**, *46*, 6227–6240. doi:10.1039/c7cs00226b
74. Cheung, K. P. S.; Sarkar, S.; Gevorgyan, V. *Chem. Rev.* **2022**, *122*, 1543–1625. doi:10.1021/acs.chemrev.1c00403
75. Zhao, W.; Wurz, R. P.; Peters, J. C.; Fu, G. C. *J. Am. Chem. Soc.* **2017**, *139*, 12153–12156. doi:10.1021/jacs.7b07546
76. Xia, H.-D.; Li, Z.-L.; Gu, Q.-S.; Dong, X.-Y.; Fang, J.-H.; Du, X.-Y.; Wang, L.-L.; Liu, X.-Y. *Angew. Chem., Int. Ed.* **2020**, *59*, 16926–16932. doi:10.1002/anie.202006317
77. Mao, Y.; Zhao, W.; Lu, S.; Yu, L.; Wang, Y.; Liang, Y.; Ni, S.; Pan, Y. *Chem. Sci.* **2020**, *11*, 4939–4947. doi:10.1039/d0sc02213f
78. Zhang, Y.; Zhang, D. *Org. Biomol. Chem.* **2020**, *18*, 4479–4483. doi:10.1039/d0ob00835d
79. Wang, C.; Guo, M.; Qi, R.; Shang, Q.; Liu, Q.; Wang, S.; Zhao, L.; Wang, R.; Xu, Z. *Angew. Chem., Int. Ed.* **2018**, *57*, 15841–15846. doi:10.1002/anie.201809400
80. Huang, H.-M.; Koy, M.; Serrano, E.; Pflüger, P. M.; Schwarz, J. L.; Glorius, F. *Nat. Catal.* **2020**, *3*, 393–400. doi:10.1038/s41929-020-0434-0
81. Wang, G.-Z.; Shang, R.; Fu, Y. *Org. Lett.* **2018**, *20*, 888–891. doi:10.1021/acs.orglett.8b00023
82. Koy, M.; Sandfort, F.; Tlahuext-Aca, A.; Quach, L.; Daniliuc, C. G.; Glorius, F. *Chem. – Eur. J.* **2018**, *24*, 4552–4555. doi:10.1002/chem.201800813
83. Cheng, W.-M.; Shang, R.; Fu, Y. *Nat. Commun.* **2018**, *9*, 5215. doi:10.1038/s41467-018-07694-w
84. Cornella, J.; Edwards, J. T.; Qin, T.; Kawamura, S.; Wang, J.; Pan, C.-M.; Gianatassio, R.; Schmidt, M.; Eastgate, M. D.; Baran, P. S. *J. Am. Chem. Soc.* **2016**, *138*, 2174–2177. doi:10.1021/jacs.6b00250
85. Toriyama, F.; Cornella, J.; Wimmer, L.; Chen, T.-G.; Dixon, D. D.; Creech, G.; Baran, P. S. *J. Am. Chem. Soc.* **2016**, *138*, 11132–11135. doi:10.1021/jacs.6b07172
86. Wang, J.; Qin, T.; Chen, T.-G.; Wimmer, L.; Edwards, J. T.; Cornella, J.; Vokits, B.; Shaw, S. A.; Baran, P. S. *Angew. Chem., Int. Ed.* **2016**, *55*, 9676–9679. doi:10.1002/anie.201605463
87. Edwards, J. T.; Merchant, R. R.; McClymont, K. S.; Knouse, K. W.; Qin, T.; Malins, L. R.; Vokits, B.; Shaw, S. A.; Bao, D.-H.; Wei, F.-L.; Zhou, T.; Eastgate, M. D.; Baran, P. S. *Nature* **2017**, *545*, 213–218. doi:10.1038/nature22307
88. Smith, J. M.; Qin, T.; Merchant, R. R.; Edwards, J. T.; Malins, L. R.; Liu, Z.; Che, G.; Shen, Z.; Shaw, S. A.; Eastgate, M. D.; Baran, P. S. *Angew. Chem., Int. Ed.* **2017**, *56*, 11906–11910. doi:10.1002/anie.201705107
89. Qin, T.; Cornella, J.; Li, C.; Malins, L. R.; Edwards, J. T.; Kawamura, S.; Maxwell, B. D.; Eastgate, M. D.; Baran, P. S. *Science* **2016**, *352*, 801–805. doi:10.1126/science.aaf6123
90. Li, C.; Wang, J.; Barton, L. M.; Yu, S.; Tian, M.; Peters, D. S.; Kumar, M.; Yu, A. W.; Johnson, K. A.; Chatterjee, A. K.; Yan, M.; Baran, P. S. *Science* **2017**, *356*, eaam7355. doi:10.1126/science.aam7355
91. Wang, J.; Shang, M.; Lundberg, H.; Feu, K. S.; Hecker, S. J.; Qin, T.; Blackmond, D. G.; Baran, P. S. *ACS Catal.* **2018**, *8*, 9537–9542. doi:10.1021/acscatal.8b02928
92. Liu, X.-G.; Zhou, C.-J.; Lin, E.; Han, X.-L.; Zhang, S.-S.; Li, Q.; Wang, H. *Angew. Chem., Int. Ed.* **2018**, *57*, 13096–13100. doi:10.1002/anie.201806799
93. Huihui, K. M. M.; Caputo, J. A.; Melchor, Z.; Olivares, A. M.; Spiewak, A. M.; Johnson, K. A.; DiBenedetto, T. A.; Kim, S.; Ackerman, L. K. G.; Weix, D. J. *J. Am. Chem. Soc.* **2016**, *138*, 5016–5019. doi:10.1021/jacs.6b01533
94. Salgueiro, D. C.; Chi, B. K.; Guzei, I. A.; García-Reynaga, P.; Weix, D. J. *Angew. Chem., Int. Ed.* **2022**, *61*, e202205673. doi:10.1002/anie.202205673
95. Huang, L.; Olivares, A. M.; Weix, D. J. *Angew. Chem., Int. Ed.* **2017**, *56*, 11901–11905. doi:10.1002/anie.201706781
96. Kang, K.; Weix, D. J. *Org. Lett.* **2022**, *24*, 2853–2857. doi:10.1021/acs.orglett.2c00805

97. Wang, J.; Cary, B. P.; Beyer, P. D.; Gellman, S. H.; Weix, D. J. *Angew. Chem., Int. Ed.* **2019**, *58*, 12081–12085. doi:10.1002/anie.201906000
98. West, M. S.; Gabbey, A. L.; Huestis, M. P.; Rousseaux, S. A. L. *Org. Lett.* **2022**, *24*, 8441–8446. doi:10.1021/acs.orglett.2c03570
99. Gabbey, A. L.; Michel, N. W. M.; Hughes, J. M. E.; Campeau, L.-C.; Rousseaux, S. A. L. *Org. Lett.* **2022**, *24*, 3173–3178. doi:10.1021/acs.orglett.2c00918
100. Suzuki, N.; Hofstra, J. L.; Poremba, K. E.; Reisman, S. E. *Org. Lett.* **2017**, *19*, 2150–2153. doi:10.1021/acs.orglett.7b00793
101. Polites, V. C.; Badir, S. O.; Keess, S.; Jolit, A.; Molander, G. A. *Org. Lett.* **2021**, *23*, 4828–4833. doi:10.1021/acs.orglett.1c01558
102. Jin, S.; Haug, G. C.; Nguyen, V. T.; Flores-Hansen, C.; Arman, H. D.; Larionov, O. V. *ACS Catal.* **2019**, *9*, 9764–9774. doi:10.1021/acscatal.9b03366
103. Yu, L.; Tang, M.-L.; Si, C.-M.; Meng, Z.; Liang, Y.; Han, J.; Sun, X. *Org. Lett.* **2018**, *20*, 4579–4583. doi:10.1021/acs.orglett.8b01866
104. Gao, L.; Wang, G.; Cao, J.; Yuan, D.; Xu, C.; Guo, X.; Li, S. *Chem. Commun.* **2018**, *54*, 11534–11537. doi:10.1039/c8cc06152a
105. Gao, L.; Wang, G.; Cao, J.; Chen, H.; Gu, Y.; Liu, X.; Cheng, X.; Ma, J.; Li, S. *ACS Catal.* **2019**, *9*, 10142–10151. doi:10.1021/acscatal.9b03798
106. Ishii, T.; Kakeno, Y.; Nagao, K.; Ohmiya, H. *J. Am. Chem. Soc.* **2019**, *141*, 3854–3858. doi:10.1021/jacs.9b00880
107. Kakeno, Y.; Kusakabe, M.; Nagao, K.; Ohmiya, H. *ACS Catal.* **2020**, *10*, 8524–8529. doi:10.1021/acscatal.0c02849
108. Ishii, T.; Ota, K.; Nagao, K.; Ohmiya, H. *J. Am. Chem. Soc.* **2019**, *141*, 14073–14077. doi:10.1021/jacs.9b07194
109. Chen, K.-Q.; Wang, Z.-X.; Chen, X.-Y. *Org. Lett.* **2020**, *22*, 8059–8064. doi:10.1021/acs.orglett.0c03006
110. Chen, X.; Luo, X.; Peng, X.; Guo, J.; Zai, J.; Wang, P. *Chem. – Eur. J.* **2020**, *26*, 3226–3230. doi:10.1002/chem.201905224
111. Mo, Y.; Lu, Z.; Rughoobur, G.; Patil, P.; Gershenfeld, N.; Akinwande, A. I.; Buchwald, S. L.; Jensen, K. F. *Science* **2020**, *368*, 1352–1357. doi:10.1126/science.aba3823
112. Niu, K.; Song, L.; Hao, Y.; Liu, Y.; Wang, Q. *Chem. Commun.* **2020**, *56*, 11673–11676. doi:10.1039/d0cc05391k
113. Liu, Y.; Xue, L.; Shi, B.; Bu, F.; Wang, D.; Lu, L.; Shi, R.; Lei, A. *Chem. Commun.* **2019**, *55*, 14922–14925. doi:10.1039/c9cc08528a
114. Li, H.; Breen, C. P.; Seo, H.; Jamison, T. F.; Fang, Y.-Q.; Bio, M. M. *Org. Lett.* **2018**, *20*, 1338–1341. doi:10.1021/acs.orglett.8b00070
115. Palkowitz, M. D.; Laudadio, G.; Kolb, S.; Choi, J.; Oderinde, M. S.; Ewing, T. E.-H.; Bolduc, P. N.; Chen, T.; Zhang, H.; Cheng, P. T. W.; Zhang, B.; Mandler, M. D.; Blaszczak, V. D.; Richter, J. M.; Collins, M. R.; Schioldager, R. L.; Bravo, M.; Dhar, T. G. M.; Vokits, B.; Zhu, Y.; Echeverria, P.-G.; Poss, M. A.; Shaw, S. A.; Clementson, S.; Petersen, N. N.; Mykhailiuk, P. K.; Baran, P. S. *J. Am. Chem. Soc.* **2022**, *144*, 17709–17720. doi:10.1021/jacs.2c08006
116. Harwood, S. J.; Palkowitz, M. D.; Gannett, C. N.; Perez, P.; Yao, Z.; Sun, L.; Abruña, H. D.; Anderson, S. L.; Baran, P. S. *Science* **2022**, *375*, 745–752. doi:10.1126/science.abn1395
117. Gu, J.; Rodriguez, K. X.; Kanda, Y.; Yang, S.; Ociepa, M.; Wilke, H.; Abrishami, A. V.; Jørgensen, L.; Skak-Nielsen, T.; Chen, J. S.; Baran, P. S. *Proc. Natl. Acad. Sci. U. S. A.* **2022**, *119*, e2200814119. doi:10.1073/pnas.2200814119
118. Guo, R.; Witherspoon, B. P.; Brown, M. K. *J. Am. Chem. Soc.* **2020**, *142*, 5002–5006. doi:10.1021/jacs.0c00359
119. Merchant, R. R.; Oberg, K. M.; Lin, Y.; Novak, A. J. E.; Felding, J.; Baran, P. S. *J. Am. Chem. Soc.* **2018**, *140*, 7462–7465. doi:10.1021/jacs.8b04891

License and Terms

This is an open access article licensed under the terms of the Beilstein-Institut Open Access License Agreement (<https://www.beilstein-journals.org/bjoc/terms>), which is identical to the Creative Commons Attribution 4.0 International License (<https://creativecommons.org/licenses/by/4.0>). The reuse of material under this license requires that the author(s), source and license are credited. Third-party material in this article could be subject to other licenses (typically indicated in the credit line), and in this case, users are required to obtain permission from the license holder to reuse the material.

The definitive version of this article is the electronic one which can be found at:
<https://doi.org/10.3762/bjoc.20.35>